APPENDIX H

Shell Puget Sound Refinery (PSR) Rail Unloading Facility Dispersion, Fire, and Explosion Analysis

Executive Summary 7
Introduction 10
Analysis Parameters 12
Technical Approach 15
Results 23
Conclusions 53
References 56
Appendix A – Summary Report 57
Appendix B – Selection of Surface Roughness Length 174

This page intentionally left blank

Evaluation of Hydrocarbon Releases from Crude-by-Rail Incidents Using Trajectory, Fate, and Effects Modeling for the Shell ARUF EIS

Prepared for: HDR, Inc.

Project Number:
2015-193

Date Submitted:
7/6/2016

Version:
DRAFT Report

Project Manager
Matthew Horn, Ph.D.

RPS ASA
55 Village Square Dr.
South Kingstown, RI USA
02879-8248

Release	File Name	Date Submitted	Notes
Final	Appendix_G_RPS_Spill_Analysis	7/6/2016	Complete Technical Appendix for submission to HDR following secondary internal HDR review and response to comments
Draft HDR v3	Shell ARUF EIS – RPS ASA Technical Report 20150422	4/22/2016	Complete Technical Appendix for submission to HDR following secondary Internal HDR review and response to comments
Draft HDR v2	Shell ARUF EIS - RPS ASA Technical Report 20150415	4/15/2016	Complete Technical Appendix for submission to HDR following internal HDR review and response to comments
Draft HDR v1	Shell ARUF EIS - RPS ASA Technical Report 20150321	3/21/2016	Complete Draft Technical Appendix for submission to HDR for internal HDR review
Draft RPS ASA v2	Shell ARUF EIS – RPS ASA Technical Report	3/18/2016	Complete Draft Technical Appendix for secondary internal RPS ASA review
Draft RPS ASA v1	Shell ARUF EIS – RPS ASA Technical Report	3/14/2016	Complete Draft Technical Appendix for primary internal RPS ASA review

DISCLAIMER:

This document contains confidential information that is intended only for use by the client and is not for public circulation, publication, nor any third party use without the prior written notification to RPS ASA. While the opinions and interpretations presented are based on information from sources that RPS ASA considers reliable, the accuracy and completeness of said information cannot be guaranteed. Therefore, RPS ASA, its agents, assigns, affiliates, and employees accept no liability for the result of any action taken or not taken on the basis of the information given in this report, nor for any negligent misstatements, errors, and omissions. RPS ASA shall not be liable or responsible for any loss, cost damages or expenses incurred or sustained by anyone resulting from an interpretation of this document. Except with permission from RPS, this report may only be used in accordance with the previously agreed terms. It must not be reproduced or redistributed, in whole or in part, to any other person than the addressees or published, in whole or in part, for any purpose without the express written consent of RPS. The reproduction or publication of any excerpts, other than in relation to the Admission Document, is not permitted without the express written permission of RPS.

List of Contributors

Matthew Horn, PhD – Project Lead and Senior Scientist

matt.horn@rpsgroup.com

Jeremy Fontenault – Modeler, senior GIS Specialist, report preparation

Lisa McStay – Modeler, report preparation, figure generation

Jenna Ducharme – GIS Specialist and figure generation

Alicia Morandi – Biologist and report preparation

Deborah Crowley – Hydrodynamics and report preparation

Richard Balouskus – Biologist and report preparation

Yong Kim – Hydrodynamics

Kathy Jayko – Modeler developer

Cheryl Morse – Model developer

Cathleen Turner – Chemist

Executive Summary

The Shell Puget Sound Refinery (PSR) proposes to construct and operate a rail unloading facility at the Shell PSR facility on March Point near Anacortes, Washington in Skagit County. The proposed project includes building a rail spur from the existing adjacent Anacortes Subdivision onto the Shell PSR property to accommodate unit trains transporting Bakken crude oil from the mid-continent area.

Oil spill trajectory, fate, and effects modeling and analyses were performed for the proposed project. The modeling was used to support evaluation of the ecological and human health risks resulting from hypothetical releases of crude oil into aquatic environments from the proposed unit trains traveling on BNSF railway lines to the Shell PSR.

Several criteria were used to select locations along the railway corridor including their proximity to the proposed facility, populated areas, and sensitive aquatic ecosystems; the general geographic and environmental conditions; and the presence of variable environmental conditions. For this assessment, three representative locations were modeled for hypothetical releases of oil: the Swinomish Channel Swing Bridge, the Skagit River Bridge Crossing, and the Edmonds Ferry Terminal.

The investigation included modeling the variability of targeted environmental conditions that could affect oil trajectory, fate, and potential effects including tides, river flow, and wind conditions. At the Swinomish Channel Swing Bridge, scenarios were modeled in the summer with spring tide flux conditions, and in the winter with neap tide flux conditions. The scenarios modeled at the Skagit River Bridge Crossing targeted high river flow (summer) and low river flow (winter) for seasonal conditions. Seasons considered at the Edmonds Ferry Terminal included the summer (low-wind speeds) and the winter (high-wind speeds). While the variability in certain environmental parameters was targeted for each scenario, it is important to note that seasonally appropriate corresponding values for all modeled environmental parameters (hydrodynamics, winds, temperature, concentration of total suspended solids, etc.) were characterized at each location based on the identified season. Therefore, seasonally appropriate hydrodynamics would include variability in general circulation, river flows, and tidal fluctuations. For each scenario, this would be coupled with the appropriate temperature, wind speed and direction, and other values for all of the other environmental parameters. Data inputs for the modeling efforts were obtained from independent sources with rigorous quality standards.

Two release volumes of a conditioned Bakken crude were modeled at each location, based on a 90th percentile discharge (90PD) of 20,000 barrels (bbl), and a 30th percentile discharge (30PD) of 5,700 bbl. It was assumed that both releases took 10 minutes for the full volume to enter the environment.

A combination of the two-dimensional overland and downstream trajectory and fate model, OILMAP Land™, and the three-dimensional in-water oil fate and biological impacts model, SIMAP™, were used to characterize the trajectory, fates, and potential biological impacts in the event of a release. Each scenario was simulated (tracked) for a total of 48 hours. All modeled releases were assumed to be unmitigated, meaning that no response efforts were undertaken (e.g., booming, burning, skimming, collection). In total, three locations, two environmental conditions, and two release volumes resulted in 12 individual deterministic trajectory and fates scenarios.

An overlay analysis was used to determine the potential impacts a release could have on identified resources located near the hypothetical release locations. The overlay assessment included a count of any identified resource features (points, lines, or polygons) that were intersected by the trajectory of the released oil. Identified resources included socioeconomic resources (e.g., parks, management areas, public access points, fishing areas), aquatic resources (e.g., shellfish locations, fish spawning areas, seal haulout points), and avian and terrestrial resources (e.g., bird colonies, nesting areas, wetlands, biodiversity corridors, and wildlife observations). In addition, biological impacts modeling was used to predict the equivalent areas of 100-percent mortality for each scenario for surface and shoreline impacts, as well as in-water impacts at two different sensitivity thresholds including 5 micrograms per liter (µg/L), which represented sensitive species, and 50 µg/L, which represented average sensitivity species.

The environmental impact statement (EIS) team collaborated with Skagit County and the Washington State Department of Ecology (co-lead agencies) to identify a modeling approach, select hypothetical release locations, identify seasonal conditions, and specify scenario-specific inputs. These criteria would be representative of locations along the route, address public concerns, and consider variable geographic and environmental factors. Site and scenario selection was finalized in collaboration with the co-lead agencies at an in-person meeting at the Washington State Department of Ecology State Government Office Building in Olympia, Washington on December 17, 2015.

The results of this analysis are provided for each modeled scenario. They include estimates of the weathering and fate of the oil for the entire model duration as a fraction of the oil spilled (mass balance information), as well as maps of the hydrocarbon trajectories, surface oil thickness, water column concentrations of dissolved aromatics components of the oil, and shoreline/sediment impacts. In general, the 90PD and 30PD scenarios at each of the release locations resulted in similar trajectory extents, as they experienced the same environmental forcing. The following conclusions can be drawn from the modeling performed.

At the Swinomish Channel Swing Bridge release location, the spring tide conditions in the summer season led to further transport, more extensive areal coverage, and more impacted resources when

compared with the neap tide in the winter. Hydrocarbon concentrations from the 90PD and 30PD scenarios in the summer (spring tide), on the water surface, or on the shorelines could cause mortality in roughly 24 to 27 square kilometers (km^2) for dabbling waterfowl, and 76 to 100 + km^2 for surface diving birds. Acute impacts were predicted for cetaceans and terrestrial life. Additionally, acute impacts were predicted for fish and shellfish. In the winter (neap tide), the hydrocarbon concentrations from the 90PD and 30PD scenarios on the water surface or on the shorelines could cause mortality in roughly 7 to 9 km^2 for dabbling waterfowl and 9 to 11 km^2 for surface diving birds. Small areas of mortality were predicted for cetaceans and terrestrial life. Additionally, limited acute impacts were predicted for fish and shellfish.

At the Skagit River Crossing release location, high flow river conditions in the summer resulted in further transport, and more extensive shoreline and surface oiling coverage. Those conditions resulted in larger numbers of impacted resources when compared with the low river flow present in the winter. Hydrocarbon concentrations, from the 90PD and 30PD scenarios in the summer (high flow), on the water surface or on the shorelines could cause mortality in roughly 16 to 35 km^2 for dabbling waterfowl and 51 to 914 + km^2 for surface diving birds. Limited acute impacts were predicted for cetaceans and terrestrial life. Additionally, limited acute impacts were predicted for fish and shellfish. In the winter (low river flow), the resulting hydrocarbon concentrations from the 90PD and 30PD scenarios on the water surface or on the shorelines had the potential to cause mortality to roughly 3 to 11 km^2 for dabbling waterfowl and 8 to 21 km^2 for surface diving birds. Small areas of mortality were predicted for cetaceans and terrestrial life. Additionally, limited acute impacts were predicted for fish and shellfish.

At the Edmonds Ferry Terminal release location, the high-wind speeds in the winter resulted in further transport, more extensive areal coverage, and larger numbers of impacted resources when compared with the low-wind speeds in the summer. Hydrocarbon concentrations from the 90PD and 30PD scenarios in the summer (high flow), on the water surface, or on the shorelines could cause mortality to roughly 4 km^2 for aerial seabirds and 69 to 74 km^2 for surface diving birds. Limited acute impacts were predicted for cetaceans and terrestrial life. Additionally, limited acute impacts were predicted for fish and shellfish. In the winter (low flow), the hydrocarbon concentrations from the 90PD and 30PD scenarios on the water surface or on the shorelines could cause mortality in roughly 1 to 3 km^2 for dabbling waterfowl and 17 to 28 km^2 for surface diving birds. Small areas of mortality were predicted for cetaceans and terrestrial life. Additionally, limited acute impacts were predicted for fish and shellfish.

Trajectory and fates results were used to demonstrate that although roughly 50 percent of the oil was predicted to evaporate within the 48-hour modeled period, extensive shoreline and surface oiling would be possible. Furthermore, under high-wind conditions, surface oil could be entrained into the water column. A portion of this entrained oil could dissolve into the water and result in sediment oiling.

In general, larger volumes (90PD compared with 30PD) of oil resulted in larger numbers of potentially affected resources and larger acute biological impacts. Environmental conditions that resulted in further transport of oil also resulted in larger numbers of potentially affected resources and greater impacts (i.e., acute mortality). Generally, the 90PD scenario led to larger numbers of potentially affected resources and more acute biological impacts.

A crude-by-rail derailment that results in a loss of containment and the release of oil into the environment is a rare occurrence. Compounded with the likelihood that a response would be organized in a short amount of time, an unmitigated release scenario would be even more unlikely. While it is understood that the identified scenarios are in no way intended to predict a specific future event, the results presented in this document demonstrate that there is a range of potential trajectory and fates and predictable impacts that may result from geographic factors, environmental variability, or biological sensitivities. In the unlikely event that a derailment and loss of containment of the magnitude modeled here were to occur and enter a waterway, the resulting impacts would have the potential to be both significant and adverse.

Table of Contents

Executive Summary 4
Table of Contents i
List of Figures iv
List of Tables x
1 Introduction 1
2 Hypothetical Release Locations and Scenarios 3
2.1 Swinomish Channel Swing Bridge 5
2.2 Skagit River Crossing 7
2.3 Edmonds Ferry Terminal 8
2.4 Release Scenarios 11
2.4.1 Identification of Timeframes for Scenarios 11
2.4.2 Seasonal Conditions for Each Modeled Scenario 19
3 Model Descriptions 26
3.1 SIMAP Physical Fates Model 27
3.1.1 Modeled SIMAP Oil Fate Processes 29
3.1.2 Summary of Spill Dynamics 32
3.1.3 SIMAP Model Oil Fates Algorithms 34
3.1.3.1 Transport 34
3.1.3.2 Shoreline Stranding 35
3.1.3.3 Spreading 35
3.1.3.4 Evaporation 36
3.1.3.5 Entrainment 36
3.1.3.6 Emulsification (Mousse Formation) 38
3.1.3.7 Dissolution 38
3.1.3.8 Volatilization from the Water column 38
3.1.3.9 Adsorption and Sedimentation 39
3.1.3.10 Degradation 39

SIMAP Model Physical Fates Output Description 40
3.2 SIMAP Biological Impacts Model for Evaluating Acute Toxic Impacts 40
Aquatic Biota 41
3.1.4 Oil Toxicity 42
Wildlife 46
3.2.1 SIMAP Model Biological Output Description 48
3.2.2
3.3 OILMAP Land Overland Flow Modeling 49
3.2.3
3.2.4 OILMAP Land Model Description 49
3.3.1.1 Overland Release Model 50
3.3.1 3.3.1.2 Surface Water Transport Model 53
3.3.1.3 Evaporation 55
OILMAP Land Model Output Description 55
3.3.2 3.4 Model Uncertainty and Validation 56
4 Model Input Data 58
4.1 SIMAP Model Input Data 58
4.1.1 Geographic and Habitat Data 58
4.1.2 4.1.1.1 Shoreline Oil Retention 64
Environmental Data 65
4.1.2.1 Wind 65
4.1.2.2 Water Temperature and Salinity 73
4.1.3 4.1.2.3 Suspended Particulate Matter 73
4.1.2.4 Horizontal and Vertical Dispersion 74
4.2.1 Hydrodynamic Data 74
4.2.2
4.2 OILMAP Land Model Inputs 75
4.2.3
Elevation 75
Storm Water Drainage System 76
Land Cover 78
4.3 Oil Properties and Acute Toxicity 79
5 Model Application 82

6 Trajectory and Fate Analysis 83
6.1 Trajectory and Fate Results 83
6.2 Swinomish Channel Swing Bridge 84
6.2.1 Swinomish Channel Swing Bridge – Summer (Spring Tide Flux) 86
6.2.2 Swinomish Channel Swing Bridge – Winter (Neap Tide Flux) 91
6.3 Skagit River Crossing 96
6.3.1 Skagit River Crossing – Summer (High Flow) 98
6.3.2 Skagit River Crossing – Winter (Low Flow) 103
6.4 Edmonds Ferry Terminal 108
6.4.1 Edmonds Ferry Terminal – Summer (Low-Wind Speeds) 111
6.4.2 Edmonds Ferry Terminal – Winter (High-Wind Speeds) 116
7 Potential Impacts Model Results 121
7.1 Overlay and Biological Impacts Analyses 121
7.2 Swinomish Channel Swing Bridge 123
7.2.1 Overlay Analysis for Swinomish Channel Swing Bridge 123
7.2.2 Biological Impacts for Swinomish Channel Swing Bridge 126
7.3 Skagit River Crossing 131
7.3.1 Overlay Analysis for Skagit River Crossing 131
7.3.2 Biological Impacts for Skagit River Crossing 135
7.4 Edmonds Ferry Terminal 140
7.4.1 Overlay Analysis for Edmonds Ferry Terminal 140
7.4.2 Biological Impacts for Edmonds Ferry Terminal 144
8 Discussion and Conclusions 150
9 References 155
10 Appendix A: Overlay Analysis Resource Figures 166

List of Figures

Figure 2-1: Map of the study area, including the three hypothetical release locations. Dotted lines represent the northern and southern modeling extents used for habitat grid development. The tide current proxy site was used for qualitative discussions of the level of the tide below. 4

Figure 2-2: Map of the hypothetical release location at the Swinomish Channel Swing Bridge and surrounding area. 6

Figure 2-3: Map of the Skagit River Crossing hypothetical release location and surrounding area. 8

Figure 2-4: Map of the Edmonds Ferry Terminal hypothetical release location and surrounding area. ... 10

Figure 2-5: Illustration of current speed at the tidal current proxy site for 2008. The hourly current data is plotted in blue. The solid pink (start) to dashed pink (end) lines represent the summer season, while the solid red (start) to dashed red (end) lines represent the winter season. 14

Figure 2-6: Hourly current speeds over 16-day periods (blue) at the tidal current proxy site for summer spring tide (top) and winter neap tide (bottom). The dashed lines bound the 48-hour simulation timeframe used in modeling. 15

Figure 2-7: Hourly current speed (blue) over 2008 at the Skagit River Crossing, along with the 48-hour running average (green). The solid pink and red lines delineate the summer season start and winter season start, respectively. The dashed pink lines bound the 48-hour simulation timeframes for the summer high flow scenarios, while the red lines bound the winter low flow timeframes. 17

Figure 2-8: Wind speed (blue) over 2008 at the Edmonds Ferry Terminal at 6-hour intervals. The 48-hour running average is overlaid in green. The solid pink and red lines delineate the summer season start and winter season start, respectively. The dashed pink lines bound the 48-hour simulation timeframes for the summer low-wind speed scenarios, while the red lines bound the winter high-wind speed timeframes. 18

Figure 2-9: Winds and currents during the summer – spring tide simulation at the Swinomish Channel Swing Bridge. The upper panel illustrates the wind speed with color-contoured arrows and the arrow position reflects the direction the wind was headed. The bottom panel illustrates the current speed at the release location as well as at the tidal current proxy site. The dashed black lines indicate the start and end of the model simulation. 20

Figure 2-10: Winds and currents during the winter – neap tide simulation at the Swinomish Channel Swing Bridge. The upper panel illustrates the wind speed with color-contoured arrows and the arrow position reflects the direction the wind was headed. The bottom panel illustrates the current speed at the release location as well as at the tidal current proxy site. The dashed black lines indicate the start and end of the model simulation. 21

Figure 2-11: Winds and currents during the summer – high river flow simulation at the Skagit River Crossing. The upper panel illustrates the wind speed with color-contoured arrows and the arrow position reflects the direction the wind was headed. The bottom panel illustrates the current speed at the release location as well as at the tidal current proxy site. The dashed black lines indicate the start and end of the model simulation. 22

Figure 2-12: Winds and currents during the winter – low river flow simulation at the Skagit River Crossing. The upper panel illustrates the wind speed with color-contoured arrows and the arrow position reflects the direction the wind was headed. The bottom panel illustrates the current speed at the release location as well as at the tidal current proxy site. The dashed black lines indicate the start and end of the model simulation. 23

Figure 2-13: Winds and currents at during the summer – low-wind simulation at the Edmonds Ferry Terminal. The upper panel illustrates the wind speed with color-contoured arrows and the arrow position reflects the direction the wind was headed. The bottom panel illustrates the current speed at the release location as well as at the tidal current proxy site. The dashed black lines indicate the start and end of the model simulation. 24

Figure 2-14: Winds and currents during the winter – high-wind simulation at the Edmonds Ferry Terminal. The upper panel illustrates the wind speed with color-contoured arrows and the arrow position reflects the direction the wind was headed. The bottom panel illustrates the current speed at the release location as well as at the tidal current proxy site. The dashed black lines indicate the start and end of the model simulation. 25

Figure 3-1: Simulated oil fates processes in lakes and rivers. 30

Figure 3-2: Illustration of percent mortality as a function of concentration (left). The LC50 is at the center of the log-normal function, aligning with 50-percent mortality. The LC50 of dissolved oil PAH mixtures as a function of exposure duration and temperature (right). 42

Figure 3-3: Diagram showing how the OILMAP Land™ model searches the eight neighboring cells to determine the steepest downslope gradient and resulting direction of flow. 50

Figure 3-4: Conceptual diagram of the land transport model depicting the possible fate of oil as it moves over the land surface. 52

Figure 3-5: Conceptual diagram of the downstream transport model depicting the possible fate of oil entering the surface water network. 54

Figure 4-1: Bathymetry grid (water depth in meters) near Swinomish Channel (purple star) and Skagit River (orange star) hypothetical release locations. 60

Figure 4-2: Habitat grid for Swinomish Channel Swing Bridge (purple star) hypothetical release locations. 60

Figure 4-3: Bathymetry grid (water depth in meters) for the Skagit River Crossing (orange star) hypothetical release location. 61

Figure 4-4: Habitat grid for Skagit River Crossing (orange star) and Swinomish Channel Swing Bridge (purple star) hypothetical release locations. 61

Figure 4-5: Bathymetry grid (water depth in meters) near Edmonds Ferry Terminal (red star) hypothetical release location. 62

Figure 4-6: Habitat grid for Edmonds Ferry Terminal (red star) hypothetical release location (red star). 62

Figure 4-7: Annual wind rose (A) and monthly average wind speeds (B) for the Swinomish Channel Swing Bridge hypothetical release location. 67

Figure 4-8: Seasonal wind rose plots (winter, summer, high flow, low flow) for Swinomish Channel Swing Bridge hypothetical release location. 68

Figure 4-9: Annual wind rose (A) and monthly average wind speeds (B) for the Skagit River Crossing hypothetical release location. 69

Figure 4-10: Seasonal wind rose plots (winter, summer, high flow, low flow) for the Skagit River Crossing hypothetical release location. 70

Figure 4-11: Annual wind rose (A) and monthly average wind speeds (B) for the Edmonds Ferry Terminal hypothetical release location. 71

Figure 4-12: Seasonal wind rose plots (winter, summer, high flow, low flow) for the Edmonds Ferry Terminal hypothetical release location. 72

Figure 4-13: Elevation data and storm water drainage system for Edmonds Ferry Terminal. The tank car release locations for the eight-car 30PD release (top) and 28-car 90PD release (bottom) are shown. 77

Figure 6-1: Oil mass balance graphs for the 90PD (top) and 30PD (bottom) at the Swinomish Channel Swing Bridge release location during the summer (spring tide) season. Entrained and decayed oil make up approximately 1 percent of the total mass or less. 86

Figure 6-2: Oil trajectories for 90PD (top) and 30PD (bottom) at the Swinomish Channel Swing Bridge release location during the summer (spring tide) season. 87

Figure 6-3: Maximum cumulative surface oil thickness for 90PD (top) and 30PD (bottom) scenarios at the Swinomish Channel Swing Bridge release location during the summer (spring tide) season. 88

Figure 6-4: Cumulative total dissolved aromatic concentration for 90PD (top) and 30PD (bottom) scenarios at the Swinomish Channel Swing Bridge release location during the summer (spring tide) season. 89

Figure 6-5: Total hydrocarbon mass on the shore and on sediments for 90PD (top) and 30PD (bottom) scenarios at the Swinomish Channel Swing Bridge release location during the summer (spring tide) season. 90

Figure 6-6: Oil mass balance graphs for the 90PD (top) and 30PD (bottom) at the Swinomish Channel Swing Bridge release location during the winter (neap tide) season. Entrained and decayed oil make up approximately 1 percent of the total mass or less. 91

Figure 6-7: Oil trajectories for 90PD (top) and 30PD (bottom) at the Swinomish Channel Swing Bridge release location during the winter (neap tide) season. 92

Figure 6-8: Maximum cumulative surface oil thickness for 90PD (top) and 30PD (bottom) scenarios at the Swinomish Channel Swing Bridge release location during the winter (neap tide) season. 93

Figure 6-9: Cumulative total dissolved aromatic concentration for 90PD (top) and 30PD (bottom) scenarios at the Swinomish Channel Swing Bridge release location during the winter (neap tide) season. 94

Figure 6-10: Total hydrocarbon mass on the shore and sediments for 90PD (top) and 30PD (bottom) scenarios at the Swinomish Channel Swing Bridge release location during the winter (neap tide) season. 95

Figure 6-11: Oil mass balance graphs for the 90PD (top) and 30PD (bottom) at the Skagit River Crossing release location during the summer (high flow) season. Entrained and decayed oil make up approximately 1 percent of the total mass or less. 98

Figure 6-12: Oil trajectories for 90PD (top) and 30PD (bottom) at the Skagit River Crossing release location during the summer (high flow) season. 99

Figure 6-13: Maximum cumulative surface oil thickness for 90PD (top) and 30PD (bottom) scenarios at the Skagit River Crossing release location during the summer (high flow) season. 100

Figure 6-14: Cumulative total dissolved aromatic concentration for 90PD (top) and 30PD (bottom) scenarios at the Skagit River Crossing release location during the summer (high flow) season. 101

Figure 6-15: Total hydrocarbon mass on the shore and on sediments for 90PD (top) and 30PD (bottom) scenarios at the Skagit River Crossing release location during the summer (high flow) season. 102

Figure 6-16: Oil mass balance graphs for the 90PD (top) and 30PD (bottom) at the Skagit River Crossing release location during the winter (low flow) season. Entrained and decayed oil make up approximately 1 percent of the total mass or less. 103

Figure 6-17: Oil trajectories for 90PD (top) and 30PD (bottom) at the Skagit River Crossing release location during the winter (low flow) season. 104

Figure 6-18: Maximum cumulative surface oil thickness for 90PD (top) and 30PD (bottom) scenarios at the Skagit River Crossing release location during the winter (low flow) season. 105

Figure 6-19: Cumulative total dissolved aromatic concentration for 90PD (top) and 30PD (bottom) scenarios at the Skagit River Crossing release location during the winter (low flow) season. 106

Figure 6-20: Total hydrocarbon mass on the shore and on sediments for 90PD (top) and 30PD (bottom) scenarios at the Skagit River Crossing release location during the winter (low flow) season. 107

Figure 6-21: Overland flow of oil downslope and through the storm water drainage system for Edmonds Ferry Terminal. The tank car release locations (orange circles) for the eight-car 30PD release (top) and 28-car 90PD release (bottom) depict three distinct water entry points. 109

Figure 6-22: Oil mass balance graphs for the 90PD (top) and 30PD (bottom) at the Edmonds Ferry Terminal release location during the summer (low wind) season. Entrained and decayed oil make up approximately 1 percent of the total mass or less. 111

Figure 6-23: Oil trajectories for 90PD (top) and 30PD (bottom) at the Edmonds Ferry Terminal release location during the summer (low wind) season. 112

Figure 6-24: Maximum cumulative surface oil thickness for 90PD (top) and 30PD (bottom) scenarios at the Edmonds Ferry Terminal release location during the summer (low wind) season. 113

Figure 6-25: Cumulative total dissolved aromatic concentrations for 90PD (top) and 30PD (bottom) scenarios at the Edmonds Ferry Terminal release location during the summer (low wind) season. 114

Figure 6-26: Total hydrocarbon mass on the shore and on sediments for 90PD (top) and 30PD (bottom) scenarios at the Edmonds Ferry Terminal release location during the summer (low wind) season. 115

Figure 6-27: Oil mass balance graphs for the 90PD (top) and 30PD (bottom) at the Edmonds Ferry Terminal release location during the winter (high wind) season. 116

Figure 6-28: Oil trajectories for 90PD (top) and 30PD (bottom) at the Edmonds Ferry Terminal release location during the winter (high wind) season. 117

Figure 6-29: Maximum cumulative surface oil thickness for 90PD (top) and 30PD (bottom) scenarios at the Edmonds Ferry Terminal release location during the winter (high wind) season..... 118

Figure 6-30: Cumulative total dissolved aromatic concentration for 90PD (top) and 30PD (bottom) scenarios at the Edmonds Ferry Terminal release location during the winter (high wind) season. 119

Figure 6-31: Total hydrocarbon mass on the shore and on sediments for 90PD (top) and 30PD (bottom) scenarios at the Edmonds Ferry Terminal release location during the winter (high wind) season. 120

List of Tables

Table 2-1: Hypothetical release locations and targeted seasonal conditions varied in each scenario. 3

Table 2-2: Hypothetical release locations and environmental conditions varied in each scenario. 11

Table 2-3: Summary of identified model timeframes based on current data 19

Table 3-1: Definition of four distillation cuts and the eight pseudo-components in the model (monoaromatic hydrocarbons, MAHs; benzene + toluene + ethybenzene + xylene, BTEX; polycyclic aromatic hydrocarbons, PAHs). 29

Table 4-1: Basemap and habitat mapping data sources used for the study area. 58

Table 4-2: Classification of habitat types in SIMAP. Seaward (Sw) and landward (Lw) system codes are listed. Fringing types (indicated by 'F') are only as wide as the intertidal zone or shoreline width where oiling might occur. Other types (indicated by 'W' for 'water') are a full grid-cell wide and have a fringing type on the landward side.) 63

Table 4-3: Maximum oil thickness for various shore types as a function of oil viscosity, measured in centistokes (cSt). 64

Table 4-4: Water temperature (˚C) and salinity (psu) for each release location and seasonal condition.. 73

Table 4-5: Suspended sediment concentrations (SPM) modeled at each release location and seasonal condition. 74

Table 4-6: Mapping used to convert the NLCD 2011 land cover categories to OILMAP Land™ classification scheme. 78

Table 4-7: Oil parameters for the spilled conditioned Bakken crude oil. 79

Table 4-8: Aromatic (AR), aliphatic (AL), and total hydrocarbon concentration (THC) and percentage composition of fresh whole oil for conditioned Bakken crude. THC is the sum of AR and AL. (Numbers of carbons in the included compounds are listed, e.g., >C8-C10 indicates greater than 8 carbons and including 9- and 10-carbon hydrocarbons.) 80

Table 6-1: Summary of the mass balance information at the Swinomish Channel Swing Bridge release location at the end of the 48-hour simulation. All values represent a percentage of the total spilled oil. 84

Table 6-2: Summary of the mass balance information at the Skagit River Crossing release location at the end of the 48-hour simulation. All values represent a percentage of the total spilled oil. 96

Table 6-3: Summary of the mass balance information at the Edmonds Ferry Terminal release location at the end of the 48-hour simulation. All values represent a percentage of the total spilled oil. 108

Table 7-1: Geographic data layers used for the overlay analysis. 121

Table 7-2: Overlay analysis for Swinomish Channel Swing Bridge summer (spring tide) and winter (neap tide) 30PD and 90PD scenarios. Numbers indicate the counts of public access and socioeconomic resource areas potentially affected by oil. 124

Table 7-3: Overlay analysis for Swinomish Channel Swing Bridge summer (spring tide) and winter (neap tide) 30PD and 90PD scenarios. Numbers indicate the counts of aquatic resources and sensitive areas potentially affected by oil. 125

Table 7-4: Overlay analysis for Swinomish Channel Swing Bridge summer (spring tide) and winter (neap tide) 30PD and 90PD scenarios. Numbers indicate the counts of avian and terrestrial resources and sensitive areas potentially affected by oil. 126

Table 7-5: Equivalent area (km^2) of up to 100-percent-predicted mortality for behavior groups of wildlife, fish, and invertebrates by threshold for the Swinomish Channel Swing Bridge summer (spring tide) 90PD release. Values are the equivalent area of 100-percent mortality for species of high and medium sensitivity to dissolved PAHs from the representative spill. 127

Table 7-6: Equivalent area (km^2) of up to 100-percent-predicted mortality for various behavior groups of wildlife, fish, and invertebrates by threshold for the Swinomish Channel Swing Bridge summer (spring tide) 30PD release. Values are the equivalent area of 100-percent mortality for species of high and medium sensitivity to dissolved PAHs from a representative spill. 128

Table 7-7: Equivalent area (km^2) of up to 100-percent-predicted mortality for various behavior groups of wildlife, fish, and invertebrates by threshold for the Swinomish Channel Swing Bridge winter (neap tide) 90PD release. Values are the equivalent area of 100-percent mortality for species of high and medium sensitivity to dissolved PAHs from a representative spill. .. 129

Table 7-8: Equivalent area (km^2) of up to 100-percent-predicted mortality for various behavior groups of wildlife, fish, and invertebrates by threshold for the Swinomish Channel Swing Bridge winter (neap tide) 30PD release. Values are the equivalent area of 100-percent mortality for species of high and medium sensitivity to dissolved PAHs from a representative spill. .. 130

Table 7-9: Overlay analysis for Skagit River Crossing summer (high flow) and winter (low flow) 30PD and 90PD scenarios. Numbers indicate the counts of public access and socioeconomic resource areas potentially affected by oil. 133

Table 7-10: Overlay analysis for Skagit River Crossing summer (high flow) and winter (low flow) 30PD and 90PD scenarios. Numbers indicate the counts of aquatic resources and sensitive areas potentially affected by oil. 134

Table 7-11: Overlay analysis for Skagit River Crossing summer (high flow) and winter (low flow) 30PD and 90PD scenarios. Numbers indicate the counts of avian and terrestrial resources and sensitive areas potentially affected by oil. 135

Table 7-12: Equivalent area (km^2) of up to 100-percent-predicted mortality for various behavior groups of wildlife, fish, and invertebrates by threshold for the Skagit River Crossing high river flow (June) 90PD release. Values are the equivalent area of 100-percent mortality for species of high and medium sensitivity to dissolved PAHs from a representative spill. 136

Table 7-13: Equivalent area (km^2) of up to 100-percent-predicted mortality for various behavior groups of wildlife, fish, and invertebrates by threshold for the Skagit River Crossing high river flow (June) 30PD release. Values are the equivalent area of 100-percent mortality for species of high and medium sensitivity to dissolved PAHs from a representative spill. 137

Table 7-14: Equivalent area (km^2) of up to 100-percent-predicted mortality for various behavior groups of wildlife, fish, and invertebrates by threshold for the Skagit River Crossing low river flow (December) 90PD release. Values are the equivalent area of 100-percent mortality for species of high and medium sensitivity to dissolved PAHs from a representative spill. 138

Table 7-15: Equivalent area (km^2) of up to 100-percent-predicted mortality for various behavior groups of wildlife, fish, and invertebrates by threshold for the Skagit River Crossing low river flow (December) 30PD release. Values are the equivalent area of 100-percent mortality for species of high and medium sensitivity to dissolved PAHs from a representative spill. 139

Table 7-16: Overlay analysis for the Edmonds Ferry Terminal summer (low wind) and winter (high wind) 30PD and 90PD scenarios. Numbers indicate the counts of public access and socioeconomic resource areas potentially affected by oil. 142

Table 7-17: Overlay analysis for the Edmonds Ferry Terminal summer (low wind) and winter (high wind) 30PD and 90PD scenarios. Numbers indicate the counts of aquatic resources and sensitive areas potentially affected by oil. 143

Table 7-18: Overlay analysis for the Edmonds Ferry Terminal summer (low wind) and winter (high wind) 30PD and 90PD scenarios. Numbers indicate the counts of avian and terrestrial resources and sensitive areas potentially affected by oil. 144

Table 7-19: Equivalent area (km^2) of up to 100-percent-predicted mortality for various behavior groups of wildlife, fish, and invertebrates by threshold for the Edmonds Ferry Terminal summer low-wind (August) 90PD release. Values are the equivalent area of 100-mortality for species of high and medium sensitivity to dissolved PAHs from a representative spill. .. 145

Table 7-20: Equivalent area (km^2) of up to 100-percent predicted mortality for various behavior groups of wildlife, fish, and invertebrates by threshold for the Edmonds Ferry Terminal summer low-wind (August) 30PD release. Values are the equivalent area of 100-percent mortality for species of high and medium sensitivity to dissolved PAHs from a representative spill. 146

Table 7-21: Equivalent area (km^2) of up to 100-percent-predicted mortality for various behavior groups of wildlife, fish, and invertebrates by threshold for the Edmonds Ferry Terminal winter high-wind (January) 90PD release. Values are the equivalent area of 100-percent mortality for species of high and medium sensitivity to dissolved PAHs from a representative spill. 147

Table 7-22: Equivalent area (km^2) of up to 100-percent-predicted mortality for various behavior groups of wildlife, fish, and invertebrates by threshold for the Edmonds Ferry Terminal winter high-wind (January) 30PD release. Values are the equivalent area of 100-percent mortality for species of high and medium sensitivity to dissolved PAHs from a representative spill. 148

1 Introduction

RPS ASA has provided modeling and data analysis services to HDR, Inc. as part of the Environmental Impact Statement (EIS) for the proposed Shell Puget Sound Refinery (PSR) rail unloading facility at March Point, near Anacortes, Washington in Skagit County. This work serves as Part Two of a three-part environmental assessment that includes contributions from Environmental Research Consulting for a probability analysis, RPS ASA for an oil spill release consequence analysis, and Risknology, Inc. for a fire and explosion risk analysis.

The three portions of the EIS include:

1. *Probability Analysis:* A risk assessment to predict the probability of hydrocarbon releases along the rail corridor (conducted by ERC)
2. *Oil Spill Release Consequence Analysis:* A trajectory, fate, and effects assessment to predict where the spilled hydrocarbons may move in the environment and how they may impact resources within the environment (conducted by RPS ASA and reported herein)
3. *Fire and Explosion Risk Analysis:* A fire and explosion assessment to predict the probability of occurrence and impacts of a fire or explosion associated with the release of combustible fluids from the rail corridor (conducted by Risknology)

At the proposed Shell PSR rail unloading facility, crude oil would be received on unit trains (four locomotives and 102 tank cars) arriving daily, with a maximum of six unit trains per week. It is expected that a maximum of 612 fully loaded tank cars would arrive at the facility, would be unloaded, and that all 612 empty tank cars would leave the facility each week. A single tank car contains between 680 to 720 barrels of crude oil, depending on the density of the product. Therefore, each unit train would be carrying approximately 66,300 to 68,901 barrels of oil per trip, for a total of 397,800 to 413,406 barrels of oil entering the facility each week. This assessment focuses on Washington State, where oil is transported along the railway corridor from the Idaho-Washington border, into Washington State to the west, along the Columbia River, and then north along the coastline of Puget Sound, before reaching the facility at Anacortes.

For this assessment, hypothetical crude oil releases were modeled from multiple locations along the proposed railway corridor using a combination of the OILMAP Land™ and SIMAP™ modeling systems. OILMAP Land™ is a two-dimensional overland and downstream trajectory and fate model. SIMAP™ is a three-dimensional, in-water oil trajectory, fate, and biological impacts model used to assess acute impacts and provide data to estimate ecological and socioeconomic impacts of spills in marine and freshwater environments. Unmitigated releases were simulated at three representative spill sites along

the rail corridor using a range of site-specific environmental conditions over multiple seasons. The risk assessment approach taken for this EIS consisted of quantitative trajectory and fate modeling, a quantitative biological impacts assessment, and a semi-quantitative analysis of potentially affected resources.

This work has been jointly overseen by the co-lead agencies, which include the Skagit County Planning and Development Services and the Washington State Department of Ecology. HDR, Inc. is conducting the EIS process.

This report describes in detail the release scenario simulations performed (Section 2); the approach used to simulate the releases and analyze their impacts using the OILMAP Land™ and SIMAP™ models (Section 3); the input datasets obtained and methods used in the modeling (Section 4); the model settings and parameters used (Section 5); the trajectory and fate results of the oil spill modeling (Section 6); and the results of the overlay and biological impacts analyses (Section 7).

2 Hypothetical Release Locations and Scenarios

Three sites along the rail corridor were selected as representative locations to model hypothetical releases of crude oil. Several criteria were used to select these locations including their proximity to the proposed facility, populated areas, and sensitive aquatic ecosystems; the general geographic and environmental conditions; and the presence of variable environmental conditions, including river flow rates and tide fluxes. The EIS team collaborated with the co-lead agencies to select sites, seasonal conditions, and specific scenarios that would be representative of locations along the route, address public concerns, and consider variable geographic and environmental factors. Site and scenario selection was finalized in collaboration with the co-lead agencies at an in-person meeting at the Washington State Department of Ecology State Government Office Building in Olympia, Washington on December 17, 2015. The three sites that were selected for this analysis include (Figure 2-1):

- Swinomish Channel Swing Bridge
- Skagit River Crossing
- Edmonds Ferry Terminal

A total of 12 scenarios were modeled for this assessment, including the three release locations, two seasonal environmental conditions, and two release volumes (3 locations x 2 seasons x 2 volumes = 12 fates scenarios). Table 2-1 provides the coordinates of each release location along with the targeted seasonal conditions that were modeled for each scenario. The site-specific and detailed conditions used for modeling at each location are provided in Section 2.4.2.

Table 2-1: Hypothetical release locations and targeted seasonal conditions varied in each scenario.

Site Name	Latitude	Longitude	Seasonal Scenario 1	Seasonal Scenario 2
Swinomish Channel Swing Bridge	48.458°	122.515°	Summer – July (spring tide flux)	Winter – March (neap tide flux)
Skagit River Crossing	48.445°	122.325°	Summer – June (high river flow)	Winter - December (low river flow)
Edmonds Ferry Terminal	47.813°	-122.383°	Summer – August (lowest wind speed)	Winter – January (highest wind speed)

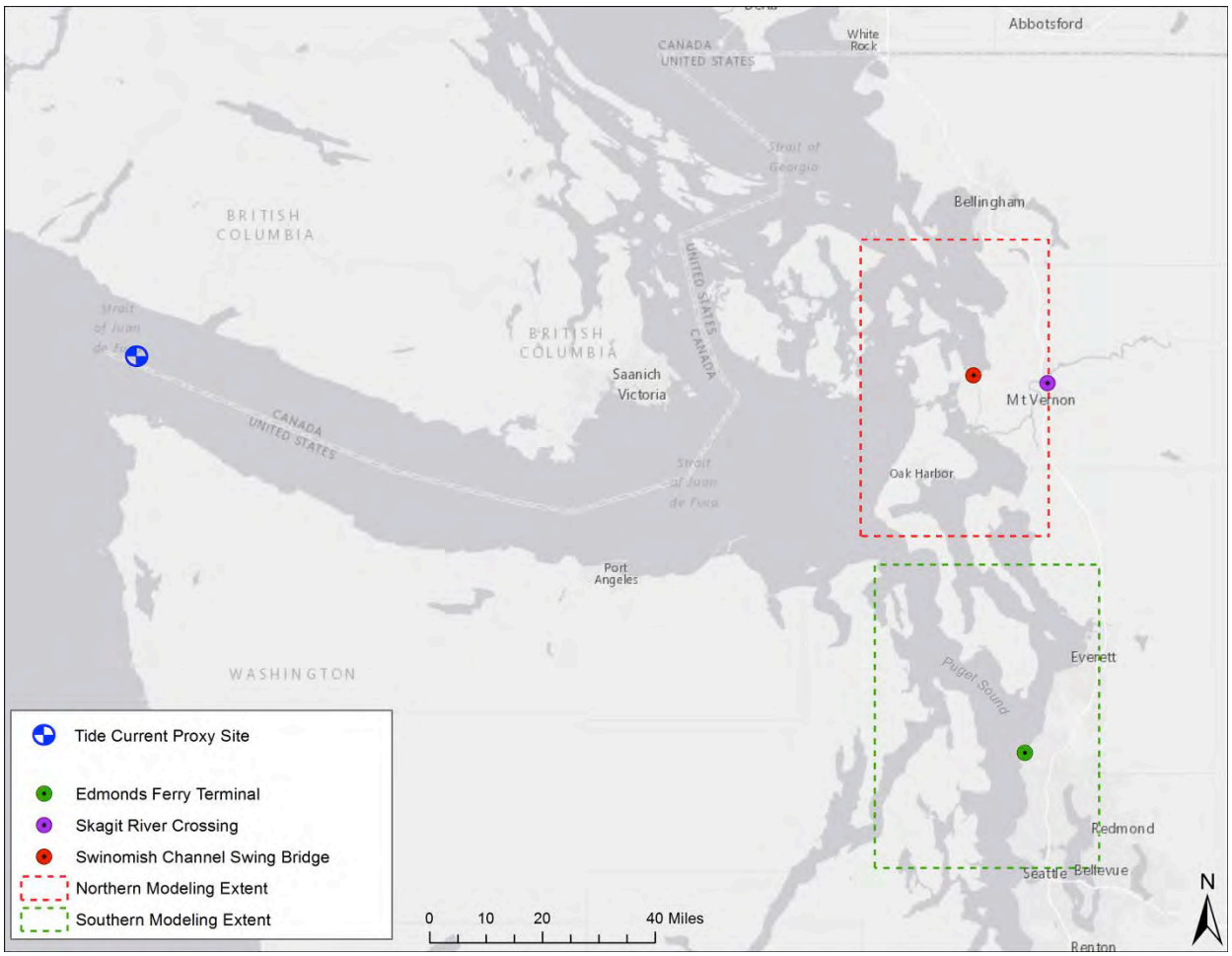

Figure 2-1: Map of the study area, including the three hypothetical release locations. Dotted lines represent the northern and southern modeling extents used for habitat grid development. The tide current proxy site was used for qualitative discussions of the level of the tide below.

The two release volumes modeled were highly conservative, erring on the side of larger release volumes than are typically observed in releases to date. The 90th percentile discharge (90PD) scenarios represent a derailment and complete release of 28 tank cars for a total of 20,000 barrels of oil. This volume is twice that of the largest oil release from a train in U.S. history (Etkin 2016). The 30th percentile discharge (30PD) scenarios represent a complete release of eight tank cars for a total of 5,700 barrels of oil. This volume is consistent with the average number of rail cars typically involved in a derailment, but with the highly conservative assumption that all of the derailed cars would rupture. Typically, less than 20 percent of derailed rail cars release their contents (Etkin 2016). For this modeling exercise, a release duration of 10 minutes was applied, implying that the entire volume of crude oil from each ruptured

tank car would be released into the environment over the course of 10 minutes. The crude oil was then tracked within the environment for a total of 48 hours.

In addition to the 12 oil fates scenarios, two acute toxicity endpoints were investigated at each site/scenario combination to capture multiple biological sensitivity thresholds within an ecosystem. Highly sensitive species had a 5 micrograms per liter (µg/L) endpoint, representing the 2.5th percentile, which would be protective of 97.5 percent of species or life stages in the aquatic environments of concern. Average sensitivity species had a 50 µg/L endpoint, representing the 50th percentile. A total of 24 biological scenarios were modeled (12 oil fates scenarios x 2 biological sensitivities).

2.1 Swinomish Channel Swing Bridge

The Swinomish Channel is an 18-kilometer-long, partially-dredged saltwater channel that connects Padilla Bay to Skagit Bay in Skagit County, Washington. The channel runs in a north-south direction, parallel to the Swinomish Reservation. The railway swing bridge is located near the northern end of the channel, just north of Memorial Highway (State Route [SR] 20) and east of Whitmarsh Junction. This site was chosen as a representative location for releases into relatively confined saltwater environments with extensive tidal flats and marshy areas. The location is a region of concern, as it is adjacent to the Swinomish Reservation and is in an area with sensitive aquatic receptors such as migratory bird populations and crabs that are harvested for human consumption.

For the hypothetical releases at the Swinomish Channel Swing Bridge, it was assumed that 100 percent of the total volume of oil from the tank cars spilled directly into the waterway (Figure 2-2). The winter season scenario for this site (March) was based on the presence of heron and migratory bird populations (WA DOE 2015) and represented the lowest tide flux (neap tide) in the region. Low tides would minimize the potential extent of trajectories and lead to maximum surface oiling thicknesses in the model and higher potential impacts on birds. The summer season scenario (July) was based on peak crab harvest times in the area (WA DOE 2015) and represented the highest tide flux (spring tide) in the region. High tides would maximize the transport of oil and lead to larger potential areas of water column contamination from dissolved aromatics and entrained oil.

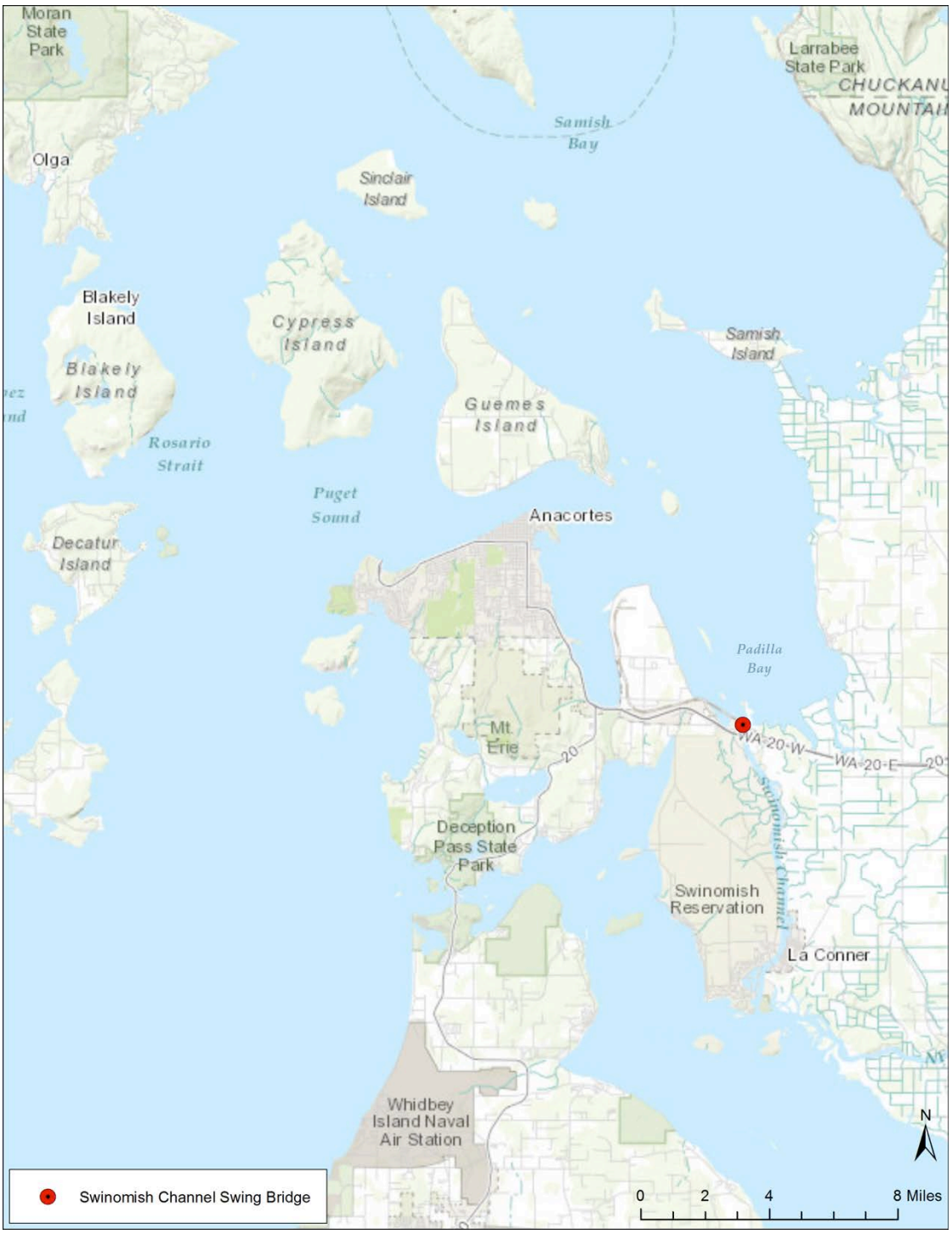

Figure 2-2: Map of the hypothetical release location at the Swinomish Channel Swing Bridge and surrounding area.

2.2 Skagit River Crossing

The Skagit River is a 240-kilometer waterbody that runs through southwestern British Columbia, Canada and northwestern Washington State, and empties into Puget Sound. The Skagit River Crossing occurs east of I-5 and Riverside Drive, connecting the cities of Burlington and Mount Vernon. About 13 km south of the hypothetical release location, the river splits around Fir Island and two branches enter Skagit Bay via a network of channels flowing into intertidal mud flats. The release location is approximately 23.8 km or 24.7 km upstream along the South Fork Skagit River and the North Fork Skagit River, respectively. This site was chosen as a representative location for releases into a freshwater environment with a high potential for extensive oiling of shorelines before entering Skagit Bay. The site also has the potential for oil to sink due to oil interactions with suspended particulate matter (SPM). The location is a region of concern, as there is a municipal drinking water intake in the river downstream of the hypothetical release location. The Skagit River is also the only large river system in Washington that provides spawning habitat for all five native salmon species and two trout species. It also supports one of the largest wintering bald eagle populations in the U.S. (NPS 2016).

For the hypothetical releases at the Skagit River Crossing, it was assumed that 100 percent of the total volume of oil from the tank cars spilled directly into the waterway (Figure 2-3). The winter season scenario for this site (December) was selected as it corresponded with the lowest river flow and represented the shortest potential downstream trajectory of spilled oil over the model run. The summer season scenario (June) was selected at the time of highest river flow (spring snow melt) and captured the farthest potential downstream trajectory, when the largest volume of water was moving through the river channel at higher velocity.

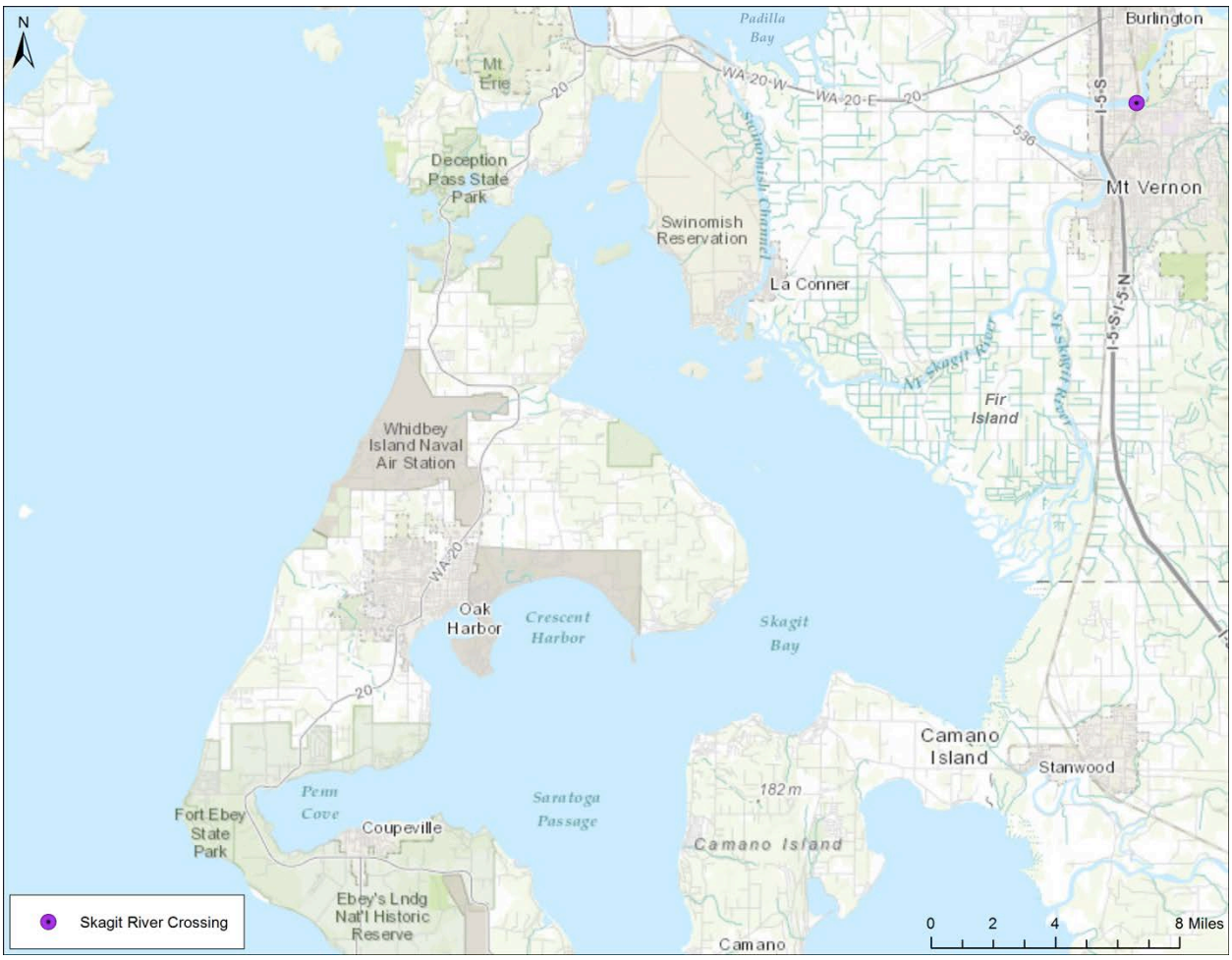

Figure 2-3: Map of the Skagit River Crossing hypothetical release location and surrounding area.

2.3 Edmonds Ferry Terminal

The Edmonds Ferry Terminal is located 18 kilometers north of Seattle, Washington on the eastern shore of the Central/Main Basin of Puget Sound. The railroad track passes through Edmonds and follows the coast for over 50 km from Shilshole Bay in the south to the Snohomish River in the north, typically within 30 meters of the shoreline. There is a ferry route that crosses Puget Sound between Edmonds and Kingston. This location was selected as being representative for releases into less confined areas within Puget Sound, with a high potential for transport of surface oil due to currents, winds, and larger "open water" areas compared with the other sites. The ferry terminal was chosen for modeling because of its proximity to residential areas, high ferry traffic, and large influx of tourists during the summer months.

For the hypothetical releases on the railway adjacent to the Edmonds Ferry Terminal, oil would travel over land before entering Puget Sound (Figure 2-4). OILMAP Land™ was used to determine the amounts and locations of oil entering Puget Sound from derailed tank cars near the ferry terminal. While the retention of oil on land was reported, it is assumed that 100 percent of the total volume of oil from the tank cars spilled directly into the waterway. The summer season scenario for this site (August) represented high ferry traffic and peak tourism, and had the lowest wind speeds, which affect surface oil transport and the vapor plume modeling performed by Risknology for the fire and explosion portion of the project. The winter season (January) had the highest average wind speeds of the year and would result in a higher potential for surface oil transport and potential entrainment of oil into the water column through surface breaking waves.

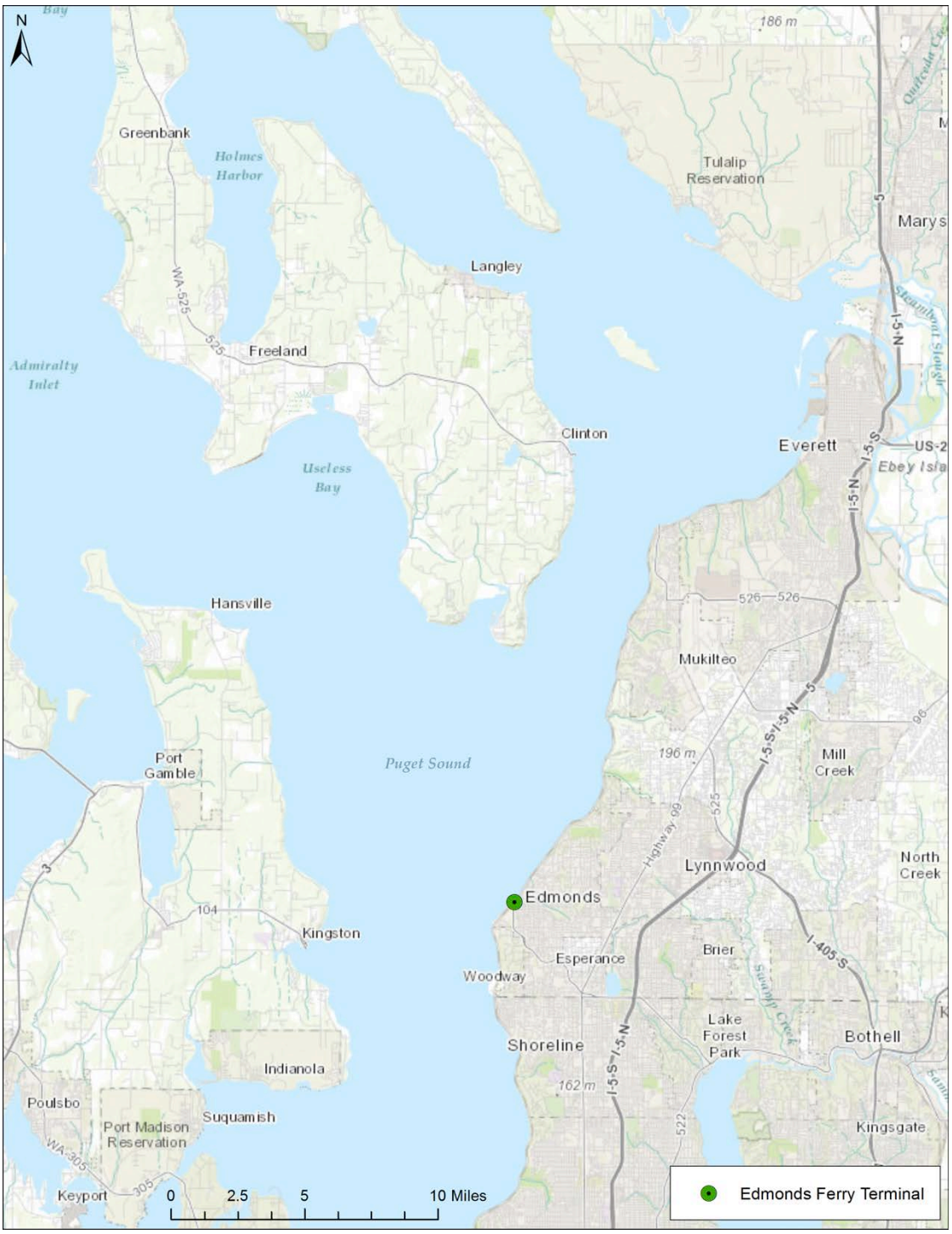

Figure 2-4: Map of the Edmonds Ferry Terminal hypothetical release location and surrounding area.

2.4 Release Scenarios

All three sites are located within Puget Sound basins, each with unique physical features that result in different dominating environmental factors that would affect the fate and transport of an oil release. While all environmental forcing (tides, river flow, winds) play a role to some degree at each site, a single environmental parameter was selected as the dominant variability for each site, and also affected the local receptors.

Table 2-2: Hypothetical release locations and environmental conditions varied in each scenario.

Scenario	Release Location	Seasonal / Environmental Condition	Release Volume
1	Swinomish Channel Swing Bridge	Summer - Spring Tide	20,000 bbl
2			5,700 bbl
3		Winter - Neap Tide	20,000 bbl
4			5,700 bbl
5	Skagit River Crossing	Summer – High River Flow	20,000 bbl
6			5,700 bbl
7		Winter – Low River Flow	20,000 bbl
8			5,700 bbl
9	Edmonds Ferry Terminal	Summer – Low Wind	20,000 bbl
10			5,700 bbl
11		Winter – High Wind	20,000 bbl
12			5,700 bbl

2.4.1 Identification of Timeframes for Scenarios

The simulation timeframes were delineated by both seasons (e.g., summer vs. winter) and characteristic environmental conditions (e.g., spring/neap tide, high/low river flow, high/low wind speed) occurring within the identified timeframes to capture the variable environmental conditions at each site. Details on the delineation of specific timeframes to capture the desired environmental conditions for each scenario are presented in Section 2.4.1. A summary of the environmental conditions during the simulation periods is provided in Section 2.4.2.

The hydrodynamic dataset that was used for the trajectory modeling included general circulation, riverine inputs, and tide flux (see Section 4.1.3). However, all of these forcings were superimposed on one another producing a single field of time-varying, three-dimensional current velocity (i.e., magnitude

and direction). To depict the level of the tide for a qualitative description of environmental conditions, a location was selected to serve as a tidal proxy. This location was away from riverine sources, islands, embayments, and other complex shoreline structures that could increase the likelihood of improperly understanding the tides. As the hydrodynamic set was a depiction of currents, maximum current velocities corresponded with peak ebb and peak flood conditions. Minimum current velocities corresponded with high tide and low tide. It is important to note that this current tidal proxy site was used only in the qualitative discussion of the environmental conditions for each hypothetical release location. For the trajectory modeling, released oil would be forced by the local current at each specific point in time and space.

The calendar seasons of summer (June, July, or August) and winter (December, January, or March) were chosen to represent different species' abundance and sensitivity in the study area. Details on the identification of timeframes that represented the characteristic environmental conditions at each site are provided below.

Swinomish Channel Swing Bridge

The Swinomish Channel is a narrow channel that runs north to south connecting Padilla Bay to Skagit Bay (Figure 2-2). Tidal currents dominate the flow through the channel and further dictate the flooding and drying of the extensive surrounding intertidal mud flats. In order to capture tidal variability, the scenarios were delineated such that a spring tide was simulated in the summer and a neap tide was simulated in the winter.

The flooded extent (i.e., area of land that is wetted and hydraulically connected) near the Swinomish Channel release location changes as tidal elevations fluctuate, with the greatest flooded extent occurring at high tide and the smallest flooded extent occurring at low tide. This flooding and drying action is cyclical with tides that are dominated by semi-diurnal (twice daily) and diurnal (once daily) forces. These forces result in a total tidal signal that has two high tides and two low tides within each day. The oil fate and transport simulations were run for 48 hours and captured approximately four of the semi-diurnal tidal cycles.

The tidal amplitude varied with time due to differences in the phases (timing) of each individual tidal forcing, namely in response to the relative positioning and gravitational forces of the sun and the moon to Earth. When the moon aligns with Earth and the sun twice monthly during full and new moons, the forces are stronger with higher tidal amplitudes ("spring tides"). When the moon and the sun are at a 90-degree angle twice monthly during quarter moons, the forces are weaker and tidal amplitudes are lower ("neap tides"). Therefore, over a two-week period, a site would experience both a spring and a neap tide. The overall amplitude can also vary over longer timescales due to longer-period forcing

factors; however, most of the variability in the modeling was captured in the spring-neap cycle. Because tidal elevations are greater during the spring tide, the flooded extent may be higher and persist longer during the spring tide than during the neap tide.

Near the release location, the tidal signal within the channel was not easily identified by the hydrodynamic dataset of current speeds due to low speeds or compounding factors such as regional river discharge or wind-driven circulation. Therefore, a tidal proxy site located at the entrance of the Strait of Juan da Fuca, immediately west of the Pacific Ocean (see area overview map Figure 2-1), was used to provide a more distinct response to the tides. Figure 2-5 illustrates the range in current speed, and therefore the timing of the tides for the available record (January 1 through December 31, 2008). Figure 2-6 depicts a shorter timescale view of the currents selected to represent the summer spring tide and the winter neap tide. These figures were used to delineate periods of spring tide and neap tide, based on visual assessment of the magnitude of the currents during the targeted month. Note that neap tidal variation would result in the smallest magnitude maximum current speeds, while spring tides would result in the largest magnitude maximum current speeds. At the tidal current proxy site, the currents peak at nearly twice the magnitude during spring tide (~ 1.0 meters per second [m/s]) compared with neap tide (~ 0.5 m/s).

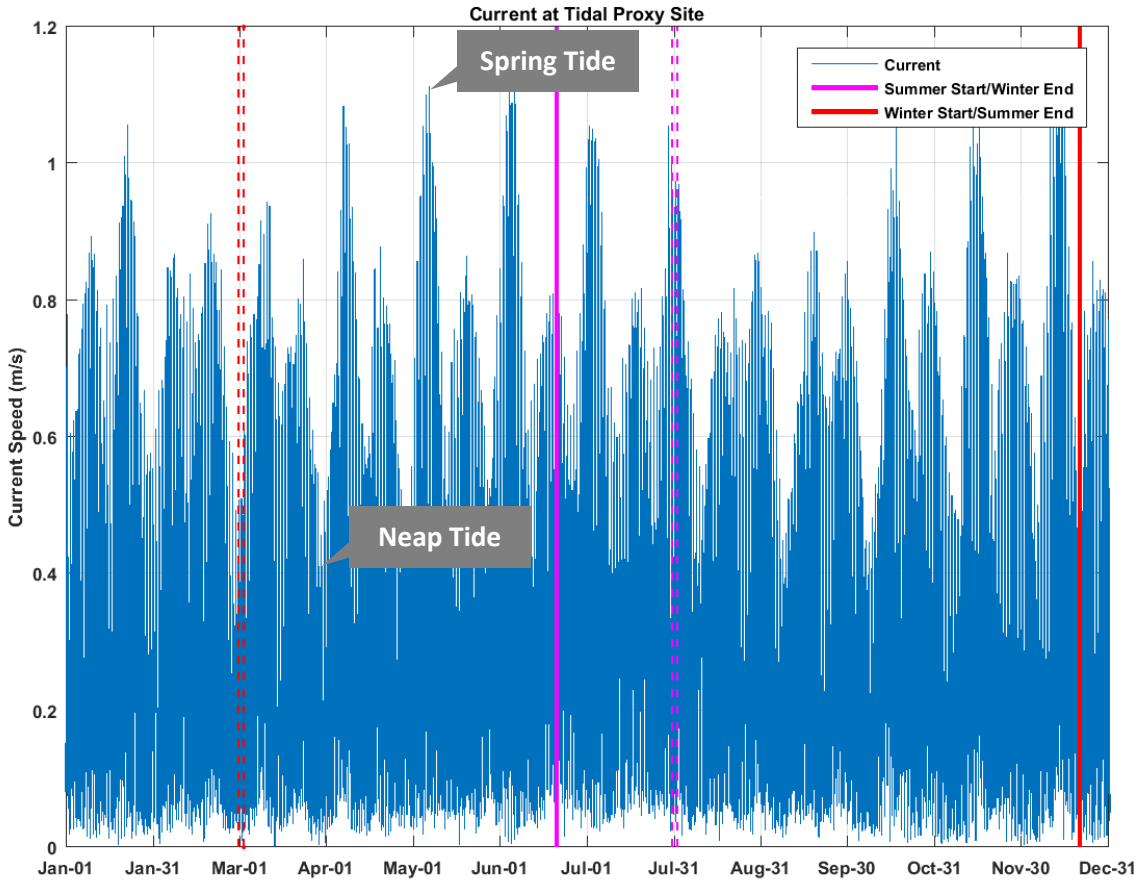

Figure 2-5: Illustration of current speed at the tidal current proxy site for 2008. The hourly current data is plotted in blue. The solid pink (start) to dashed pink (end) lines represent the summer season, while the solid red (start) to dashed red (end) lines represent the winter season.

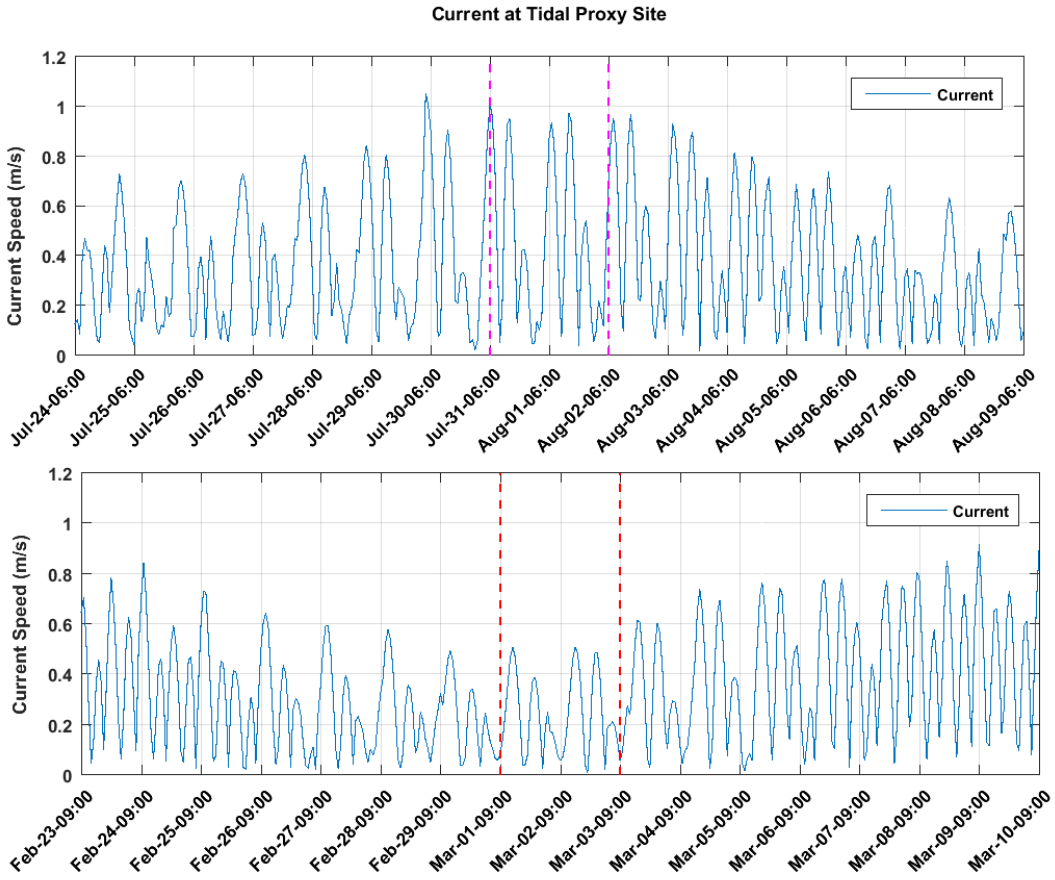

Figure 2-6: Hourly current speeds over 16-day periods (blue) at the tidal current proxy site for summer spring tide (top) and winter neap tide (bottom). The dashed lines bound the 48-hour simulation timeframe used in modeling.

Skagit River Crossing

The Skagit River Crossing site is located within the Skagit River, which flows into Skagit Bay (Figure 2-3). In the immediate vicinity of the modeled spill site, freshwater river flow was the driving force of oil transport, predominantly flowing downstream. The tide was not typically strong enough to reverse the flow except for some regions much farther downstream, near the bay. During periods of low freshwater flows, the force of the tide rivaled the river flow, which was evident by the oscillating current speeds (though not direction) at the release location. Farther downstream from the release location and within the bay, the currents reversed direction in response to the ebbing and flooding of the tide.

The Skagit River downstream current speeds were evaluated from the hydrodynamic data set at the release location. The 48-hour periods with relatively high current speeds were identified during the summer to reflect high river flow; relatively low current speeds were identified during the winter to reflect low river flow. To do this, a running 48-hour average was calculated for the time series and the minimum and maximum current speeds were identified. Model run times were centered around these points. Figure 2-7 depicts the downstream current and further indicates the summer period of representative high river flow and the winter period of representative low river flow used for the modeling timeframes.

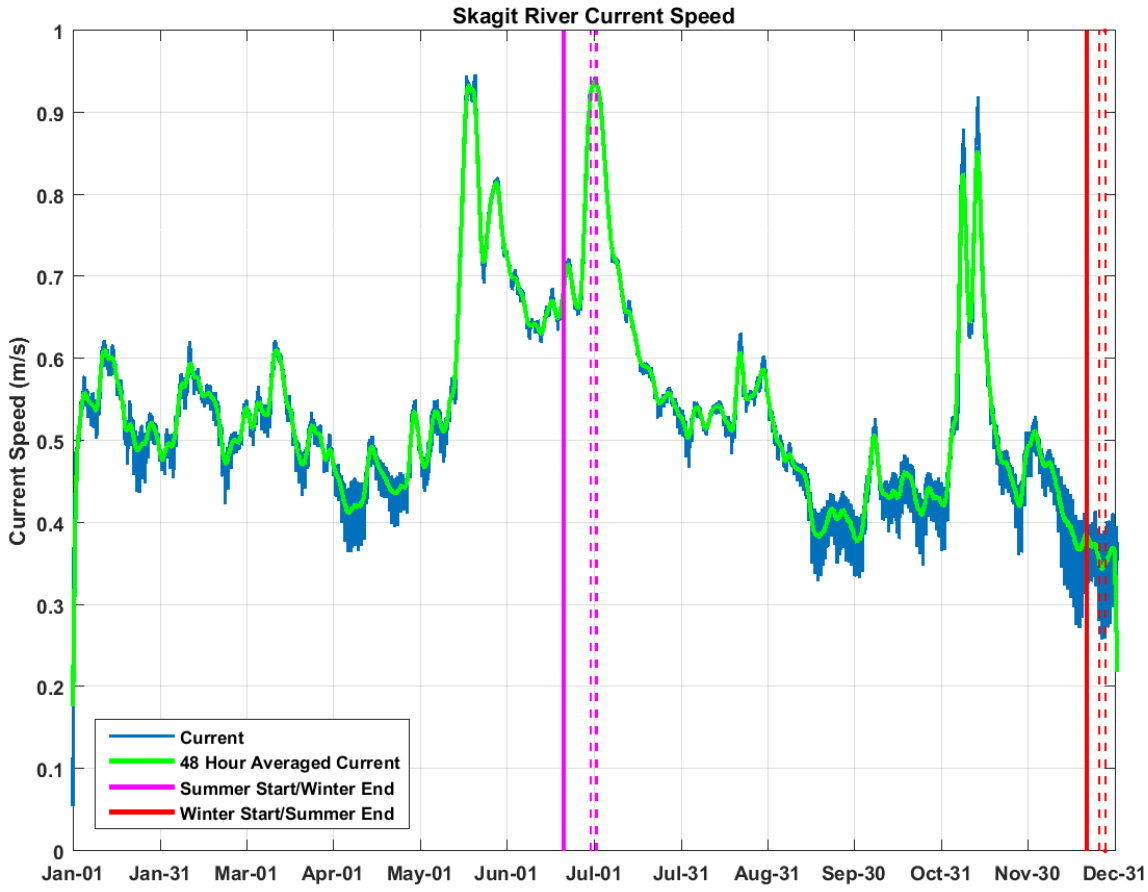

Figure 2-7: Hourly current speed (blue) over 2008 at the Skagit River Crossing, along with the 48-hour running average (green). The solid pink and red lines delineate the summer season start and winter season start, respectively. The dashed pink lines bound the 48-hour simulation timeframes for the summer high flow scenarios, while the red lines bound the winter low flow timeframes.

Edmonds Ferry Terminal

The Edmonds Ferry Terminal is located in east central Puget Sound (Figure 2-4). The waters near the release location are relatively deep and void of extensive intertidal mudflats, unlike the Swinomish Channel and Skagit River. The Edmonds Ferry Terminal site has greater potential for wind-driven transport due to the relatively larger open water areas; therefore, wind speed was used to characterize the modeling timeframes. The model scenario timeframes were delineated by identifying the 48-hour periods with the lowest wind speeds for summer scenarios and the highest average wind speeds for

winter scenarios. Figure 2-8 depicts the 48-hour running average for wind speed and further indicates the time periods for representative low winds during the summer and high winds during the winter.

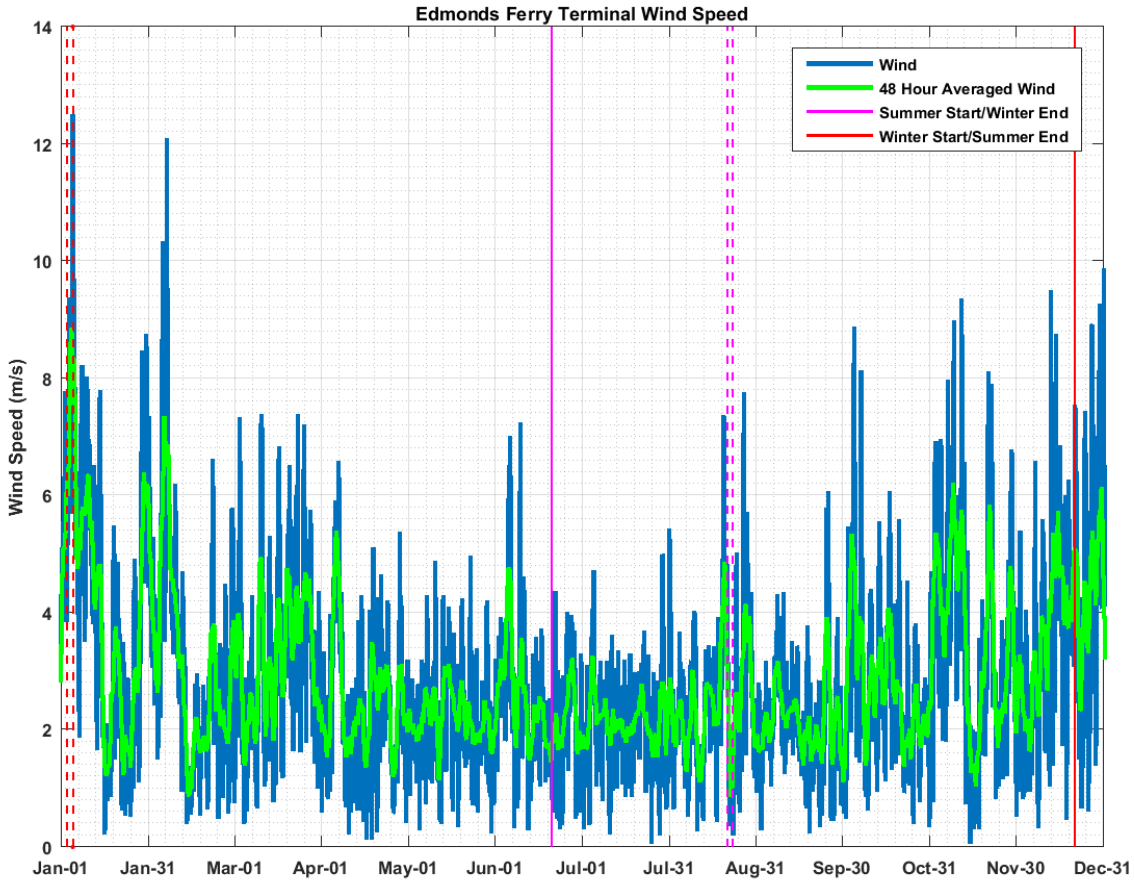

Figure 2-8: Wind speed (blue) over 2008 at the Edmonds Ferry Terminal at 6-hour intervals. The 48-hour running average is overlaid in green. The solid pink and red lines delineate the summer season start and winter season start, respectively. The dashed pink lines bound the 48-hour simulation timeframes for the summer low-wind speed scenarios, while the red lines bound the winter high-wind speed timeframes.

A summary of the identified timeframes for simulation are provided in Table 2-3.

Table 2-3: Summary of identified model timeframes based on current data

Release location	Season	Simulation Start Time	Simulation End Time
Swinomish Channel Swing Bridge	Summer - Spring Tide	7/31/2008 6:00	8/2/2008 6:00
	Winter - Neap Tide	3/1/2008 9:00	3/3/2008 9:00
Skagit River Crossing	Summer - High Flow	6/30/2008 11:00	7/2/2008 11:00
	Winter - Low Flow	12/25/2008 14:00	12/27/2008 14:00
Edmonds Ferry Terminal	Summer - Low Wind	8/21/2008 23:00	8/23/2008 23:00
	Winter - High Wind	1/3/2008 6:00	1/5/2008 6:00

2.4.2 Seasonal Conditions for Each Modeled Scenario

As previously stated, the oil fate and transport model required definition of environmental parameters for the simulation period. The figures and tables below summarize the current conditions used in the modeling for each scenario. Both winds and currents, along with the proxy for tidal current, are presented for: Swinomish Channel Swing Bridge under summer spring tide (Figure 2-9) and winter neap tide (Figure 2-10); Skagit River Crossing under summer high flow conditions (Figure 2-11) and winter low flow conditions (Figure 2-12); and Edmonds Ferry Terminal under summer low-wind conditions (Figure 2-13) and winter high-wind conditions (Figure 2-14).

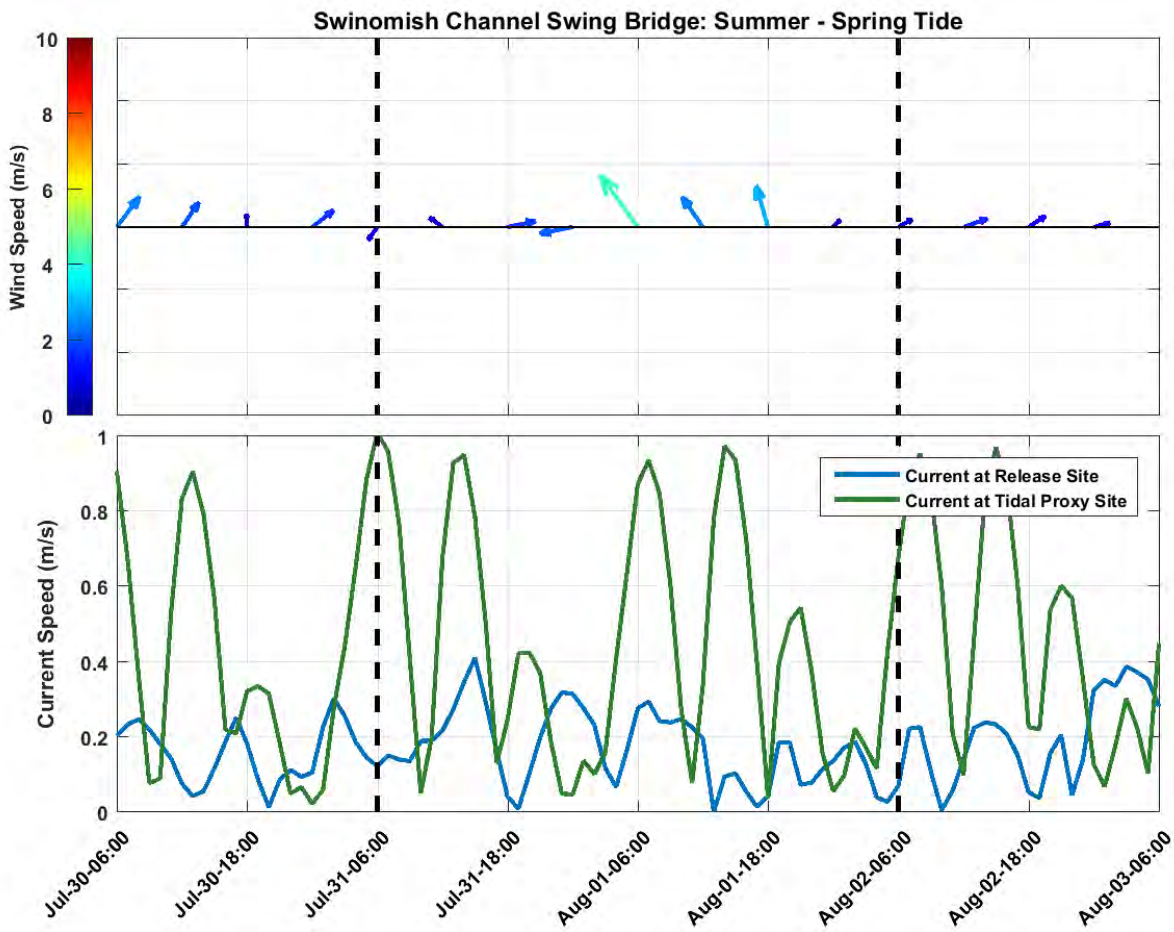

Figure 2-9: Winds and currents during the summer – spring tide simulation at the Swinomish Channel Swing Bridge. The upper panel illustrates the wind speed with color-contoured arrows and the arrow position reflects the direction the wind was headed. The bottom panel illustrates the current speed at the release location as well as at the tidal current proxy site. The dashed black lines indicate the start and end of the model simulation.

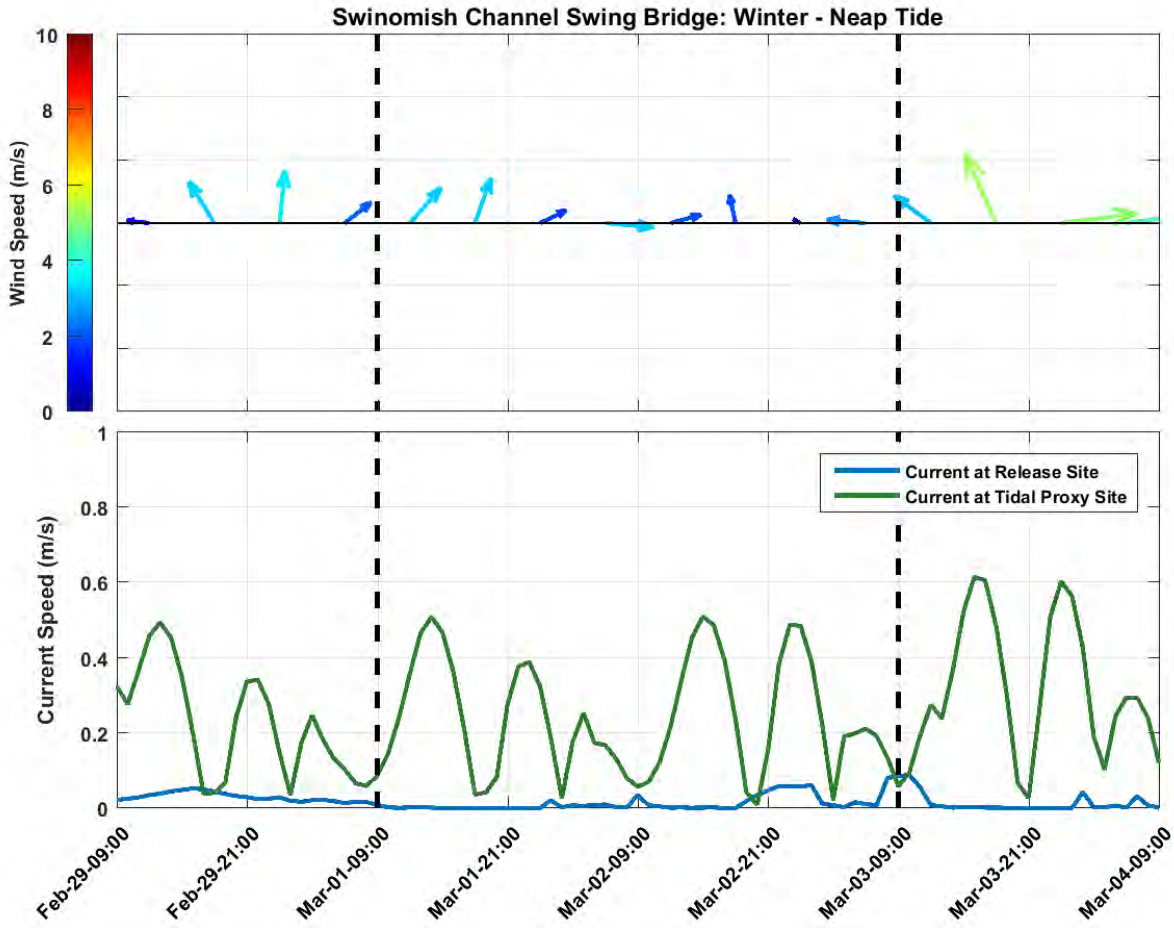

Figure 2-10: Winds and currents during the winter – neap tide simulation at the Swinomish Channel Swing Bridge. The upper panel illustrates the wind speed with color-contoured arrows and the arrow position reflects the direction the wind was headed. The bottom panel illustrates the current speed at the release location as well as at the tidal current proxy site. The dashed black lines indicate the start and end of the model simulation.

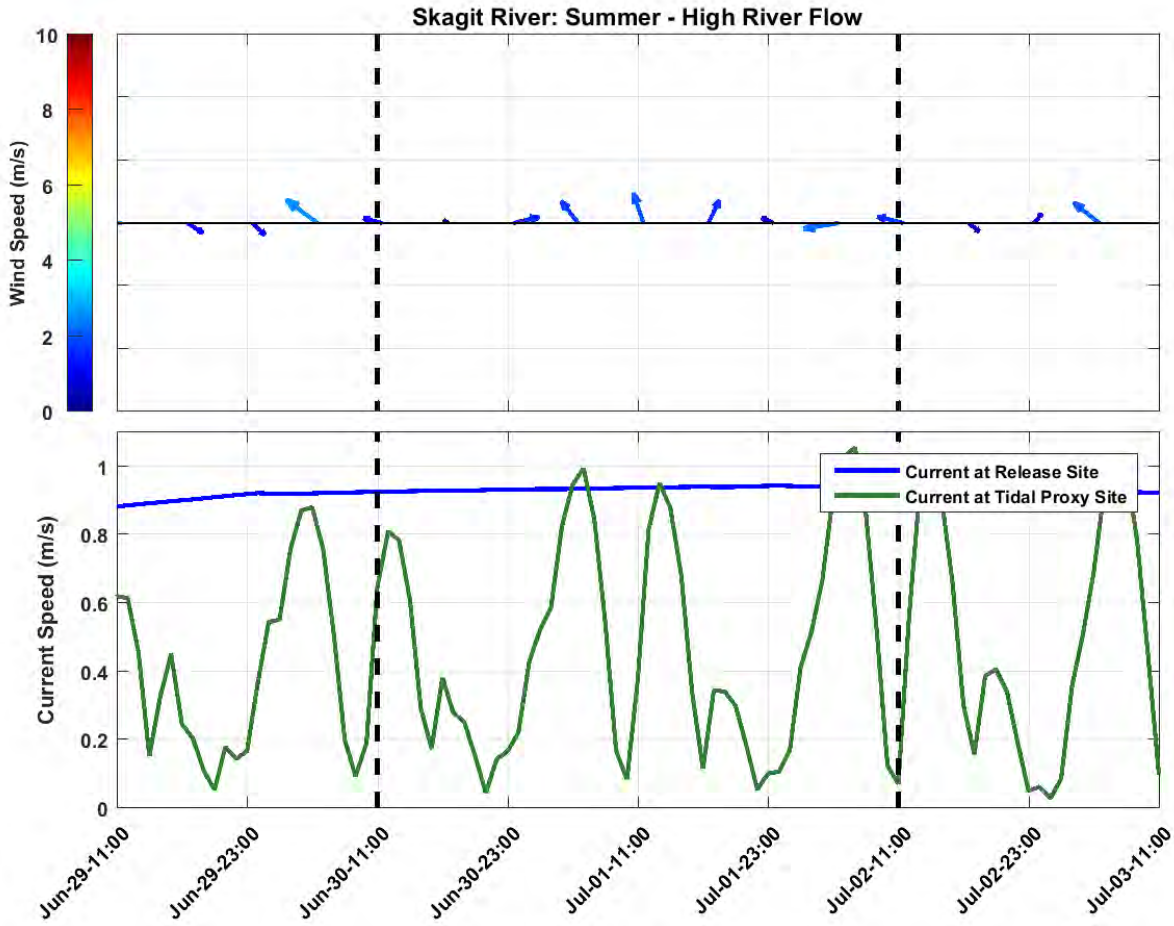

Figure 2-11: Winds and currents during the summer – high river flow simulation at the Skagit River Crossing. The upper panel illustrates the wind speed with color-contoured arrows and the arrow position reflects the direction the wind was headed. The bottom panel illustrates the current speed at the release location as well as at the tidal current proxy site. The dashed black lines indicate the start and end of the model simulation.

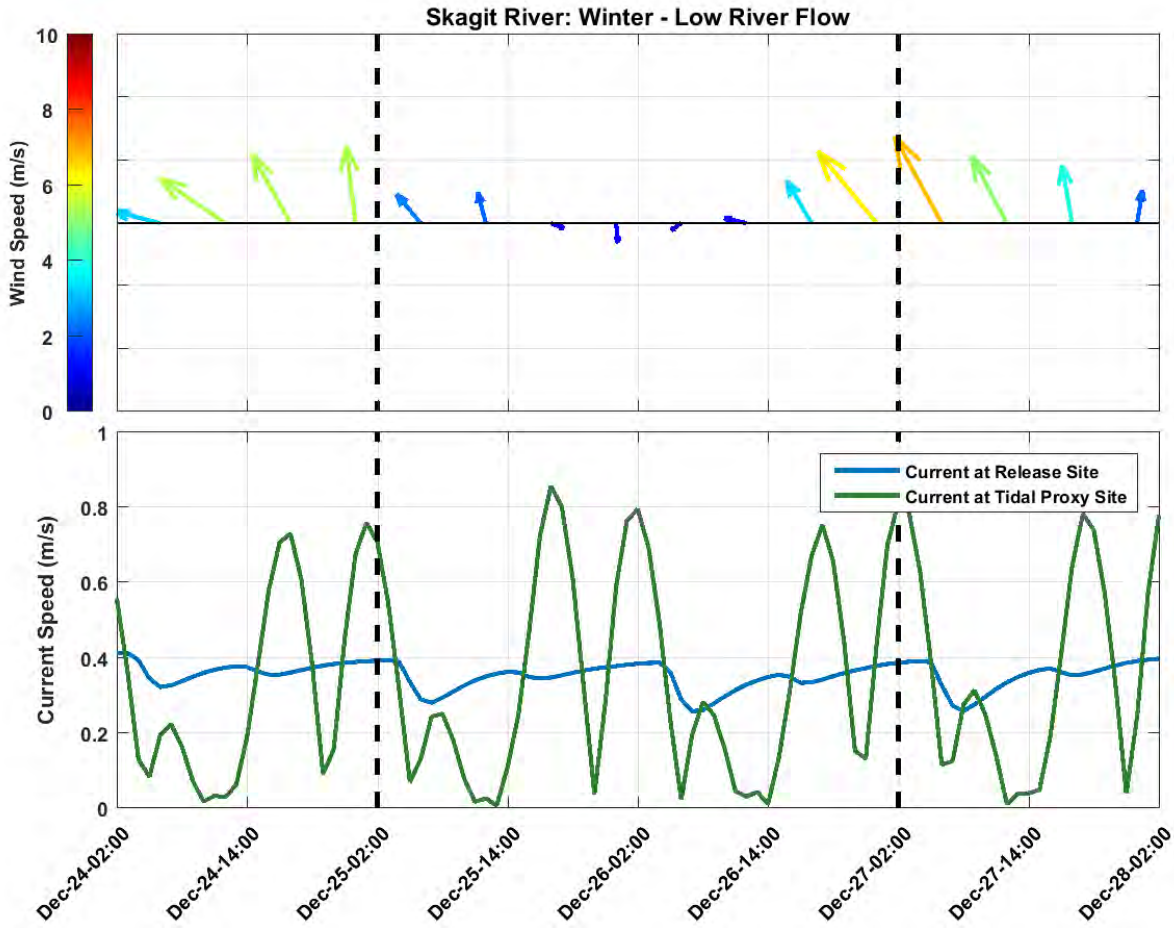

Figure 2-12: Winds and currents during the winter – low river flow simulation at the Skagit River Crossing. The upper panel illustrates the wind speed with color-contoured arrows and the arrow position reflects the direction the wind was headed. The bottom panel illustrates the current speed at the release location as well as at the tidal current proxy site. The dashed black lines indicate the start and end of the model simulation.

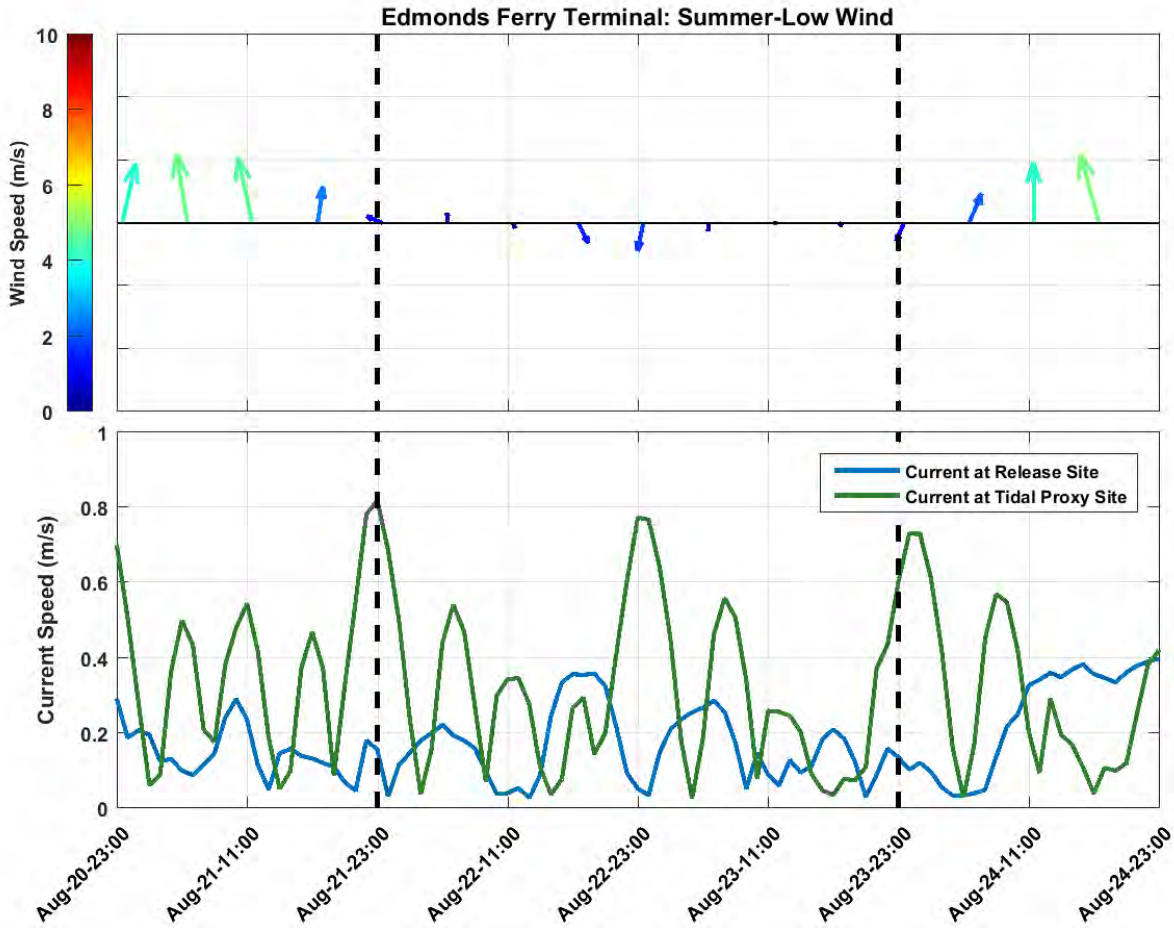

Figure 2-13: Winds and currents at during the summer – low-wind simulation at the Edmonds Ferry Terminal. The upper panel illustrates the wind speed with color-contoured arrows and the arrow position reflects the direction the wind was headed. The bottom panel illustrates the current speed at the release location as well as at the tidal current proxy site. The dashed black lines indicate the start and end of the model simulation.

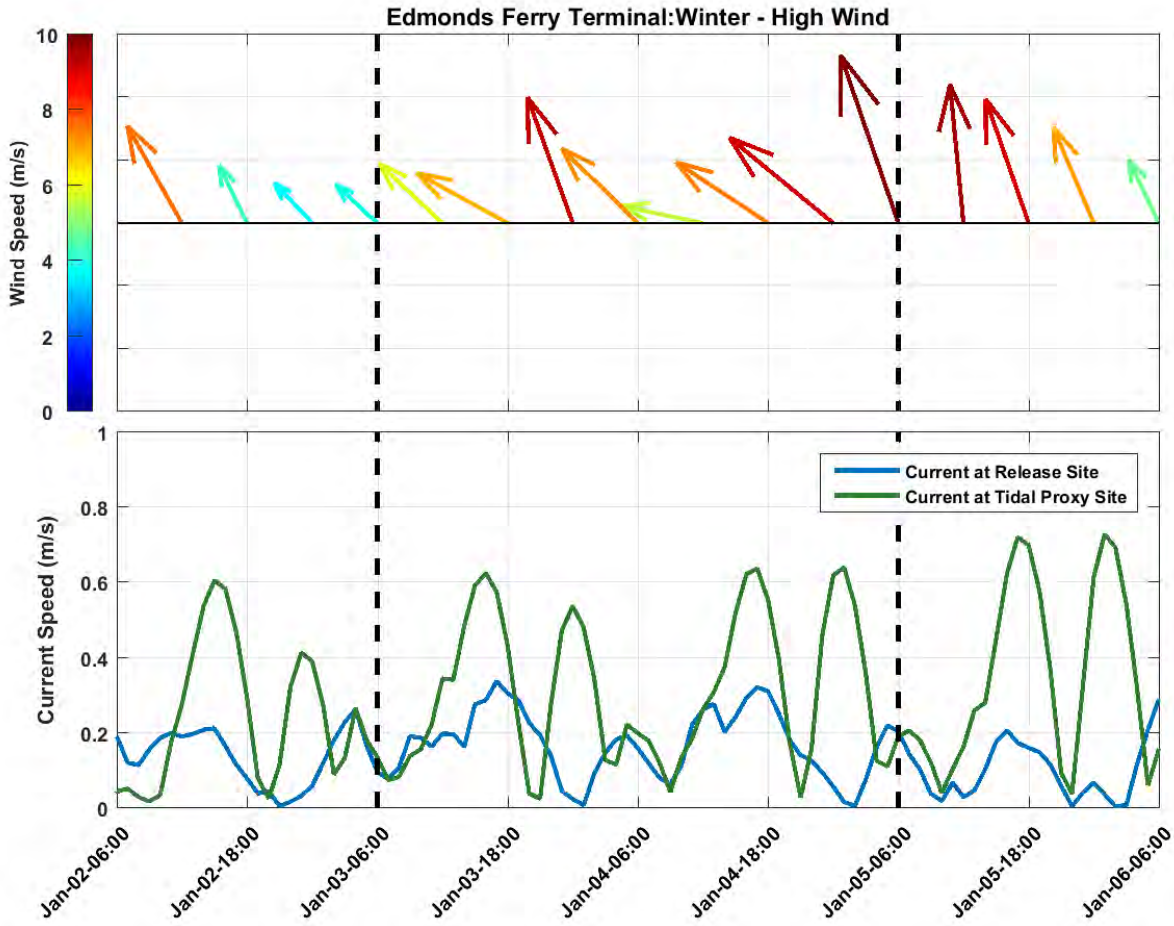

Figure 2-14: Winds and currents during the winter – high-wind simulation at the Edmonds Ferry Terminal. The upper panel illustrates the wind speed with color-contoured arrows and the arrow position reflects the direction the wind was headed. The bottom panel illustrates the current speed at the release location as well as at the tidal current proxy site. The dashed black lines indicate the start and end of the model simulation.

3 Model Descriptions

The analysis for this project was primarily performed using the SIMAP™ (Spill Impact Model Analysis Package) modeling system, developed by RPS ASA (formerly Applied Science Associates, or ASA). SIMAP™ originated from the oil fates and biological impacts submodels in the Natural Resource Damage Assessment Models for Coastal and Marine Environments (NRDAM/CME) and Great Lakes Environments (NRDAM/GLE), which ASA developed in the early 1990s for the U.S. Department of the Interior for use in "type A" Natural Resource Damage Assessment (NRDA) regulations under the Comprehensive Environmental Response, Compensation and Liability Act of 1980 (CERCLA). The most recent version of the type A models, the NRDAM/CME (Version 2.4, April 1996) was published as part of the CERCLA type A NRDA Final Rule (Federal Register, May 7, 1996, Vol. 61, No. 89, pp. 20559–20614). The technical documentation for the NRDAM/CME is in French et al. (1996). This technical development involved several in-depth peer reviews, as described in the Final Rule.

While the NRDAM/CME and NRDAM/GLE were developed for simplified natural resource damage assessments of small spills in the U.S., SIMAP™ was designed to evaluate fate and impacts of both real and hypothetical spills in marine, estuarine, and freshwater environments worldwide. Additions and modifications to prepare SIMAP™ were made to increase model resolution, allow modification and site-specificity of input data, allow incorporation of spatially and temporally varying current data, evaluate subsurface releases and movements of subsurface oil, track multiple chemical components of the oil, enable stochastic modeling, and facilitate analysis of results.

The consideration of the impacts of subsurface oil is important, particularly in the evaluation of impacts on aquatic organisms. Surface floating oil primarily affects wildlife (birds, mammals, reptiles, and adult amphibians) and shoreline biota (emergent vegetation), rather than aquatic biota (fish, invertebrates, early life-stages of amphibians, aquatic plants) in submerged habitats. In turbulent waters (e.g., riverine environments) and at higher wind speeds beginning at about 12 knots (or at lower wind speeds if dispersant is applied), oil will entrain into the water column, unless it has become too viscous to do so after weathering and the formation of mousse. Once oil is entrained in the water in the form of small droplets, monoaromatics (MAHs) and polycyclic aromatic hydrocarbons (PAHs) dissolve into the water column over time. The MAHs and PAHs are the most toxic portion of the oil by virtue of their relative solubility in water, making them available to aquatic biota for uptake. The dissolution rate of MAHs and PAHs from entrained oil is very sensitive to the droplet size because it involves mass transfer across the surface area of the droplet. Also, the amount of hydrocarbon mass dissolved is a function of the mass entrained and droplet size distribution. These are, in turn, a function of the soluble hydrocarbon content of the oil, the amount of evaporation of these components before entrainment, oil viscosity (which

increases as the oil weathers and emulsifies), oil surface tension (which may be reduced by surfactant dispersants), and the energy in the system (the higher the energy, the smaller the droplets). Large droplets (greater than a few hundred microns in diameter) resurface rapidly, and so their dissolution is inconsequential. Dispersant application facilitates the entrainment of oil into the water in a smaller size distribution than would occur naturally, with the median droplet size of about 20 μm (Lunel 1993a; 1993b).

Therefore, the fate of MAHs and lighter or more volatile PAHs in surface oil is primarily volatilization to the atmosphere, rather than to the water unless entrainment of the surface oil into the water is significant. If oil is entrained before it has weathered and lost the lower molecular weight aromatics to the atmosphere, dissolved MAHs and PAHs in the water can reach concentrations where they can affect water column organisms or bottom communities (French McCay and Payne 2001).

Below are brief descriptions of the fates and impacts models presented in SIMAP™. Detailed descriptions of the algorithms and assumptions in the model are in published papers (French McCay 2002; 2003; 2004; 2009). The model has been validated with more than 20 case histories, including the *Exxon Valdez* and other large spills (French and Rines 1997; French McCay 2003; 2004; French McCay and Rowe 2004), as well as with test spills designed to verify the model (French et al. 1997).

3.1 SIMAP Physical Fates Model

The three-dimensional physical fates model estimates distribution (as mass and concentrations) of whole oil and oil components on the water surface, on shorelines, in the water column, and in sediments. Oil fate processes included are oil spreading (gravitational and by shearing), evaporation, transport, randomized dispersion, emulsification, entrainment (natural and facilitated by dispersant), dissolution, volatilization of dissolved hydrocarbons from the surface water, adherence of oil droplets to suspended sediments, adsorption of soluble and sparingly-soluble aromatics to suspended sediments, sedimentation, and degradation.

Oil is a mixture of hydrocarbons of varying physical, chemical, and toxicological characteristics. That means oil hydrocarbons have varying fates and impacts on organisms. In the model, oil was represented by component categories, and the fate of each component was tracked separately. The “pseudo-component” approach (Payne et al. 1984, 1987; French et al. 1996; Jones 1997; Lehr et al. 2000) was used, where chemicals in the oil mixture were grouped by physical-chemical properties, and the resulting component category behaved as if it were a single chemical with characteristics typical of the chemical group.

The most toxic components of oil to aquatic organisms are low molecular weight aromatic compounds (monoaromatic and polycyclic aromatic hydrocarbons, MAHs and PAHs), which are both volatile and soluble in water. Their acute toxic impacts are caused by nonpolar narcosis, where toxicity is related to the octanol-water partition coefficient (K_{ow}), a measure of hydrophobicity. The more hydrophobic the compound, the more toxic it is likely to be. However, as K_{ow} increases, the compound also becomes less soluble in water, so there is less exposure to aquatic organisms. The toxicity of compounds with log (K_{ow}) values greater than about 5.6 is limited by its very low solubility in water and consequent low bioavailability (French McCay 2002; Di Toro et al. 2000). Therefore, the potential for acute impacts is the result of a balance between bioavailability, toxicity once exposed, and duration of exposure. French McCay (2002) contains a full description of the oil toxicity model in SIMAP™ and French McCay (2002) describes the implementation of the toxicity model in SIMAP™.

Because of these considerations, the SIMAP™ fates model focuses on tracking the lower molecular weight aromatic components divided into chemical groups based on volatility, solubility, and hydrophobicity. In the model, the oil is treated as comprising eight components (defined in Table 3-1). Six of the components (i.e., all but the two nonvolatile residual components representing nonvolatile aromatics and aliphatics) evaporate at rates specific to the pseudo-component. Solubility is strongly correlated with volatility, and the solubility of aromatics is higher than aliphatics of the same volatility. The MAHs are the most soluble, the 2-ring PAHs are less soluble, and the 3-ring PAHs slightly soluble (Mackay et al. 1992). Both the solubility and toxicity of the nonaromatic hydrocarbons are much lower than for the aromatics, and dissolution (and water concentrations) of nonaromatics is safely ignored. Therefore, dissolved concentrations are calculated only for each of the three soluble aromatic pseudo-components.

This number of components provided sufficient accuracy for the evaporation and dissolution calculations, particularly given the time frame (minutes) over which dissolution occurred from small droplets and the rapid resurfacing of large droplets (see discussion above). The alternative approach of treating oil as a single compound with empirically-derived rates (e.g., Mackay et al. 1980; Stiver and Mackay 1984) does not provide sufficient accuracy for environmental impacts analyses. The impacts to water column organisms are caused by MAHs and PAHs, which have specific properties that differ from the other volatile and soluble compounds. The model was validated both in predicting dissolved concentrations and their resulting toxic impacts, thereby supporting the adequacy of the use of this number of pseudo-components (French McCay 2003).

Table 3-1: Definition of four distillation cuts and the eight pseudo-components in the model (monoaromatic hydrocarbons, MAHs; benzene + toluene + ethybenzene + xylene, BTEX; polycyclic aromatic hydrocarbons, PAHs).

Characteristic	Volatile and Highly Soluble	Semi-Volatile and Soluble	Low Volatility and Slightly Soluble	Residual (nonvolatile and very low solubility)
Distillation cut	1	2	3	4
Boiling Point (°C)	< 180	180 - 265	265 - 380	> 380
Molecular Weight	50 - 125	125 - 168	152 - 215	> 215
Log(K_{ow})	2.1 - 3.7	3.7 - 4.4	3.9 - 5.6	> 5.6
Aliphatic pseudo-components: Number of carbons	volatile aliphatics: C4 - C10	semi-volatile aliphatics: C10 - C15	low-volatility aliphatics: C15 - C20	nonvolatile aliphatics: > C20
Aromatic pseudo-component name: included compounds	MAHs: BTEX, MAHs to C3-benzenes	2 ring PAHs: C4-benzenes, naphthalene, C1-, C2-naphthalenes	3 ring PAHs: C3-, C4-naphthalenes, 3-4 ring PAHs with log(K_{ow}) < 5.6	≥ 4 ring aromatics: PAHs with log(K_{ow}) > 5.6 (very low solubility)

The lower molecular weight aromatics dissolved from the whole oil and were partitioned in the water column and sediments according to equilibrium partitioning theory (French et al. 1996; French McCay 2004). The residual fractions in the model were composed of nonvolatile and insoluble compounds that remained in the "whole oil" that spread, were transported on the water surface, stranded on shorelines, and dispersed into the water column as oil droplets or remains on the surface as tar balls. This is the fraction that composes black oil, mousse, and sheen.

3.1.1 Modeled SIMAP Oil Fate Processes

The schematic in Figure 3-1 shows oil fate processes simulated in the model near shore and riverine environments. Because oil contains many chemicals with varying physical-chemical properties and the fact that the environment is spatially and temporally variable, the oil rapidly separates into different phases or parts of the environment:

- Surface oil
- Emulsified oil (mousse) and tar balls
- Oil droplets suspended in the water column
- Oil adhering to suspended particulate matter in the water
- Dissolved lower molecular weight components (MAHs, PAHs, and other soluble components) in the water column

- Oil on and in the sediments
- Dissolved lower molecular weight components (MAHs, PAHs, and other soluble components) in the sediment pore water
- Oil on and in the shoreline sediments and surfaces

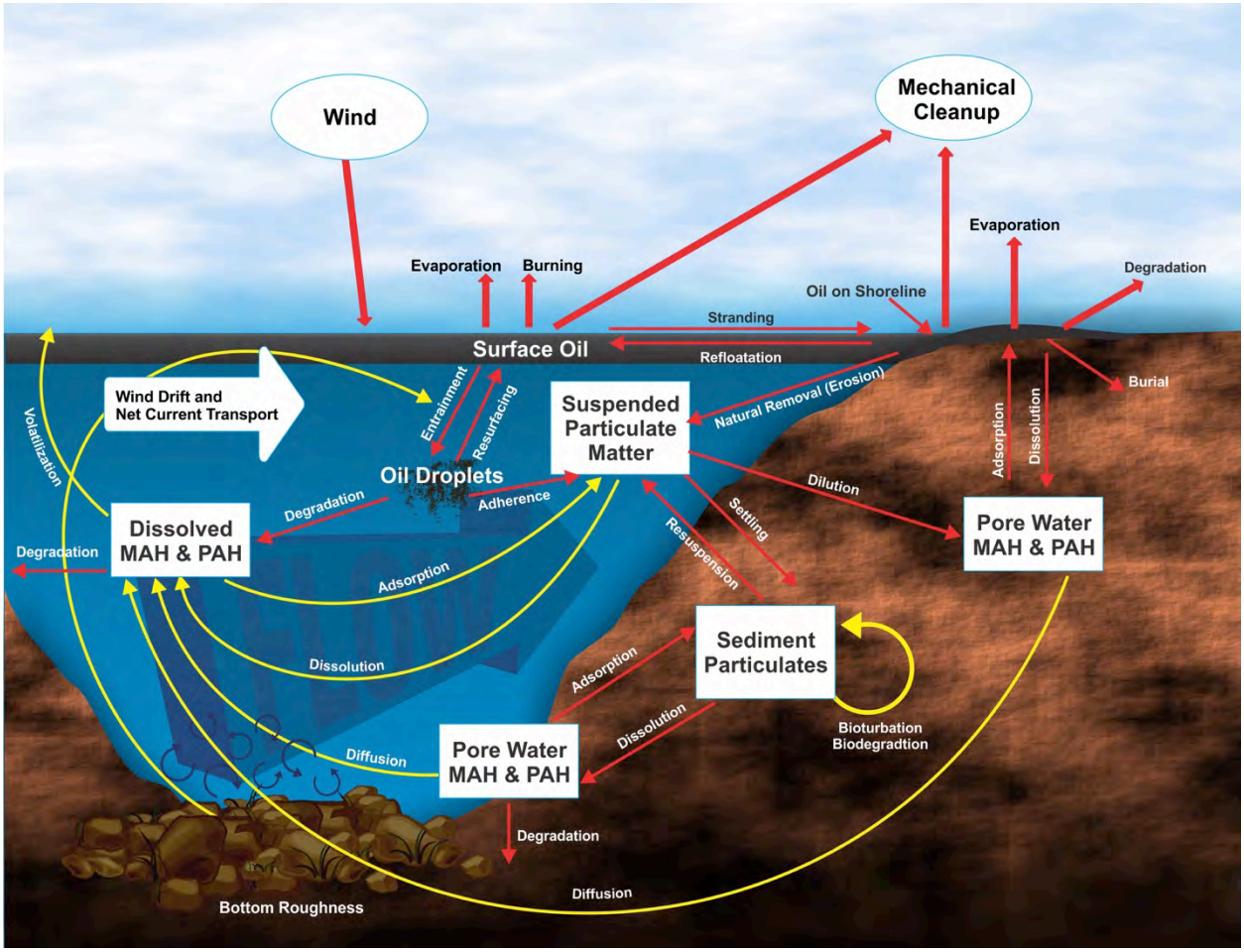

Figure 3-1: Simulated oil fates processes in lakes and rivers.

The schematic in Figure 3-1 represents oil fate processes that are simulated in the model:

- **Spreading** is the thinning and broadening of surface slicks caused by gravitational forces and surface tension. This occurs rapidly after oil is spilled on the water surface. The spreading rate is faster when oil viscosity is lower at higher temperatures. Viscosity increases as oil emulsifies.
- **Transport** is the process by which oil is carried by currents.
- **Turbulent dispersion** is the process by which turbulence ("sub-scale" currents that mix oil in three dimensions) spreads oil components on the surface and into the water column.

- **Evaporation** is the diffusion of volatile compounds from oil into a gaseous phase in the atmosphere. Evaporation from surface and shoreline oil increases as the oil surface area, temperature, and wind speed increase. As lighter components evaporate, the remaining "weathered" oil becomes more viscous.
- **Emulsification** is the mixture of water into the oil, such that the oil forms a matrix with embedded water droplets. The resulting mixture is commonly called mousse, which is technically a water-in-oil emulsion. The rate of emulsification escalates with increasing wind speed and turbulence on the surface of the water. Viscosity increases as oil emulsifies.
- **Entrainment** is the process by which waves break over surface oil and carry oil droplets into the water column. At higher wind speeds (about 12 knots, or 6 m/s) or where currents and bottom roughness induce turbulence in a river or stream, wave heights may reach a threshold where they break. Thus, entrainment becomes increasingly important (higher rate of mass transfer to the water) with higher wind speeds.
- **Resurfacing** of entrained oil occurs rapidly for larger oil droplets. Smaller droplets resurface when the wave turbulence decreases. The smallest droplets do not resurface, as typical turbulence levels in the water keep them indefinitely suspended. Local winds at the water surface can also prevent oil from surfacing.
- **Dissolution** is the diffusion of water-soluble components out of the oil and into the water. The dissolution rate increases as the surface area of the oil, relative to its volume, increases. Since the surface-area-to-volume ratio is higher for smaller spherical droplets, smaller droplet sizes have higher dissolution rates.
- **Volatilization** of dissolved components from the water to the atmosphere occurs as they mix, diffuse to the water surface boundary, and enter the gas phase. Volatilization rates escalate with increasing air and water temperatures.
- **Adsorption** of dissolved components to particulate matter in the water occurs because the soluble components (MAHs and PAHs) preferentially adsorb to particulates when the latter are present. The higher the concentration of suspended particulates, the more adsorption occurs. Also, the higher the molecular weight of the compound, the less soluble it is, and the more it tends to adsorb to particulate matter.
- **Adherence** is a combination of oil droplets with particles in the water. If the particles are suspended sediments, the combined oil/suspended sediment agglomerate is heavier than the oil and the surrounding water. If turbulence subsides, the oil-sediment agglomerates will settle.
- **Sedimentation (settling)** is the process whereby oil-sediment agglomerates and particles with adsorbed sparingly-soluble components (MAHs and PAHs) settle to the bottom sediments. Sedimentation can be an important oil pathway in nearshore areas when waves are strong and

subsequently subside. Generally, oil-sediment agglomerates transfer more PAHs to the bottom than sediments with PAHs adsorbed from the dissolved phase in the water column.

- **Resuspension** of settled oil-sediment agglomerates and particles with adsorbed sparingly-soluble components (MAHs and PAHs) may occur if current speeds and turbulence exceed threshold values for overcoming cohesive forces.
- **Diffusion** is the process whereby dissolved compounds move from higher to lower concentration areas by random motion of molecules and micro-scale turbulence. Dissolved components in bottom and shoreline sediments can diffuse out to the water column where concentrations are relatively low. Bioturbation, groundwater discharge, and hyporheic flow of water through streambed sediments can greatly increase the rate of diffusion from sediments (see below).
- **Hyporheic flow** is the movement of water through streambed sediments, induced by pressure differentials associated with streambed irregularities or groundwater discharge.
- **Dilution** occurs when water of lower concentration is mixed into water with higher concentration by turbulence, currents, or shoreline groundwater.
- **Bioturbation** is the process by which benthic fauna mix the surface sediment layer while burrowing, feeding, or passing water over their gills. In open-water, soft-bottom environments, bioturbation impactively mixes the top 10 centimeters (cm) of the sediment layer (in nonpolluted areas).
- **Degradation** is when oil components are changed either chemically or biologically (biodegradation) into another compound. Degradation occurs through breakdown to simpler organic carbon compounds by bacteria and other organisms, photo-oxidation by solar energy, and other chemical reactions. Higher temperature and higher light intensity (particularly ultraviolet wavelengths) increase the rate of degradation.

3.1.2

- **Stranding and refloatation** occur when floating oil meets the shorelines and then refloats as water levels rise, allowing the oil to move farther downcurrent or downstream.

Summary of Spill Dynamics

For a spill on the water surface, gravitational spreading occurs very rapidly (within hours) to a minimum thickness, which makes the area exposed to evaporation high relative to the oil volume. Evaporation proceeds faster than dissolution. Therefore, most of the volatiles and semi-volatiles evaporate, with a smaller fraction dissolving into the water. Degradation (photo-oxidation and biodegradation) also occurs at a relatively slow rate compared with these processes.

Evaporation is more rapid as the wind speed increases. However, beginning at about 12 knots (6 m/s) of wind speed and in open water, white caps begin to form and the breaking waves entrain oil as droplets into the water column. Higher wind speeds (and turbulence) increase entrainment and result in smaller droplet sizes. From Stoke's Law, larger droplets resurface faster and form surface slicks. Therefore, a dynamic balance evolves between entrainment and resurfacing. As high-wind events occur, the entrainment rate increases. When the winds subside to less than 12 knots, the larger oil droplets resurface and remain floating. Similar dynamics occur in turbulent streams.

The smallest oil droplets remain entrained in the water column for an indefinite period. Larger oil droplets rise to the surface at varying rates. While the droplets are under water, dissolution of the light and soluble components occurs. Dissolution rate is a function of the surface area available. That means that most dissolution occurs from droplets rather than from surface slicks, as droplets have a higher surface-area-to-volume ratio, and they are not in contact with the atmosphere (and so the soluble components do not preferentially evaporate as they do from surface oil).

If oil is released or driven underwater, it forms droplets of varying sizes. The more turbulent the conditions, the smaller the droplets. From Stoke's Law, larger droplets rise faster and surface if the water is shallow. Resurfaced oil behaves as surface oil after gravitational spreading has occurred. The surface oil may be re-entrained. The smallest droplets in most cases remain in the water permanently. As a result of the higher surface area per volume of small droplets, the dissolution rate is much higher from subsurface oil than from floating oil on the water surface.

Because of these interactions, the majority of dissolved constituents (which are of concern because of potential impacts on aquatic organisms) are from droplets entrained in the water. For a given spill volume and oil type/composition, with increasing turbulence either at the water surface and/or at the streambed: (1) there is an increasing amount of oil entrained; (2) the oil is increasingly broken up into smaller droplets; (3) there is more likelihood of the oil remaining entrained rather than resurfacing; and (4) the dissolved concentrations will be higher. Entrainment and dissolved concentrations increase with (1) higher wind speeds, (2) increased turbulence from other sources of turbulence (waves on a beach, rapids, and waterfalls in rivers, etc.), (3) subsurface releases (especially under higher pressure and turbulence), and (4) application of chemical dispersants. Chemical dispersants both increase the amount of oil entrained and decrease the oil droplet size. Therefore, chemical dispersants increase the dissolution rate of soluble components. (Note that chemical dispersants are unlikely to be used in a stream when impacts on aquatic biota are a primary concern.)

Processes that increase the rate of supply of dissolved constituents are balanced by loss terms in the model: (1) transport (dilution), (2) volatilization from the dissolved phase to the atmosphere, (3) adsorption to SPM and sedimentation, and (4) degradation (photo-oxidation or biologically mediated).

Also, other processes slow the entrainment rate: (1) emulsification increases viscosity and slows or eliminates entrainment; (2) adsorption of oil droplets to SPM and settling removes oil from the water; (3) stranding on shorelines removes oil from the water; and (4) mechanical cleanup and burning removes mass from the water surface and shorelines. Therefore, the model-predicted concentrations are the resulting balance of all these processes and the best estimates based on our quantitative understanding of the individual processes.

3.1.3 SIMAP Model Oil Fates Algorithms

The algorithms used to model oil fate processes are described in French McCay (2004). Lagrangian elements (spillets) are used to simulate the movements of oil components in three dimensions over time. Surface floating oil, subsurface droplets, and dissolved components are tracked in separate spillets. Transport is the sum of advective velocities by currents input to the model, surface wind drift, vertical movement according to buoyancy, and randomized turbulent diffusive velocities in three dimensions. The vertical diffusion coefficient is computed as a function of wind speed in the surface wave-mixed layer. The horizontal and deeper water vertical diffusion coefficients are model inputs.

The oil (whole and as pseudo-components) separates into different phases or parts of the environment, i.e., surface slicks; emulsified oil (mousse) and tar balls; oil droplets suspended in the water column; dissolved lower molecular weight components (MAHs and PAHs) in the water column; oil droplets adhered and hydrocarbons adsorbed to suspended particulate matter in the water; hydrocarbons on and in the sediments; dissolved MAHs and PAHs in the sediment pore water; and hydrocarbons on and in the shoreline sediments and surfaces.

The algorithms used to calculate these fates processes are briefly described in the subsections below.

3.1.3.1 Transport

Lagrangian particles (spillets) are moved in three dimensions over time. For each model time step, the new vector position of the spillet center is calculated from the old location plus the vector sum of east-west, north-south, and vertical components of advective and diffusive velocities:

$$X_t = X_{t-1} + \Delta t \, (U_t + D_t + R_t + W_t)$$

where X_t is the vector position at time t, X_{t-1} is the vector position the previous time step, Δt is the time step, U_t is the sum of all the advective (current) velocity components in three dimensions at time t, D_t is the sum of the randomized diffusive velocities in three dimensions at time t, R_t is the rise or sinking velocity of whole oil droplets in the water column, and W_t is the surface wind transport ("wind drift"). The magnitudes of the components of D_t are scaled by horizontal and vertical diffusion coefficients (Okubo and Ozmidov 1970; Okubo 1971). The vertical diffusion coefficient is computed as a function of

wind speed in the surface wave-mixed layer (which ranges from centimeter scales in rivers and near lee shorelines to potentially meters in large water bodies away from shore when wind speeds are high), based on Thorpe (1984). R_t is computed by Stokes law, where velocity is related to the difference in density between the particle and the water, and to the particle diameter. The algorithm developed by Youssef and Spaulding (1993) is used for wind transport in the surface wave-mixed layer (W_t, described below).

3.1.3.2 Shoreline Stranding

The fate of spilled oil that reaches the shoreline depends on characteristics of the oil, the type of shoreline, and the energy environment. The stranding algorithm is based on work by CSE/ASA/BAT (1986), Gundlach (1987) and Reed and Gundlach (1989) in developing the COZOIL model for the U.S. Minerals Management Service. In SIMAP™, deposition occurs when an oil spillet intersects shore surface. Deposition ceases when the volume holding capacity for the shore surface is reached. Subsequent oil coming ashore is not allowed to remain on the shore surface. It is refloated by rising water, and carried away by currents and wind drift. The remaining shoreline oil is then removed exponentially with time. Data for holding capacity and removal rate are taken from CSE/ABA/BAT (1986) and Gundlach (1987), and are a function of oil viscosity and shore type. The algorithm and data are in French et al. (1996).

3.1.3.3 Spreading

Spreading determines the areal extent of the surface oil, which, in turn, influences its rates of evaporation, dissolution, dispersion (entrainment), and photo-oxidation, all of which are functions of surface area. Spreading results from the balance among the forces of gravity, inertia, viscosity, and surface tension, which increases the diameter of each spillet; turbulent diffusion, which spreads the spillets apart; and entrainment followed by resurfacing, which can spatially separate the leading edge of the oil from resurfaced oil transported in a different direction by subsurface currents.

For many years, Fay's (1971) three-regime spreading theory was widely used in oil spill models (ASCE 1996). Mackay et al. (1980; 1982) modified Fay's approach and described the oil as thin and thick slicks. Their approach used an empirical formulation based on Fay's (1971) terminal spreading behaviour. They assumed the thick slick feeds the thin slick and that 80 to 90 percent of the total slick area is represented by the thin slick. In SIMAP™, oil spillets on the water surface increase in diameter according to the spreading algorithm empirically-derived by Mackay et al. (1980; 1982). Sensitivity analyses of this algorithm led to the discovery that the solution was affected by the number of spillets used. Therefore, a formulation was derived to normalize the solution under differing numbers of surface spillets (Kolluru et al. 1994). Spreading is stopped when an oil-specific terminal thickness is reached.

3.1.3.4 Evaporation

The rate of evaporation depends on surface area, thickness, vapour pressure, and mass transport coefficient, which, in turn, are functions of the composition of the oil, wind speed, and temperature (Fingas 1996; 1997; 1998; 1999; Jones 1997). As oil evaporates, its composition changes, affecting its density and viscosity, as well as subsequent evaporation. The most volatile hydrocarbons evaporate most rapidly, typically in less than a day and sometimes in less than an hour (McAuliffe 1989). As the oil continues to weather, and particularly if it forms a water-in-oil emulsion, evaporation will be significantly decreased.

The evaporation algorithm in SIMAP™ is based on accepted evaporation theory, which follows Raoult's Law that each component will evaporate with a rate proportional to the saturation vapour pressure and mole fraction present for that component. The pseudo-component approach (Payne et al. 1984; French et al. 1996; Jones 1997; Lehr et al. 2000) is used, such that each component evaporates according to its mean vapour pressure, solubility, and molecular weight. The mass transfer coefficient is calculated using the methodology of Mackay and Matsugu (1973), as described in French et al. (1996).

3.1.3.5 Entrainment

As oil on the water surface is exposed to wind and waves, or if oil moves into a turbulent area of a stream or river, it is entrained (or dispersed) into the water column. Entrainment is a physical process whereby globules of oil are transported from the water surface into the water column due to breaking waves or other turbulence. It has been observed that entrained oil is broken into droplets of varying sizes. Smaller droplets spread and diffuse in the water column, while larger ones rise back to the surface.

Entrainment by Breaking Surface Wave Action

In open waters, breaking waves created by the action of wind and waves on the water surface are the primary sources of energy for entrainment. Entrainment is strongly dependent on turbulence and is greater in areas of high wave energy (Delvigne and Sweeney 1988).

Delvigne and Sweeney (1988), using laboratory and flume experimental observations, developed a relationship for entrainment rate and oil droplet size distribution as a function of turbulent energy level and oil viscosity. Entrained droplets in the water column rise according to Stokes law, where velocity is related to the difference in density between the particle and the water, and to the particle diameter. The data and relationships in Delvigne and Sweeney (1988) are used in SIMAP™ to calculate mass and particle size distribution of droplets entrained. Particle size decreases with higher turbulent energy level

and lower oil viscosity. The natural dispersion particle sizes observed by Delvigne and Sweeney (1988) are confirmed by field observations by Lunel (1993a; 1993b).

Use of chemical dispersants (not modeled in the scenarios examined here, nor likely to occur in freshwater) decreases the median particle size, increasing the number of droplets in the < 70 μm range (Daling et al. 1990; Lunel 1993a; 1993b). Particle size distributions for dispersed oil are available for several oils from these studies. When dispersant is applied, the model entrains surface oil, creating subsurface droplets in the appropriate size distribution for dispersant use. The median particle size for permanently dispersed droplets is set at 20 microns, the median size observed by Lunel (1993a; 1993b). The fraction of oil permanently dispersed is set by the assumed dispersant efficiency. The IKU/SINTEF studies provide data on the viscosity range where oils may be dispersed chemically. Typically, dispersants are effective up to about 10,000 cP (centipoise) (Aamo et al. 1993; Daling and Brandvik, 1988; 1991; Daling et al. 1997). In the model, oil is dispersed up to 10,000 cP.

Entrained oil is mixed uniformly throughout the wave-mixed zone. Vertical mixing is simulated by random placement of particles within the wave-mixed layer each time step. Settling of particles does not occur in water depths where waves reach the bottom (taken as 1.5 times wave height). Wave height is calculated from wind speed, duration, and fetch (distance upwind to land), using the algorithms in CERC (1984). Wave height is on the scale of centimeters in small rivers and streams and near lee shorelines; whereas it may increase to meters in open waters under windy conditions.

Entrainment by Bottom Roughness in Streams

When modeling oil spills in rivers, entrainment of oil into the water column by turbulent flow over bottom structures and around obstacles must be taken into consideration. It is clear that in rapid flow where turbulence is large, rocks or other obstacles may break the surface and a plunging wake may occur where the possibility of entrainment increases. Delvigne (1993) demonstrated that breaking wave dispersion to fast flow past an obstacle, such as a pile, generates a plunging wake. This is sufficiently similar to breaking waves from alternative sources of turbulence such as the fast flow past an obstacle, flow over a dam, cataract with a hydraulic jump, or a ship crossing an oil slick. In the breaking wave model, the dispersion of energy leads to the plunging of oil into water and the formation of oil droplets. To relate this more generally to a river formulation, an energy dissipation relationship was developed. In this formulation, energy dissipation is proportional to the stream flow rate and bottom roughness, and is inversely proportional to the local depth. The generation and propagation of turbulent energy through the water column due to bottom roughness is applied with a typical quadratic stress equation to the plunging flow (Anderson et al. 1995). The dispersed mass of oil is determined by scaling the surface area covered by oil at the dispersion source and the range of oil droplet sizes, which is a function of the dispersion energy.

3.1.3.6 Emulsification (Mousse Formation)

The formation of water-in-oil emulsions, or mousse, depends on oil composition and turbulence level. Emulsified oil can contain as much as 80 percent water in the form of micrometer-sized droplets dispersed within a continuous phase of oil (Daling and Brandvik 1988; Fingas et al. 1997). Viscosities are typically much higher than that of the parent oil. The incorporation of water also dramatically increases the oil/water mixture volume.

The Mackay and Zagorski (1982) emulsification scheme is implemented in SIMAP™ for floating oil. Water content increases exponentially, with the rate related to the square of wind speed and previous water incorporation. Viscosity is a function of water content. The change in viscosity feeds back in the model to the entrainment rate.

3.1.3.7 Dissolution

Dissolution is the process by which soluble hydrocarbons enter the water from a surface slick or from entrained oil droplets. The lower molecular weight hydrocarbons tend to be both more volatile and more soluble than those of higher molecular weight. For surface slicks, because the partial pressures tend to exceed the solubilities of these lower molecular weight compounds, evaporation accounts for a larger portion of the mass than dissolution (McAuliffe 1989), except perhaps under ice. Dissolution and evaporation are competitive processes. The dissolved component concentration of hydrocarbons in water under a surface slick shows an initial increase followed by a rapid decrease after some hours due to the evaporative loss of components. Most soluble components are also volatile and direct evaporation (volatilization) from the water column depletes their concentrations in the water. Dissolution is particularly important where evaporation is low (dispersed oil droplets and ice-covered surfaces). Dissolution can be significant from entrained droplets because of the lack of atmospheric exposure and because of the higher surface area per unit of volume.

The model developed by Mackay and Leinonen (1977) is used in SIMAP™ for dissolution from a surface slick. The slick (spillet) is treated as a flat plate, with a mass flux (Hines and Maddox 1985) related to solubility and temperature. It assumes a well-mixed layer with most of the resistance to mass transfer lying in a hypothetical stagnant region close to the oil. For subsurface oil, dissolution is treated as a mass flux across the surface area of a droplet (treated as a sphere) in a calculation analogous to the Mackay and Leinonen (1977) algorithm. The dissolution algorithm was developed in French et al. (1996).

3.1.3.8 Volatilization from the Water column

The procedure outlined by Lyman et al. (1982), based on Henry's Law and mass flux (Hines and Maddox 1985), is followed in the SIMAP™ fates model. The volatilization depth for dissolved substances is

limited to the maximum of one-half the wave height. Wave height is computed from the wind speed and fetch (CERC 1984). The volatilization algorithm was developed in French et al. (1996).

3.1.3.9 Adsorption and Sedimentation

Aromatics dissolved in the water column are carried to the sediments primarily by adsorption to suspended particulates and subsequent settling. The ratio of adsorbed (C_a) to dissolved (C_{dis}) concentrations is computed from standard equilibrium partitioning theory as

$$C_a / C_{dis} = K_{oc} C_{ss}$$

K_{oc} is a dimensionless partition coefficient and C_{ss} is the concentration of SPM in the water column expressed as mass of particulate per volume of water. As a default, the model uses a mean value of total suspended solids of 10 mg/l (Kullenberg 1982); alternatively suspended sediment concentration is specified as model input.

Sedimentation of oil droplets occurs when the specific gravity of oil increases over that of the surrounding water. Several processes may act on entrained oil and surface slicks to increase density: weathering (evaporation, dissolution and emulsification), adhesion or sorption onto suspended particles or detrital material, and incorporation of sediment into oil during interaction with suspended particulates, bottom sediments, and shorelines. Rates of sedimentation depend on the concentration of suspended particulates and the rates of particulate flux into and out of an area. In areas with high suspended particulate concentrations, rapid dispersal and removal of oil is found due to sorption and adhesion (Payne and McNabb 1984).

Kirstein et al. (1987) and Payne et al. (1987) used a reaction term to characterize the water column interactions of oil and suspended particulates. The reaction term represents the collision of oil droplets and suspended matter, accounting for both oiled and unoiled particulates. The model formulation developed by Kirstein et al. (1987) is used to calculate the volume of oil adhered to particles. In the case where the oil mass is larger than the adhered sediment (i.e., the sediment has been incorporated into the oil), the buoyancy of the oil droplet will control its settling or rise rate. The Stoke's law formulation is used to adjust vertical position of these particles. If the mass of adhered droplets is small relative to the mass of the sediment it has adhered to, the sediment settling velocity will control the fate of the combined particulate.

3.1.3.10 Degradation

Degradation may occur as the result of photolysis or photo-oxidation, which is a chemical process energized by ultraviolet light from the sun, and by microbial breakdown, termed biodegradation. In the model, degradation occurs on the surface slick, deposited oil on the shore, the entrained oil and

aromatics in the water column, and oil in the sediments. A first order decay algorithm is used, with a specified (total) degradation rate for each oil type: surface oil, water column oil, and sedimented oil (French et al. 1999).

3.1.4 SIMAP Model Physical Fates Output Description

The physical fates model creates output files recording the distribution of a spilled substance in three dimensional space and time. The quantities recorded are:

- Cumulative area covered by oil and thickness on the water surface ("swept area")
- Volumes in the water column at various concentrations of dissolved aromatics
- Volumes in the water column at various concentrations of total hydrocarbons in suspended droplets
- Total hydrocarbons and aromatic mass in surface sediment
- Lengths and location of shoreline affected by oil, and volume of oil ashore in each shoreline segment

The dissolved aromatic hydrocarbon concentration in the water column is calculated from the mass in the Lagrangian elements, as follows. Concentration is contoured on a three-dimensional Lagrangian grid system. This grid is scaled at each time step to cover the volume occupied by aromatic particles, including the dispersion around each particle center. This maximizes the resolution of the contour map at each time step and reduces error caused by averaging mass over large cell volumes. Distribution of mass around the particle center is described as Gaussian in three dimensions, with one standard deviation equal to twice the diffusive distance ($2D_xt$ in the horizontal, $2D_zt$ in the vertical, where D_x is the horizontal and D_z is the vertical diffusion coefficient, and t is particle age). The plume grid edges are set at one standard deviation away from the outermost particle. These data are used by the biological impacts model to evaluate exposure, toxicity and acute impacts.

3.2 SIMAP Biological Impacts Model for Evaluating Acute Toxic Impacts

The SIMAP™ biological exposure model estimates the volume and area of water (and stream length, as appropriate) affected by surface oil, concentrations of oil components in the water, and sediment contamination. Then the SIMAP™ biological impacts model estimates losses resulting from acute exposure after a spill (i.e., losses at the time of the spill and while acutely toxic concentrations remain in the environment) in terms of direct mortality.

The area potentially affected by the spill is represented by a rectangular grid with each grid cell coded by habitat type. Habitat types are defined by depth, proximity to shoreline(s), bottom/shore type, and dominant vegetation type. The habitat grid is also used by the physical fates model to define the

shoreline location and type, as well as habitat and sediment type. A habitat is an area of essentially uniform physical and biological characteristics that is occupied by a group of organisms that are distributed throughout that area. A contiguous grouping of habitat grid cells represents an ecosystem in the biological model. The density of fish, invertebrates, wildlife, and rates of lower trophic level productivity are assumed constant for the duration of the spill simulation and evenly distributed across an ecosystem. While biological distributions are known to be highly variable in time and space, data are generally not sufficient to characterize this patchiness. Because oil is also patchy in distribution, the patchiness is assumed to be on the same scale so that the intersection of the oil and biota is equivalent to overlays of spatial mean distributions.

3.2.1 Aquatic Biota

In the model, aquatic biota (e.g., fish, invertebrates) are affected by dissolved aromatic concentrations in the water or sediment. This rationale is supported by the fact that soluble aromatics are the most toxic constituents of oil (Neff et al. 1976; Rice et al. 1977; Tatem et al. 1978; Neff and Anderson 1981; Malins and Hodgins 1981; National Research Council (NRC) 1985; 2002; Anderson 1985; French McCay 2002). Exposures in the water column are short in duration and impacts are the result of acute toxicity. In the sediments, exposure can be both acute and chronic, as the concentrations may remain elevated for longer periods of time.

The model evaluates mortality and sublethal impacts of dissolved aromatic concentrations in the water or sediment. Mortality is a function of duration of exposure—the longer the duration of exposure, the lower the impacts concentration (see review in French McCay 2002). At a given concentration after a certain period of time, all individuals that will die, will have done so. The LC50 is the lethal concentration at which 50 percent of exposed organisms will die, for a specified duration of exposure. The cumulative percent mortality is a log-normal function of concentration, with the LC50 located at the mid-point of the distribution (Figure 3-2). The incipient LC50 ($LC50_\infty$) is the asymptotic LC50 reached after infinite exposure time (or long enough that that level is approached).

French McCay (2002) provides estimates of $LC50_\infty$ for MAH and PAH mixtures in fuel and crude oils for spills under different environmental conditions. Figure 3-2 plots LC50s for total dissolved PAHs for species of average sensitivity under turbulent conditions ($LC50_\infty$ = 50 μg/L) for a range of exposure durations and temperatures. The $LC50_\infty$ for 95 percent of species fall in the range 5 to 400 μg/L parts per billion (ppb). This oil toxicity model has been validated using laboratory oil bioassay data (French McCay 2002).

In SIMAP™, $LC50_\infty$ for the dissolved aromatic mixture of the spilled oil is input to the model. For each aquatic biota behavior group, the model evaluates exposure duration and corrects the LC50 for time of

exposure and temperature to calculate mortality (Figure 3-2). The oil toxicity model is described in the next section, and in detail in French McCay (2002).

Mortality is calculated as percent loss in specified areas. This is translated into the equivalent area of 100-percent loss. That area is divided by the total area of habitat available in the region of interest to estimate a percentage of the population in the area affected. The percent mortality of the exposure group is multiplied by abundance at the time exposed and in the habitat type to calculate the species' mortality as numbers of individuals or biomass (kg).

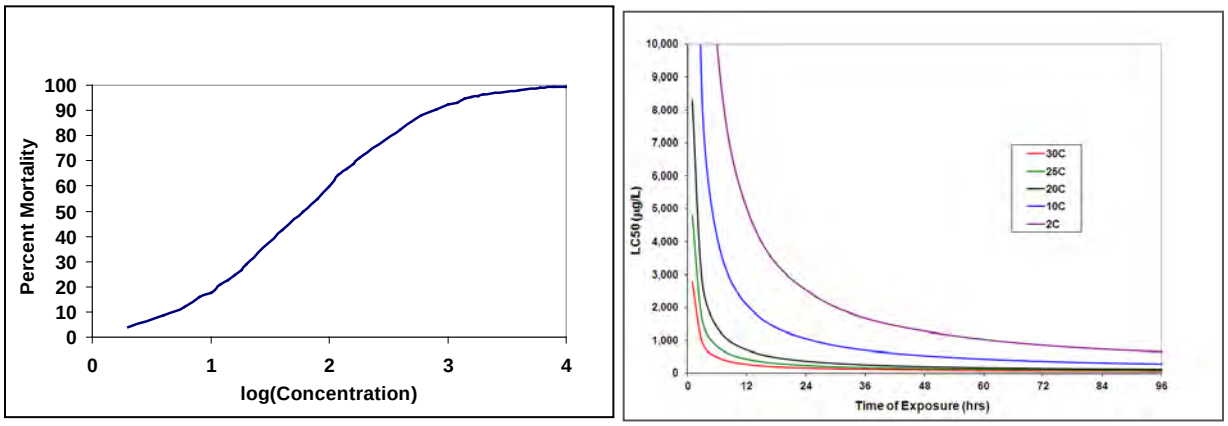

Figure 3-2: Illustration of percent mortality as a function of concentration (left). The LC50 is at the center of the log-normal function, aligning with 50-percent mortality. The LC50 of dissolved oil PAH mixtures as a function of exposure duration and temperature (right).

3.2.2 Oil Toxicity

The following describes the oil toxicity model, OilToxEx, used in the SIMAP exposure model. The full development of OilToxEx and data on which it is based are in French McCay (2001; 2002). This uses the accepted Toxic Units (TU) approach for organic compounds, including MAHs and PAHs, where the primary acute impact is narcosis (Bradbury et al. 1989). The approach was used by the U.S. Environmental Protection Agency (USEPA) for development of PAH water and sediment quality criteria (Di Toro et al. 2000; Di Toro and McGrath 2000; USEPA 2003; 2008). The oil toxicity model has been validated using laboratory oil bioassay data for both fresh and saltwater organisms (French McCay 2002) and for lobster mortality in the case of the *North Cape* spill (French McCay 2003). The underlying toxicity data used to develop the model is based on bioassays for freshwater and marine fish, invertebrate and

algal species at a variety of life stages. Below is a summary of the oil toxicity analysis in French McCay (2001; 2002).

The most toxic components of oil to pelagic (fish, plankton, amphibians) and benthic (invertebrates, algae) organisms are lower molecular-weight compounds, which are both volatile and soluble in water, especially the aromatic compounds (Anderson et al. 1987; French et al. 1996; French McCay 2001; 2002; 2003). It has been shown that toxicity of narcotic organic compounds, such as these lower molecular-weight aromatics in oil (MAHs and PAHs), is related to the octanol-water partition coefficient (K_{ow}), a measure of hydrophobicity (Nirmalakhandan and Speece 1988; Hodson et al. 1988; Blum and Speece 1990; McCarty 1986; McCarty et al. 1992a; Mackay et al. 1992; McCarty and Mackay 1993; Varhaar et al. 1992; Swartz et al. 1995; French et al. 1996; French McCay 2001; 2002; 2003). Chemicals that have a narcotic mode of action affect organisms by accumulating in lipids (such as in the cell membranes) and disrupting cellular and tissue function. At the same time, however, the more hydrophobic a compound is, the more it accumulates in the tissues, and the more severe its impact. However, the more hydrophobic the compound, the less soluble it is in water, and so the less available it is to aquatic organisms. Compounds of $\log(K_{ow}) > 5.6$ are virtually insoluble, and so are not bioavailable and therefore make no meaningful contribution to the acute toxicity of hydrocarbon mixtures to aquatic biota (French McCay 2001; 2002). Biological impacts are the result of a balance between bioavailability (dissolved-component exposure) and toxicity once exposed.

The acute toxic impacts of narcotic chemicals, including lower molecular weight aromatics, are additive (Swartz et al. 1995; French et al. 1996; Di Toro et al. 2000; Di Toro and McGrath 2000; French McCay 2001; 2002; 2003). The Toxic Unit (TU) model is used to estimate the toxicity of a mixture of narcotic chemicals. A TU is defined as the exposure concentration divided by the LC50 (lethal concentration to 50 percent of exposed organisms). For a mixture, the TUs are additive. When Σ TU = 1, the mixture is lethal to 50 percent of exposed organisms.

It has been shown (French et al. 1996; French McCay 2001; 2002) that the LC50 of the mixture ($LC50_{mix}$) is related to the LC50 of each chemical (i) in the mixture and the dissolved concentration of chemical i in the total mixture:

$$F_i = C_{w,i} / (\Sigma C_{w,i})$$

$$LC50_{mix} = 1 / \Sigma (F_i / LC50_i)$$

where $C_{w,i}$ is the dissolved concentration of chemical i in the water. The values of F_i may be measured in the field or F_i may be estimated from data on oil composition. It has been shown that for turbulent surface waters where entrainment of oil has occurred, the values of F_i are nearly proportional to the source oil aromatic composition. The values of $LC50_i$ can be estimated using regression models relating

LC50 to K_{ow} (French McCay 2001; 2002). The 95-percent confidence range of this regression provides LC50s for average (50th percentile), sensitive (2.5th percentile), and insensitive (97.5th percentile) species. This oil toxicity model is used to estimate the LC50 for the dissolved aromatic mixture originating from the spilled oil. Only the soluble compounds of $\log(K_{ow}) \leq 5.6$ are included in the additive toxicity model.

Toxicity varies with the duration of exposure, with the LC50 decreasing as exposure time increases (Sprague 1969; Kooijman 1981; McAuliffe 1987; Anderson et al. 1987; French and French 1989; French 1991; McCarty et al. 1989; 1992a; 1992b; Mackay et al. 1992; French et al. 1996). This is due to the accumulation of toxicant over time up to a critical body residue (tissue concentration) that causes mortality. The accumulation is faster at higher temperatures such that LC50 at a given (short) exposure time decreases with increasing temperature.

The following algorithm was developed in French McCay (2001; 2002). The LC50 of an aromatic in the oil mixture varies with exposure time and temperature according to:

$$LC50_{\infty} = LC50_t\,(1 - e^{-\varepsilon t})$$

$$\log_{10}(\varepsilon) = \varepsilon_1 - \varepsilon_2 \log_{10}(K_{ow})$$

$$d\varepsilon / dT = \tau\, T$$

where t is time of exposure, $LC50_t$ is LC50 at time t, $LC50_{\infty}$ is LC50 at infinite time of exposure, K_{ow} is the octanol-water partition coefficient, ε_1 =1.47 and ε_2 = 0.414, T = temperature (˚C), and τ = 0.11 (French McCay 2002).

LC50s for MAHs and PAHs from the literature were corrected for time and temperature of exposure to calculate $LC50_{\infty}$. The QSAR (Quantitative Structure Activity Relationship) regression for narcotic aromatics in oil was developed:

$$\log_{10}(LC50_{\infty}) = \log_{10}(\phi) + \gamma \log_{10}(K_{ow})$$

For 278 bioassays on individual aromatics, the slope and intercept of the regression are: $\log_{10}(\phi)$ = 4.8926 and γ = -1.0878. This QSAR describes the mean response for all species (i.e., the response of the average species) and the slope of this relationship is constant for all species (see Di Toro et al. 2000 for theory). The intercept varies by species, with 95 percent of species falling within the range $\log_{10}(\phi)$ = 3.9704 (sensitive species) and $\log_{10}(\phi)$ = 5.8147 (insensitive species). The above equation may be used to estimate $LC50_{\infty}$ for any aromatic, assuming an appropriate intercept for the species of concern.

The SIMAP™ exposure model takes into account the time and temperature of exposure, using the rearrangement of the above: $LC50_t = LC50_{\infty} / (1 - e^{-\varepsilon t})$ to correct the LC50. Time of exposure is evaluated

by tracking movements of organisms' relative concentrations greater than the concentration lethal to 1 percent of exposed organisms (LC1, approximated as 1 percent of $LC50_{\infty}$). Stationary or moving Lagrangian tracers that represent organisms record the concentrations of exposure over time and the dose (summed concentration times duration) to an organism represented by that behavior. Exposure time is the total time concentration exceeds LC1. The concentration is the average over that time, or total dose divided by exposure time. The percent mortality is then calculated using the log-normal function centered on $LC50_t$.

BTEX (benzene + toluene + ethybenzene + xylene) is very soluble in water, so exposure concentrations can be high. However, BTEX is only moderately hydrophobic (so relatively low in toxicity) and it is also very volatile. Thus, the BTEX rapidly volatilizes reducing exposure concentrations. For these reasons, the impacts due to BTEX after a spill are typically low and of short duration, except potentially for very light fuels such as gasoline or jet fuel, which may contain high percentages of BTEX.

PAHs and many of the alkyl-substituted benzenes are less soluble than BTEX, but do dissolve in significant bioavailable quantities. Because they are more hydrophobic than BTEX, they more strongly partition into the lipids in membranes and tissues. Thus, they are more toxic and can have significant impacts on aquatic organisms.

Lower molecular-weight aliphatic hydrocarbons (e.g., alkanes and cycloalkanes with boiling points less than about 380°C) may also contribute to toxicity after an oil spill. However, the aliphatics are more volatile (have higher vapor pressure), are less soluble than aromatics of the same molecular weight (Mackay et al. 1992) and would be more readily lost to the atmosphere from surface waters. They are also less toxic than the aromatics of similar molecular weight (French McCay 2001; 2002). Anderson et al. (1981) and Anderson (1985) found that 98 percent of the dissolved hydrocarbons in oil and water dispersions were aromatics (MAHs and PAHs).

The residual fraction in the model is composed of nonvolatile and relatively insoluble compounds that remain in the "whole oil" that spreads, is transported on the water surface, strands on shorelines, and disperses into the water column as oil droplets or remains on the surface as tar balls. This is the fraction that comprises black oil, mousse, and sheen. In the model, it is assumed not to be bioavailable or acutely toxic to aquatic biota, although it may have acute impacts on wildlife species and contribute to chronic impacts on aquatic biota.

The $LC50_{mix}$ of aromatic mixtures from oil were calculated using the additive model, including those aromatics that are measured in the oil and dissolved in the water (with log (K_{ow}) $\leq$ 5.6) long enough for exposure to aquatic organisms to be significant. Typically, only the PAHs are dissolved in sufficient quantity and remain in the water long enough for their TU values to be significant. The biological

impacts model uses the calculated ΣPAH (or ΣBTEX + ΣPAH if BTEX is significant) and the estimated $LC50_{mix}$ corrected for time and temperature of exposure to estimate mortality to aquatic biota. Typically, the appropriate $LC50_{mix}$ for most species is the average sensitivity, as specific data are not available for all species and the most likely LC50 for an untested species would be the mean of the observations for other species. However, for certain species known to be sensitive to organics with a narcotic mode of action, the sensitive 2.5th or some other percentile $LC50_{mix}$ may be more appropriate. Categorization of species as sensitive, average, or insensitive may be based on bioassay data reviewed in French McCay (2001) or similar data indicating the percentile of the species' sensitivity to the narcotic lower molecular weight aromatics in oil.

The dissolved concentrations are estimated by the fates model for both the water column and sediments. Dissolved concentrations in the water column result mainly from dissolution of entrained oil droplets, as the soluble compounds evaporate faster from surface slicks. In the sediments, dissolved concentrations in pore waters are calculated using the equilibrium partitioning model. Exposure and mortality of benthic organisms are a function of the dissolved concentrations in pore water. This methodology has been validated by Swartz et al. (1995) and used in sediment quality criteria for PAHs (Di Toro et al. 2000; USEPA 2003; 2008).

3.2.3 Wildlife

The likelihood of encounter with oil will be different for each wildlife type depending on specific wildlife behavior. For example, terrestrial mammals and birds that do not feed in aqueous habitats would likely avoid the oil, except for those attracted to carrion (e.g., foxes, coyotes, wolverines, bald eagles). Scavengers and wildlife that obtain part of their diet from aquatic habitats (e.g., racoons, moose) would have a moderate probability of becoming oiled. Aquatic mammals (e.g., muskrat, beaver, otter, and mink), waterfowl, wading birds, and turtles would have a high likelihood of being oiled.

In this report, "wildlife" includes the air-breathing vertebrates that occupy primarily terrestrial habitats but also interact with the aquatic environment. Accordingly, wildlife includes birds, mammals, reptiles, and adult stages of amphibians. The potential impacts on wildlife that are in the spill-affected area are evaluated based on the probability of encounter with floating and/or shoreline oil and the amount of oil that is likely to accumulate on an individual animal. The threshold of oil thickness that would impart a lethal dose to intersecting wildlife is 10 microns (~10 g/m^2), based on literature reviews by Engelhardt (1983), Clark (1984), Geraci and St. Aubin (1988), Jenssen (1994) and other oil impacts literature on aquatic birds and marine mammals. Varoujean et al. (1983) state that 1 g/m^2 of oil on the water surface is 100-percent lethal to birds when confined to the oil slick in an enclosure, while 0.1 g/m^2 is not enough to cause acute mortality. Peakall et al. (1985) state that blue sheen oil < 1 µm thick (NRC 1985) is not

harmful to seabirds. Jenssen and Ekker (1991a; 1991b) studied the impacts of exposure of eiders to oil at various doses. The required dose for an impact on metabolism was > 20 mL of crude oil on the skin or feathers, with hydrocarbons being adsorbed directly and ingested via preening. However, their literature review revealed that an order of magnitude more oil is the required dose for significant and potentially lethal impacts.

Birds incubating eggs can transfer oil to the egg from their plumage (Albers and Szaro 1978; King and Lefever 1979; Albers 1980). Clutches of common eider eggs treated with 20 μL of fuel oil had significantly greater embryonic mortality than control clutches (Albers and Szaro 1978). Hatching success was significantly reduced for mallards with plumage exposed to 100 mL/m^2 (0.1 mm) of Prudhoe Bay crude oil for 48 hours while incubating eggs, whereas the reduction in hatching success was not significant at 5 mL/m^2 of oil exposure. However, survival rates of newly hatched ducklings and adults exposed to up to 100 mL/m^2 oil were not significantly lowered (Albers 1980). Mortality rates of mallard eggs treated with 1 and 5 μL South Louisiana crude oil were 35 percent and 91 percent, respectively. For chicken eggs, with applications of 1, 5, and 10 μL of oil, mortality rates were 38 percent, 80 percent, and 98 percent, respectively (Hoffman 1978). As these amounts of oil covered only small fractions of the eggshell surface, impacts were likely due to chemical toxicity and not to physical causes such as reduced gas exchange rates.

To determine the impacts on mammalian receptors, Wolfe and Esher (1981) exposed rice rats to 200 mL/m^2 (~200 g/m^2) and 20 mL/m^2 (~20 g/m^2) of crude oil on the water surface. These studies were conducted in laboratory test chambers, with 1 m^2 water and two islands. In both exposures, willingness to enter the water and swim was reduced. Survival 24 hours later was significantly lowered in the higher exposure treatment. Survival rate was not measured beyond 24 hours after exposure. These results suggest that mortality would occur for other semi-aquatic mammals, such as muskrat, mink, and otter that swim through oil. River otters were observed to be killed by *Exxon Valdez* oil (Spies et al. 1996).

Little research is available to quantify oil exposure impacts on aquatic reptiles. Much of what is available regarding reptiles includes work on sea turtles, synthesized by Vargo et al. (1986). In addition to direct mechanical and chemical toxicity, impacts include reduced hatching rates and developmental deformities (Milton et al. 2003). For turtles of all ages, ingestion of tar balls is a major issue because turtles eat anything that appears to be the same size as their preferred prey. Ingestion can result in starvation from gut blockage, decreased absorption efficiency, absorption of toxins, buoyancy problems from buildup of fermentation gasses, and other impacts (Milton et al. 2003). Inhalation of vapor is also of concern for turtles. Sea turtles have not been shown to exhibit avoidance behavior when surrounded by petroleum fumes (Milton et al. 2003) and presumably freshwater turtles would behave similarly.

The SIMAP model uses an estimate of the minimum external dose of oil that is lethal. During testing that was conducted, there was one observation of a 70 mL dose causing a significant change in metabolic rate; however, 200 to 500 mL has been observed as the lethal dose when applied to the plumage of ducks (Jenssen 1994). In the SIMAP model, 350 mL is assumed to be the lethal dose for all wildlife. Assuming that a swimming bird has a width of 15 cm, it would need to swim through 23 m of oil of 100 µm thickness, 230 m of oil of 10 µm thickness, or 2300 m of oil of 1 µm thickness, to obtain a dose of 350 milliliters (mL). This distance spent in oil need not be in a straight line. If an animal swims at a rate of 10 m/min, then 23 m would be covered in about 2 minutes. Carrying this calculation forward, 230 m would be covered in 23 min and 2300 m would be covered in 230 min (3.8 hours). A slick thickness of 10 µm is assumed as a threshold thickness for oiling mortality, given the sizes of the water bodies involved and likely exposure times of animals within them (French McCay 2009). Those animals oiled above a threshold lethal dose may die, given the environmental temperatures involved and the possibility that timely capture and treatment may not be possible.

3.2.4 SIMAP Model Biological Output Description

The biological impacts model (French et al. 1996; French McCay 2003; 2004; 2009) estimates short-term (acute) exposure of biota to floating oil and subsurface oil contamination (in-water and sediments), and predicts the resulting percent mortality. Toxicity to aquatic biota in the water column and sediments is estimated from dissolved aromatic concentrations and exposure duration, using laboratory-based bioassay data for oil hydrocarbon mixtures (French McCay 2002). In each habitat grid cell, acute toxicity to aquatic biota in water column and demersal (bottom 1 meter of the water immediately above the sediments) habitats are evaluated by tracking exposure for these different behaviour groups. In the rivers, where water depths are near or less than 1 m, the affected areas for water column and demersal biota are the same. Areas in which impacts on wildlife might occur are estimated based on the area swept by surface oil over a threshold thickness for acute toxic impacts.

The dissolved aromatic modeling results for all fates scenarios were post-processed to analyze the extent of dissolved aromatic concentrations and the potential for impacts on aquatic organisms (e.g., fish, invertebrates, algae, amphibians). The threshold value for species toxicity in the water column is based on global data from French McCay (2002), which showed that species sensitivity to dissolved aromatics exposure > 4 days (96 hour LC50) varied from 5 to 400 µg/L (ppb) with an average of 50 µg/L. This range covered 95 percent of aquatic organisms (fish, invertebrates and eggs) tested. Biological impacts were evaluated for species with high sensitivity to dissolved aromatics (e.g., 5 µg/L level) to indicate a protection of 97.5 percent of species, and for species with an average sensitivity to dissolved aromatics (e.g., 50 µg/L level) to indicate average losses.

The results of the biological exposure model provide estimates of the equivalent area (in km^2) of 100-percent mortality by behavior group for wildlife and fish/invertebrates. Potential acute impacts following a release can vary greatly by space, time, and percent kill. In some cases, 100-percent mortality may be experienced in some localized regions, while much broader areas may experience only partial impacts (e.g. 10-percent mortality). To normalize results, the equivalent areas of 100-percent predicted mortality were estimated for both the surface/shoreline and in the water column. This implies that the equivalent area of 100-percent mortality would be the same for a release that resulted in 100-percent mortality over 1 km^2 versus 1-percent mortality over 100 km^2. This example is an oversimplification; however, as the SIMAP model will predict the likely percent mortality by grid cell for the entire modeled domain.

It should be noted that injury resulting from nonacute mortality due to a spill (e.g., chronic impacts, delayed mortality such as reduced cardiac fitness (Incardona et al. 2015)) are not accounted for in the exposure model. Therefore, the results predicted by the biological exposure model may be considered underestimates for fish and wildlife. This metric was evaluated for both pelagic and demersal species, benthic and planktonic organisms, and other avian, wildlife, and mammalian receptors.

The area of potential impacts on wildlife is presented as the area of the open water or shoreline that was covered by oil above the thickness threshold for acute impacts at any time during the scenario. In this case, the threshold thickness was 10 µm. It is important to note that this area does not imply direct impacts on all wildlife in that area because the actual impacts will be different for each wildlife type depending on the percent likelihood of encountering oil, which is based on behavior.

3.3 OILMAP Land Overland Flow Modeling

The RPS ASA OILMAP Land™ two-dimensional spill modeling system was used to simulate the overland flow of release from Edmonds Ferry Terminal site, to predict the locations where oil from a derailment at this land-based site would enter Puget Sound. Once in Puget Sound, the oil fate and transport was modeled using SIMAP™, as it was for the other two release locations. The purpose of the overland flow modeling is to estimate the downslope path and loss of oil to the land surface to calculate the volume of oil that would likely reach the nearby waterway.

3.3.1 OILMAP Land Model Description

The OILMAP Land™ model simulates the flow of oil or chemicals over land from a given container rupture point (i.e., derailed train car). The release is modeled as it propagates over the land surface and into any surface water network until the entire amount of product is released. Oil flow over land is governed by the physical characteristics and slope of the land surface. The overland model calculates an

oil mass balance that includes losses from oil adhesion to land over the oiled path, the formation of small puddles, oil pooling in large depressions on the land surface, and oil evaporation to the atmosphere.

When oil reaches a waterway, the water transport model simulates the downstream movement of oil on the water surface in streams (or drainage pipes, as in this project) at a defined velocity. As oil moves downstream, estimates of the amount of oil lost to the shore from adhesion and to the atmosphere by evaporation are made. Any oil entering a lake is allowed to spread over the water surface of the lake in a radial pattern to a minimum thickness that reflects the density and viscosity of the released oil.

While OILMAP Land™ does provide an indication of the downstream extent of oiling and mass balance of oil within the modeled 24-hour period, it is not able to provide detailed predictions of three-dimensional oil fate and transport. These processes, such as entrainment of oil into the water column, dissolution of soluble fractions of hydrocarbons, emulsion formation, potential biological impacts from exposure to oil, and other complex interactions, were modeled within SIMAP™ after spill sites and volumes were identified from the OILMAP Land ™ output.

3.3.1.1 Overland Release Model

In OILMAP Land ™, the overland flow of oil is simulated using a square land elevation grid. Starting at the release location, the model searches the eight neighboring cells to determine the steepest down slope direction. The adjacent cell with the lowest elevation becomes the next starting location (Figure 3-3). This process repeats successively until a flat or depression area is reached. In a flat area, the model searches beyond adjacent cells to determine the minimum distance path to a next lowest cell. In a depression area, the area is assumed to fill with liquid until the elevation of the surface of the pool equals the elevation of a grid cell on its boundary. At this point, the boundary of the pool is breached and the grid cell becomes the next starting point for further downslope movement of oil. The lowest elevation cell becomes the next starting location.

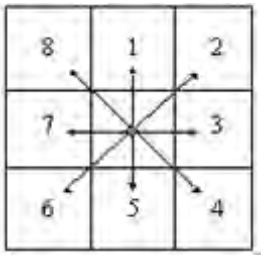

Figure 3-3: Diagram showing how the OILMAP Land™ model searches the eight neighboring cells to determine the steepest downslope gradient and resulting direction of flow.

As a release path is established, the release area is calculated and the loss of oil is computed as a function of three processes: adherence, pooling, and evaporation, as shown in Figure 3-4. Adherence, or depression storage, is the process by which oil is lost to the ground surface and vegetation as it spreads overland. Depression storage values vary by land type (as a function of surface area and roughness) and oil type (as a function of viscosity). Depression storage represents both the puddling of oil within small surface depressions on a scale smaller than the elevation grid and physical adhesion of oil on surfaces. Pooling is a larger-scale process by which oil is trapped within depressions in the local topography (i.e., depressions that can be resolved at the resolution of the available elevation grid). Such depressions are assumed to fill with oil before additional downslope transport occurs. Evaporation is the process by which the volatile portion of the liquid oil becomes a gas that enters the atmosphere.

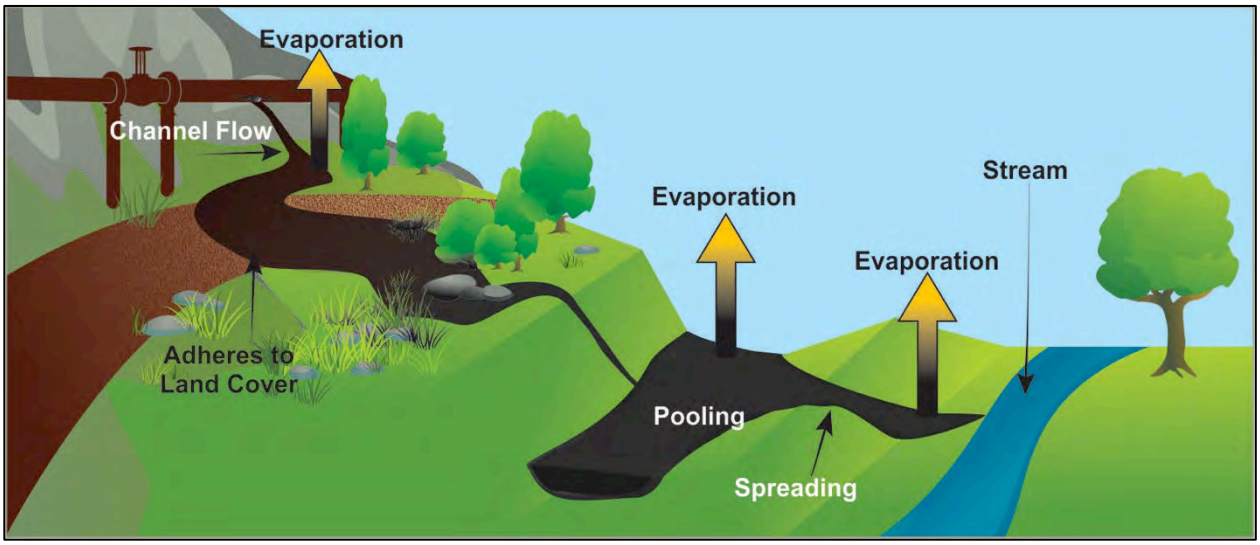

Figure 3-4: Conceptual diagram of the land transport model depicting the possible fate of oil as it moves over the land surface.

The rate of oil loss to adhesion and puddle formation depends primarily on the physical characteristics of the land surface (vegetation type, land cover, slope) and the physical and chemical characteristics of the released oil. A data grid specifying land cover type is used to determine the amount of oil retention on each grid cell. As oil traverses the land, a variable loss rate is calculated based on changes in land cover type. Oil retention loss values vary by five orders of magnitude, between 0.02 and >200 mm, based on surface hydrologic studies (ASCE 1969; Kouwen et al. 2002; Schwartz et al. 2002).

The second loss term includes oil lost to pooling on the land surface, known as depression storage or puddling. This is defined as the volume of oil that would be retained within depressions defined by the land elevation grid. Essentially, released oil would need to fill a depression before any additional oil would be allowed to travel downslope. When combined, the oil lost to the ground is the sum of adhesion and pooling.

The third loss term includes the evaporation of oil into the atmosphere. Evaporative loss depends on the chemical and physical parameters of the oil, as well as the shape of the release, and environmental conditions. Some or all of the remaining released product may evaporate.

The leading edge of a release travels with a specific velocity (V) as the oil moves over the land surface. The velocity of the oil is determined using Manning's Equation, which uses the slope of the land surface and the width of the oil plume:

$$V = 1/n\ R^{2/3}\ S^{1/2}$$

Where R is the hydraulic radius, S is the slope, and n is a dimensionless number that characterizes the flow resistance from surface roughness. The surface roughness n is 0.05 for all land types. The hydraulic radius is a slope-dependent metric of cross-sectional area of flow divided by the wetted perimeter. It is calculated iteratively at each time step and is based on flow rate. Typically, R is approximately 0.122 m, which corresponds with the velocity calculation that is dependent on slope alone:

$$V = 4.92\ S^{1/2}\ (m/s)$$

Downslope speed never reaches more than a few meters per second and has a minimum of 0.001 m/s. The maximum advance rate is limited by the release rate of the released oil.

In many cases, the elevation grid defining the land surface is not of sufficient resolution to define channels that direct the path of the oil. The width of the flow path increases as the slope decreases and downslope velocity slows. Conversely, the path width decreases to a narrower channel with increasing land surface slope and increasing downslope velocity. The model uses the land surface slope to calculate the path width of the oil, which is typically around 1 m, and cannot exceed the dimension of the land elevation grid cells.

The total volume of oil loss is equal to the sum of adherence, pooled oil, and evaporation losses. If total oil loss equals the total release volume during overland flow, then the release is terminated at this point. If the release volume is not a limiting factor, release propagation over land terminates when the leading edge encounters a surface water feature, or when the model's set duration is reached.

3.3.1.2 Surface Water Transport Model

Once the released product encounters a surface water feature, it is transported through the surface water network at a velocity defined by the speed and direction of each stream segment. As oil is transported down the surface water network, there are two potential loss terms including:

- Adhesion of the released product to the stream shoreline
- Loss of the released product through evaporation to the atmosphere

A diagram is provided to illustrate the modeled portions of the downstream release model and the factors influencing a release in surface waters (Figure 3-5).

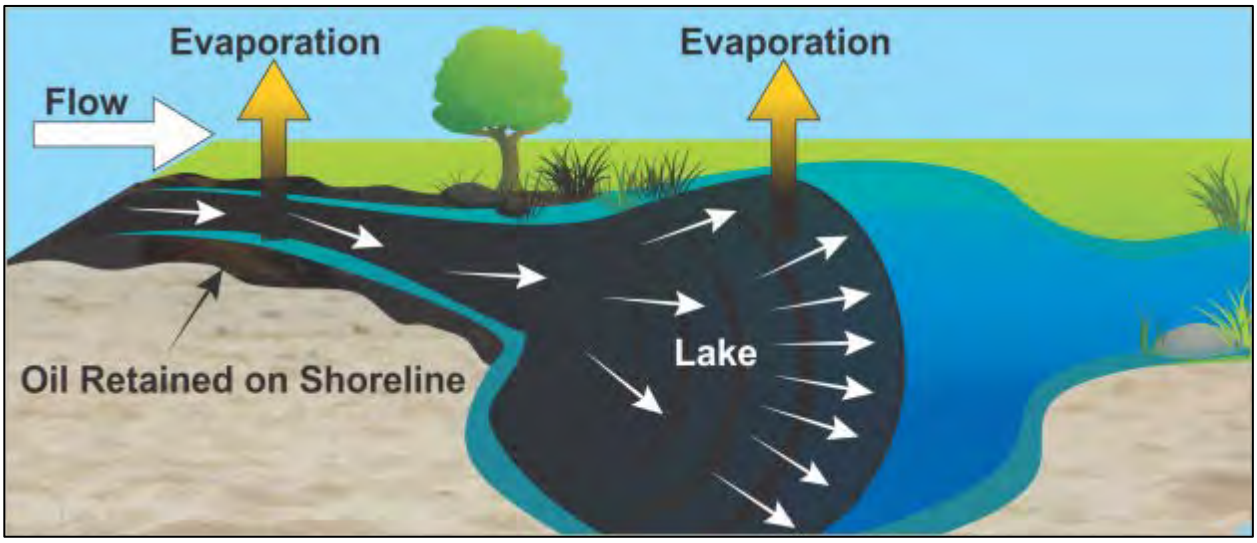

Figure 3-5: Conceptual diagram of the downstream transport model depicting the possible fate of oil entering the surface water network.

The distance oil is allowed to travel downstream is limited by one of three factors including:

- Reaching a user-specified travel time limit (i.e., model duration)
- Adherence of all available released product on the water surface to the stream bank as shoreline oiling
- Loss of all available /remaining released product to evaporation

User-specified travel times are typically defined in release response plans as the time required to respond to a catastrophic release.

The amount of oil adhering to the stream shoreline varies according to the stream shore type and oil type, which can be specified by the user. Five different stream shore types are defined, each with a specified bank width and range of oil retention thickness. Oil volume lost to the shoreline is calculated as the product of the length of the shoreline oiled, the specified bank width, and the oil retention thickness, which is controlled by the density and viscosity of the oil.

Oil movement across lakes is simulated based on lake size, shape, and water flow characteristics. Oil is assumed to spread radially across the lake surface until it covers the entire lake, or until the oil slick reaches a specified minimum thickness. If the minimum thickness is reached, spreading stops and the oil travels no farther. The minimum slick thickness is variable and is dependent on the oil type, as density, viscosity, and other chemical and physical parameters control the behavior of oil on the water surface. Typical values for minimum slick thickness range from microns (µm) to millimeters (mm). If oil covers

the entire lake surface before reaching the minimum thickness, the remaining oil is allowed to continue to move down any out-flowing streams at the velocity defined for that specific stream segment.

For the hypothetical release at the Edmonds Ferry Terminal, the stormwater drainage system data for the City of Edmonds was used to augment the path or define the path of the "surface water network" for the downslope and downstream trajectory calculations.

3.3.1.3 Evaporation

Evaporation is the process by which volatile components of the oil diffuse out of the oil and enter a gaseous phase in the atmosphere. Several simplifying assumptions are made that directly affect the amount of oil predicted to evaporate as it spreads over land and water. In general, the rate of evaporation depends on surface area, oil thickness, and vapor pressure, which are functions of the composition of the oil, wind speed, and air and land temperatures. The mass of oil evaporated is particularly sensitive to the surface area of the spreading oil and the time period over which evaporation is calculated. On the land surface, the exposed surface area and evaporation time are functions of the slope, which is defined by the elevation grid. Steeper slopes cause the oil to travel faster but along a narrower path, while a lower slope slows the speed of advance and increases the width of the oiled path. In general evaporation from surface and shoreline oil increases as the oil surface area, temperature, and wind speed increase.

In the stream network, the surface area of oiled water is a function of the total length of the oiled stream, times the average width. The total length oiled is a function of stream velocity. The surface area of the oil then defines the rate of evaporation. Oil loss to evaporation ceases once the total oil volume is released and the simulation is terminated. Termination may occur for a number of reasons including:

- Oil loss to the ground surface, stream banks, and evaporation
- The stream travel time is exceeded
- The release reaches its minimum thickness on a lake surface
- The release reaches a dead end in the stream network or the coastline

3.3.2 In reality, oil will continue to evaporate from the ground or water surface, increasing the total evaporation amount. This conservative calculation of evaporative loss is consistent with a worst-case scenario approach.

OILMAP Land Model Output Description

The output from the OILMAP Land™ model for this assessment includes the overland trajectory of oil and resulting location(s) where oil will enter Puget Sound. Two release volumes were modeled with

slightly different areal extents. Therefore, the model will provide the proportion of the total volume released at each location, should oil enter the waterway at multiple locations.

3.4 Model Uncertainty and Validation

The SIMAP™ model has been developed over many years to include as much information as possible to simulate the fates and impacts of oil spills. However, as in all science, there are limits to the complexity of processes that can be modeled, as well as gaps in knowledge regarding the environment that is affected, and the behavior of organisms and ecosystems. As described in the preceding sections, assumptions based on available scientific information and professional judgment were made in the development of the model, which represent a best assessment of the processes and potential mechanisms for impacts that could result from oil spills.

The major sources of uncertainty in the oil fates and biological impacts models are:

- Oil contains thousands of chemicals of differing physical and chemical properties that determine their fate in the environment. The model must, of necessity, treat the oil as a mixture of a limited number of components, grouping chemicals by physical and chemical properties.
- The fates model contains a series of algorithms that are simplifications of complex physical-chemical processes. These processes are understood to varying degrees.
- Biological organisms are assumed to be uniformly distributed in habitats they occupy for the duration of the spill simulation. The accuracy of this assumption varies between organism types, but the objective is to assess potential impacts for an average-expected condition, which this assumption most closely resembles.
- Biological impacts are quantified based on acute exposure and toxicity of contaminant concentrations as a function of magnitude and duration of exposure. The SIMAP™ model is not designed to address long-term, chronic exposure to pollutants.
- The model treats each spill as an isolated, singular event and does not account for any potential cumulative impacts.
- A number of physical parameters including but not limited to hydrodynamics, water depth, river width, total suspended solids concentration, wind speed, etc., were not sampled extensively at each hypothetical release location and throughout the entire modeled domain. However, in nearly all cases, the data that did exist was sufficient for this type of modeling. When data was lacking, professional judgment and previous experience was used to refine the model inputs.

In addition, in the unlikely event of an actual oil spill, the fates and impacts will be strongly determined by the specific environmental conditions, the precise locations and types of organisms present, and a myriad of details related to the event. Thus, the results are a function of the scenarios simulated and the

accuracy of the input data used. The goal of this study was not to forecast every detail that could occur, but to describe a range of possible consequences so that an informed analysis could be made as to the likely impacts of oil spills under various scenarios. The model inputs are designed to provide representative conditions to inform such an analysis for the scenarios considered.

Despite the uncertainty inherent in this type of modeling, the OilToxEx model in SIMAP™ and the data upon which it is based (French McCay 2001; 2002) have been validated through various studies and applications. The toxic units approach was used by USEPA for development of PAH water and sediment quality criteria (Di Toro et al. 2000; Di Toro and McGrath 2000; USEPA 2003; 2008). The oil toxicity model has been validated using laboratory oil bioassay data for both fresh and saltwater organisms (French McCay 2002) and for lobster mortality in the case of the North Cape spill (French McCay 2003). The underlying toxicity data used to develop the model is based on bioassays for freshwater and marine fish, invertebrate and algal species at a variety of life stages.

The biological impacts model has been validated using simulations of over 20 spill events where data were available for comparison (French and Rines 1997; French McCay 2003; 2004; French McCay and Rowe 2004). In most cases (French and Rines 1997; French McCay 2004; French McCay and Rowe 2004), only the wildlife acute impacts could be verified because of limitations of the available observational data. However, in the North Cape spill simulations, both wildlife and in-water hydrocarbon exposure impacts could be verified (French McCay 2003).

4 Model Input Data

4.1 SIMAP Model Input Data

4.1.1 Geographic and Habitat Data

For geographical reference, SIMAP™ uses a rectilinear grid to designate the location of the shoreline, the water depth (bathymetry), slope, bottom roughness, and the shore or habitat type. The grid is generated from a digital shoreline or other geographical information using the ESRI Arc/Info compatible Spatial Analyst program. The cells are coded for depth and habitat type and the model identifies the shoreline using this grid. Therefore, in model outputs, the land-water map is only used for visual reference; it is the habitat grid that defines the actual location of the shoreline in the model.

Geographical data including digital shoreline basemap and habitat mapping were obtained from the sources listed in Table 4-1. Basemap data were used to define the land/water boundary, and habitat data were used to define the types of habitats present within the study area. Habitat grids define the bottom type and vegetation found in subtidal areas, areas of extensive mud flats and wetlands, and the shore type. A variety of sources were used and combined to make the final habitat grids. Two grids were prepared: a northern extent for the Swinomish Channel Swing Bridge and Skagit River Crossing sites, and a southern extent for the Edmonds Ferry Terminal site.

Table 4-1: Basemap and habitat mapping data sources used for the study area.

Data Type	Data Source	Data Layers Used	Geographic Coverage	Citation
Basemap	NOAA Environmental Sensitivity Index	hydro_polygon	Puget Sound	NOAA, 2016a
Basemap	USGS National Hydrographic Dataset	NHDArea	Lower Skagit basin	USGS, 2016a
Habitat	NOAA Environmental Sensitivity Index	ESILines, esip_polygon	Puget Sound	NOAA, 2016a
Habitat	Whatcom and Skagit County Intertidal Habitat Inventory	intertidal vegetation, intertidal substrate	northern grid extent	WA DNR, 2016
Habitat	Snohomish County Marine Resources Committee	intertidal habitats, eelgrass map service	southern grid extent	Snohomish County MRC, 2016
Habitat	State of Washington Department of Ecology Coastal Atlas	shoreline photos	data gaps	WA DOE, 2014
Habitat	Google Earth and ESRI base maps	aerial photography	data gaps	n/a

Data Type	Data Source	Data Layers Used	Geographic Coverage	Citation
Bathymetry	NOAA National Centers for Environmental Information	1/3 arc-secondNAVD 88 DEM	Port Townsend and Puget Sound	NOAA, 2016b
Bathymetry	USACE Skagit River Levee General Investigation	bathymetry profiles	Skagit River	S&W, 2011
Bathymetry	USGS Skagit River Gage, Mount Vernon	annual average gauge height ("river stage")	Skagit River	USGS, 2016b

The grid scale resolution was slightly different for the northern and southern extent habitats depending on the geographic complexity and spatial extent of the model domain. For the Swinomish Channel Swing Bridge and the Skagit River Crossing, a 3568 E-W by 3736 N-S cell grid was composed of cells with sizes that were 10.01 m E-W by 15.02 m N-S. The Edmonds Ferry Terminal had a 3192 E-W by 2897 N-S cell grid that was composed of cells with sizes that were 13.51 m E-W by 20.04 m N-S.

Within the grid, habitats were designated as landward or seaward. Landward portions were identified as the rivers, estuaries, and inlets. The seaward portion was assigned to the open-water part of the water body. This designation allowed exposures to be evaluated in landward and seaward zones of the same habitat type (e.g., open water with sand bottom).

Where datasets overlapped, the NOAA ESI shoreline layers took precedence, followed by the Skagit River shore types, intertidal vegetation layers for the county, NOAA ESI mudflats and wetlands polygons, and subtidal substrate for the county. A default bottom type of sand was applied to fill in areas when no data was available, which was applied mainly to habitat cells that were farther away from shorelines. For the Skagit River, habitats were assigned based on interpretation of aerial photos and hand digitized.

Bathymetry data defined the water depths within the study area. Datasets were resampled into grids with the same resolution as the habitat grids. Depths for the Skagit River were obtained from bathymetry profiles within the U.S. Army Corps of Engineers (USACE) Skagit River Levee General Investigation report (S&W 2011). The profile locations were determined along the river. The maximum or average depth (the average was used when there was just a narrow deep channel in one part of the river) at each profile was determined by subtracting the annual average water level from the river bottom elevation. Depths between each profile were interpolated.

Bathymetry and habitat grids are provided for the Swinomish Channel Swing Bridge and Skagit River scenarios (Figure 4-1 through Figure 4-4), with smaller-scale maps of habitat for the Swinomish Channel (Figure 4-2) and bathymetry for the Skagit River (Figure 4-3) displayed for clarity. Bathymetry and habitat grids are also provided for the Edmonds Ferry Terminal (Figure 4-5 and Figure 4-6).

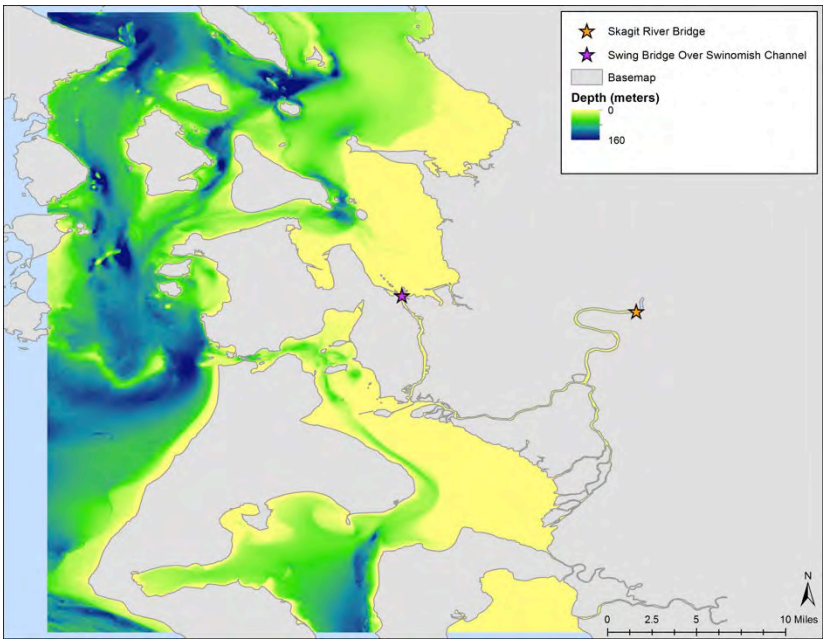

Figure 4-1: Bathymetry grid (water depth in meters) near Swinomish Channel (purple star) and Skagit River (orange star) hypothetical release locations.

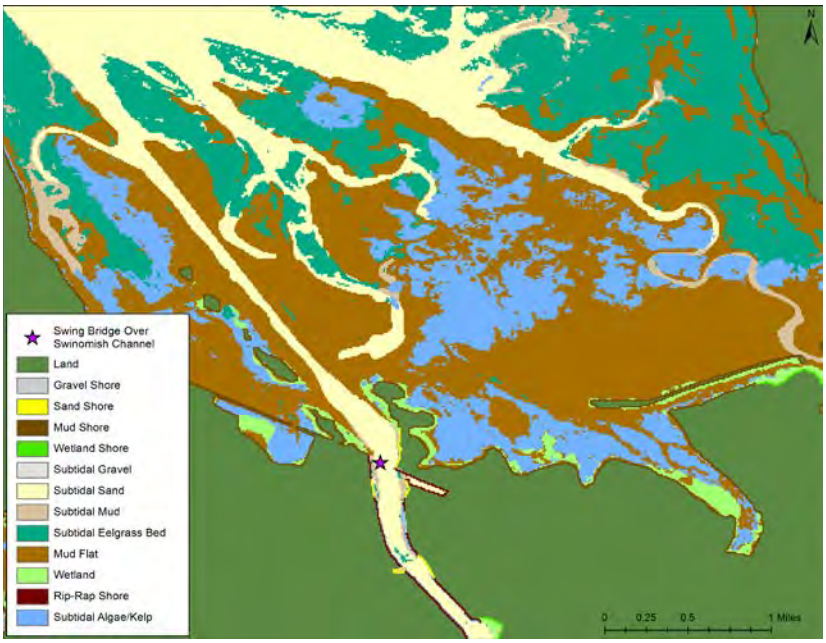

Figure 4-2: Habitat grid for Swinomish Channel Swing Bridge (purple star) hypothetical release locations.

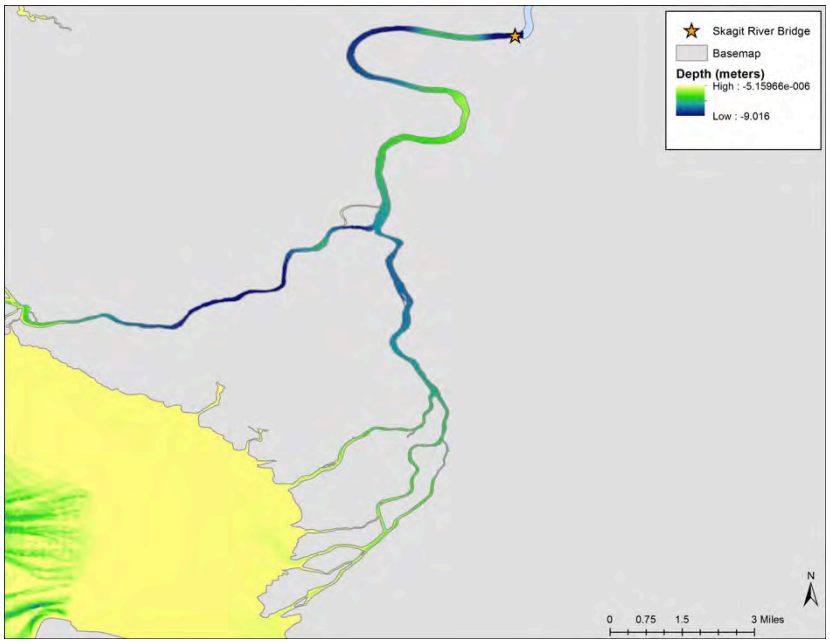

Figure 4-3: Bathymetry grid (water depth in meters) for the Skagit River Crossing (orange star) hypothetical release location.

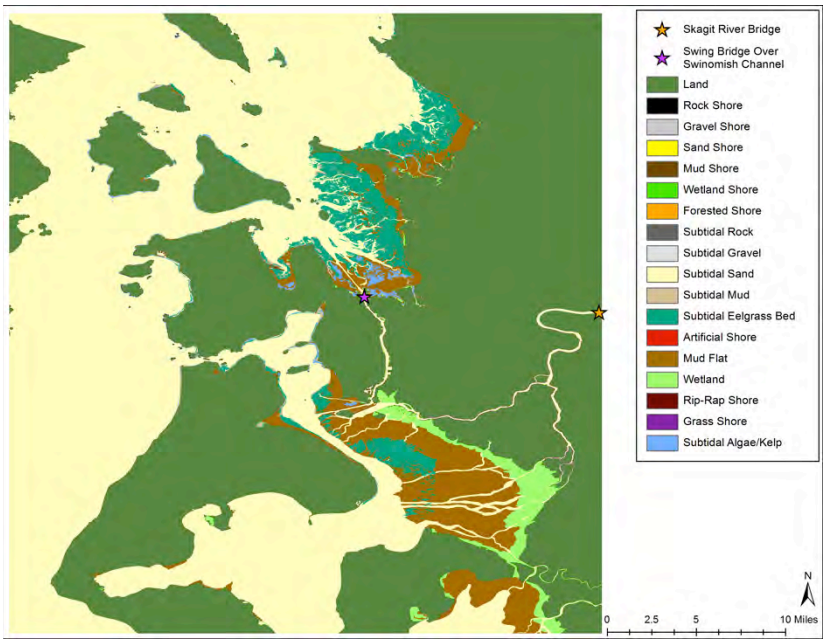

Figure 4-4: Habitat grid for Skagit River Crossing (orange star) and Swinomish Channel Swing Bridge (purple star) hypothetical release locations.

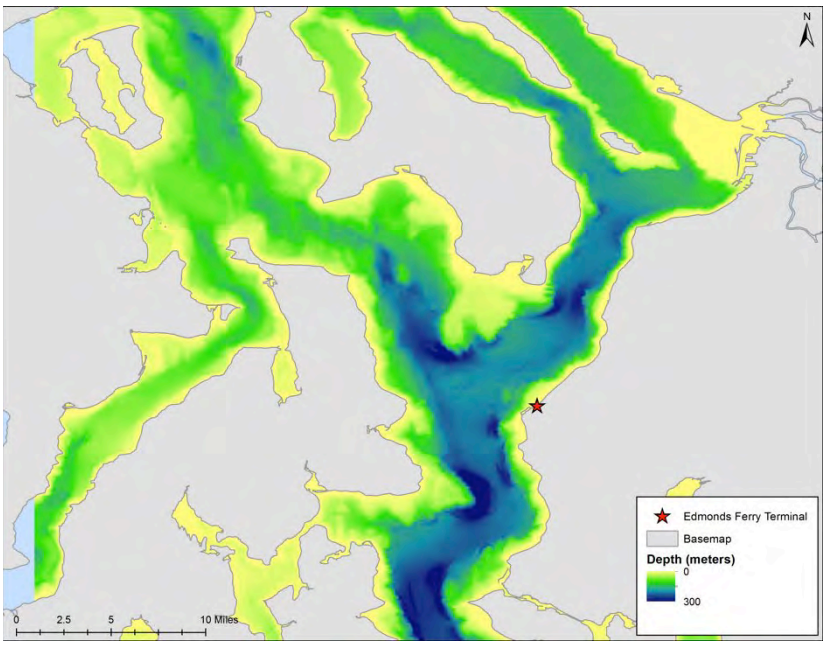

Figure 4-5: Bathymetry grid (water depth in meters) near Edmonds Ferry Terminal (red star) hypothetical release location.

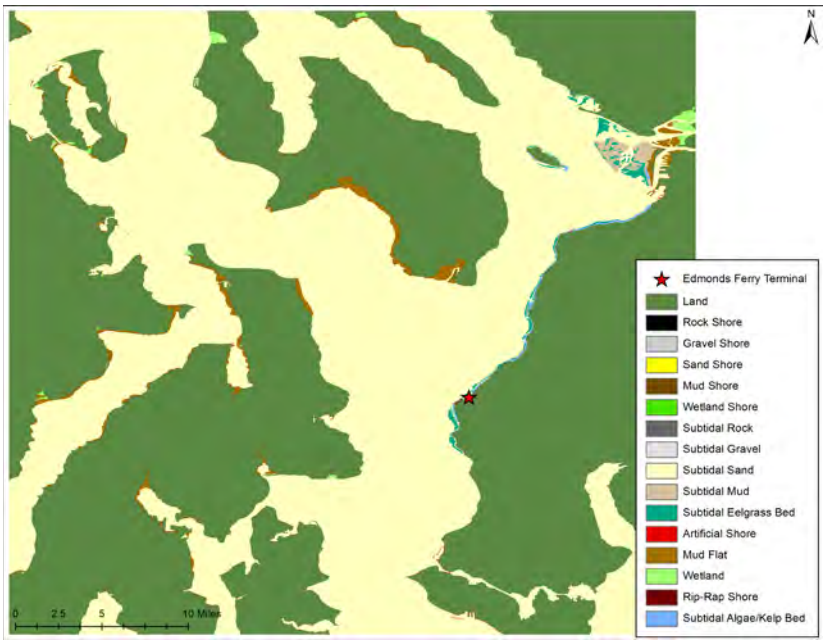

Figure 4-6: Habitat grid for Edmonds Ferry Terminal (red star) hypothetical release location (red star).

Ecological habitat types (Table 4-2) were broadly categorized into two zones within SIMAP™: shoreline (or intertidal, above spring low-water tide level) and submerged (or subtidal, below spring low-water tide level).

In riverine modeling scenarios, the shoreline habitats become oiled as surface oil makes contact with shoreline cells. Submerged/subtidal areas correspond to river bottom cells that are always underwater. Intertidal/shoreline areas can be extensive, such that they are wide enough to be represented by an entire grid cell at the resolution of the grid. These are typically either mud flats or wetlands, while all other intertidal/shoreline habitats are much narrower than the size of a grid cell. Therefore, these narrower fringing intertidal/shore types (indicated by F in Table 4-2) have typical widths associated with them in the model. Boundaries between land and water are fringing habitat types. On the waterside of fringing grid cells, there may be extensive intertidal/shoreline grid cells if the wetlands or mudflats are extensive. Otherwise, subtidal/submerged habitats border the fringing cells. Oil will strand as the tide falls and areas such as mud flats are exposed. These habitat types are based on the Environmental Sensitivity Index datasets created by the National Oceanic Atmospheric Association (NOAA 2016a) and used solely for determining the retention of oil on shorelines and substrate types during trajectory and fates modeling; the data were not used in the biological impacts model or overlay analysis for this project.

Table 4-2: Classification of habitat types in SIMAP. Seaward (Sw) and landward (Lw) system codes are listed. Fringing types (indicated by 'F') are only as wide as the intertidal zone or shoreline width where oiling might occur. Other types (indicated by 'W' for 'water') are a full grid-cell wide and have a fringing type on the landward side.)

Habitat Code (Sw, Lw)	Ecological Habitat	F or W
	Intertidal / Shore	
1, 31	Rocky Shore	F
2, 32	Gravel Shore	F
3, 33	Sand Beach or Shore	F
4, 34	Fringing Mud Flat	F
5, 35	Fringing Wetland (Emergent or Forested)	F
6, 36	Macroalgal Bed	F
7, 37	Mollusk Reef	F
8, 38	Coral Reef (marine only)	F

Subtidal / Submerged		
9, 39	Rock Bottom	W
10, 40	Gravel Bottom	W
11, 41	Sand Bottom	W
12, 42	Silt-mud Bottom	W
13, 43	Wetland (submerged areas)	W
14, 44	Macroalgal Bed	W
15, 45	Mollusk Reef	W
16, 46	Coral Reef (marine only)	W
17, 47	Submerged Aquatic Vegetation Bed	W
Intertidal / Shore		
18, 48	Man-made, Artificial	F
19, 49	Ice Edge	F
20, 50	Extensive Mud Flat	W
21, 51	Extensive Wetland (Emergent or Forested)	W

4.1.1.1 Shoreline Oil Retention

Retention of oil on a shoreline depends on the shoreline type, width and angle of the shoreline, viscosity of the oil, tidal amplitude in estuarine areas, and wave energy. In the NRDAM/CME (French et al. 1996), shore-holding capacity was based on observations from the *Amoco Cadiz* spill in France and the *Exxon Valdez* spill in Alaska (based on Gundlach 1987) and later work summarized in French et al. 1996). These data were used here (Table 4-3). The shore width (width of zone where oiling would occur) was set to 1 m in the model, as a realistic width for oiling given the spill volumes and river dimensions involved for the Skagit River scenarios.

Table 4-3: Maximum oil thickness for various shore types as a function of oil viscosity, measured in centistokes (cSt).

Oil Thickness (mm) by Oil Type			
Shore Type	**Light (< 30 cSt)**	**Medium (30 - 2000 cSt)**	**Heavy (> 2000 cSt)**
Rocky shore	1	5	10
Gravel shore	2	9	15
Sand beach	4	17	25

Oil Thickness (mm) by Oil Type			
Shore Type	**Light (< 30 cSt)**	**Medium (30 - 2000 cSt)**	**Heavy (> 2000 cSt)**
Mud flat	6	30	40
Wetland	6	30	40
Artificial	1	2	2

Source: French et al. 1996, based on Gundlach 1987

4.1.2 Environmental Data

4.1.2.1 Wind

Winds may physically transport oil on the water surface, meaning that wind speed and direction at the water surface may make a difference between limited or extensive transport. The model uses time-varying or mean wind speeds and directions for the time of the spill and simulation. For this study, modeled wind data was obtained from the National Centers for Environmental Prediction (NCEP) Climate Forecast System Reanalysis (CFSR) product. The CFSR was designed and executed as a global, high-resolution, coupled atmosphere-ocean-land surface-sea ice system to provide the best estimate of the state of these coupled domains. The CFSR global atmospheric resolution is ~38 km, with 64 vertical levels extending from the surface to 0.26 hPa. Selected CFSR time series products are available at 0.3, 0.5, 1.0 and 2.5 degree horizontal resolutions at 6-hourly intervals (Saha et al. 2010). A 10-year record (2001 to 2010) was sampled with annual wind roses and mean monthly wind speeds calculated for each station (Figure 4-7, Figure 4-9, and Figure 4-11). Seasonal wind roses present wind speeds during winter, summer, high flow, and low flow conditions (Figure 4-8, Figure 4-10, and Figure 4-12, respectively).

In addition to lateral transport, winds add to the vertical mixing of the surface water, in some instances keeping subsurface oil entrained or entraining more oil under higher wind speeds. The winds in the relatively protected Swinomish Channel and Skagit River may be slightly different than the lower resolution CFSR winds that characterize more generalized wind speed and direction. Because of these uncertainties and the expected variability in direction, we have conservatively assumed wind drift transport as zero in the Skagit River and Swinomish Channel themselves. In the bays and other open waters, wind drift was allowed. Therefore, winds did not laterally transport oil or push it ashore for the channel and riverine sections. For the Edmonds Ferry Terminal release location, both winds and currents contributed to oil transport. For the Swinomish Channel Swing Bridge site, wind direction is variable; however, the predominant yearly wind direction is from the south-southeast with an average speed of 2.4 m/s. The highest annual wind speeds (> 5 m/s) were most frequently from the southeast. Mean monthly wind speeds were highest in November-December, and lowest in August. Winds were stronger during winter, with speeds greater than 5 m/s occurring from the southeast. Summer wind speeds were

lower, typically less than 2 m/s, with primarily west-northwest and west-southwest winds. The strongest winds occur from the southeast.

At the Skagit River Crossing site, the predominant annual wind direction is south-southeasterly and easterly, with an average of 2.5 m/s. Annual wind speeds were highest most frequently from the south-southeast. Mean monthly wind speeds were highest in November and remained elevated through January, while the lowest wind speeds occur in July. Winds were notably stronger during winter, with speeds exceeding 5 m/s from the southeast. In summer, winds were most frequently between 2 to 3 m/s from the east or west-northwest, with the strongest speeds from the southeast.

Near the Edmonds Ferry Terminal site, the annual wind rose illustrates that winds were predominantly from the south-southeast with an average speed of 3 m/s. Annual wind speeds were highest most frequently from the south-southeast, but also blew strongly on occasion from the northwest. Mean monthly wind speeds were highest in December and lowest in July and August. During the winter, winds frequently exceeded 5 m/s from the south-southeast, while in the summer, winds were typically between 2-3 m/s from the northwest, but were strongest from the south-southeast.

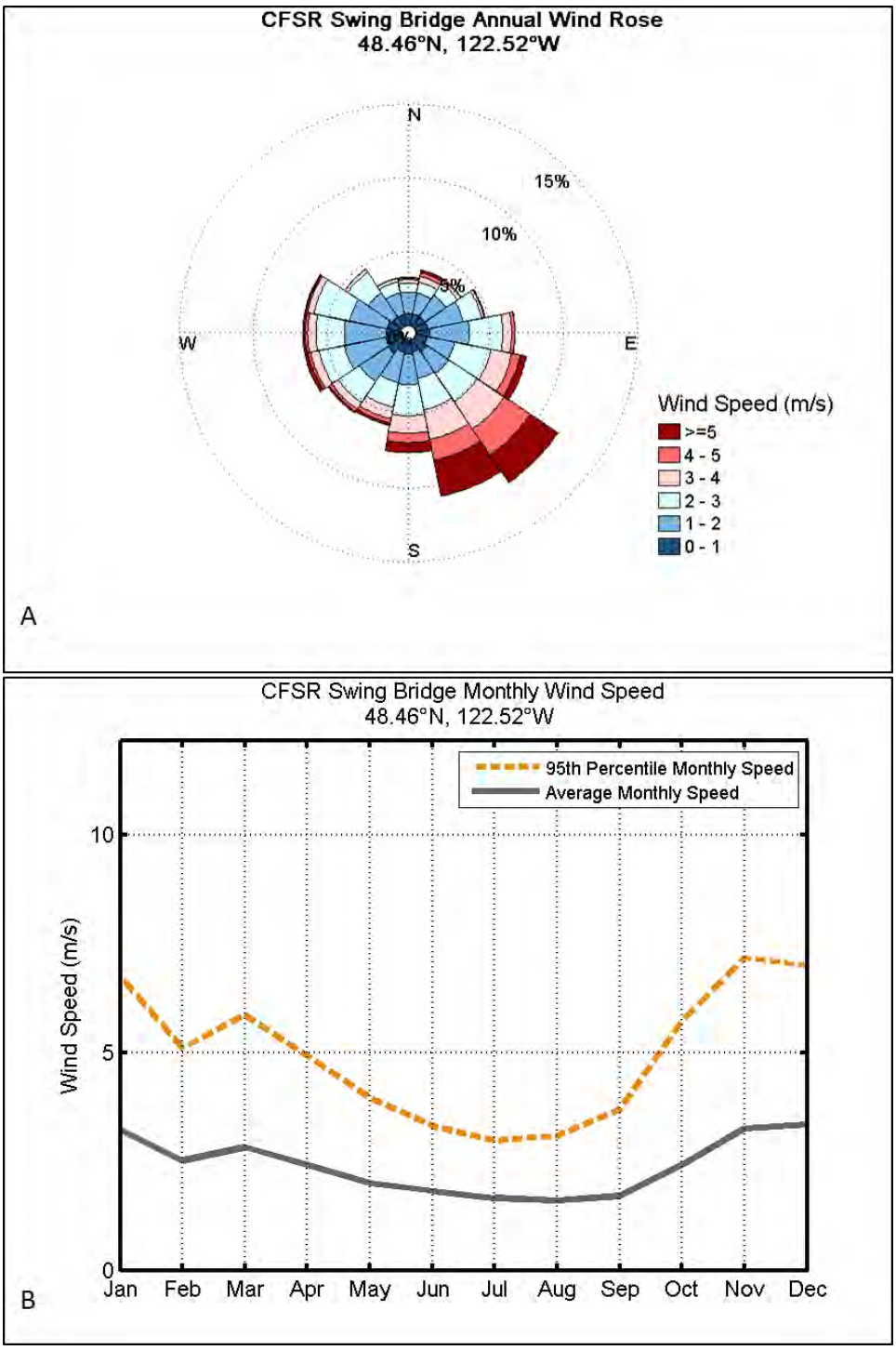

Figure 4-7: Annual wind rose (A) and monthly average wind speeds (B) for the Swinomish Channel Swing Bridge hypothetical release location.

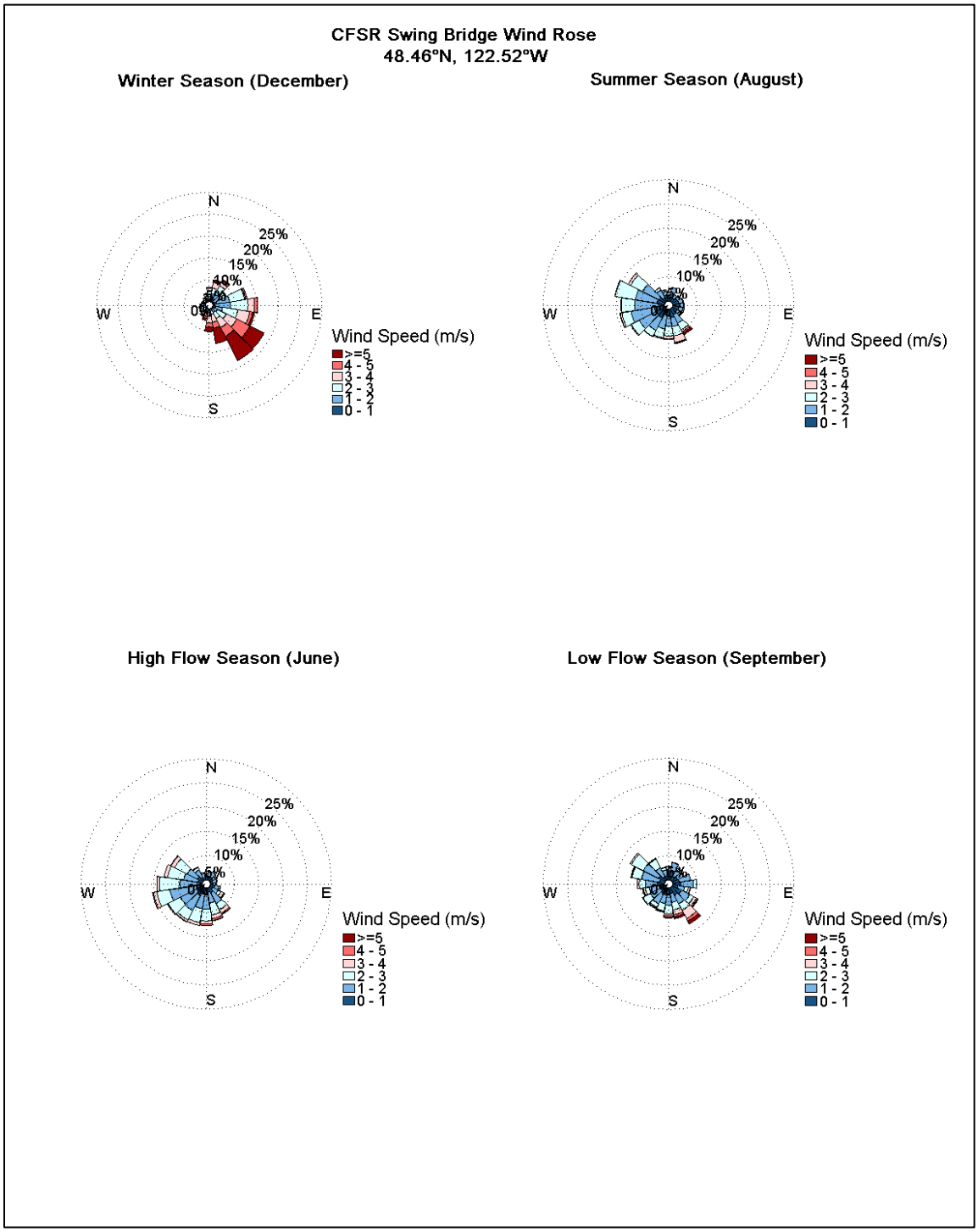

Figure 4-8: Seasonal wind rose plots (winter, summer, high flow, low flow) for Swinomish Channel Swing Bridge hypothetical release location.

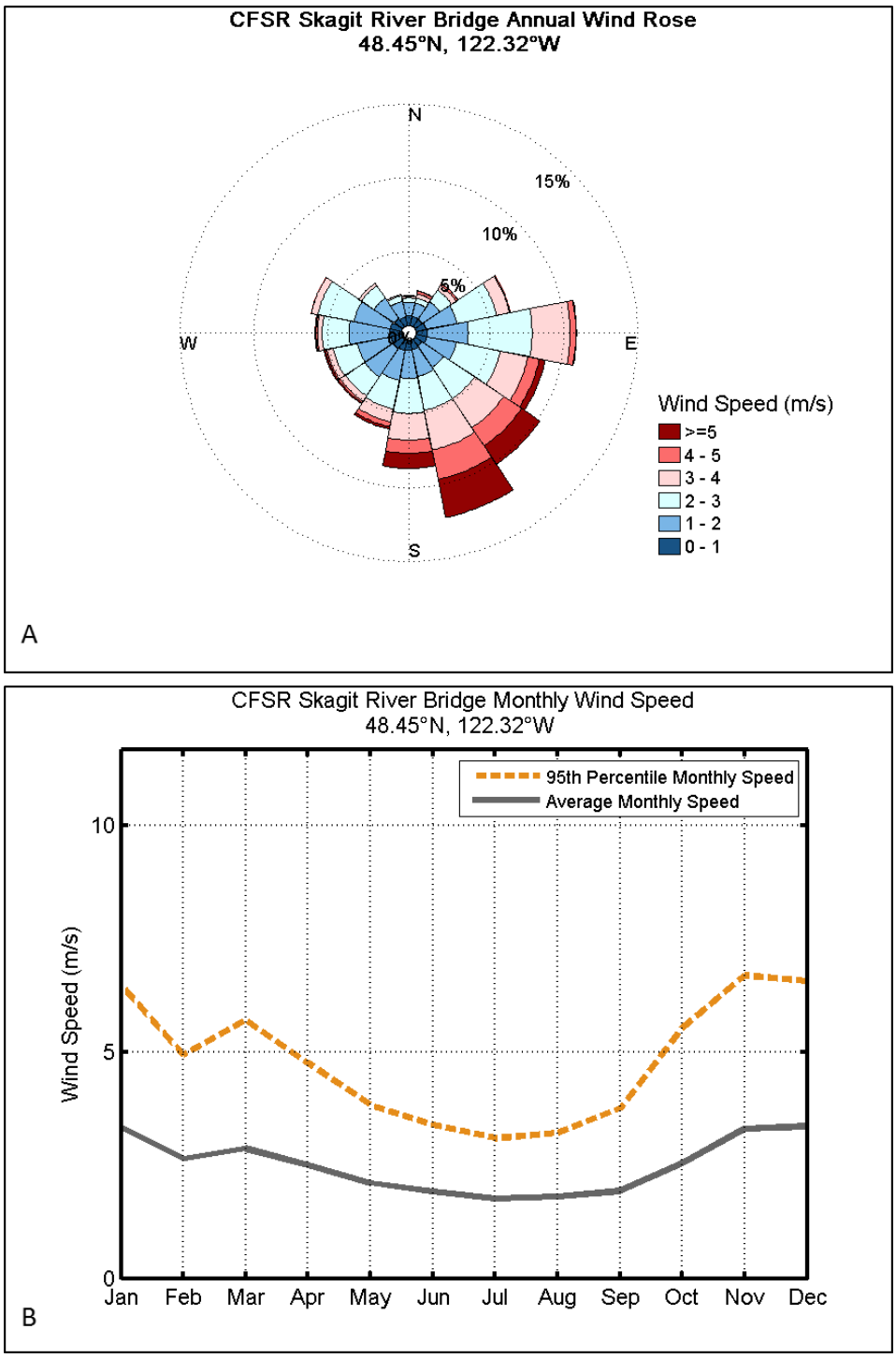

Figure 4-9: Annual wind rose (A) and monthly average wind speeds (B) for the Skagit River Crossing hypothetical release location.

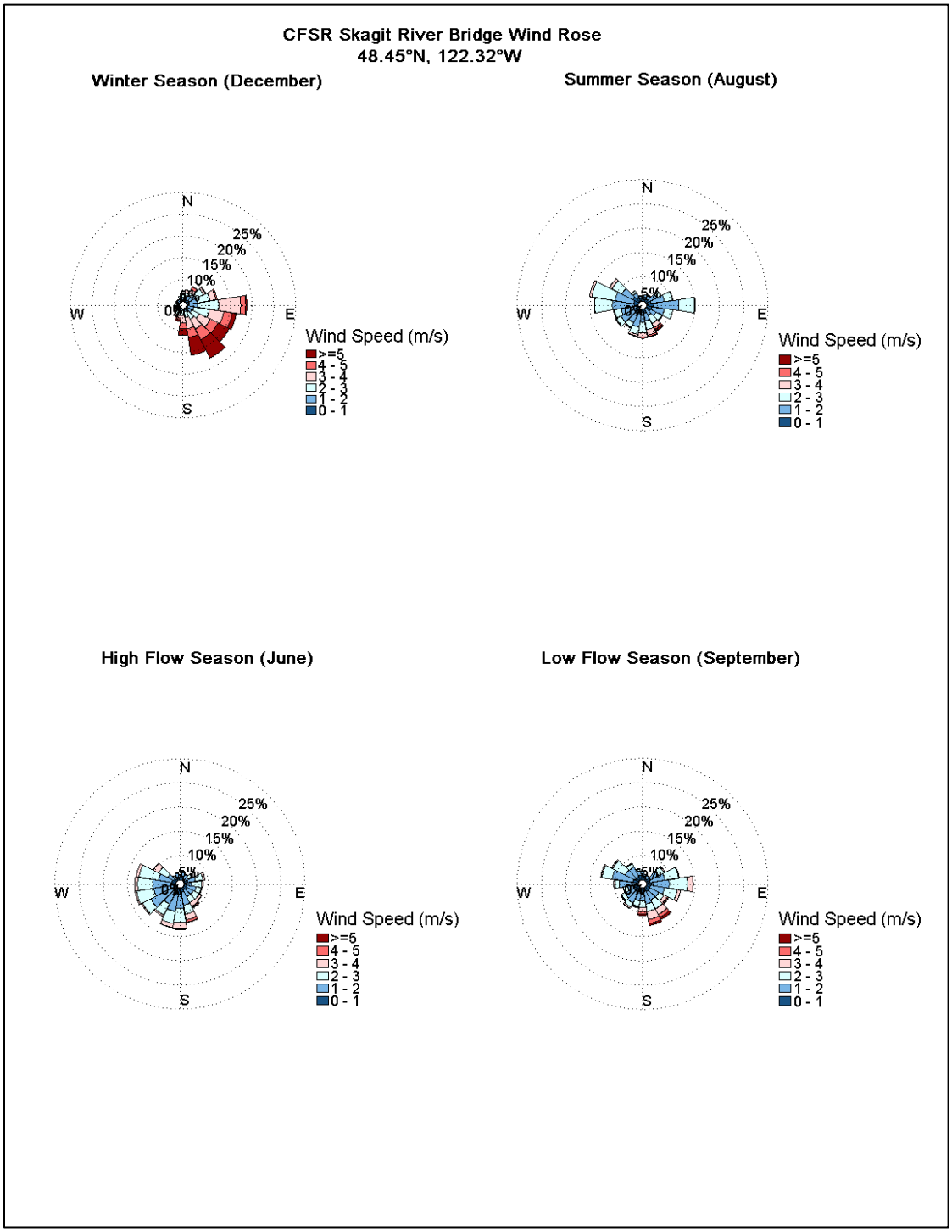

Figure 4-10: Seasonal wind rose plots (winter, summer, high flow, low flow) for the Skagit River Crossing hypothetical release location.

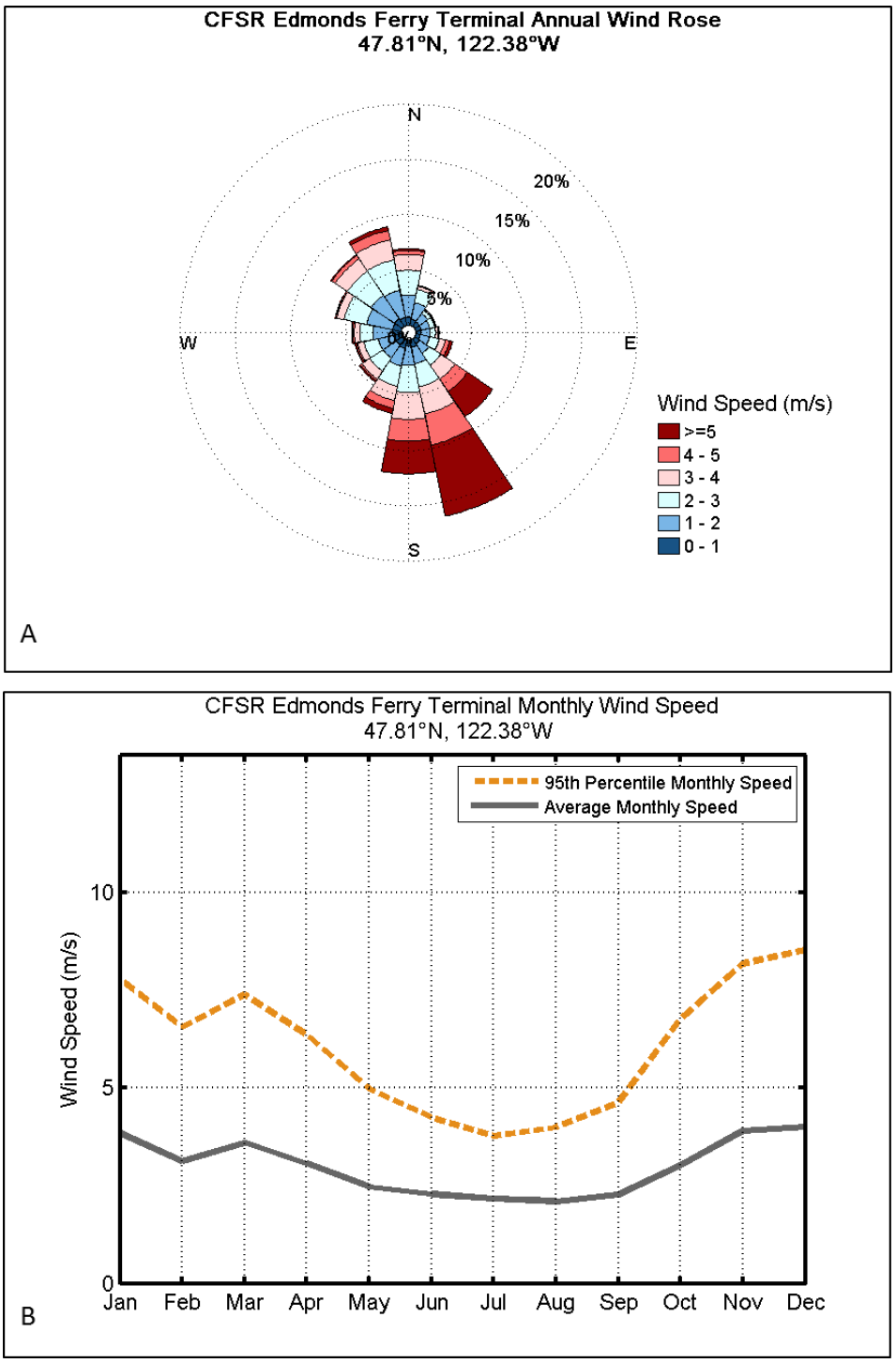

Figure 4-11: Annual wind rose (A) and monthly average wind speeds (B) for the Edmonds Ferry Terminal hypothetical release location.

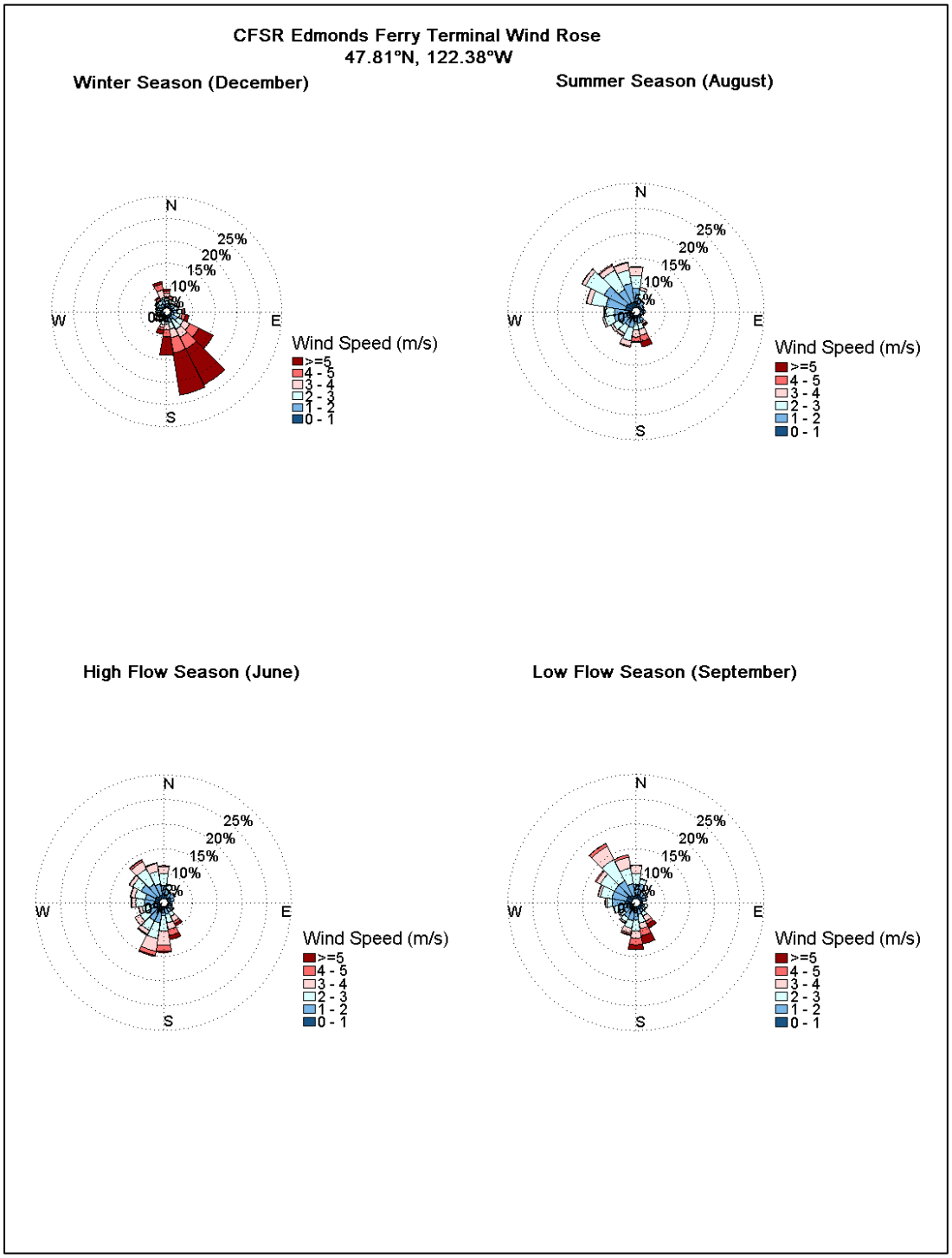

Figure 4-12: Seasonal wind rose plots (winter, summer, high flow, low flow) for the Edmonds Ferry Terminal hypothetical release location.

4.1.2.2 Water Temperature and Salinity

Water temperature varies throughout the year. The air immediately above the water was assumed to have the same temperature as the water surface, which is the best estimate of the air temperature in contact with floating oil. Temperatures for the study area were extracted from a U.S. Geological Survey (USGS) technical report on nearshore circulation and water column properties in the Skagit River Delta and northern Puget Sound (Grossman et al. 2007).

The salinity value assumed in the model has little influence on the fate of the oil, as salinity is used along with temperature to calculate water density, which is then used to calculate buoyancy. The salinities for the Skagit River and Swinomish Channel study areas were extracted from Grossman et al. (2007) while salinities for the Edmonds Ferry Terminal came from NOAA's 2012 Overview of Puget Sound Marine Waters (Moore et al. 2012). The water temperatures and salinities used for each model scenario are presented in Table 4-4 below.

Table 4-4: Water temperature (˚C) and salinity (psu) for each release location and seasonal condition.

Site	Season	Temperature (˚C)	Salinity (psu)
Swinomish Channel Swing Bridge	Summer – Spring Tide	14	25
	Winter – Neap Tide	7	21
Skagit River Crossing	Summer – High Flow	10	0.15
	Winter – Low Flow	8	0.15
Edmonds Ferry Terminal	Summer – Low Winds	12	28
	Winter – High Winds	9	29

4.1.2.3 Suspended Particulate Matter

The amount of sediment transport can change by several orders of magnitude based on location and flow conditions, with extensive sediment transport during high flow conditions (especially storm events), and very low sediment transport and clear water during low flow conditions. Oil droplets may stick to suspended sediments and settle to the bottom. Surface water data from the USGS station Skagit River near Mount Vernon, Washington (station 12200500) was used to determine the total SPM concentrations during high and low flow months for the Skagit River (USGS 2016b; 2016c). SPM concentrations varied for each scenario and season with typical ranges between 5 mg/L for neap tide low flow conditions at Swinomish Channel, and up to 135 mg/L for high flow river conditions in the Skagit River. The settling rate was set to 1 m/d for all scenarios. The SPM concentration used for each model scenario is presented in Table 4-5 below.

Table 4-5: Suspended sediment concentrations (SPM) modeled at each release location and seasonal condition.

Site	Season	SPM (mg/L)
Swinomish Channel Swing Bridge	Summer – Spring Tide	8
	Winter – Neap Tide	5
Skagit River Crossing	Summer – High Flow	135
	Winter – Low Flow	37
Edmonds Ferry Terminal	Summer – Low Winds	10
	Winter – High Winds	10

4.1.2.4 Horizontal and Vertical Dispersion

The horizontal dispersion (randomized mixing) coefficient was assumed as 1 m^2/s for all locations except for the Skagit River. Due to resolution of the river hydrodynamics, the horizontal dispersion at the surface was assumed to be 3 m^2/s in the main channel. The vertical dispersion (randomized mixing) coefficient was assumed to be 1 cm^2/s throughout. Vertical dispersion values may keep the water column well mixed and slow the resurfacing of entrained oils. Dispersion values are reasonable for coastal and riverine waters based on empirical data (Fischer 1973; Okubo and Ozmidov 1970; Okubo 1971; Seo and Baek 2004; Socolofsky and Jirka 2004) and modeling experience.

4.1.3 Hydrodynamic Data

Currents are critical data inputs that have substantial influence on the trajectory and fate of oil. For this study, an available FVCOM hydrodynamic solution (Khangaonkar et al. 2011; Khangaonkar et al. 2016) of spatially- and temporally-varying currents in the study area was used. The hydrodynamic data domain covered the Salish Sea, which encompasses Puget Sound, Georgia Strait, and the Strait of Juan de Fuca, as well as many major rivers within the area, and included the Skagit River (see study area overview map, Figure 2-1). The data set spanned the 12-month period between January 1, 2008 and December 31, 2008. While the entire year of data was available, only specific timeframes that reflected varying hydrodynamic conditions were used for the model runs (Section 2.4.1). The model grid was unstructured, which allowed for variable cell sizes at high resolutions to capture relatively small coastline and bathymetric features where needed. Typically, higher resolution cells are used along shorelines and at constriction points, while lower resolution grid cells are used in the open waters. Model forcing included tides, water column temperature and salinity (i.e., density), and river flows. It also included meteorological surface forcing driven by surface heat flux, radiation, and winds. The model

output available in the dataset included hourly current speed and direction at every grid cell for the modeled time period. The model data was available in three dimensions; however, surface oil transport in coastal areas predominately requires only the surface layer of data.

4.2 OILMAP Land Model Inputs

As discussed previously, the release location at the Edmonds Ferry Terminal consisted of a terrestrial release that moved overland before entering the water. The trajectory and fate of the overland surface release was characterized in two dimensions using the OILMAP Land™ model, with inputs described in the following sections, until the oil entered Puget Sound.

4.2.1 Elevation

The OILMAP Land™ model uses land elevation data to determine the overland pathways of releases occurring in the terrestrial environment (Figure 4-13). The elevation data are stored in a grid (raster) format and the model calculates the downslope pathway by determining the direction of the steepest slope as the leading edge of the release moves from grid cell to grid cell.

The ability of the model to accurately determine the overland release pathways is, in large part, controlled by the vertical and horizontal resolution of the elevation grid. The horizontal resolution refers to the size of the individual grid cells of the elevation data in north-south and east-west directions. Greater horizontal resolution is important to be able to see smaller terrain features present in the elevation data. This may include roads, ditches, and other smaller-scale features. Each horizontal grid cell is assigned a single elevation value, so small-scale features would be flattened or smoothed in the larger grid cell and have limited impacts on the elevation. The vertical resolution refers to the level of precision available for each cell's elevation value. Sub-meter precision is critical for accurate modeling of flow over a land surface. Without the small sub-meter variations in the elevation surface, larger areas of no apparent elevation change may be present. In this case, the surface flow model will have greater difficulty in determining an overland flow direction, as multiple cells need to be crossed to find the downslope gradient.

Elevation data for the study were obtained from the Puget Sound Lidar Consortium (PSLC 2016). Data were collected in the Lower Puget Sound area from 2000 to 2005, and compiled into one dataset; for this project, the data used were collected from Snohomish County in 2003. The bare earth digital elevation model (DEM) data product was derived from Light Detection and Ranging (LiDAR) collected at resolution of approximately one per square meter. The horizontal resolution of the DEM was 6 feet (2 meters) and the vertical resolution was less than 1/10 of an inch (0.25 cm). The accuracy is reported as ±30 cm RMSE (root-mean-square error) in the vertical.

4.2.2 Storm Water Drainage System

The OILMAP Land™ release model uses networked streams and lake data to model the pathways of oil once it reaches surface water. Streams and rivers must be represented as a polyline feature of the stream centerline, which has been digitized according to the flow direction. The streams must be networked in a way such that the model can determine where each single stream segment joins the next, as the downstream movement of oil is modeled.

No surface water streams or lakes were present at the Edmonds Ferry Terminal. However, there were a significant number of storm water drainage systems that could affect the trajectory of released oil (Figure 4-13). Storm water drainage system data was available on the City of Edmonds GIS website (City of Edmonds 2016). In the model, these drainage features were treated as if they were streams or rivers that transported the released oil from the land surface into Puget Sound at their respective outfalls. Oil was allowed to enter the drainage network only at locations of the catch basins (i.e., storm water grates, frames, and curb inlets). From there, the oil travelled through drainage lines or drainage ditches and was released into Puget Sound at each respective endpoint.

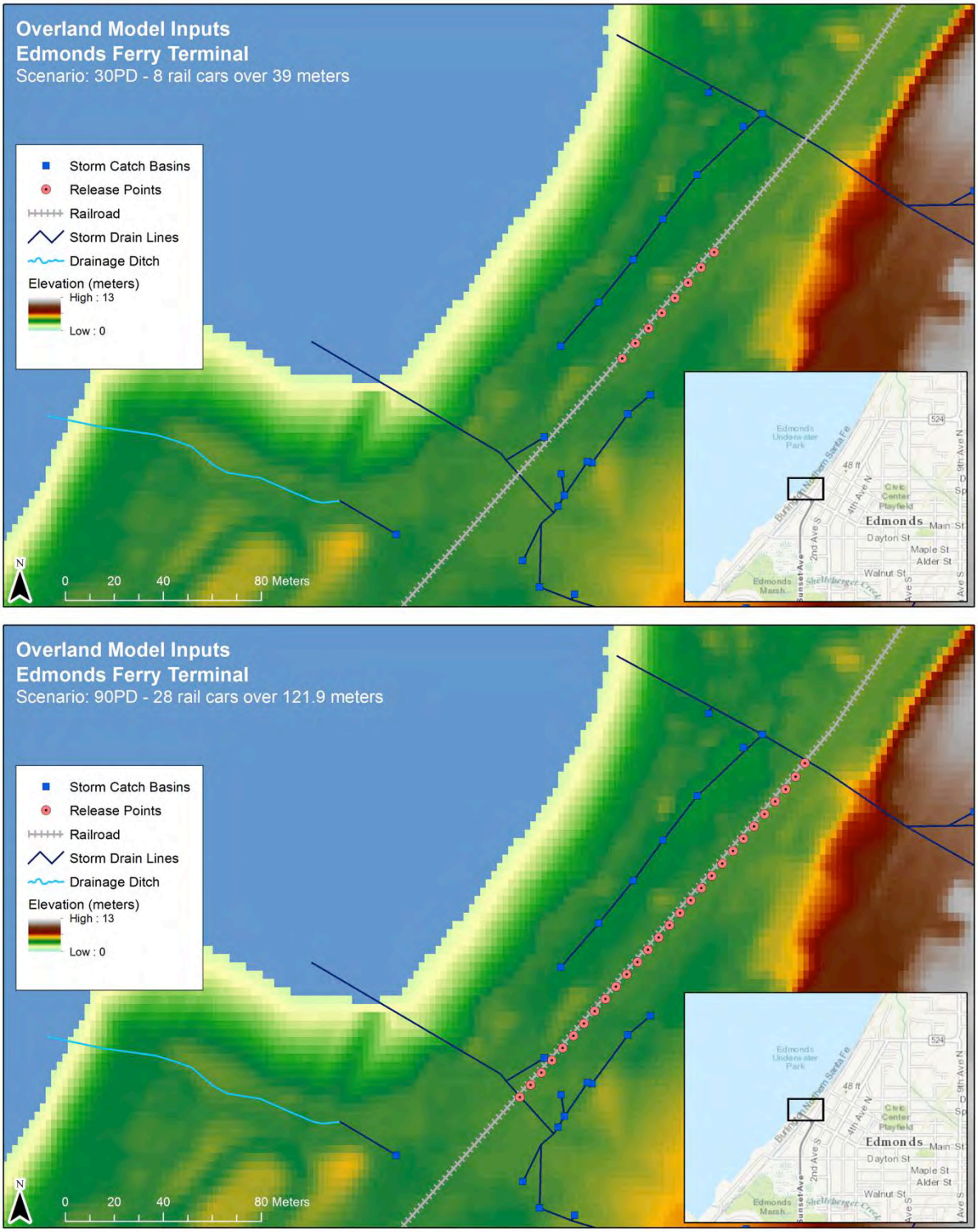

Figure 4-13: Elevation data and storm water drainage system for Edmonds Ferry Terminal. The tank car release locations for the eight-car 30PD release (top) and 28-car 90PD release (bottom) are shown.

4.2.3 Land Cover

The OILMAP Land™ model uses land cover data to vary the amount of oil that adheres to the land surface as oil moves downslope. The land cover data are used in a gridded format, with each grid cell value representing the type of land cover at that specific location. Land cover code values are matched to the categories that define oil retention, so that the loss by retention can be accurately calculated as oil flows over the land surface.

The land cover data used was the National Land Cover Database (NLCD) 2011, created by the Multi-Resolution Land Characteristics Consortium (Homer et al. 2015). The NLCD 2011 is based on a decision-tree classification of 2011 Landsat satellite data with 30-meter resolution.

The NLCD 2011 data was transformed to the required coordinate system. The dataset required reclassification of land cover classes to assign them appropriate OILMAP Land™ values. The classification conversions for the NLCD 2011 data are provided in Table 4-6.

Table 4-6: Mapping used to convert the NLCD 2011 land cover categories to OILMAP Land™ classification scheme.

NLCD 2011 Code	NLCD 2011 Description	OILMAP Land™ Code	OILMAP Land™ Description
11	Open Water	5	Water
12	Perennial Snow/Ice	12	Perennial Ice/Snow
21	Developed, open space	21	Low Intensity Residential
22	Developed, Low Intensity	21	Low Intensity Residential
23	Developed, Medium Intensity	22	High Intensity Residential
24	Developed, High Intensity	22	High Intensity Residential
31	Barren Land (Rock/Sand/Clay)	31	Bare Rock/Sand/Clay
41	Deciduous Forest	41	Deciduous Forest
42	Evergreen Forest	42	Evergreen Forest
43	Mixed Forest	43	Mixed Forest
51	Dwarf Scrub	51	Shrubland
52	Shrub/Scrub	51	Shrubland
71	Grasslands/Herbaceous	71	Grasslands/Herbaceous
72	Sedge/Herbaceous	92	Emergent Herbaceous Wetlands
73	Lichens	98	Barren Land
74	Moss	98	Barren Land
81	Pasture/Hay	81	Pasture/Hay
82	Cultivated Crops	82	Row Crops
90	Woody Wetlands	91	Woody Wetlands
95	Emergent Herbaceous Wetlands	92	Emergent Herbaceous Wetlands

4.3 Oil Properties and Acute Toxicity

A single oil type was modeled across all scenarios, including a conditioned Bakken crude oil. Summaries of the physical parameters for the conditioned Bakken crude oil are provided in Table 4-7 with sources indicated in notes following the table. The three aromatic pseudo-components and three aliphatic pseudo-components were then modeled in SIMAP, along with the total hydrocarbons. The volatile aliphatics evaporate and volatilize from the surface water and so their mass is accounted for in the overall mass balance. However, as they do not dissolve in significant amounts, they have no influence on the biological impacts on water column and benthic organisms. Minimum oil slick thicknesses were determined based on McAuliffe (1987). The aromatic and aliphatic concentrations and the percentage of fresh whole oil are included in Table 4-8.

Table 4-7: Oil parameters for the spilled conditioned Bakken crude oil.

Oil Property	Conditioned Bakken Crude
Oil Type	Crude
Minimum Slick Thickness (µm)[1]	0.1
Surface tension (dyne/cm) [2]	27.3
Pour Point (°C)[3]	-82.2
API Gravity[3]	43.67
Density (g/cm^3) at 16°C[4]	0.80765
Viscosity (cP) at 50°C[4]	4.968[5]

[1] RPS ASA 2013 - CRC categories and observations of oil spills.
[2] Environment Canada Oil Property Database: Sweet Blend (http://www.etcentre.org/spills) as described in Jokuty et al. (1999). Jokuty, P., S. Whiticar, Z. Wang, M. Fingas, B. Fieldhouse, P. Lambert, and J. Mullin 1999. Properties of Crude Oil.
[3] Data provided by Shell, from Crude Oil Evaluation Data Sheet (COED), Reference BAKK20140703, Bakken Hi API (Norco RDCC of N0452) generated on November 30, 2015.
[4] Calculated from API

Table 4-8: Aromatic (AR), aliphatic (AL), and total hydrocarbon concentration (THC) and percentage composition of fresh whole oil for conditioned Bakken crude. THC is the sum of AR and AL. (Numbers of carbons in the included compounds are listed, e.g., >C8-C10 indicates greater than 8 carbons and including 9- and 10-carbon hydrocarbons.)

Conditioned Bakken Crude Oil	% AR[6]	% AL[7]	% THC[8]
1 (AR = BTEX & MAHs >C8-C10) (AL = >C6-C10)	3.9278	33.6082	37.5360
2 (AR = MAHs and PAHs >C10-C12) (AL= >C10-C12)	1.9342	14.7362	16.6704
3 (AR = PAHs >C12-C16) (AL = >C12-C16)	2.9437	18.9379	21.8816

For oil spills at the water surface, six- to eight-carbon MAHs (i.e., BTEX) do not have a significant impact on aquatic organisms for the following reasons. BTEX compounds are soluble, and so some become bioavailable (dissolved). However, they are also very volatile, and will volatilize (from the water surface and water column) very quickly after a spill. The threshold for toxic impacts for these compounds is about 500 ppb for sensitive species (French McCay 2002). BTEX compounds evaporate faster than they dissolve, such that toxic concentrations are not reached. Small concentrations of BTEX in the water will quickly be diluted to levels well below toxic thresholds immediately after a spill. Therefore, the assumed values for BTEX concentrations in the oil, as well as their fates, have little influence on model results. The percentages of PAHs and more highly substituted benzenes (i.e., with nine or more total carbons in the molecule) have a significant influence on the model results. Therefore, data for well-defined oils were used in the modeling to develop acute toxic endpoints, and the LC50s assumed were for total dissolved PAH concentrations in the water (LC50mix, see Section 3.2.2). The substituted benzenes have similar toxicity to the soluble and sparingly-soluble PAHs.

[6] AR adjusted from calculated THC values from distillation data from Crude Oil Evaluation Data Sheet (COED). Reference BAKK20140703, Bakken Hi API (Norco RDCC of N0452) generated on November 30, 2015. AR and THC data used for the adjustment calculations are from: A Survey of Bakken Crude Oil Characteristics Assembled for the U.S. Department of Transportation. Submitted by American Fuel & Petrochemical Manufacturers. Prepared by Dangerous Goods Transport Consulting, Inc. May 14, 2014.
[7] Calculated by difference THC2-AR2.
[8] Calculated from distillation data from Crude Oil Evaluation Data Sheet (COED), Reference BAKK20140703, Bakken Hi API (Norco RDCC of N0452) generated on November 30, 2015.

To estimate $LC50_{mix}$ values for dissolved PAHs in the water, the additive model described in French McCay (2002) was used (Section 3.2.2). French McCay (2002) estimated $LC50_{mix}$ = 50 ppb for typical fuels at infinite exposure time and for the average species and life stage. Ninety-five percent of species and life stages have LC50s between 5 and 400 µg/L (ppb).

The LC50s above are for the concentration of dissolved PAHs that would be lethal to 50 percent of organisms exposed for a long enough time for mortality to occur. For PAHs, this duration of exposure is at least 10 days at warm temperatures. For chemicals in general, toxicity is higher, and the LC50 lower, at a longer duration of exposure and at higher temperatures (French et al. 1996; French McCay 2002). The model corrects this LC50 to temperature and duration of exposure for each group of organisms exposed.

For this exposure assessment, modeling was performed using two acute toxicity endpoints for in-water impacts: the $LC50_{mix}$ for species of average sensitivity (50 µg/L), and for sensitive species (5 µg/L). The lower value (5 µg/L) would be protective of 97.5 percent of species or life stages in the aquatic environments of concern. For surface and shoreline impacts, a toxicity endpoint of 10 µm was used.

5 Model Application

For each of the three release locations, four hypothetical release scenarios were modeled to outline the expected behavior of two release volumes (30PD and 90PD) of conditioned Bakken crude oil under two seasonal conditions. Together, this included 12 trajectory and fates scenarios. The intent was to provide a range of representative trajectories and fates to understand the range of potential biological impacts under different geographic and environmental conditions. Two additional biological model runs were conducted for each scenario to capture a range of biological sensitivities to contaminants. Together, this included 24 biological scenarios.

A deterministic modeling approach was used to provide a prediction of a representative individual release, based on specific parameters for each single event. The deterministic trajectory simulations provided representative estimates of the oil's fate and transport for a specific set of environmental conditions. Each scenario was simulated as a 10-minute release, where the trajectory, fate, and impacts were tracked for the following 48 hours after the release.

All modeled releases were assumed to be unmitigated, meaning that no response efforts were undertaken (e.g. booming, burning, skimming, collection).

The results of the deterministic simulations provided a time history of oil weathering over the duration of the spill (mass balance), expressed as the percentage of spilled oil on the water surface, on the shoreline, evaporated, entrained in the water column, and decayed. In addition, time-series snapshots of the individual trajectories showing the location of floating surface oil, shoreline oil, and the concentration of dissolved aromatics in the water column (surface and profile view) are provided. These results are described in in Section 6.

All modeled releases were assumed to enter the water directly at the Swinomish Channel and Skagit River release locations. The Edmonds Ferry Terminal site required the OILMAP Land™ model, an additional overland trajectory and fate model, to predict the downslope path and the amount of oil that could pool in depressions or adhere to land. The volumes of oil and entry-specific points reaching Puget Sound were calculated and used as inputs for the in-water SIMAP™ modeling portion.

It is important to note that because of the high degree of variability in environmental conditions within the study region, a spill occurring at a different date or time than those modeled could result in slightly different trajectory, fate, and potential impacts than reported here. Therefore, the area of surface oiling, mass of oil along the shoreline, and mass of oil within the water column, may be different for each modeled run. Overall, this modeling methodology provided a range of representative results for trajectory, fate, and biological impacts for each modeled hypothetical release.

6 Trajectory and Fate Analysis

This section provides modeled predictions of the expected trajectory and fate information for conditioned Bakken crude oil releases under multiple environmental conditions at three hypothetical release locations in the study area. Trajectory and fates results are shown for large 90th percentile discharges (90PD; 28 cars or 20,000 bbl oil) and smaller 30th percentile discharges (30PD; eight cars or 5,700 bbl oil) scenarios modeled for each season. A set of figures is provided for each modeled scenario.

6.1 Trajectory and Fate Results

The hydrocarbon trajectory provides a history of oil transport throughout the modeled domain in both time and space. Components of the oil are tracked as entrained droplets of oil, dissolved aromatic, floating surface oil, stranded oil on shorelines, and oil in the sediment. The following points describe the types of figures produced through the modeling process and the information they portray. Summary figures of trajectory and fate are provided for each location, season, and release volume. Mass balance information at the end of the 48-hour simulation is provided in tables for each of the release scenarios in terms of percent of oil spilled.

1. **Mass Balance**: Provide an estimate of the oil's weathering and fate for a specific run for the entire model duration as a fraction of the oil spilled up to that point. Components of the oil tracked over time include the amount of oil on the water surface, the total entrained hydrocarbons in the water column, the amount of oil on shore, the oil evaporated into the atmosphere, the oil in sediments, and the amount of oil that has decayed (accounts for both photo-oxidation and biodegradation).
2. **Hydrocarbon Trajectory Maps:** Provide maps showing the history of each individual particle of oil throughout the modeled domain in both time and space. Components of the oil are tracked as entrained droplets of oil, dissolved aromatic constituents, floating surface oil, and stranded shoreline oil. Darker colours indicate the presence of a portion of the oil after the 48-hour modeled period, at the last time step. The lighter shade of each type (surface oil as grey, entrained oil as light blue, and dissolved aromatics as light green) indicates that oil with that characteristic had previously passed through the region over the 48-hour modeled period, as a swept area or time history.
3. **Surface Oil Thickness Maps:** Provide maps depicting the footprint of maximum floating surface oil and the associated thicknesses (mm) over all time steps (cumulative view) of each individual 48-hour spill simulation.
4. **Water Column Concentration Maps:** Provide maps depicting the footprint of maximum water column concentration of dissolved aromatics (ppb) over all time steps (cumulative view) of each individual 48-hour spill simulation. Dissolved aromatics are the portion of the oil having the

greatest potential to affect water column biota, and the footprints from this analysis were typically smaller than the extent of total oil contamination in the water column. Water column contamination figures show only concentrations ≥ 1 ppb. Concentrations below 1 ppb are considered low and result in little water column impact.

5. **Shoreline and Sediment Impact:** Provide a figure depicting the total mass of oil deposited onto the shoreline and on sediments. Note that 1 µm thickness is roughly equivalent to 1 g/m^2.

6.2 Swinomish Channel Swing Bridge

The mass balance predictions in Figure 6-1 and Figure 6-6 show that the oil from hypothetical releases from the swing bridge during both the summer and winter seasons evaporated rapidly during the 48-hour simulation due to the large quantity of oil that remained on the water surface. As the oil evaporated and clung to the shoreline, the amount of oil floating on the surface decreased, respectively. There was very little entrainment and decay from the spills modeled at this spill location. Table 6-1 provides a summary of the mass balance information at the end of the 48-hour simulation.

Table 6-1: Summary of the mass balance information at the Swinomish Channel Swing Bridge release location at the end of the 48-hour simulation. All values represent a percentage of the total spilled oil.

Summary of Mass Balance Information at the End of the 48-hour Simulation (Percentage of Spilled Oil)						
Scenario	**Surface (%)**	**Evaporated (%)**	**Water Column (%)**	**Sediment (%)**	**Ashore (%)**	**Decayed (%)**
90PD Summer (Spring Tide)	31.6	53.1	0.1	0.0	14.1	1.0
30PD Summer (Spring Tide)	28.0	53.1	0.1	0.0	17.7	1.0
90PD Winter (Neap Tide)	32.9	53.0	0.0	0.0	13.0	1.0
30PD Winter (Neap Tide)	19.5	52.0	0.0	0.0	27.4	1.0

During the summer season, floating surface oil generally traveled north into Padilla Bay, toward Bellingham Bay (Figure 6-2). As the currents shifted with the tide (Figure 2-9), a fraction of the surface oil traveled south toward Skagit Bay. The aromatic fraction of the oil traveled farther than the floating surface oil both south into Skagit Bay and west into the Rosario Strait. As shown on Figure 6-3, the thickest oil stayed within the Swinomish Channel and Padilla Bay, with a thickness greater than 1 mm. The extent of oiling during the winter season (Figure 6-8) at the Swinomish Channel release location was much smaller. Although oil traveled south in the Swinomish Channel, it did not reach Skagit Bay. Additionally, the oil that traveled north remained within Padilla Bay. The thickest oil (> 1 mm) was within the channel and directly north of the channel.

Figure 6-4 illustrates that the highest maximum total dissolved aromatic concentration during the summer season was within Padilla Bay and south in Skagit Bay for both the 90PD and 30PD simulations. There was very little oil that adhered to sediments in the region of the Swinomish Channel. As shown on Figure 6-5, the majority of oil that did adhere to sediments was less than 0.01 g/m^2 and occurred within the Swinomish Channel and Padilla Bay. The total hydrocarbon concentration on most oiled shorelines was greater than 500 g/m^2, although there were some segments of shoreline with total hydrocarbon concentrations between 100 and 500 g/m^2.

During the winter season, the highest maximum total dissolved aromatic concentration was within Padilla Bay (Figure 6-9). Note that the concentrations are higher, but localized to a smaller area, when compared to the summer season release. Total hydrocarbon concentrations on sediments were very low (less than 0.01 g/m^2) (Figure 6-10). Concentrations on the shoreline were high (greater than 500 g/m^2) and were primarily present within Swinomish Channel, although there was some shoreline oiling to the north and east of the spill site (Figure 6-10).

Swinomish Channel Swing Bridge – Summer (Spring Tide Flux)

6.2.1

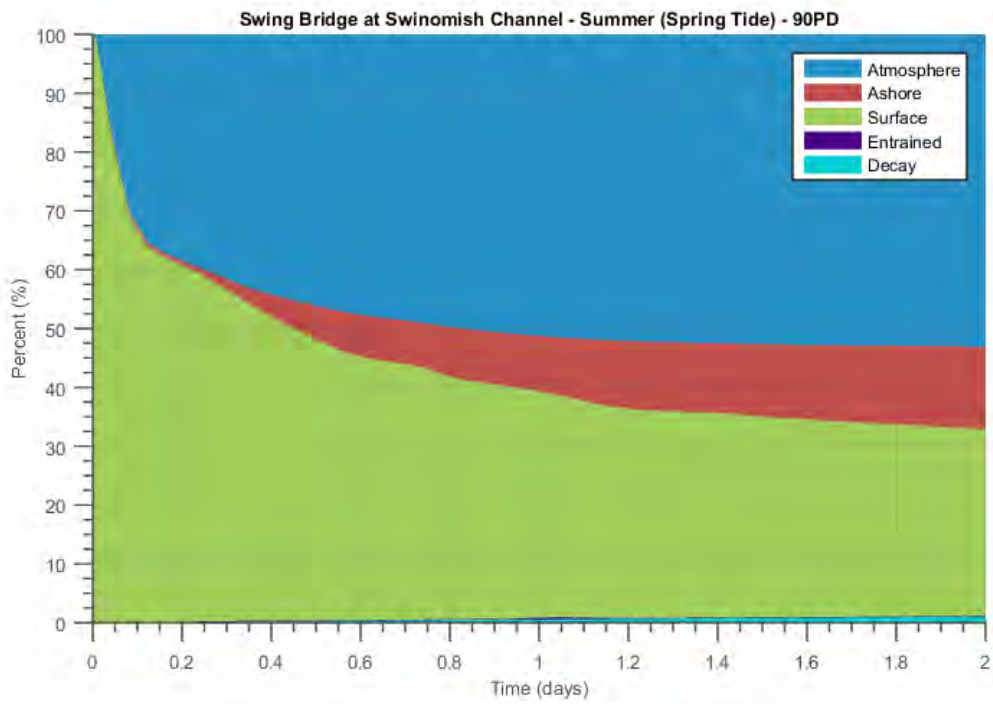

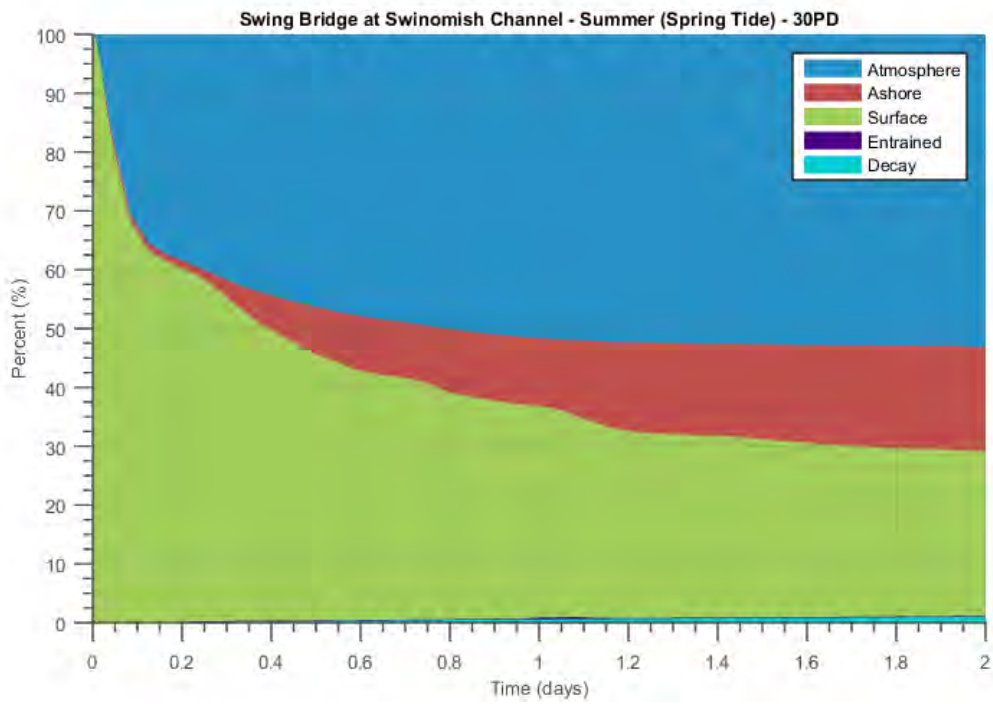

Figure 6-1: Oil mass balance graphs for the 90PD (top) and 30PD (bottom) at the Swinomish Channel Swing Bridge release location during the summer (spring tide) season. Entrained and decayed oil make up approximately 1 percent of the total mass or less.

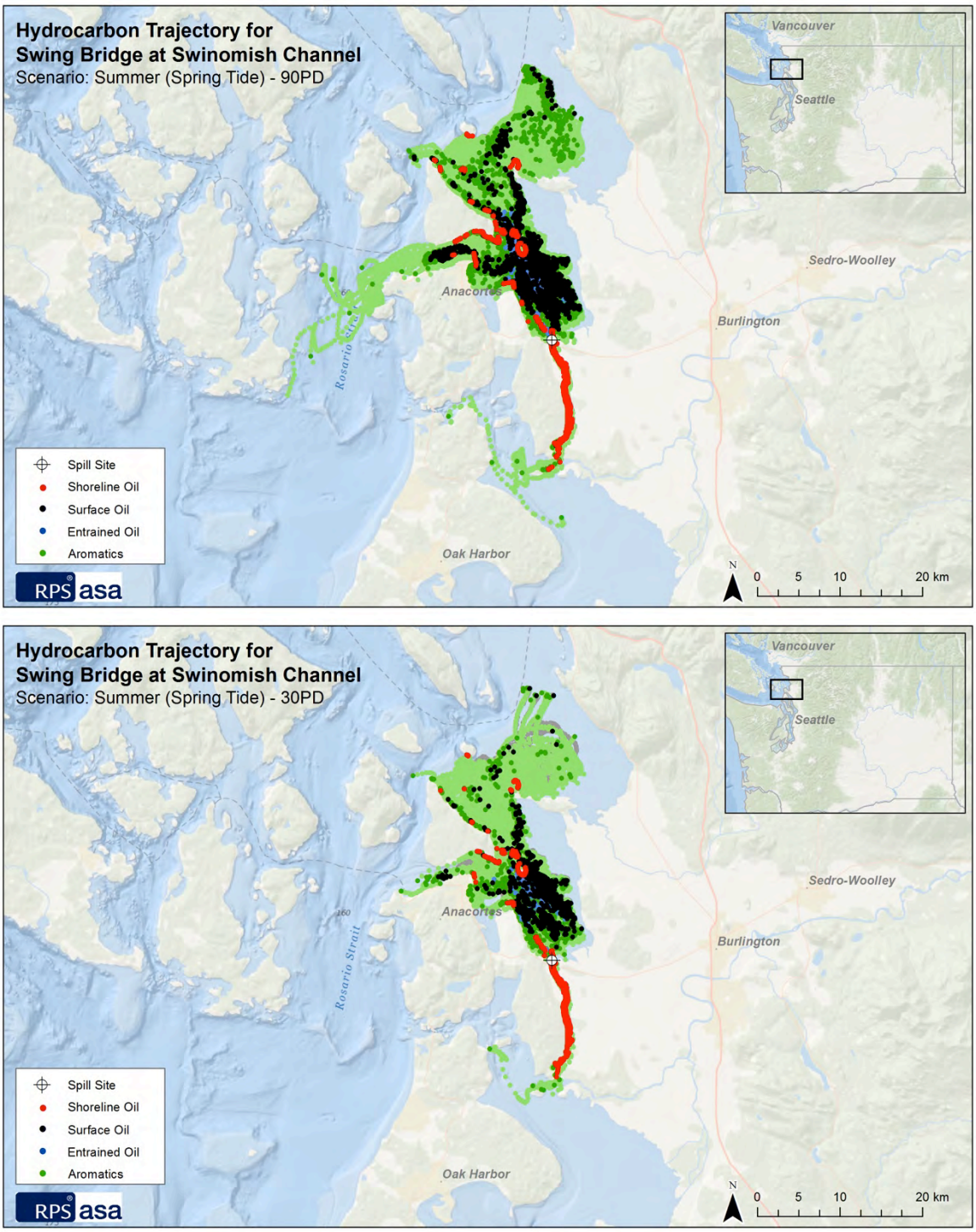

Figure 6-2: Oil trajectories for 90PD (top) and 30PD (bottom) at the Swinomish Channel Swing Bridge release location during the summer (spring tide) season.

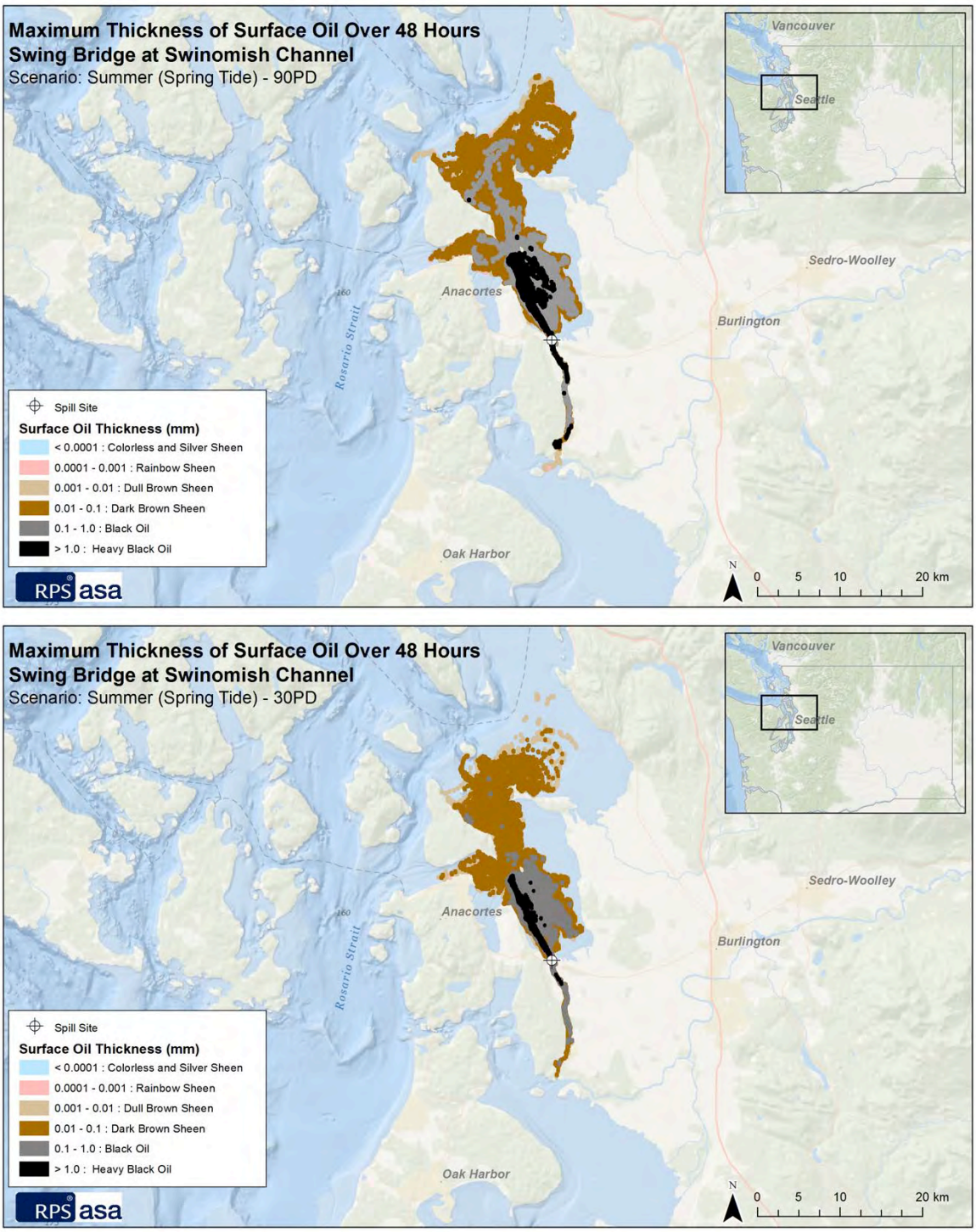

Figure 6-3: Maximum cumulative surface oil thickness for 90PD (top) and 30PD (bottom) scenarios at the Swinomish Channel Swing Bridge release location during the summer (spring tide) season.

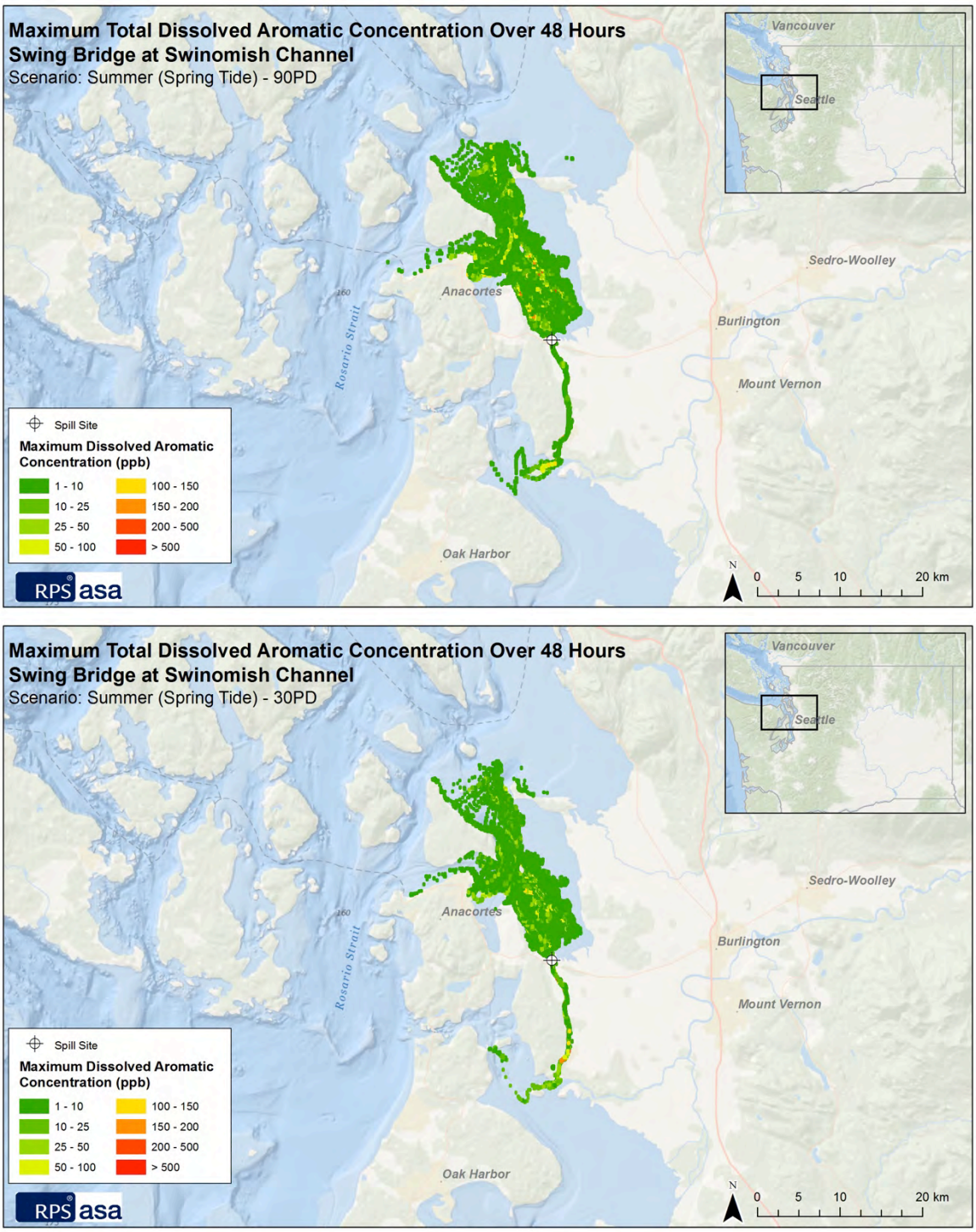

Figure 6-4: Cumulative total dissolved aromatic concentration for 90PD (top) and 30PD (bottom) scenarios at the Swinomish Channel Swing Bridge release location during the summer (spring tide) season.

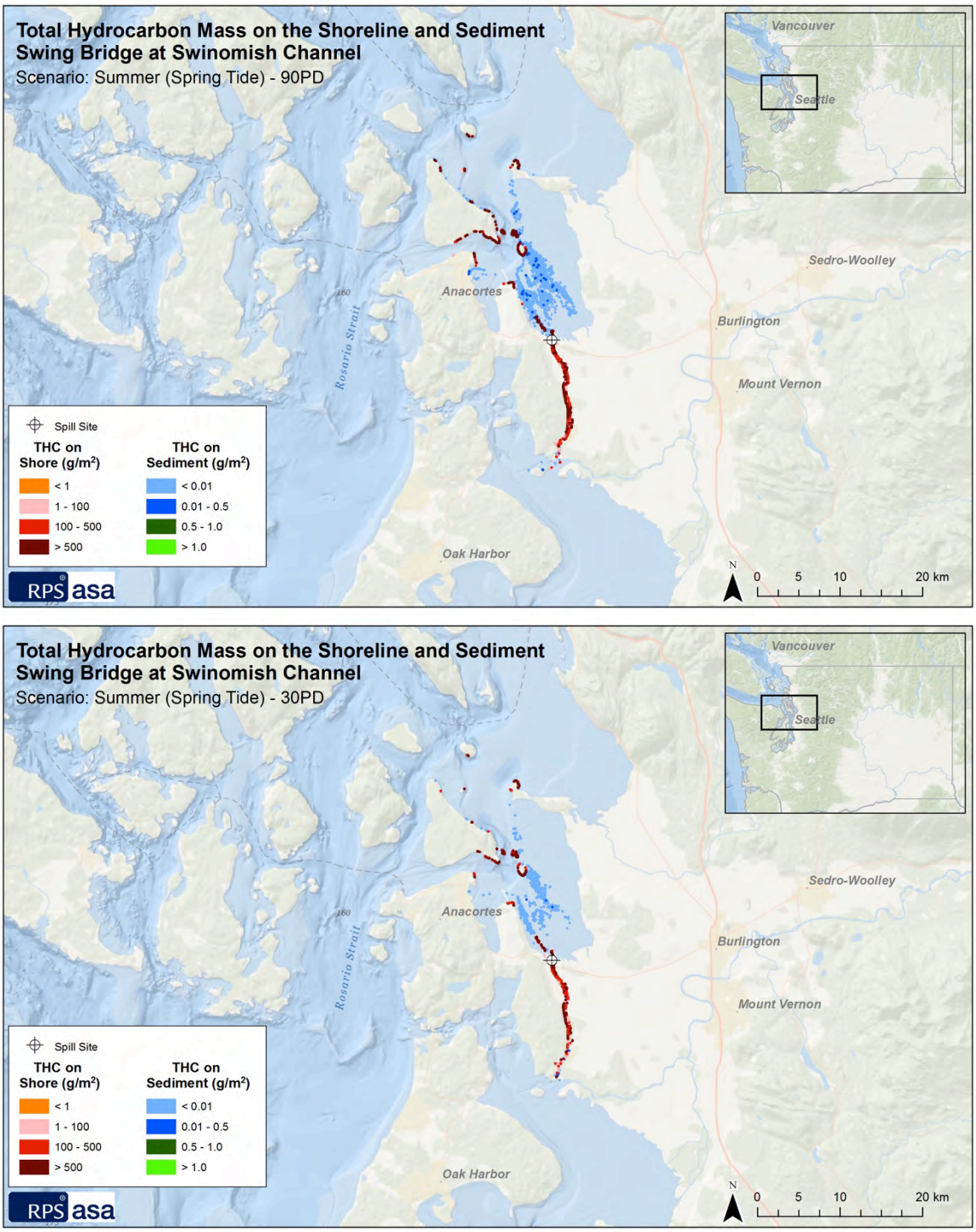

Figure 6-5: Total hydrocarbon mass on the shore and on sediments for 90PD (top) and 30PD (bottom) scenarios at the Swinomish Channel Swing Bridge release location during the summer (spring tide) season.

Swinomish Channel Swing Bridge – Winter (Neap Tide Flux)

6.2.2

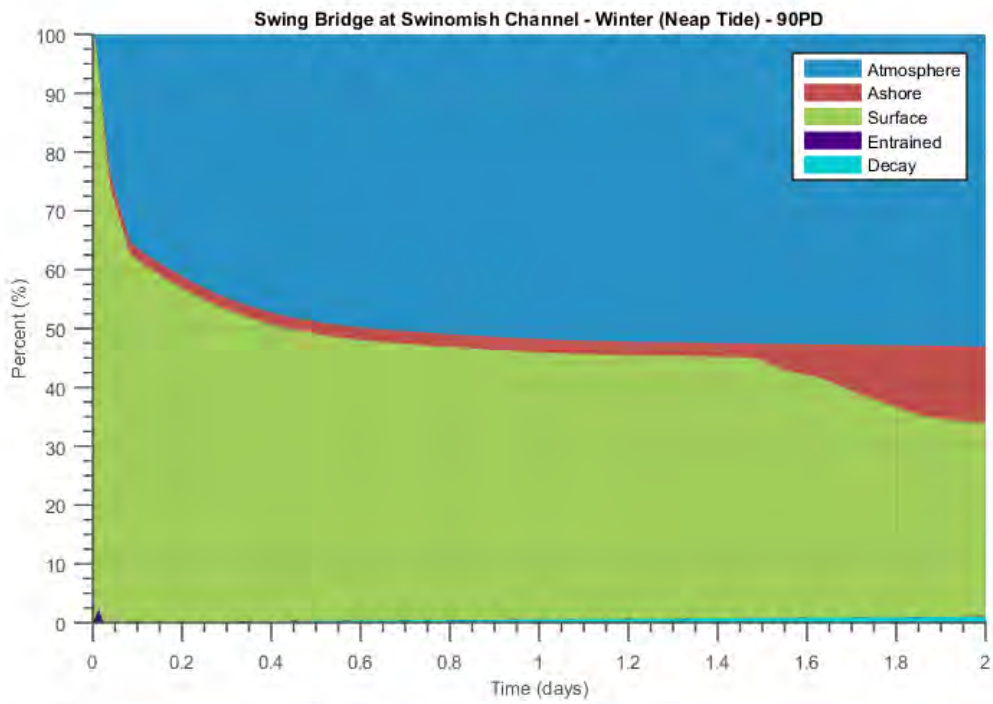

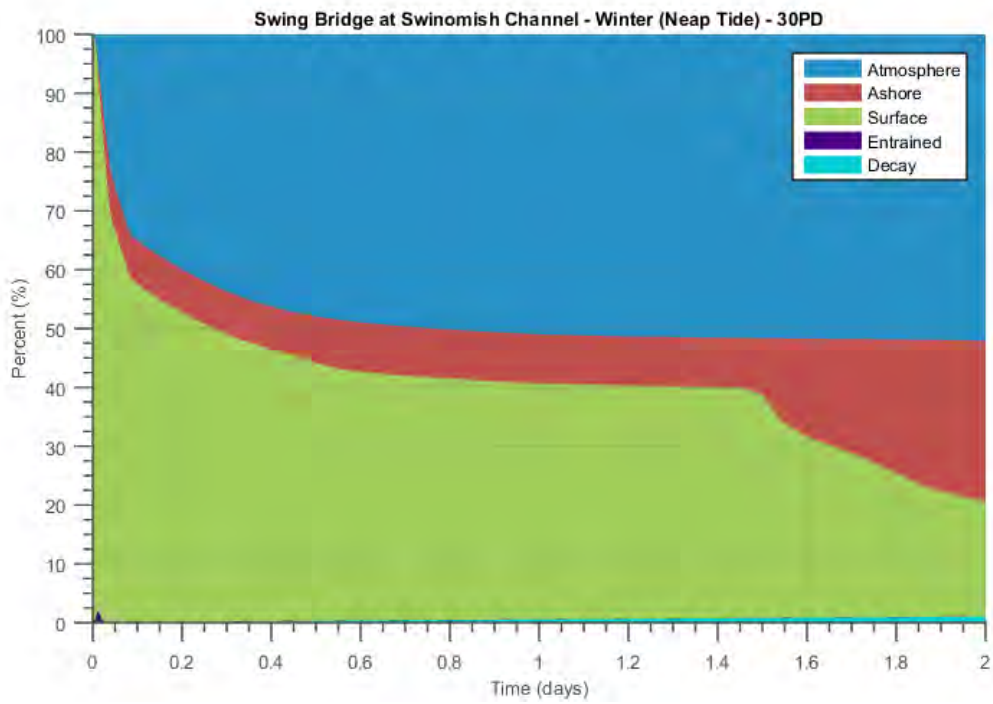

Figure 6-6: Oil mass balance graphs for the 90PD (top) and 30PD (bottom) at the Swinomish Channel Swing Bridge release location during the winter (neap tide) season. Entrained and decayed oil make up approximately 1 percent of the total mass or less.

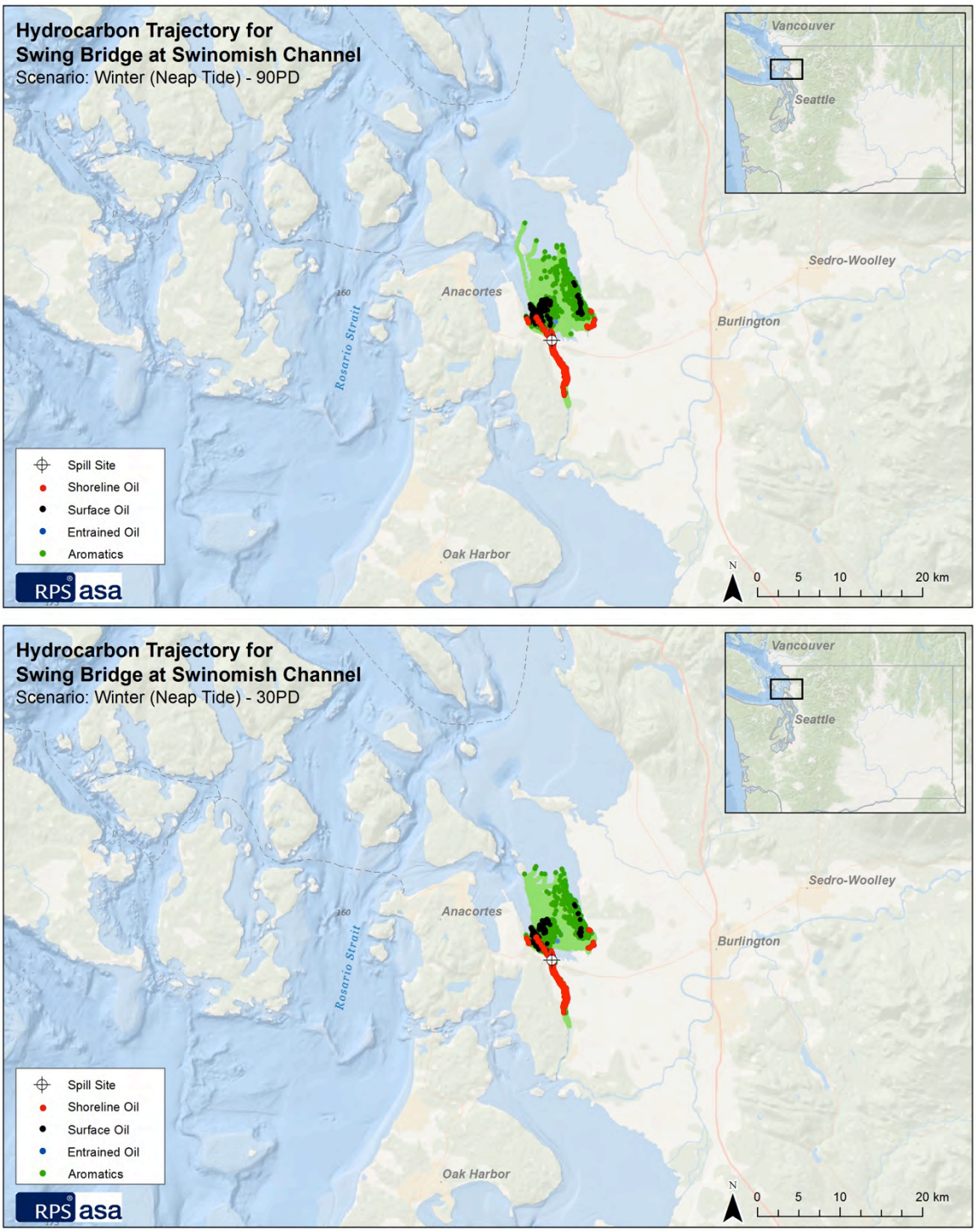

Figure 6-7: Oil trajectories for 90PD (top) and 30PD (bottom) at the Swinomish Channel Swing Bridge release location during the winter (neap tide) season.

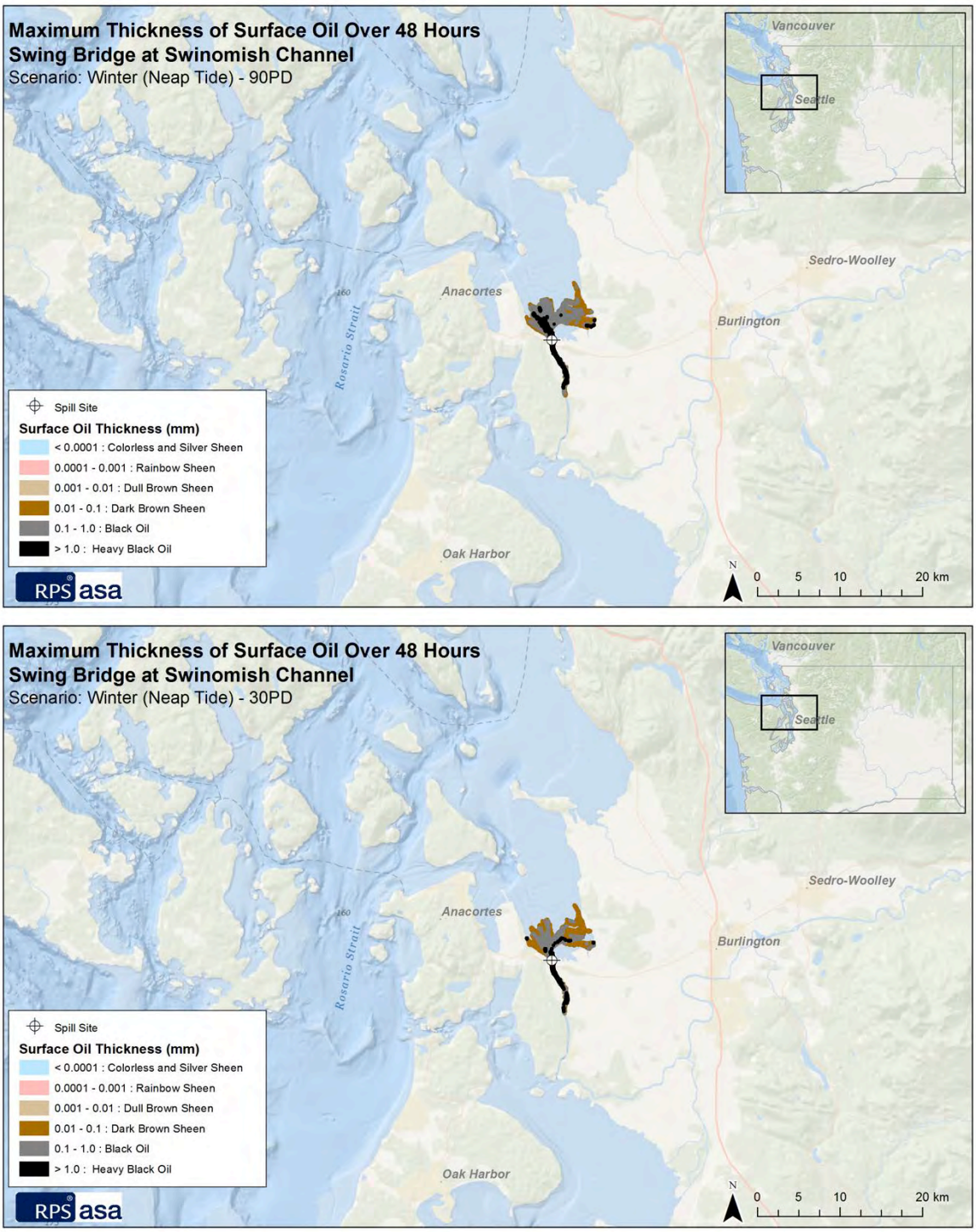

Figure 6-8: Maximum cumulative surface oil thickness for 90PD (top) and 30PD (bottom) scenarios at the Swinomish Channel Swing Bridge release location during the winter (neap tide) season.

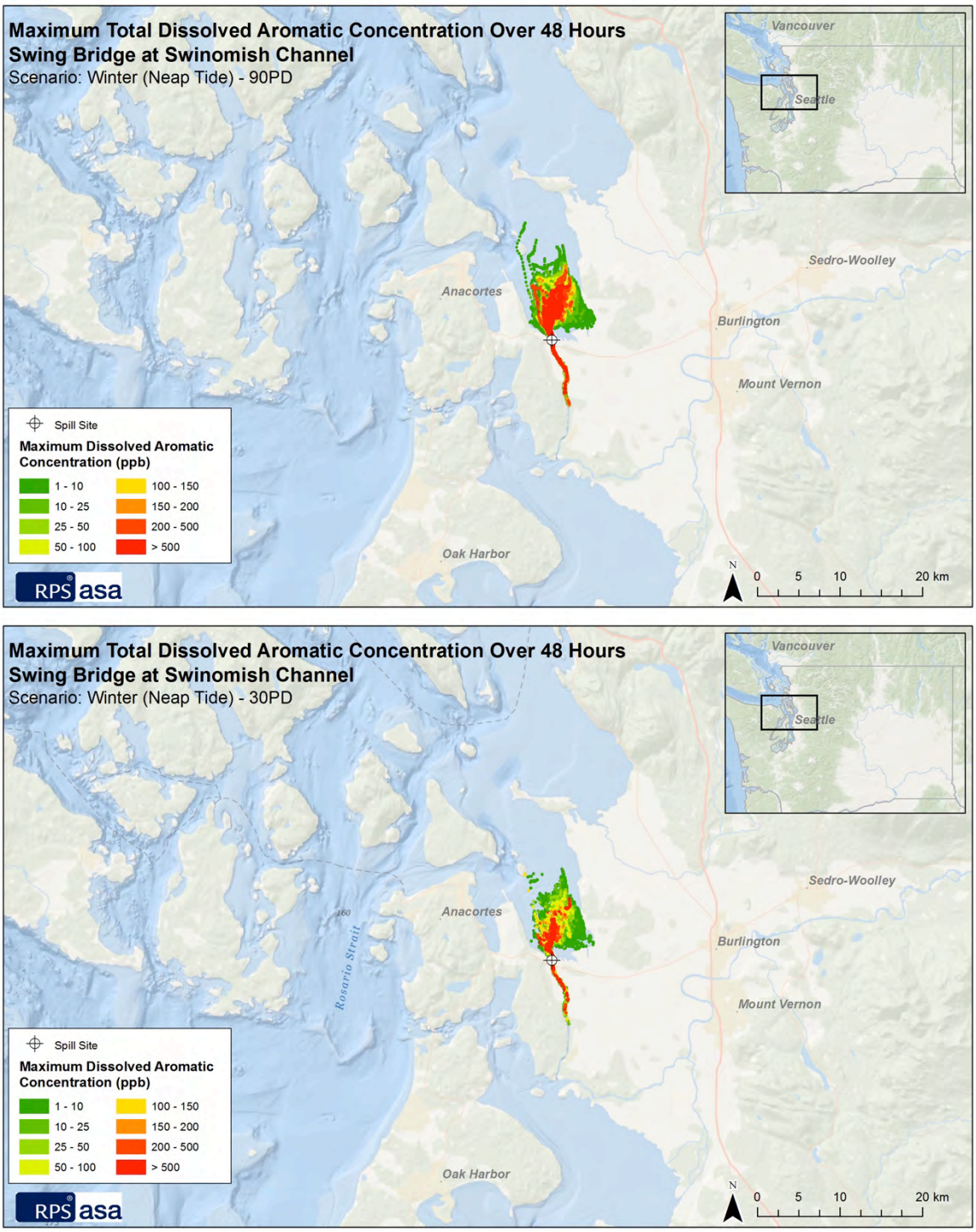

Figure 6-9: Cumulative total dissolved aromatic concentration for 90PD (top) and 30PD (bottom) scenarios at the Swinomish Channel Swing Bridge release location during the winter (neap tide) season.

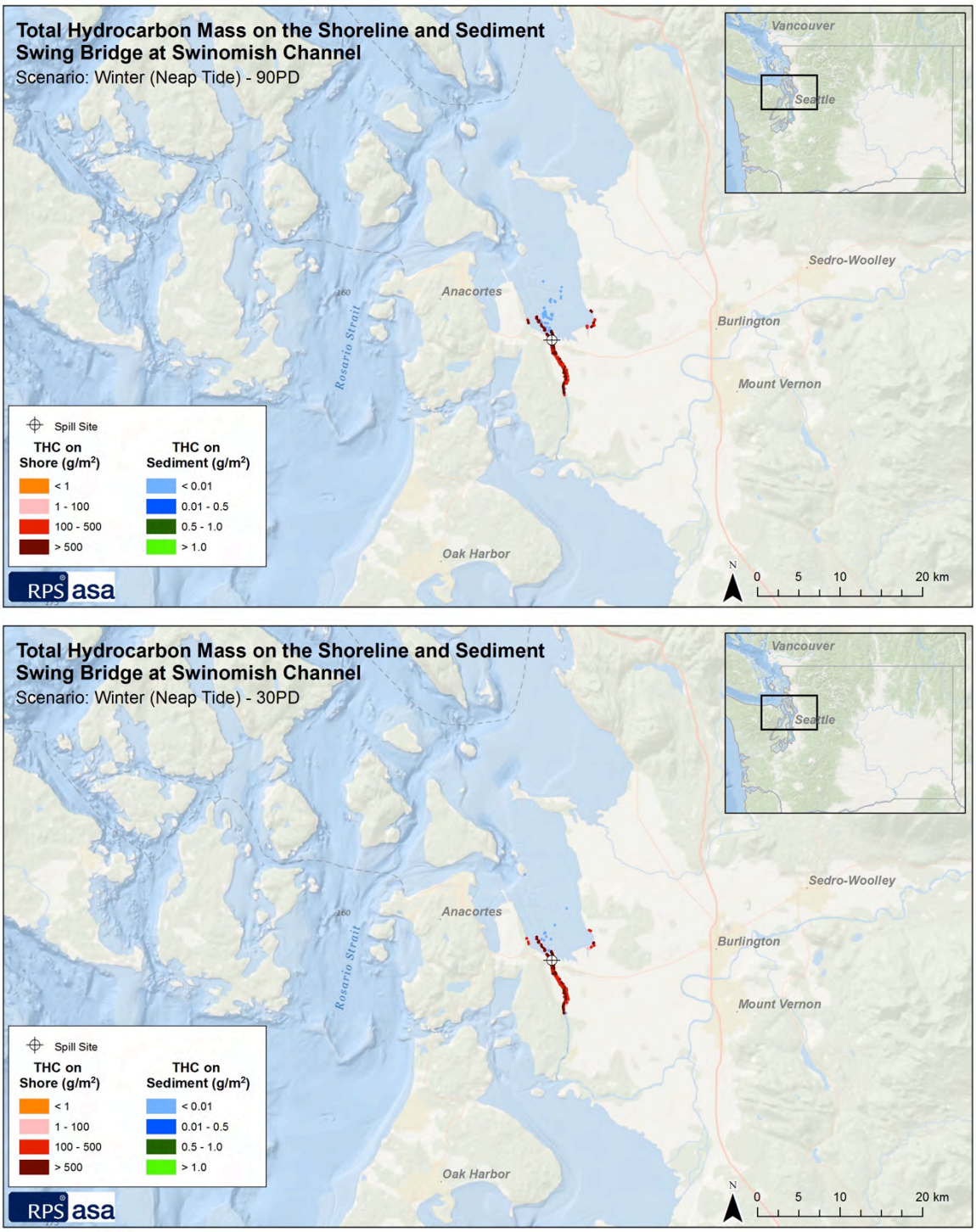

Figure 6-10: Total hydrocarbon mass on the shore and sediments for 90PD (top) and 30PD (bottom) scenarios at the Swinomish Channel Swing Bridge release location during the winter (neap tide) season.

6.3 Skagit River Crossing

The mass balance predictions in Figure 6-11 and Figure 6-16 depict that the oil from hypothetical spills from the Skagit River Crossing during the summer and winter seasons both stranded on the shoreline and evaporated rapidly over the 48-hour simulation. As the oil evaporated and clung to the shoreline, the amount of oil floating on the water's surface decreased, respectively. There was very little entrainment, sedimentation, and decay from the spills originating at this release location. Table 6-2 provides a summary of the mass balance information at the end of the 48-hour simulation.

Table 6-2: Summary of the mass balance information at the Skagit River Crossing release location at the end of the 48-hour simulation. All values represent a percentage of the total spilled oil.

Summary of Mass Balance Information at the End of the 48-hour Simulation (Percentage of Spilled Oil)						
Scenario	**Surface (%)**	**Evaporated (%)**	**Water Column (%)**	**Sediment (%)**	**Ashore (%)**	**Decayed (%)**
90PD Summer (High Flow)	2.3	48.8	0.1	0.0	47.7	1.1
30PD Summer (High Flow)	1.7	50.3	0.1	0.0	46.8	1.1
90PD Winter (Low Flow)	6.9	52.3	0.2	0.1	39.4	1.1
30PD Winter (Low Flow)	0.0	43.6	0.0	0.0	55.1	1.2

During the high flow summer season, the oil originating from the hypothetical Skagit River Crossing release location traveled down the Skagit River, through both the north and south forks, into Skagit Bay. Shorelines along the Skagit River and within Skagit Bay were oiled extensively. Once the oil reached Skagit Bay, the dissolved aromatics and surface oil traveled northwest, around Pass Island, through Canoe and Deception passes, and into the Rosario Strait. Additionally, oil traveled south in Skagit Bay around Camano Island (Figure 6-12). As shown by Figure 6-13, the thickest floating surface oil (greater than 1 mm) was confined to the Skagit River, with thinner dark brown, dull brown, and rainbow sheens present on the surface of Skagit Bay.

During the low flow winter season, oil in the 90PD scenario reached Skagit Bay and traveled up the Swinomish Channel into Padilla Bay (Figure 6-17). However, oil originating from the low flow 30PD scenario did not travel up the Swinomish Channel. The overall extent of oiling during the low flow season was much smaller when compared with the high flow season. As in the high flow scenarios, the thickest floating surface oil (greater than 1 mm) was found within the Skagit River, with almost no surface oil present in Skagit Bay. The small amount of surface oil outside of the Skagit River was only

observed in the 90PD release as mainly dark brown and dull brown sheens localized to the northern-most region of Skagit Bay, the Swinomish Channel, and the southern end of Padilla Bay.

Due to the confinement within the river channel and the large extent of the spills during the high flow and low flow seasons, the highest maximum dissolved aromatic concentrations (greater than 500 ppb) extended beyond the Skagit River into Skagit Bay (Figure 6-14 and Figure 6-19). During the high flow summer season, the maximum total hydrocarbon concentration on sediments was in the 0.01 to 0.5 g/m^2 range (within both Skagit River and Skagit Bay). This was due to the higher SPM concentrations and potential for oil to adhere to particulates and sink. The total hydrocarbon concentrations on the shoreline were high, primarily greater than 500 g/m^2. During the low flow winter season, the maximum total hydrocarbon concentration on the shoreline (greater than 500 g/m^2.) was within the Skagit River (Figure 6-20). During the 90PD scenario, the shorelines in the Swinomish Channel had maximum concentrations ranging from 100 to 500 ppb. Total hydrocarbon concentrations on sediments did not exceed 0.5 g/m^2 in the low flow winter scenarios.

6.3. Skagit River Crossing – Summer (High Flow)

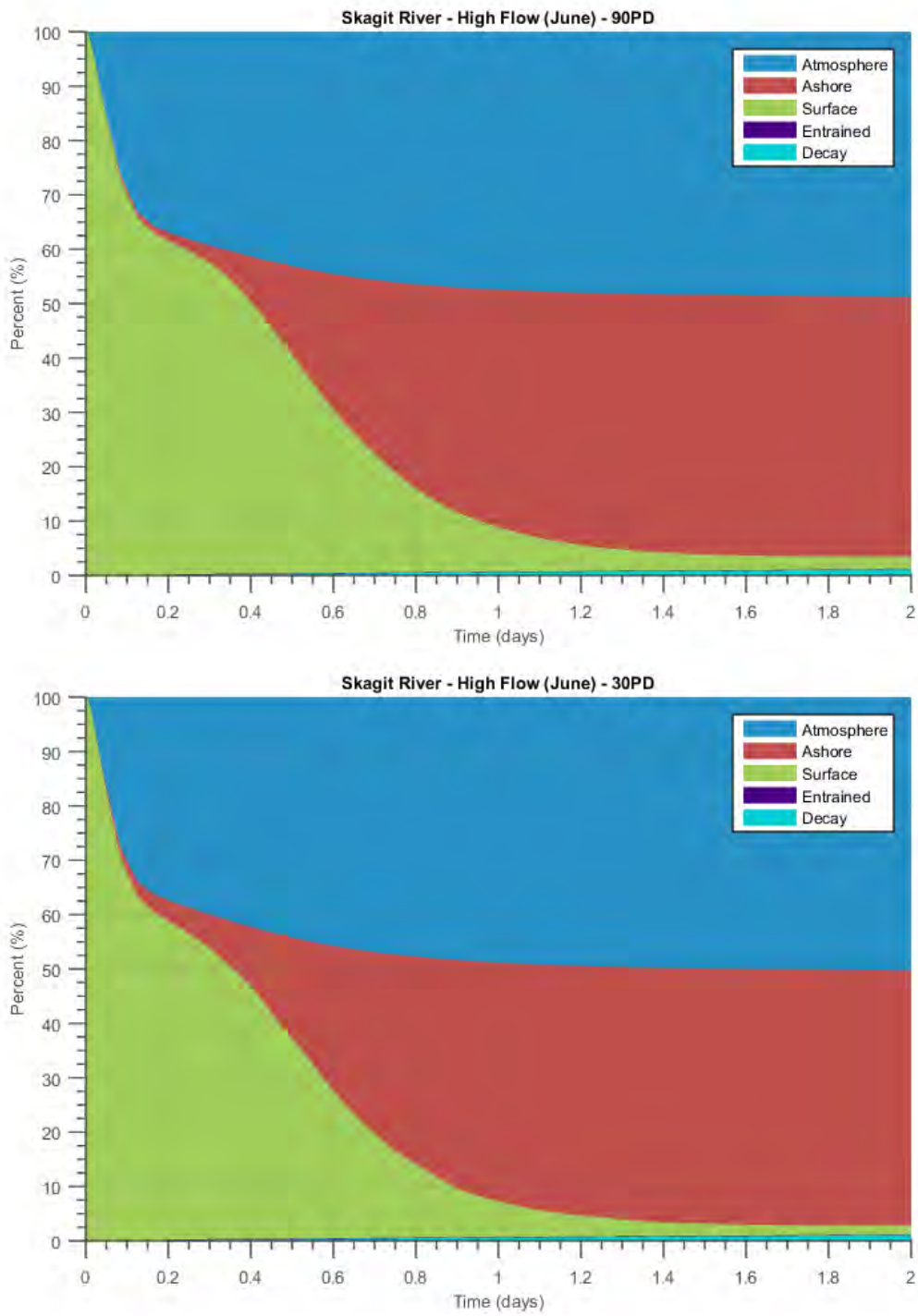

Figure 6-11: Oil mass balance graphs for the 90PD (top) and 30PD (bottom) at the Skagit River Crossing release location during the summer (high flow) season. Entrained and decayed oil make up approximately 1 percent of the total mass or less.

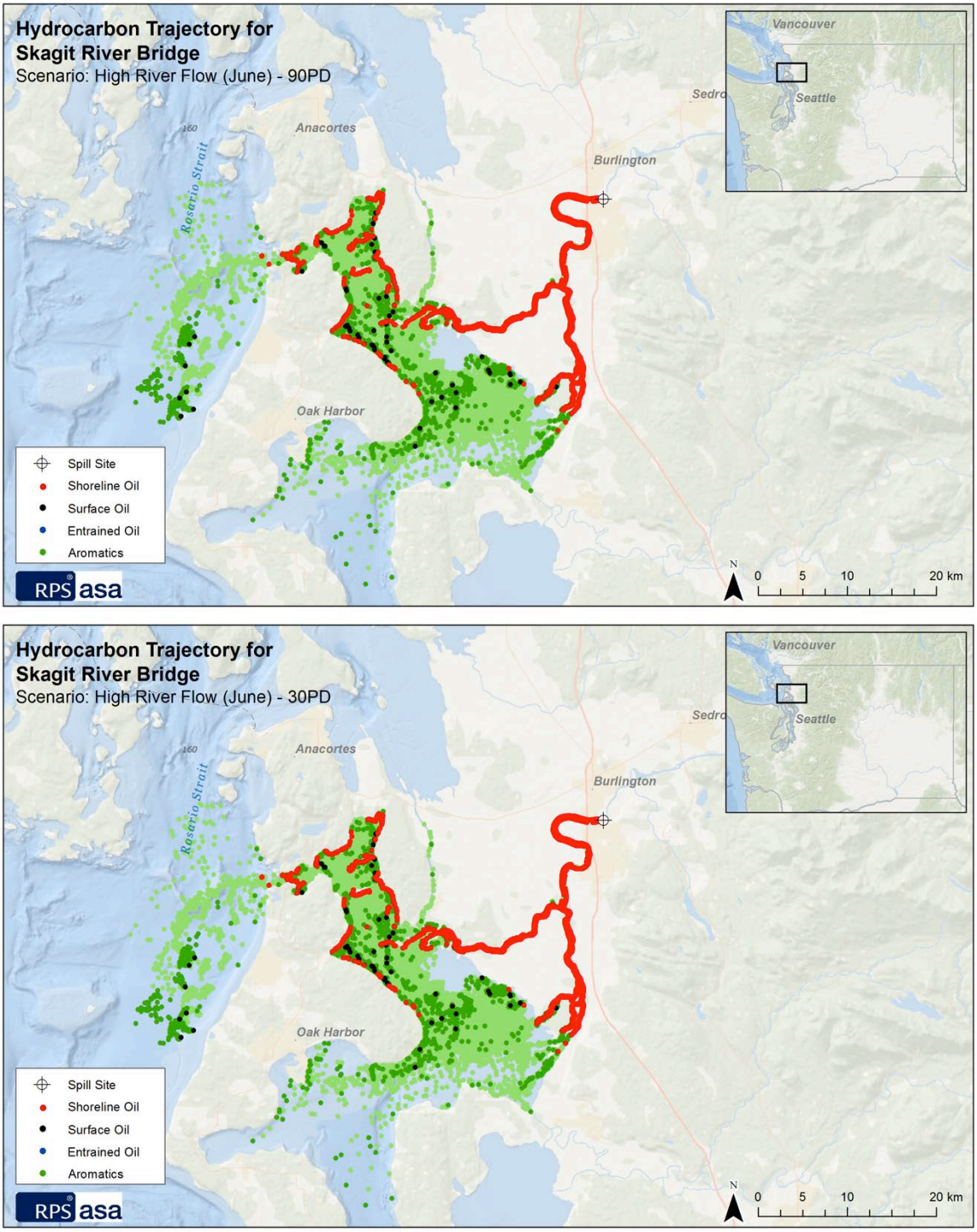

Figure 6-12: Oil trajectories for 90PD (top) and 30PD (bottom) at the Skagit River Crossing release location during the summer (high flow) season.

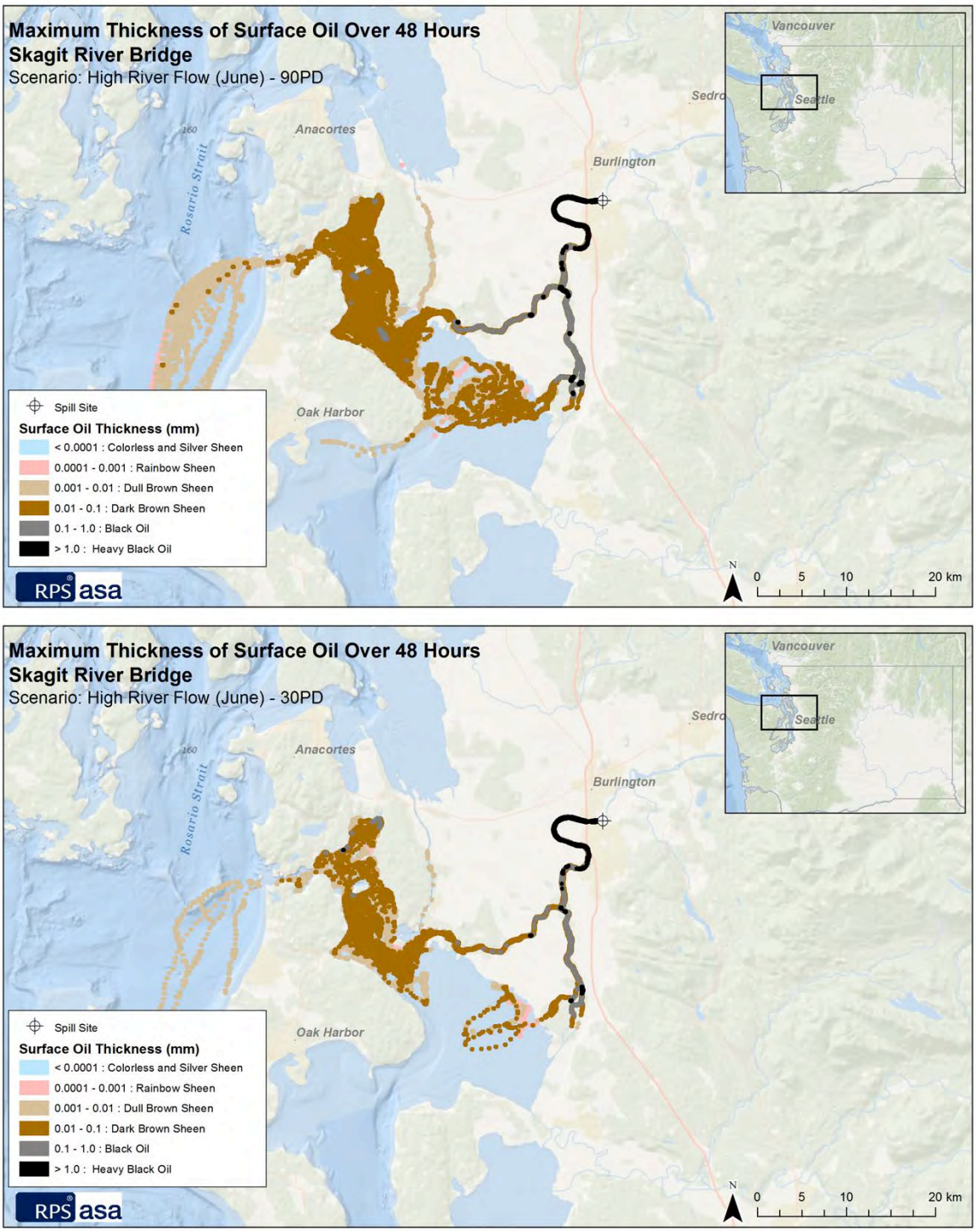

Figure 6-13: Maximum cumulative surface oil thickness for 90PD (top) and 30PD (bottom) scenarios at the Skagit River Crossing release location during the summer (high flow) season.

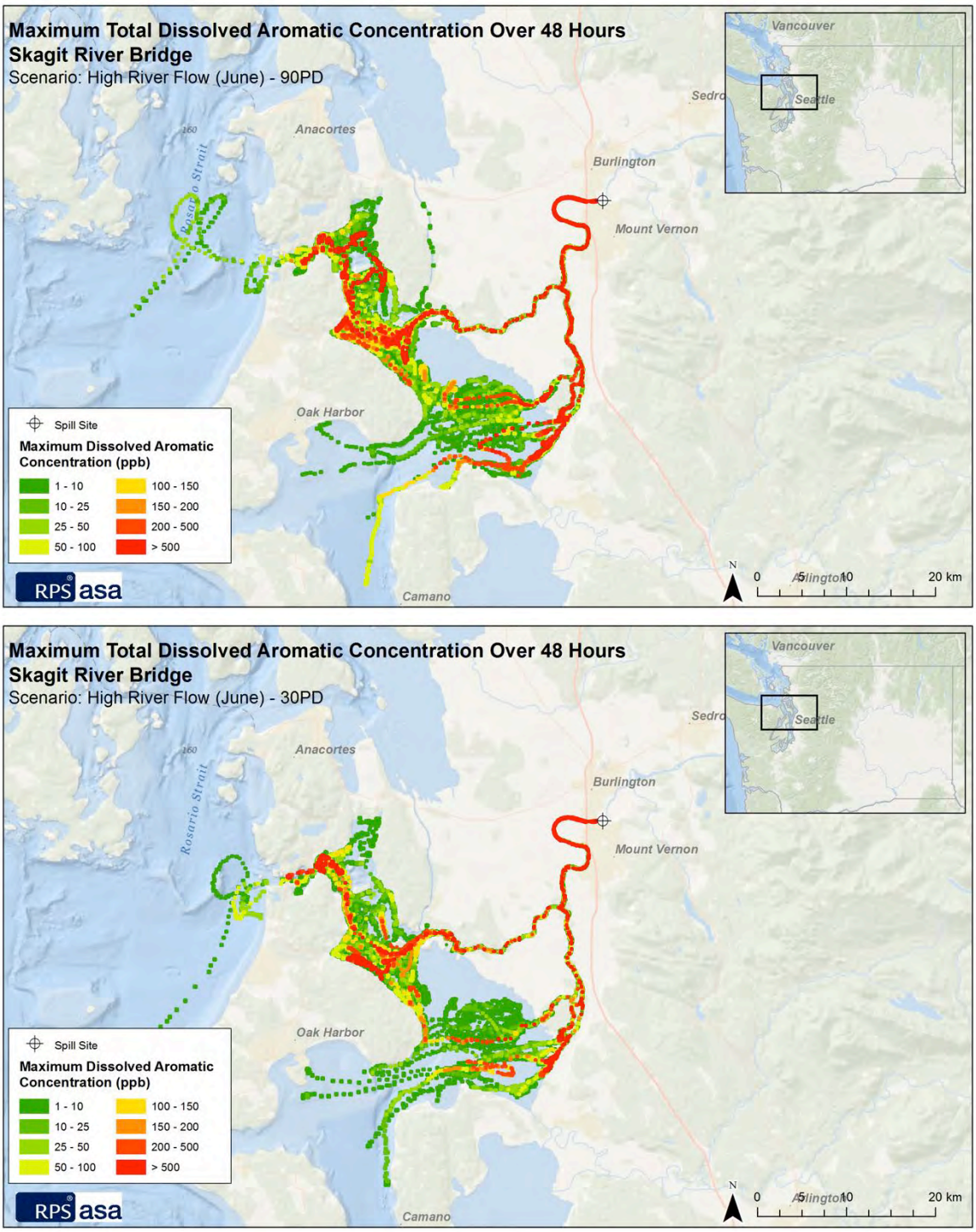

Figure 6-14: Cumulative total dissolved aromatic concentration for 90PD (top) and 30PD (bottom) scenarios at the Skagit River Crossing release location during the summer (high flow) season.

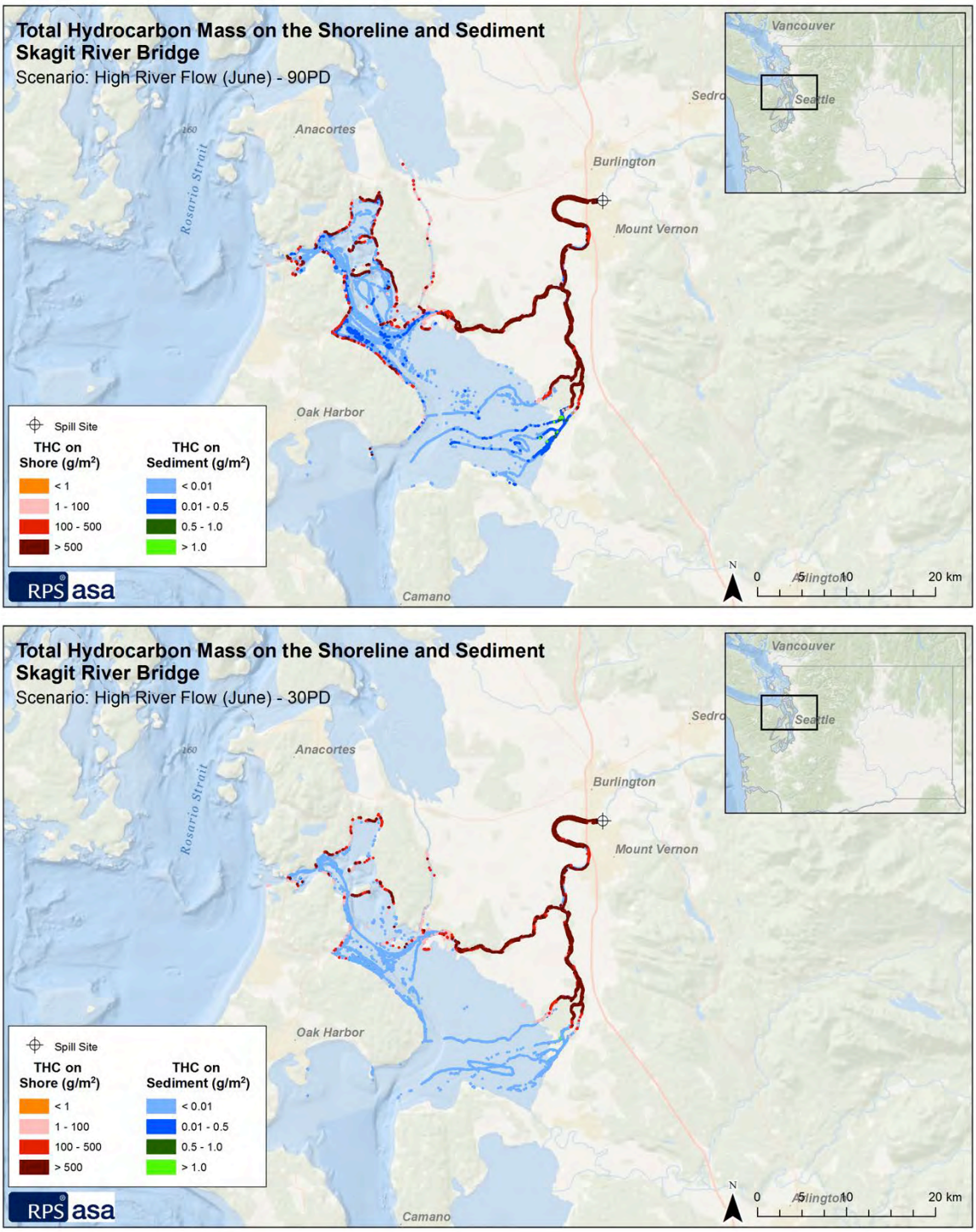

Figure 6-15: Total hydrocarbon mass on the shore and on sediments for 90PD (top) and 30PD (bottom) scenarios at the Skagit River Crossing release location during the summer (high flow) season.

Skagit River Crossing – Winter (Low Flow)

6.3.

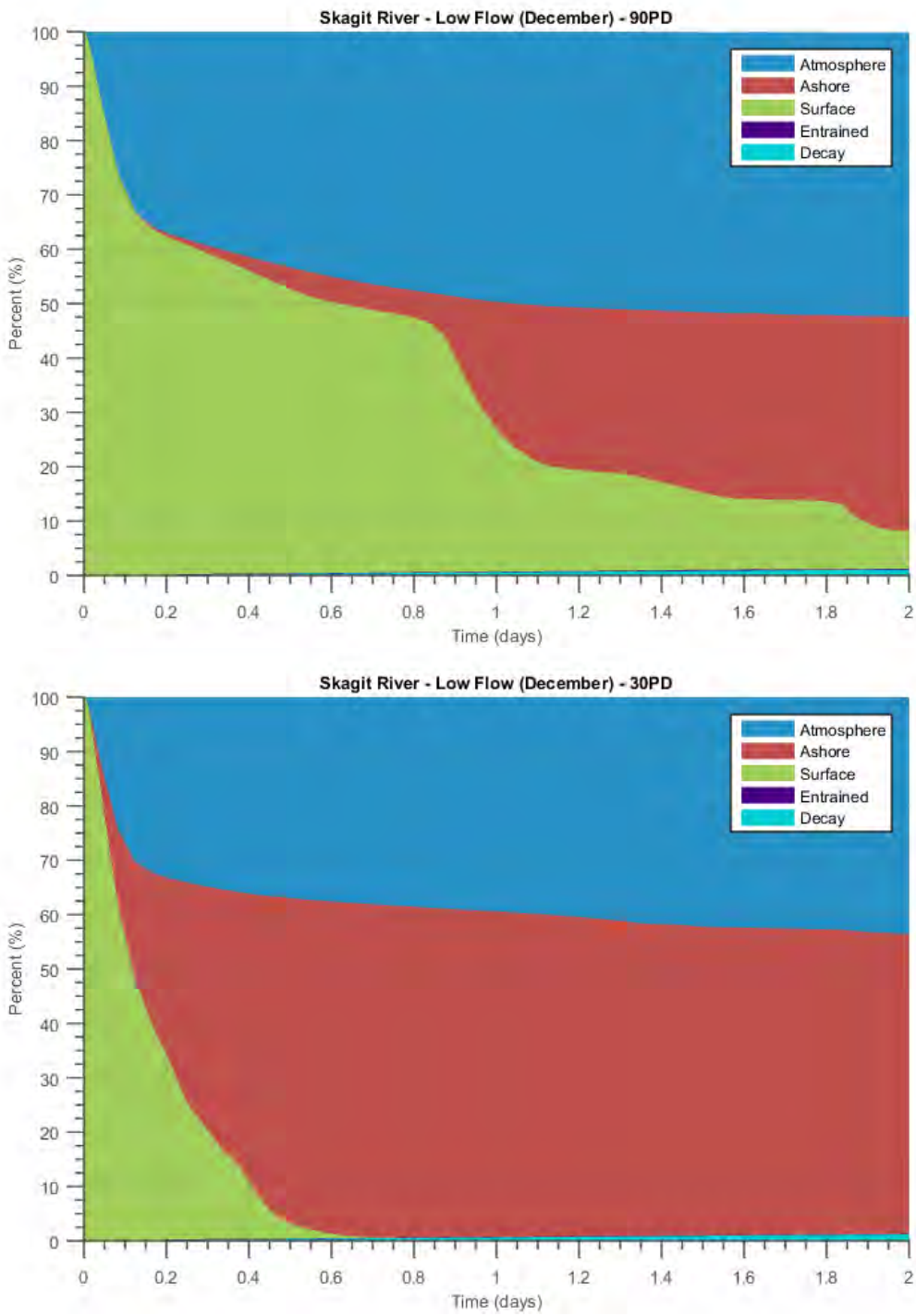

Figure 6-16: Oil mass balance graphs for the 90PD (top) and 30PD (bottom) at the Skagit River Crossing release location during the winter (low flow) season. Entrained and decayed oil make up approximately 1 percent of the total mass or less.

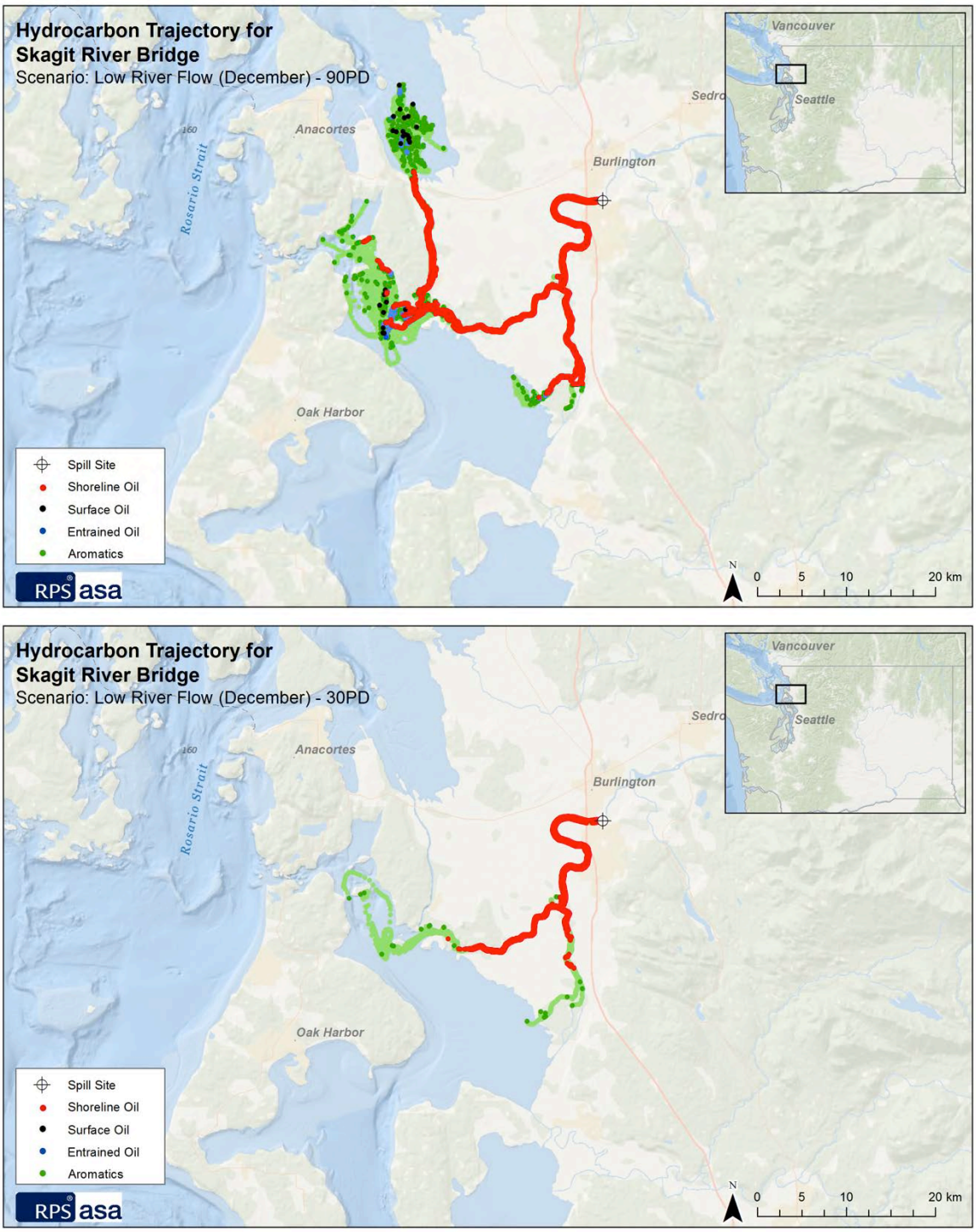

Figure 6-17: Oil trajectories for 90PD (top) and 30PD (bottom) at the Skagit River Crossing release location during the winter (low flow) season.

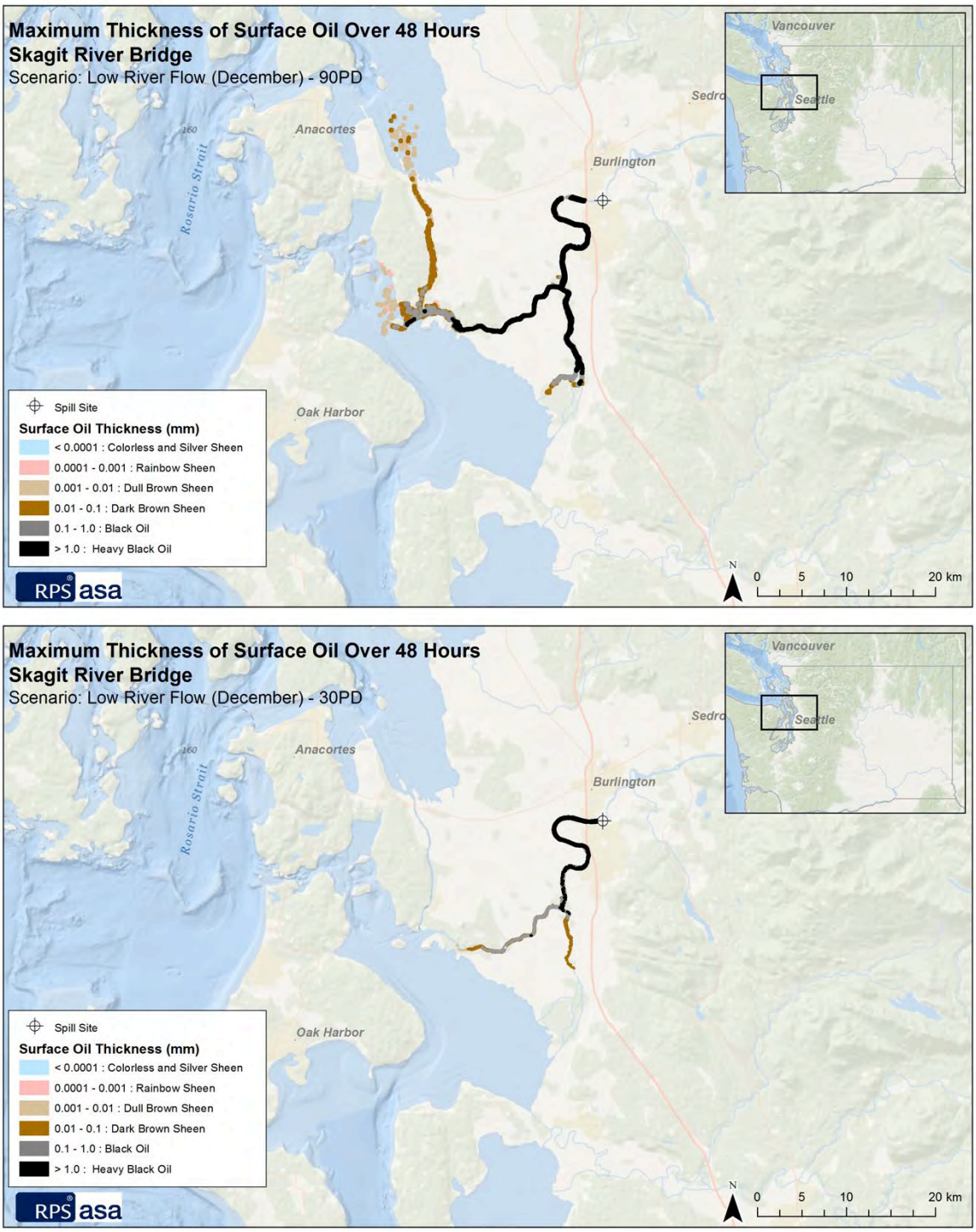

Figure 6-18: Maximum cumulative surface oil thickness for 90PD (top) and 30PD (bottom) scenarios at the Skagit River Crossing release location during the winter (low flow) season.

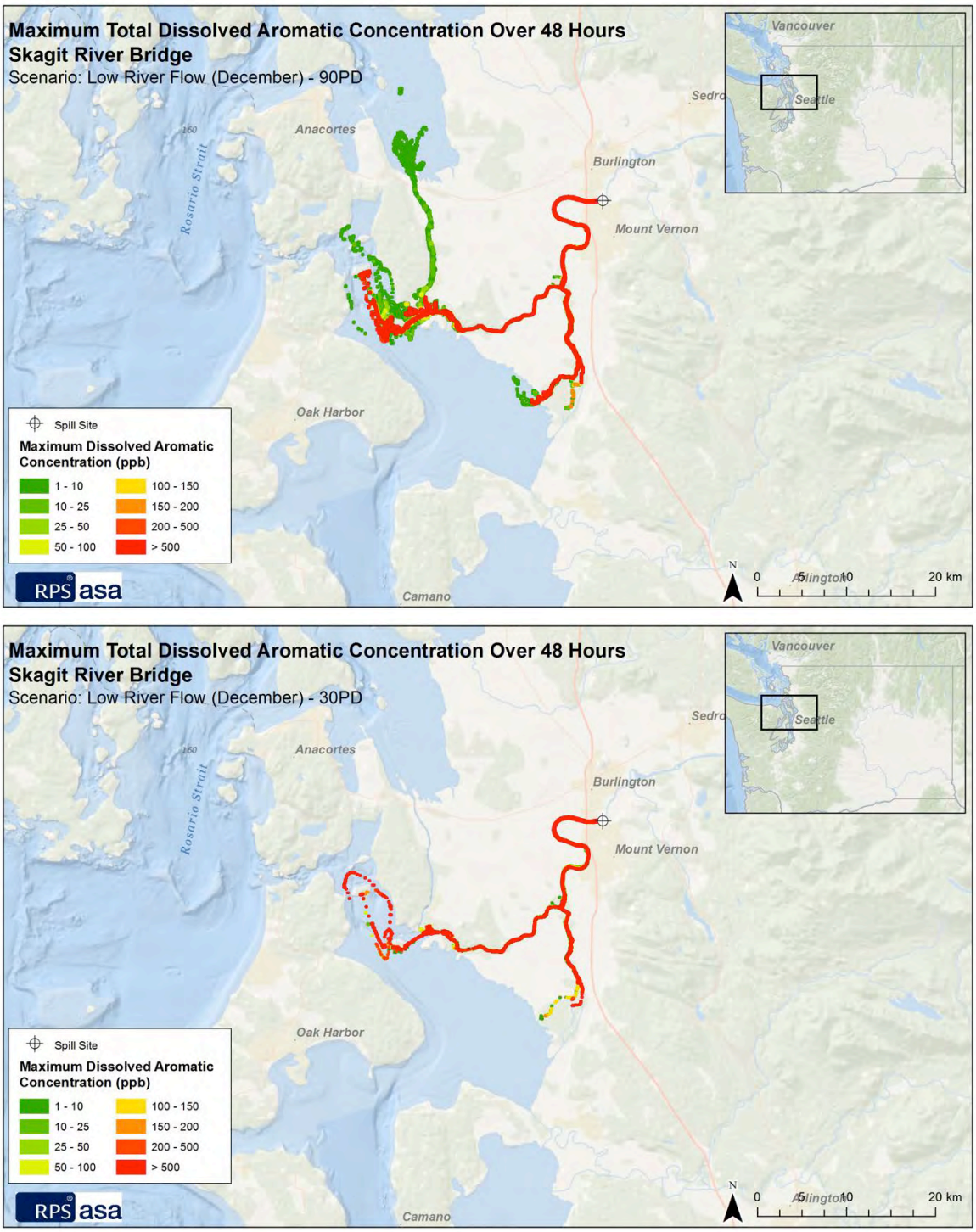

Figure 6-19: Cumulative total dissolved aromatic concentration for 90PD (top) and 30PD (bottom) scenarios at the Skagit River Crossing release location during the winter (low flow) season.

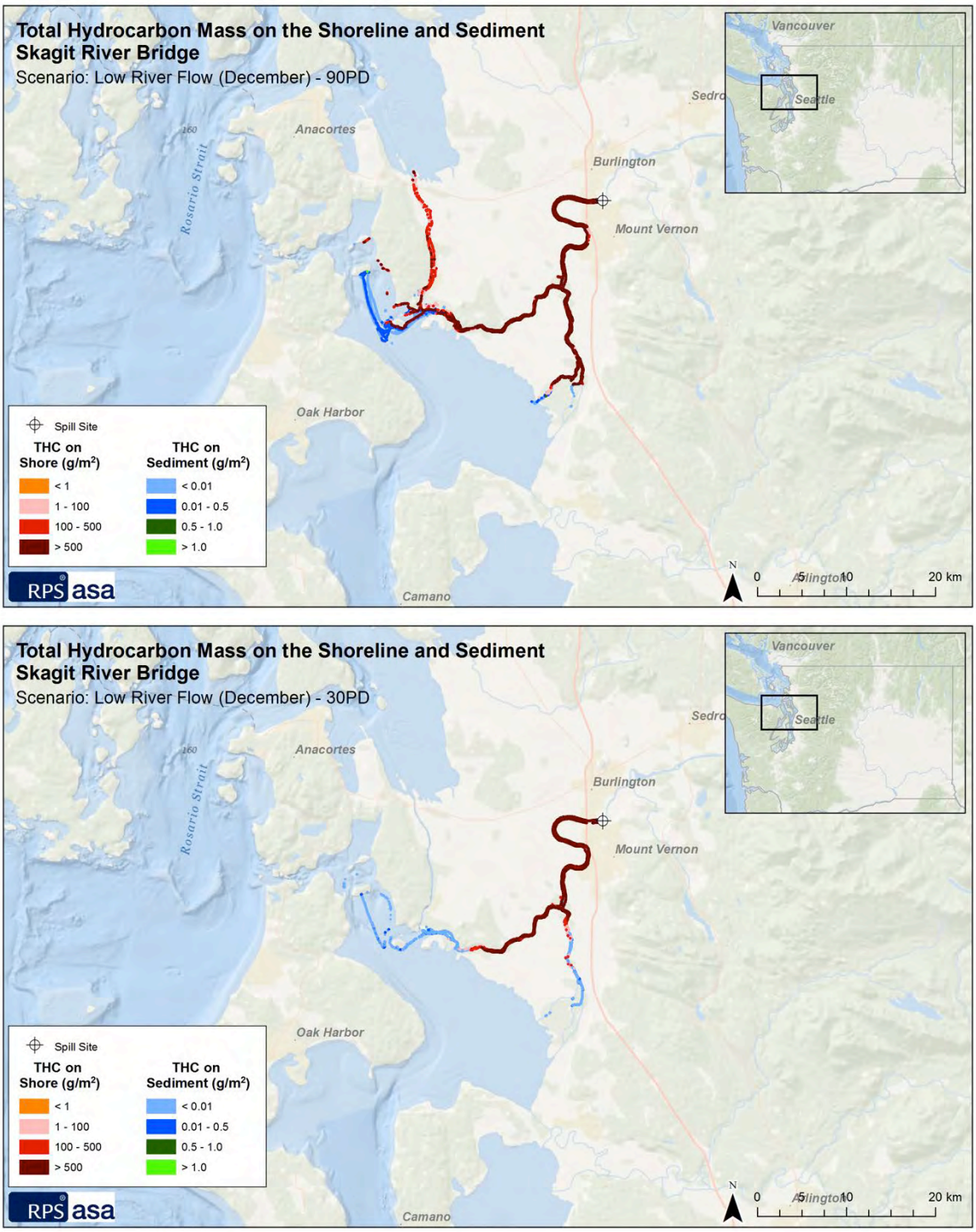

Figure 6-20: Total hydrocarbon mass on the shore and on sediments for 90PD (top) and 30PD (bottom) scenarios at the Skagit River Crossing release location during the winter (low flow) season.

6.4 Edmonds Ferry Terminal

Releases at the Edmonds Ferry Terminal required initial OILMAP Land™ overland trajectories to determine the amounts and locations of oil entering the waterway from ruptured tank cars on land (Figure 6-21). Modeling that incorporated the storm water drainage network into OILMAP Land™ resulted in three points of entry for oil into Puget Sound for the 90PD scenarios, and a single point of entry for the 30PD scenarios. Release volumes at each of the three entry points varied and were calculated based on the proportion of oil that would enter each branch of the drainage network for the individual tank car spill locations modeled.

The mass balance graphs in Figure 6-22 and Figure 6-27 depict that the oil from hypothetical spills originating near the Edmonds Ferry Terminal during the low-wind summer season evaporated rapidly over the 48-hour simulation due to the large quantity of oil that remained on the water surface throughout the 48-hour simulation. A lower percentage of oil is found on the water surface under high-wind scenarios, when compared to low-wind scenarios. During the high-wind (winter) scenarios, large quantities of oil stranded on shorelines. In addition, the high winter winds resulted in surface breaking waves, causing oil to entrain in the water column, adhere to SPM, and sink to the sediments. There was very little decay from the spills originating at this release location. Table 6-3 provides a summary of the mass balance information at the end of the 48-hour simulation.

Table 6-3: Summary of the mass balance information at the Edmonds Ferry Terminal release location at the end of the 48-hour simulation. All values represent a percentage of the total spilled oil.

Summary of Mass Balance Information at the End of the 48-hour Simulation (Percentage of Spilled Oil)						
Scenario	**Surface (%)**	**Evaporated (%)**	**Water Column (%)**	**Sediment (%)**	**Ashore (%)**	**Decayed (%)**
90PD Summer (Low Wind)	43.4	52.4	0.1	0.0	3.0	1.1
30PD Summer (Low Wind)	42.7	53.2	0.2	0.0	2.8	1.0
90PD Winter (High Wind)	11.7	52.8	10.8	11.9	11.9	0.9
30PD Winter (High Wind)	4.9	52.4	4.5	8.8	28.5	0.9

Figure 6-21: Overland flow of oil downslope and through the storm water drainage system for Edmonds Ferry Terminal. The tank car release locations (orange circles) for the eight-car 30PD release (top) and 28-car 90PD release (bottom) depict three distinct water entry points.

Surface oil originating from the Edmonds Ferry Terminal hypothetical release location during the low-wind summer season traveled both south and west, oiling the respective coastlines of Puget Sound (Figure 6-23). Dissolved aromatics traveled northwest toward Whidbey Island. The majority of the thickest surface floating oil (greater than 1 mm) directly occurred at and south of the spill site (Figure 6-24). Hydrodynamic conditions and winds from the east and northeast prevented surface oil transport to the north and resulted in an east-west boundary of predicted surface oiling. During the high-wind winter season, the oil traveled primarily toward the north, oiling the southern coastlines of Whidbey Island and Camano Island (Figure 6-28). The thickest surface floating oil (greater than 1 mm) existed in a plume that traveled north toward Whidbey Island (Figure 6-29).

The highest maximum dissolved aromatic concentrations (500 ppb) during the summer were found to the west and south of the Edmonds Ferry Terminal site (Figure 6-25). Figure 6-26 shows that the maximum total hydrocarbon concentrations (greater than 500 g/m^2) on the shoreline during the low-wind summer season were also found to the west and south of the release location. Total hydrocarbon concentrations on suspended sediments were generally low (less than 0.01 g/m^2).

In the high-wind winter season 90PD scenario, the extent of highest maximum dissolved aromatic concentration (greater than 500 ppb) covered most of the entire extent of dissolved aromatics (Figure 6-30). The extent of highest maximum dissolved aromatic concentration during the 30PD scenario (Figure 6-30) was slightly smaller than that of the 90PD. The maximum total hydrocarbon concentrations (greater than 500 g/m^2) on the shoreline during the high-wind winter season were found along the southern coastlines of Whidbey Island and Camano Island. Total hydrocarbon concentrations on sediments (Figure 6-31) did not exceed 0.5 g/m^2.

6.4. Edmonds Ferry Terminal – Summer (Low-Wind Speeds)

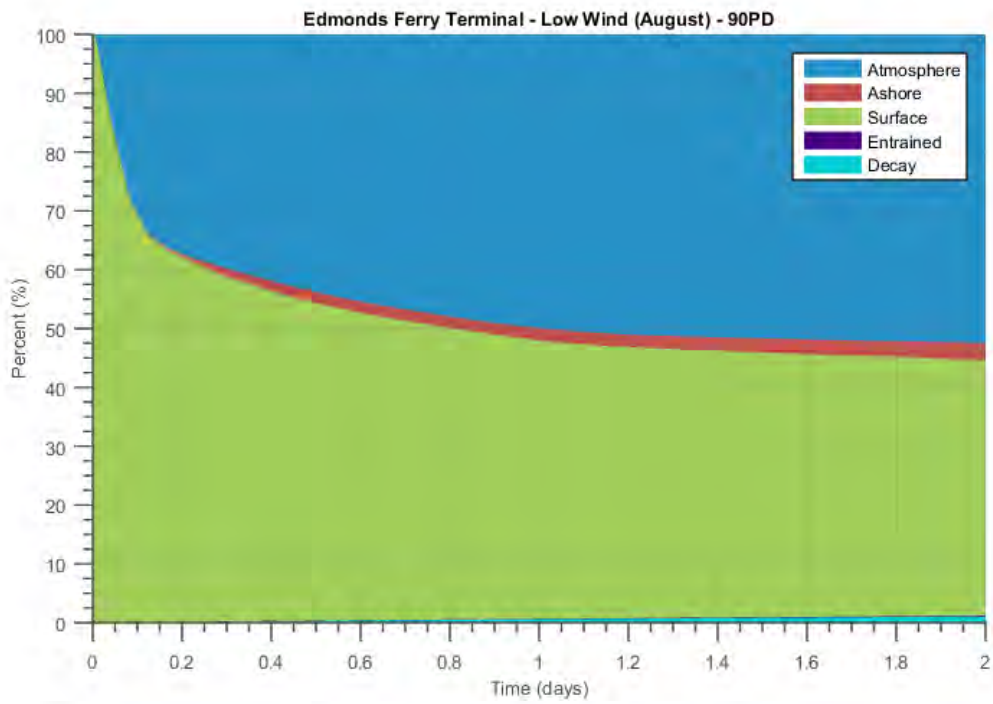

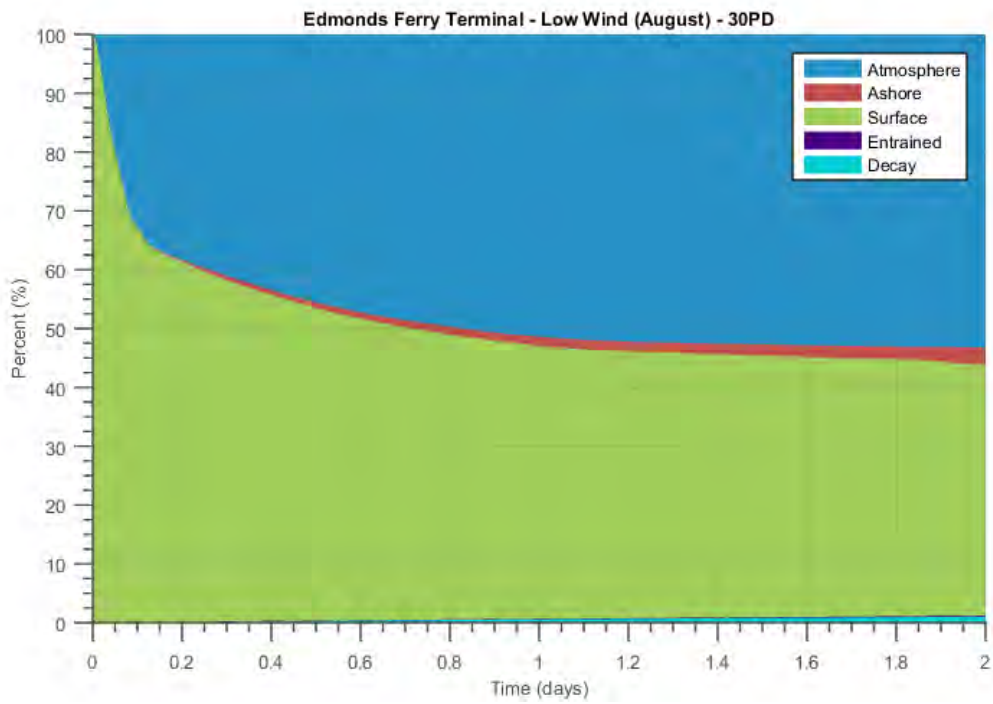

Figure 6-22: Oil mass balance graphs for the 90PD (top) and 30PD (bottom) at the Edmonds Ferry Terminal release location during the summer (low wind) season. Entrained and decayed oil make up approximately 1 percent of the total mass or less.

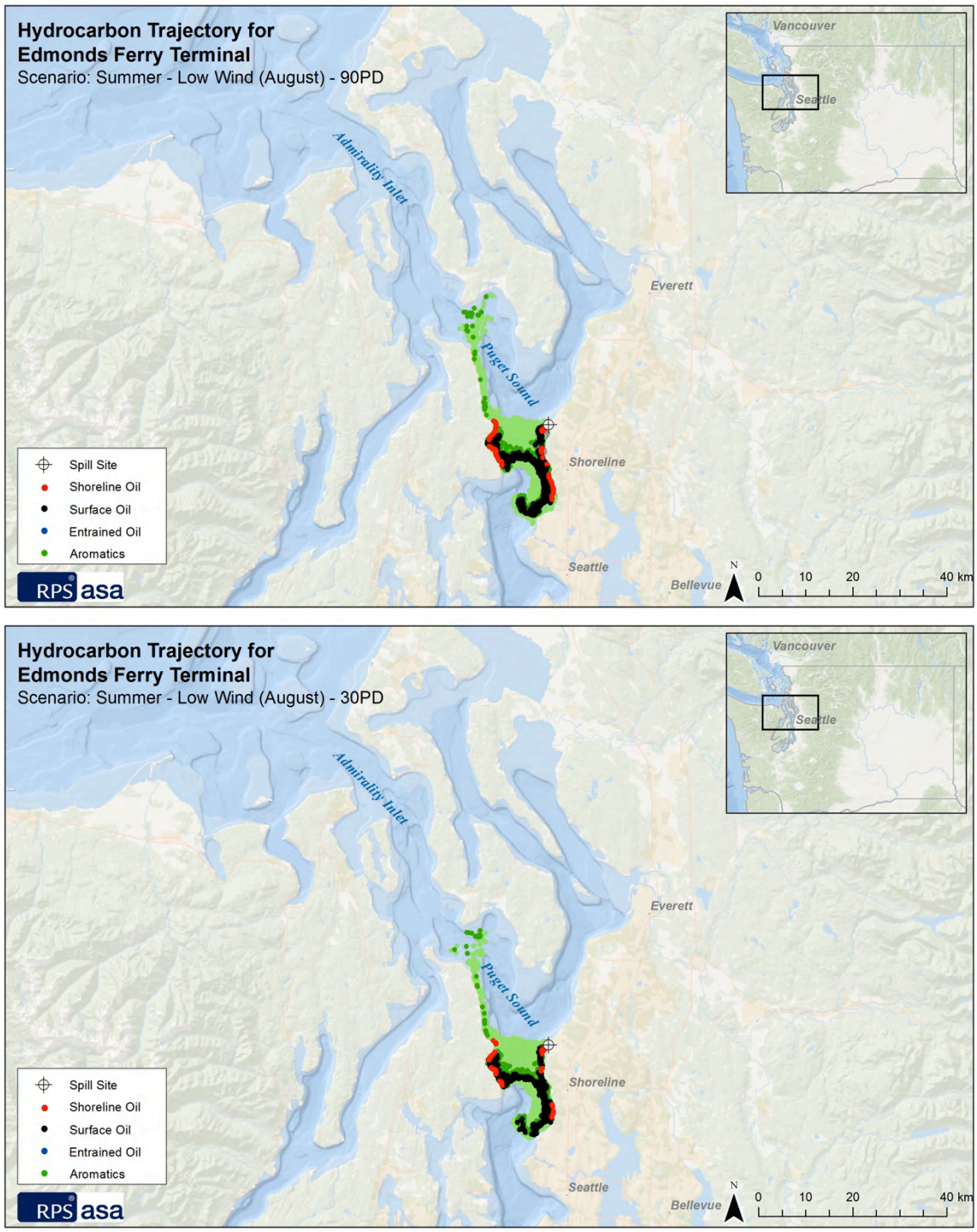

Figure 6-23: Oil trajectories for 90PD (top) and 30PD (bottom) at the Edmonds Ferry Terminal release location during the summer (low wind) season.

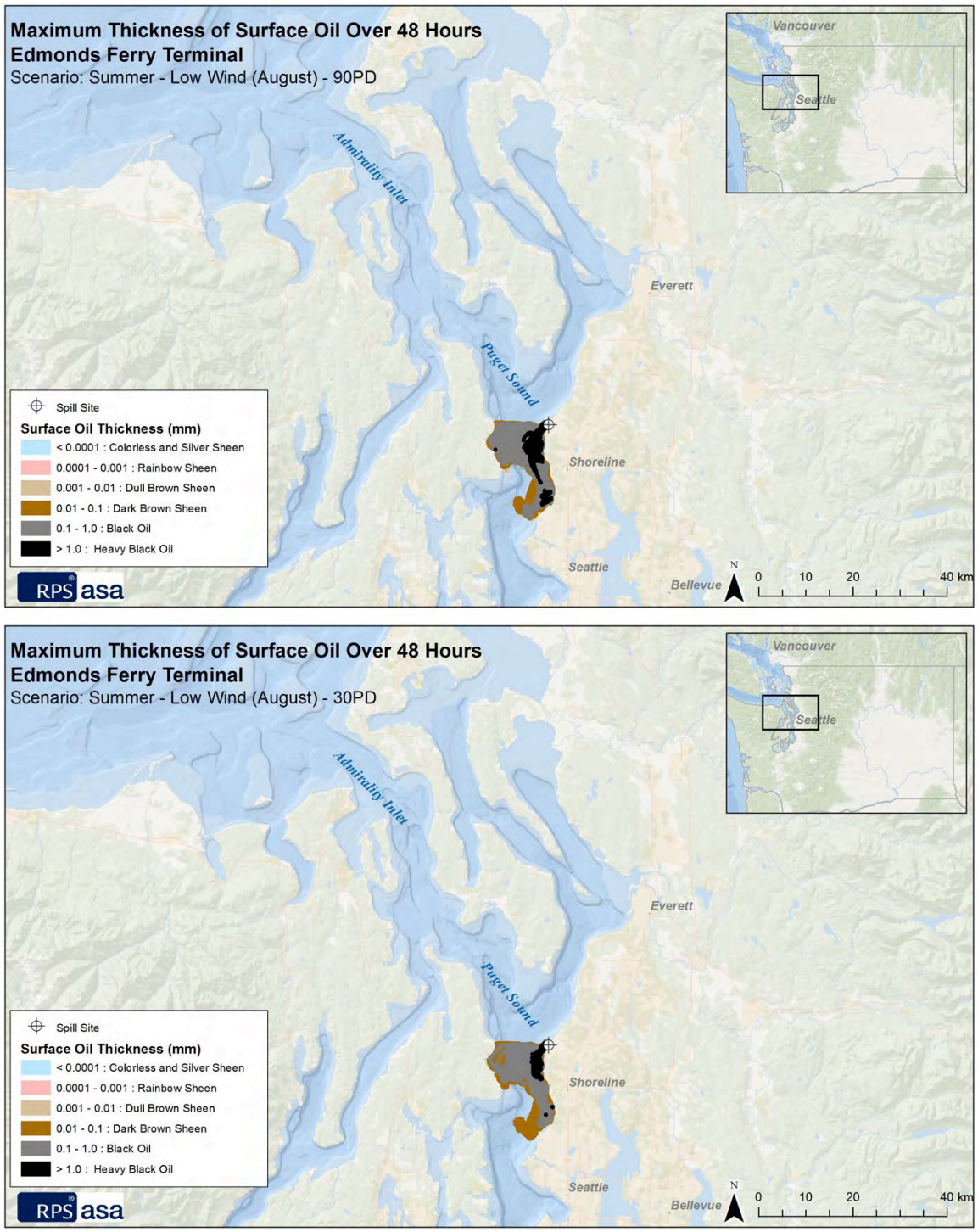

Figure 6-24: Maximum cumulative surface oil thickness for 90PD (top) and 30PD (bottom) scenarios at the Edmonds Ferry Terminal release location during the summer (low wind) season.

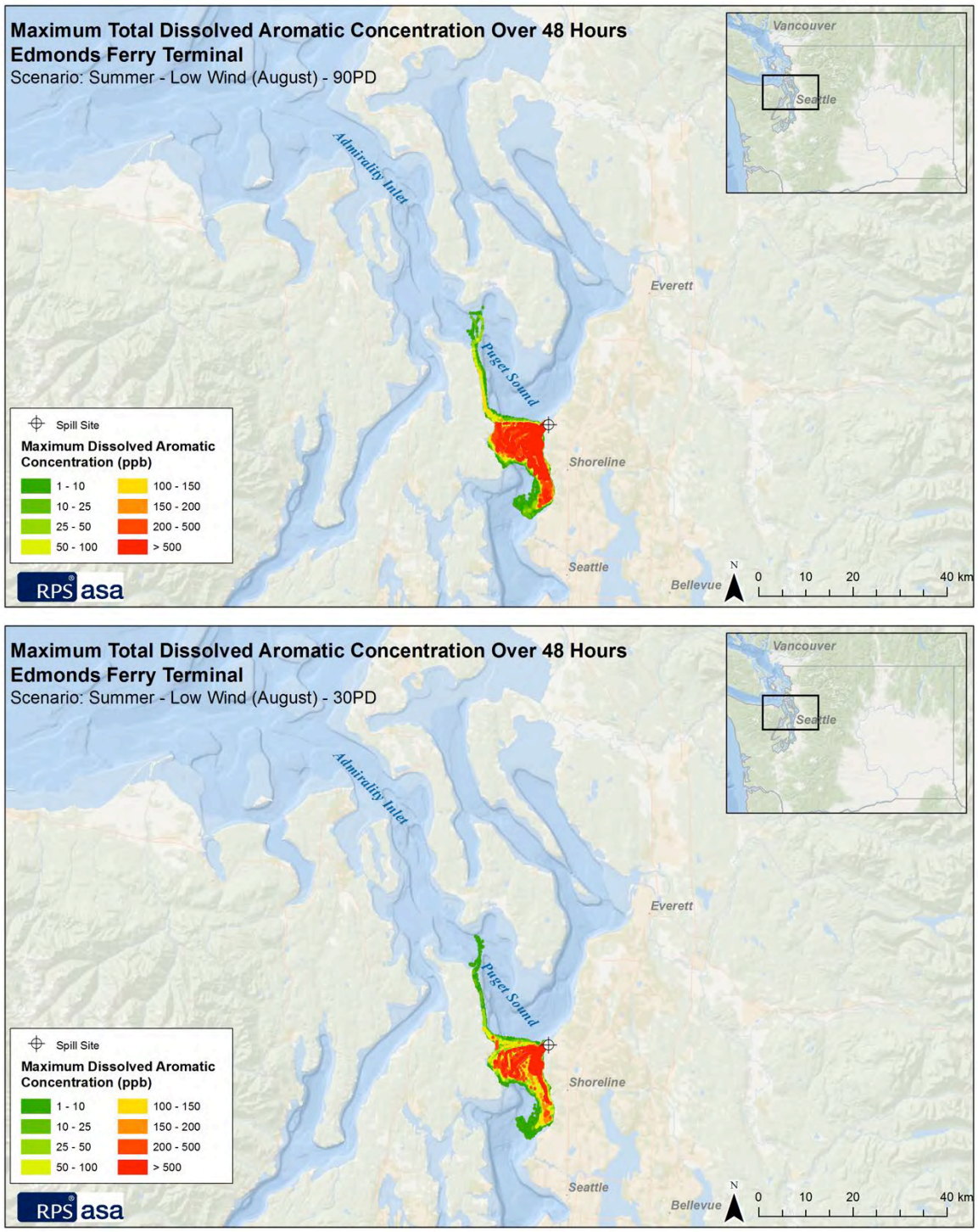

Figure 6-25: Cumulative total dissolved aromatic concentrations for 90PD (top) and 30PD (bottom) scenarios at the Edmonds Ferry Terminal release location during the summer (low wind) season.

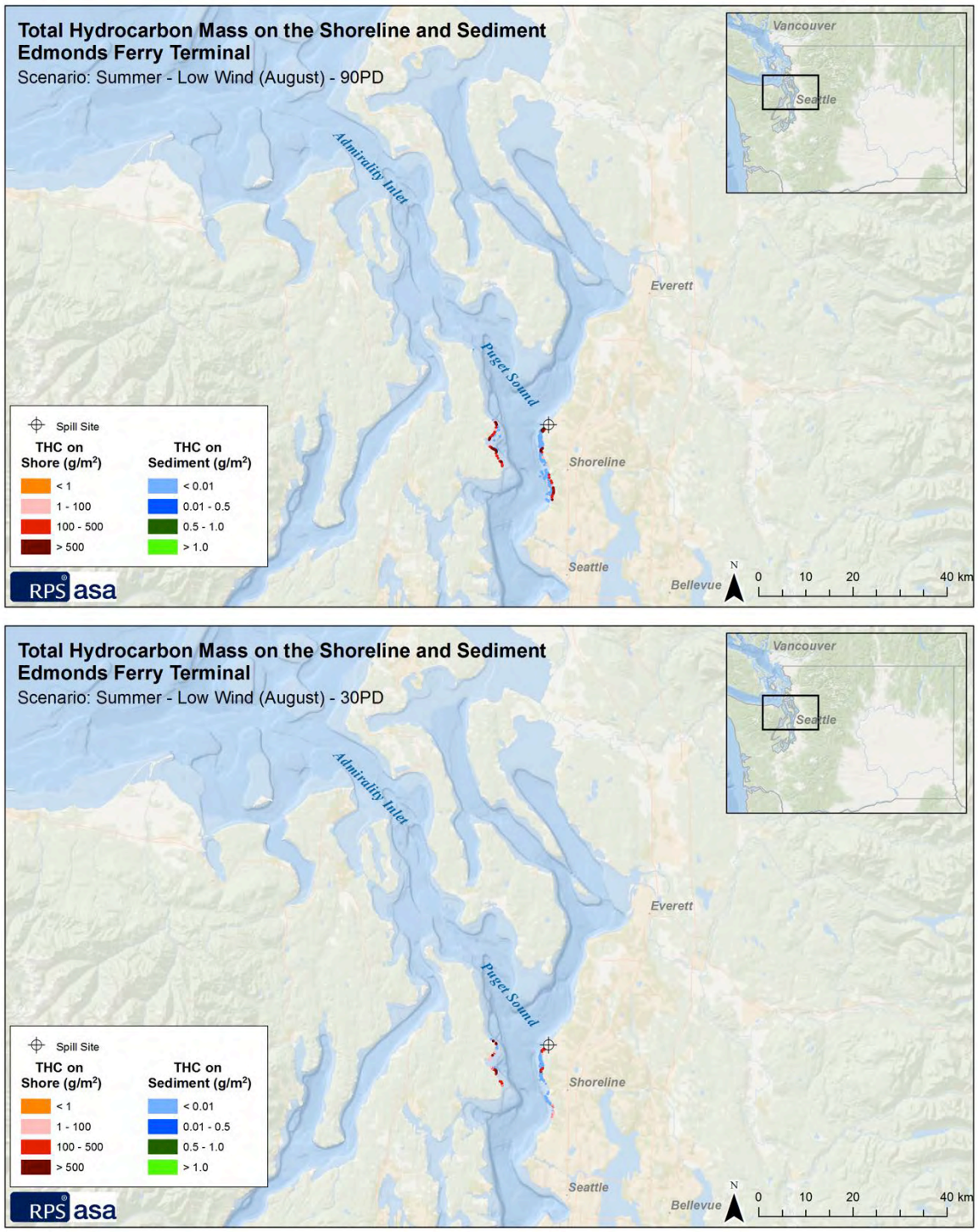

Figure 6-26: Total hydrocarbon mass on the shore and on sediments for 90PD (top) and 30PD (bottom) scenarios at the Edmonds Ferry Terminal release location during the summer (low wind) season.

Edmonds Ferry Terminal – Winter (High-Wind Speeds)

6.4.2

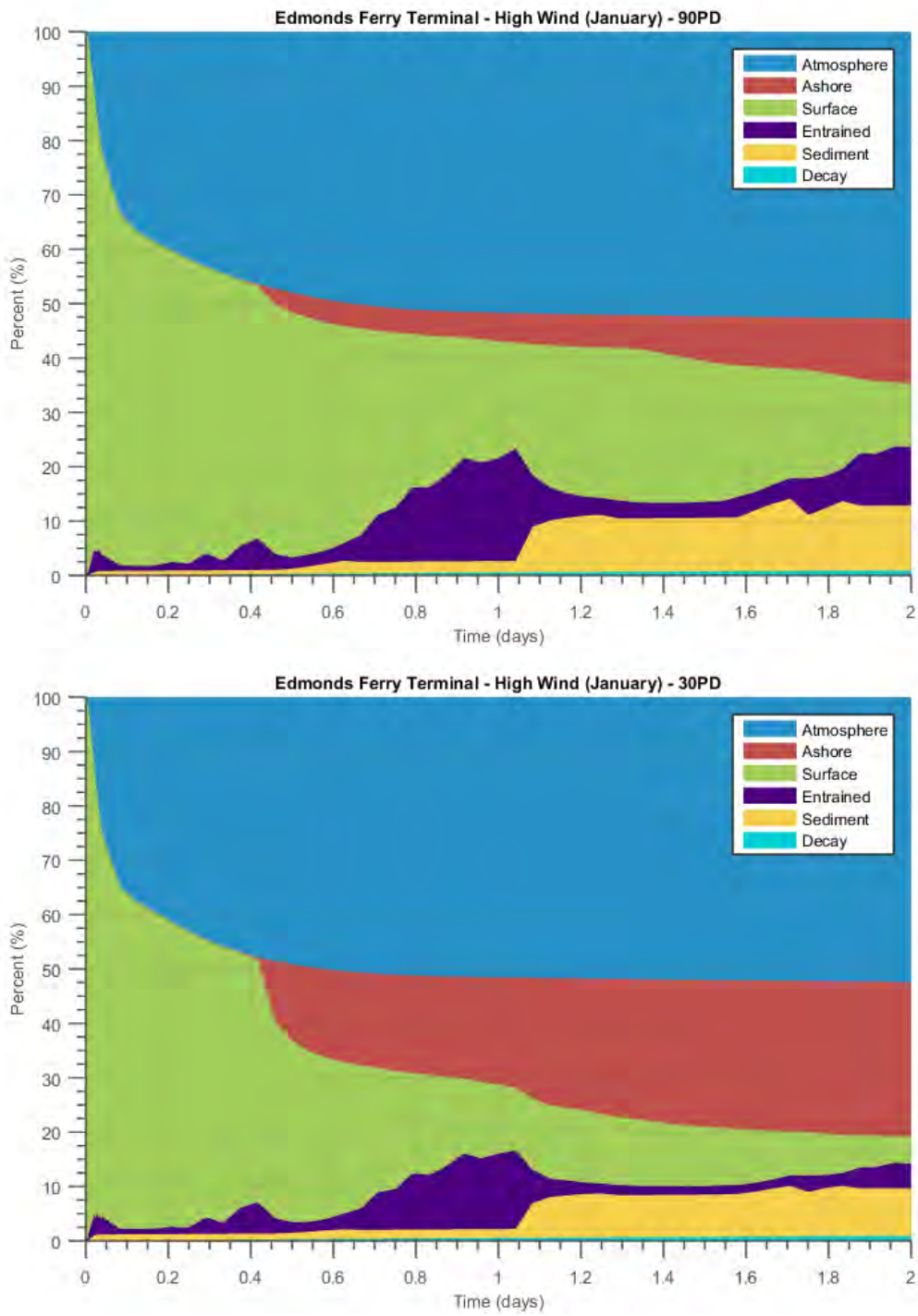

Figure 6-27: Oil mass balance graphs for the 90PD (top) and 30PD (bottom) at the Edmonds Ferry Terminal release location during the winter (high wind) season.

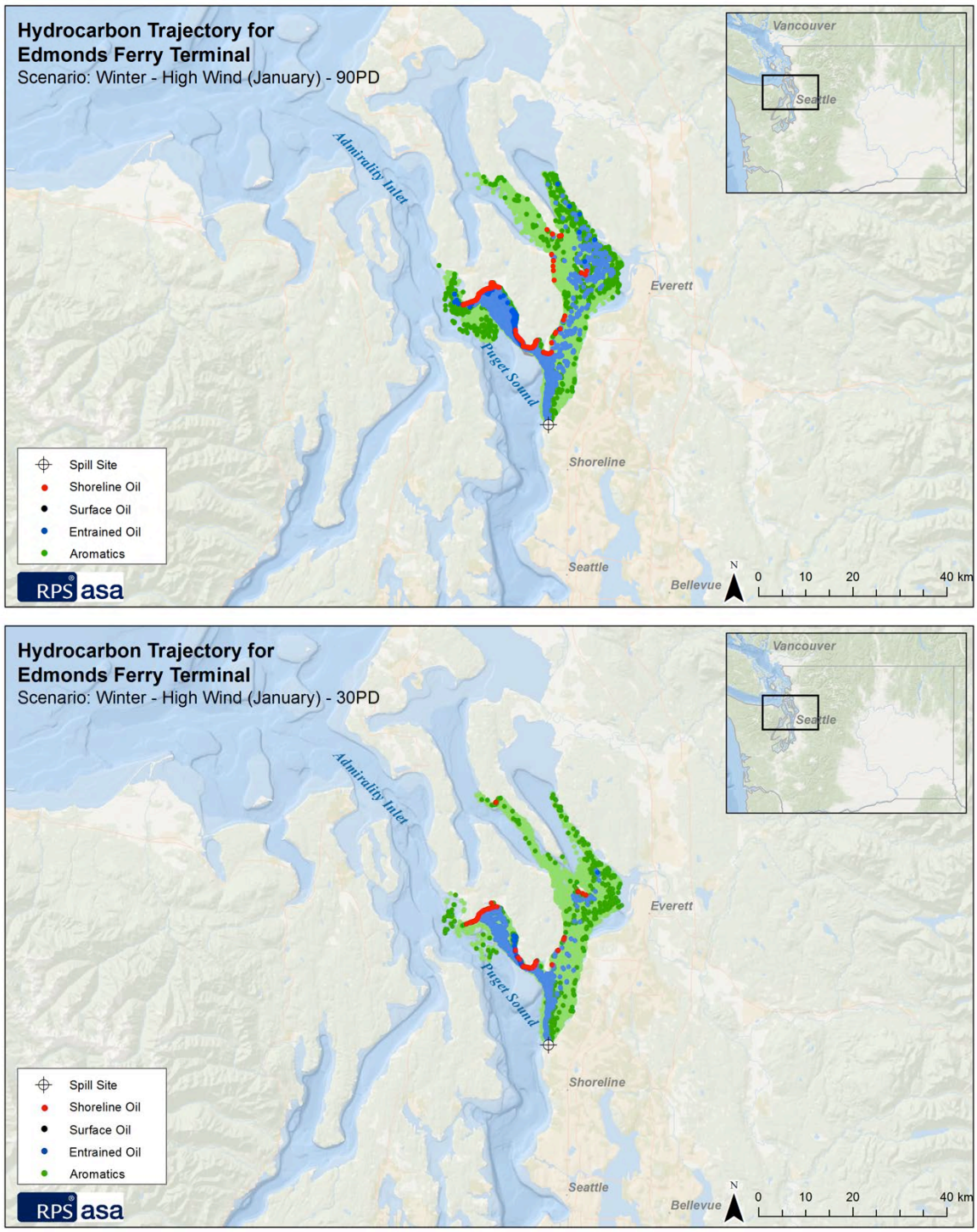

Figure 6-28: Oil trajectories for 90PD (top) and 30PD (bottom) at the Edmonds Ferry Terminal release location during the winter (high wind) season.

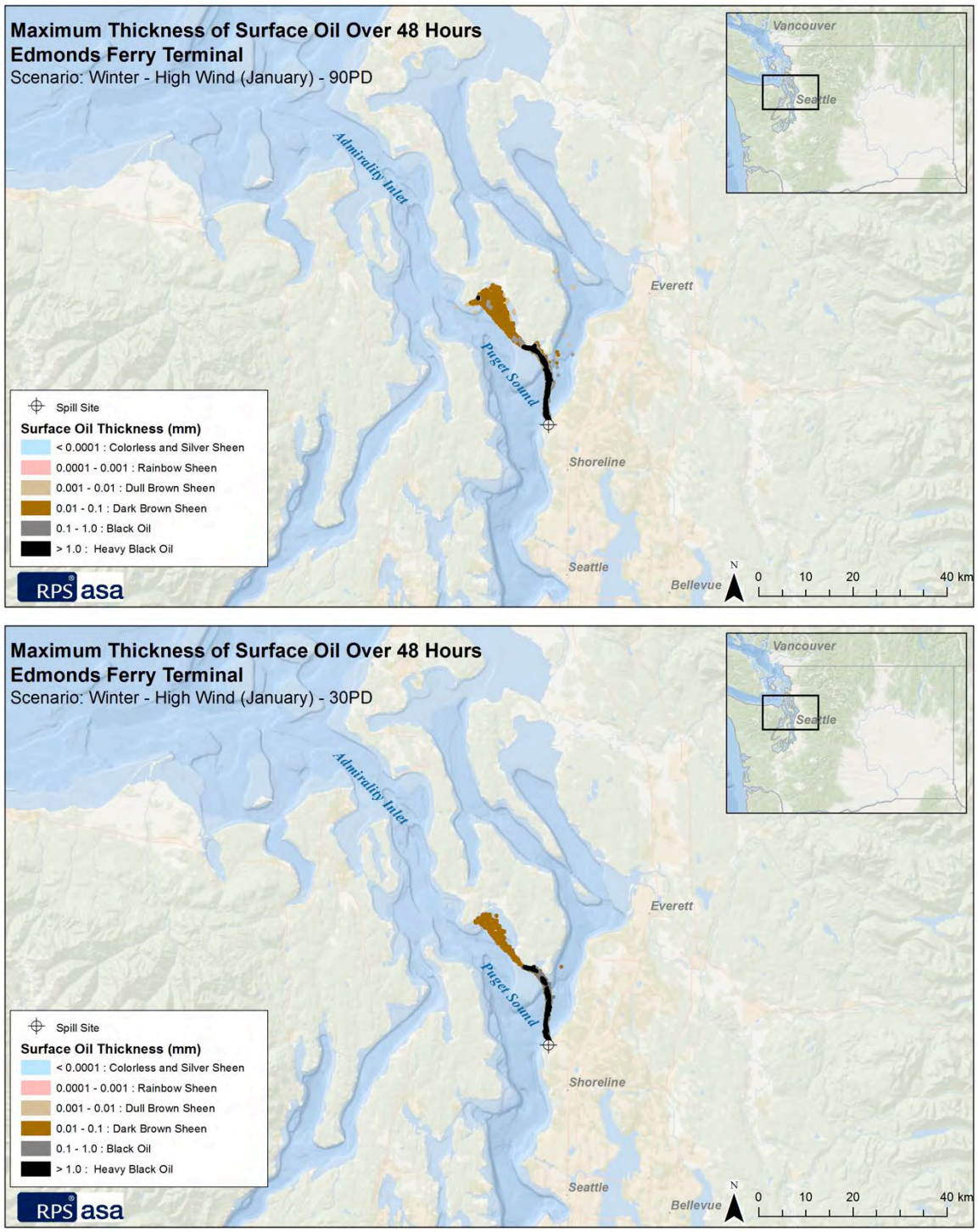

Figure 6-29: Maximum cumulative surface oil thickness for 90PD (top) and 30PD (bottom) scenarios at the Edmonds Ferry Terminal release location during the winter (high wind) season.

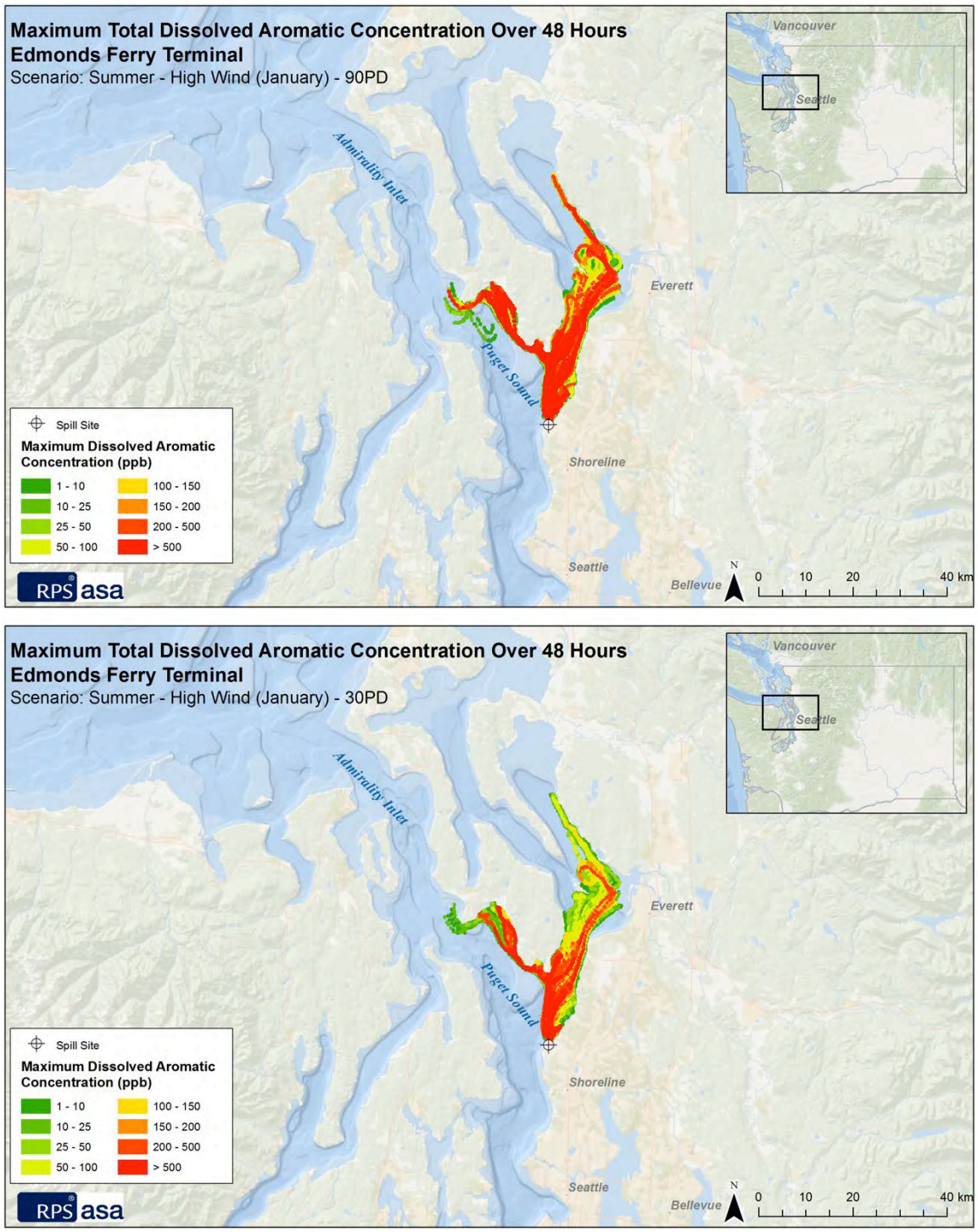

Figure 6-30: Cumulative total dissolved aromatic concentration for 90PD (top) and 30PD (bottom) scenarios at the Edmonds Ferry Terminal release location during the winter (high wind) season.

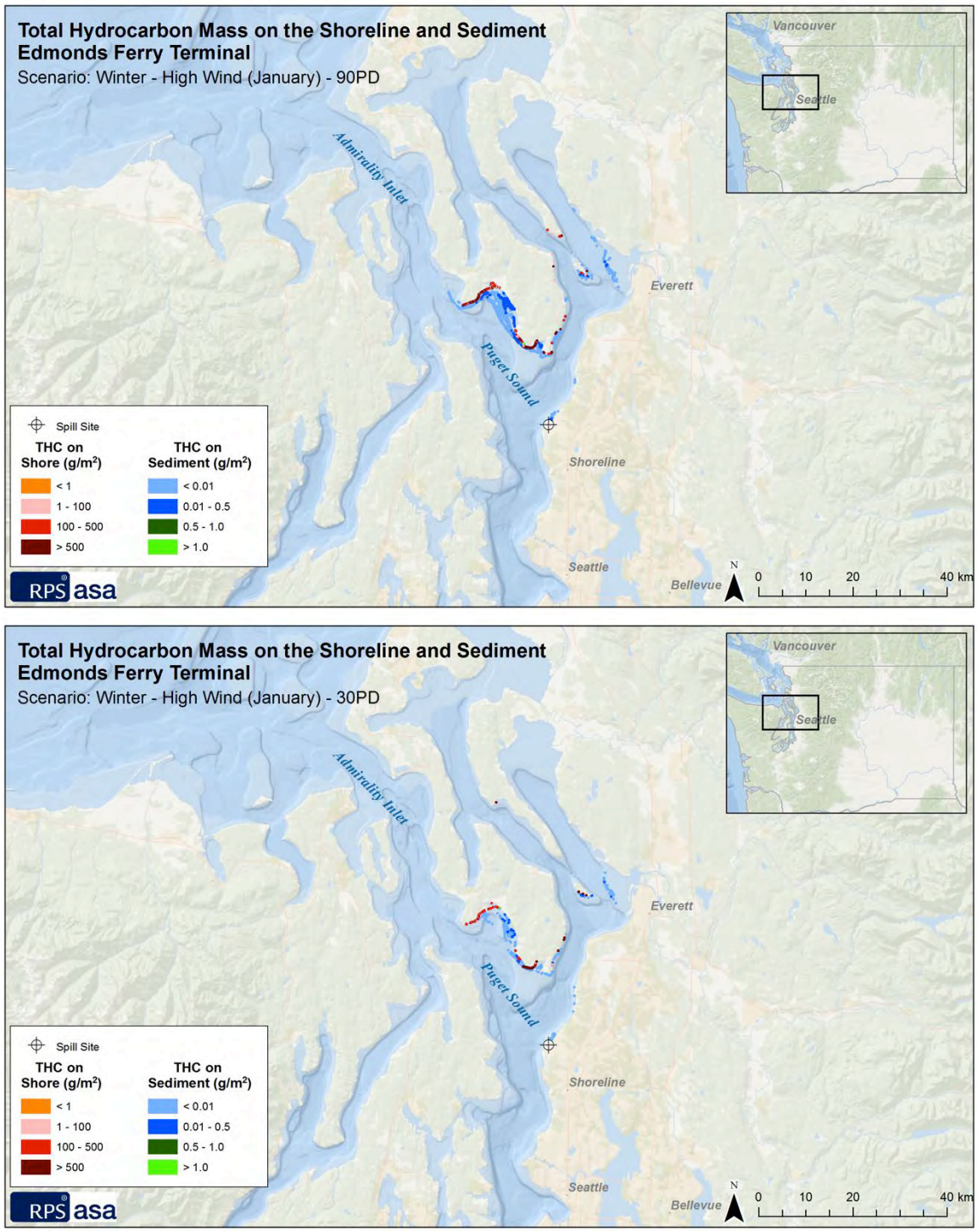

Figure 6-31: Total hydrocarbon mass on the shore and on sediments for 90PD (top) and 30PD (bottom) scenarios at the Edmonds Ferry Terminal release location during the winter (high wind) season.

7 Potential Impacts Model Results

7.1 Overlay and Biological Impacts Analyses

The trajectory and fates results from Section 6 were used in an overlay assessment to determine the potential impacts on resources located near the hypothetical release locations. The GIS overlay assessment included a count of any identified resource features (points, lines, or polygons) that were intersected by the trajectory of the released oil (Table 7-1). These data layers contained several sub-types ('Area Types' in subsequent tables) for which area counts and 'Location/Description/Species' names were combined, when appropriate. Any oil that passed through a resource was assumed to have had the potential to affect the identified resource. Any resource features that were located adjacent to shorelines, but not directly intersected by the oiling, were assumed to be affected. These data represent a snapshot of the spatial distribution of resources obtained from static datasets. The spatial distribution and extent of these resources may change over time.

Table 7-1: Geographic data layers used for the overlay analysis.

Layer ID	Data Layer Name	Geometry Type	Citation
1	NOAA ESI Socioeconomic Resource Points	Point	NOAA, 2016c
2	NOAA ESI Socioeconomic Resource Lines	Line	
3	NOAA ESI Nest Points	Point	
4	NOAA ESI Fish Lines	Line	
5	NOAA ESI Management Area Polygons	Poly	
6	NOAA ESI Invertebrate Polygons	Poly	
7	NOAA ESI Fish Polygons	Poly	
8	NOAA ESI Bird Polygons	Poly	
9	NOAA ESI Marine Mammal Points	Point	
10	Shoreline Public Access - Skagit County	Point	WA DOE, 2016
11	Shoreline Public Access - Snohomish County	Point	
16	Tribal Lands	Poly	
12	Shellfish Commercial Harvest Sites	Point	WA DOH, 2016
15	Shellfish Recreational Beaches	Line	
23	Surface Water Protection Areas	Poly	
25	Shellfish Commercial Growing Areas	Poly	
26	Wildlife Survey Occurrence Point (Generalized)	Poly	WDFW, 2016
27	Wildlife Survey Occurrence Polygon (Generalized)	Poly	
28	Wildlife Survey Occurrence Point (Nonsensitive)	Point	
29	Wildlife Survey Occurrence Polygon (Nonsensitive)	Poly	
30	Marbled Murrelet Detection Locations	Poly	
31	Marbled Murrelet Detection Adjacent Locations	Poly	

Layer ID	Data Layer Name	Geometry Type	Citation
32	Bald Eagle Nests and Communal Roosts	Poly	
33	Spotted Owl Sites	Poly	
34	Seal and Sea Lion Haulout Locations	Poly	
35	Priority Habitat & Species Regions (Generalized)	Poly	
36	Priority Habitat & Species Regions	Poly	
37	Priority Habitat Sites (Generalized)	Poly	
38	Priority Habitat Sites	Point	
39	Seabird Colonies	Point	
40	NWI Wetlands	Poly	
41	Statewide Fish Distribution	Line	
42	Salmonid Fish Stock Inventory	Line	
43	Geoduck	Poly	
44	Herring Holding Areas	Poly	
45	Herring Spawning Areas	Poly	
46	Shellfish Summary	Poly	
47	Sand Lance Spawning	Line	
48	Surf Smelt Spawning	Line	

Affected resources include the following categories of environmentally sensitive areas:

- Socioeconomic resources (e.g., parks, management areas, public access points, fishing areas)
- Aquatic resources (e.g., shellfish locations, fish spawning areas, seal haulout points)
- Avian and terrestrial resources (e.g., bird colonies, nesting areas, wetlands, biodiversity corridors, and wildlife observations)

Summary tables were prepared for each release location identifying the type and count of each resource potentially affected by the simulated oil trajectories. It is likely that in the event of a release, hydrocarbons could affect the use or suitability of each identified resource. It is important to note that the various GIS data layers contain overlapping information and that information is not quantified by area or linear distance. This analysis was strictly a count of spatial features that were intersected by the oil trajectory. Therefore, identified counts of affected features could overstate a portion of the resources potentially affected. The counts should only be used to compare the relative impacts from one modeled release to another, rather than as a quantified number of affected resources. Results can be compared between scenarios at the same release location, but caution should be exercised when comparing the counts between release locations. The spatial extents of different resource data layers vary and data for a particular resource may exist for one site but not for another. Refer to Section 10 (Appendix A) for figures representing the spatial extent of each identified resource data layer was used

in the overlay analysis. The results of this analysis are summarized in the following subsections for each release location.

The trajectory and fate modeling results were also used in a biological impacts assessment. The assessment estimated the potential short-term (acute) exposure of biota to floating oil and subsurface oil contamination (in-water and on sediments), and predicted the resulting mortality percentage. In each grid cell, acute toxicity to aquatic biota in the water column and demersal (bottom 1 meter of the water immediately above the sediments) habitats were evaluated by tracking exposure for these different behavior groups. In rivers, where water depths could be less than 1 m, the affected areas for water column and demersal biota were equal. Equivalent areas of 100-percent-predicted morality were estimated for both the surface/shoreline and the water column. Acute toxicity for the surface/shoreline was based on the area swept by surface oil over a 10 µm threshold thickness for acute effects.

Biota potentially impacted by surface and shoreline oiling includes waterfowl, aerial and diving birds, wetland and terrestrial wildlife, fur-bearing marine mammals, pinnipeds (seals and sea lions), and cetaceans (whales and dolphins). Acute toxicity for in-water impacts was based upon sensitivities of 5 µg/L for sensitive species and 50 µg/L for average-sensitivity species.

Biota potentially impacted by water column toxicity includes mobile and stationary demersal (bottom-dwelling) fish and invertebrates, small pelagic (swimming) fish and invertebrates, large pelagic fish, benthic organisms residing within the bottom sediments, and plankton that drift with the currents. The equivalent areas of predicted mortality above the stated thresholds would only occur if the organisms were present in the areas affected by spilled oil at the time of the release. A full description of the acute biological impacts modeling, including selection of thresholds of concern and validation are provided in Sections 3.2 and 3.4.

7.2.1 7.2 Swinomish Channel Swing Bridge

Overlay Analysis for Swinomish Channel Swing Bridge

The results of the overlay analysis for public access and socioeconomic resources, aquatic resources and aquatic sensitive areas, and avian/terrestrial resources and terrestrial sensitive areas for the Swinomish Channel Swing Bridge scenarios are presented in Table 7-2, Table 7-3, and Table 7-4, respectively.

Similar to the trajectory results presented in Section 6, the 90PD scenarios often affected a slightly higher count of impacted resources than the 30PD scenarios. Significantly more resources were affected during the summer (spring tide) than the winter (neap tide) scenarios. Many fewer beaches, parks, commercial and recreational fishing resources, shellfish locations, fish spawning areas, seal haulout sites, and bird nesting sites were affected during the winter scenarios than the summer scenarios. This can be attributed to the greater extents of oiling in the summer (spring tide) scenarios.

Table 7-2: Overlay analysis for Swinomish Channel Swing Bridge summer (spring tide) and winter (neap tide) 30PD and 90PD scenarios. Numbers indicate the counts of public access and socioeconomic resource areas potentially affected by oil.

Layer ID	Area Type(s)	Location/Description/Species	Summer 30PD	Summer 90PD	Winter 30PD	Winter 90PD
1	Beach, park, access	Anacortes Ferry Terminal Beach, Bayview State Park, Camp Kirby, Cap Sante Park, North Beach - Guemes Island, Samish Island Public Access, South Shore Drive Road End, Washington Park, Young County Park	5	8	1	1
	Aquaculture, boat ramp, equipment, ferry, marina	Anacortes Ferry Landing, Anacortes Marina, Anacortes net pens, Deception Pass State Park (Cornet Bay), Fidalgo net pens, LaConner City Floats, LaConner Marina, March Point, Swinomish Channel Boat Launch, Padilla Bay, Sherman St. Boat Ramp, Sidney BC - Anacortes Ferry	11	13	2	2
10	Public access	Bayview Boat Launch, Bayview State Park, Boat Harbor - East Guemes Island, Cap Sante Park, Goat Island, Huckleberry Island, LaConner Marina, Lower Cap Sante Park, March Point Recreational Beach, Swinomish Channel Boat Launch, Padilla Bay, Saddlebag Island State Park, Samish Island Recreation Area, Seafarer Park, Unknown, Young County Park North Beach	18	18	4	4
5	Park, management area, marine sanctuary, nature conservancy, Indian reservation	Cypress Island Aquatic Reserve, San Juan County/ Cypress Island MBP, Padilla Bay NERR, Jack Island, Deception Pass, Huckleberry Island, Swinomish Indian Reservation	10	15	4	4
	Unknown use, aquaculture, and commercial fishing	Unknown, East San Juans, Swinomish, Demersal groundfish fishing, pelagic groundfish fishing, rocky reef groundfish fishing, salmon fishing	15	27	1	3
	Recreational and subsistence fishing	Demersal groundfish fishing, rocky reef groundfish fishing, salmon fishing, Native American salmon fishing	6	10	1	1
12 / 25	Shellfish commercial harvest and growing areas	Upper Skagit Indian Tribe, East San Juans, Padilla Bay, Samish Bay	6	7	0	0
15	Shellfish recreational beaches	Ala Spit CP, Anacortes City Park, Bay View SP, Clark Point, Deception Pass SP, DNR-144 (Sleeper), Hope Island SP (North), March Pt Rec Area, Saddlebag Island SP, Swinomish Channel Boat Launch, Padilla Bay	7	10	2	3
16	Unknown, ceded land, reservation	Unknown, Treaty of Point Elliott, Swinomish Tribe	3	3	2	2

Table 7-3: Overlay analysis for Swinomish Channel Swing Bridge summer (spring tide) and winter (neap tide) 30PD and 90PD scenarios. Numbers indicate the counts of aquatic resources and sensitive areas potentially affected by oil.

Layer ID	Area Type(s)	Location/Description/Species	Summer 30PD	Summer 90PD	Winter 30PD	Winter 90PD
6	Invertebrate concentration area	Unknown, hardshell clams, scallops, softshell clams Dungeness crab, sea urchins, pandalid shrimp, Pacific oyster	38	51	2	3
46	Shellfish locations	Abalone, Dungeness crab, hardshell clam, pandalid shrimp, red sea urchin, subtidal hardshell clam, oyster beds	13	20	2	2
4	Fish spawning areas / beaches	Chinook salmon (fall), coho salmon, Pacific Sand lance, pink salmon, surf smelt	26	31	3	3
7	Spawning and pre-spawner areas	Pacific herring	8	8	1	2
44 / 45	Adult holding and spawning areas	Pacific herring	10	10	1	2
47	Spawning habitat	Pacific sand lance	7	16	3	3
48	Spawning habitat	Surf smelt	426	467	0	0
9	Marine mammal haulout points	Harbor seal	12	15	6	7
34	Seal and sea lion haulout locations	Belle Rock, Burrows Island/West Side reefs, Fidalgo Bay/log booms, Jack Island, Padilla Bay/Bent Piling/Indian Slough, Padilla Bay/Channels east of Saddlebag Island, Padilla Bay/Joe Leary Slough, Padilla Bay/West Channels, Padilla Bay/west of Swinomish Slough, Swinomish Channel Boat Launch, Padilla Bay, Skagit Bay/North Channels/Goat Island/Iki Island, Vendovi Island	10	13	4	5
28	Observation of listed species - haulout	California sea lion, harbor seal, Stellar sea lion	5	13	0	0

Table 7-4: Overlay analysis for Swinomish Channel Swing Bridge summer (spring tide) and winter (neap tide) 30PD and 90PD scenarios. Numbers indicate the counts of avian and terrestrial resources and sensitive areas potentially affected by oil.

Layer ID	Area Type(s)	Location/Description/Species	Summer 30PD	Summer 90PD	Winter 30PD	Winter 90PD
8	Unknown bird sites	Unknown	7	7	2	2
	Alcid bird sites	Murre, pigeon guillemot, rhinoceros auklet, common loon	8	15	0	0
	Diving bird sites	Cormorant, Pacific loon, red-throated loon, western grebe	16	17	1	1
	Gull/tern bird sites	Caspian tern, gulls	20	24	12	13
	Waterfowl bird sites	Bufflehead, long-tailed duck, scoters, waterfowl, scaup	35	37	11	13
3	Pelagic nesting sites	Seabirds	7	7	1	2
	Raptor nesting sites	Bald eagle	25	34	1	2
	Wading nesting sites	Great blue heron	1	1	0	0
32	Bald eagle nests and communal roosts	Bald eagle	52	64	6	10
39	Seabird colonies	Unknown, alcids, others	11	13	2	4
40	National Wetlands Inventory	Estuarine and marine deepwater, estuarine and marine wetland, freshwater emergent wetland, freshwater forested/shrub wetland	41	53	29	29
35 / 36	Biodiversity areas and corridors	Cap Sante Park, Fidalgo Island Open Space areas, Guemes Island Open Space, Hope Island, Skagit Wildlife Area and vicinity, Washington Park	5	6	1	1
	Priority habitats (cliffs/bluffs, islands, sloughs, wetlands)	Cliffs/bluffs, Burrows Island, Allen Island, Williamson Rocks, Padilla Bay Islands, Fidalgo Island wetlands, Guemes Island wetlands, Padilla Bay wetlands, Region 4 Saltwater wetlands, slough	7	8	3	5
	Wildlife concentrations and occurrences	Cap Sante Bald eagle winter concentration area, Fidalgo Bay waterfowl area, Guemes Island Bald eagle roost, March Point brant graveling areas, Padilla Bay shorebird concentration, Padilla Bay waterfowl area, Samish Bay, Skagit Bay waterfowl staging and wintering area, Swinomish Channel Boat Launch, Padilla Bay	10	11	3	3
38 / 29	Observation of listed species - biotic detection, nest, colony, communal roost, or concentration	Bald eagle, black oystercatcher, Caspian tern, great blue heron, peregrine falcon, purple martin, snowy owl, Townsend's big-eared bat, western toad	49	65	9	10

7.2.2

Biological Impacts for Swinomish Channel Swing Bridge

For the Swinomish Channel Swing Bridge summer (spring tide) 90PD release (Table 7-5), hydrocarbon concentrations on the water surface and on the shorelines could cause mortality in roughly 27 km^2 for dabbling waterfowl and over 100 km^2 for surface diving birds. For this release scenario, very limited acute impacts were predicted for cetaceans (whales or dolphins) and terrestrial wildlife. The results from the exposure model for water column organisms indicated there would be concentrations of

hydrocarbons in the water column (or on the sediment) that would cause small areas of mortality in each of the organism types evaluated, all < 0.9 km^2. Species of moderate sensitivity would experience extremely small regions of acute mortality, all < 0.01 km^2. This would have implications for commercial fisheries in that there would be limited acute impacts to fish and shellfish for this one release event.

Table 7-5: Equivalent area (km^2) of up to 100-percent-predicted mortality for behavior groups of wildlife, fish, and invertebrates by threshold for the Swinomish Channel Swing Bridge summer (spring tide) 90PD release. Values are the equivalent area of 100-percent mortality for species of high and medium sensitivity to dissolved PAHs from the representative spill.

Behavior Group	Equivalent Area (km^2) of up to 100%-Predicted Mortality At Threshold:	
Surface and Shoreline Impacts	**10 µm**	
Dabbling waterfowl	26.6	
Nearshore aerial birds	10.0	
Surface diving birds	100.0	
Aerial seabirds	5.7	
Wetland wildlife	9.8	
Terrestrial wildlife	< 0.1	
Cetaceans	0.1	
Fur-bearing marine mammals	78.3	
Pinnipeds	1.1	
In-Water Impacts	**5 ppb**	**50 ppb**
Demersal - move at bottom	0.8	< 0.1
Demersal – stationary	0.4	< 0.1
Small pelagic fish/invertebrates	0.5	< 0.1
Large pelagic fish	0.6	< 0.1
Benthic – in sediments	0	0
Planktonic (drift)	0.8	< 0.1

For the Swinomish Channel Swing Bridge summer (spring tide) 30PD release (Table 7-6), there could be surface and shoreline oiling at thicknesses that could cause mortality in areas of 24 km^2 for dabbling waterfowl and 76 km^2 for surface diving birds. For this spill scenario, very low acute impacts were predicted for cetaceans (whales or dolphins), pinnipeds, and terrestrial wildlife. The results from the exposure model for water column organisms indicated there would be concentrations of hydrocarbons

in the water column (or in the sediment) that would cause small areas of mortality in each of the organism types evaluated, all < 0.2 km^2. Species of moderate sensitivity would experience extremely small regions of acute mortality, all < 0.01 km^2. This would have implications for commercial fisheries in that there would be limited acute impacts to fish and shellfish for this one spill event.

Table 7-6: Equivalent area (km^2) of up to 100-percent-predicted mortality for various behavior groups of wildlife, fish, and invertebrates by threshold for the Swinomish Channel Swing Bridge summer (spring tide) 30PD release. Values are the equivalent area of 100-percent mortality for species of high and medium sensitivity to dissolved PAHs from a representative spill.

Behavior Group	Equivalent Area (km^2) of up to 100%-Predicted Mortality At Threshold:	
Surface and Shoreline Impacts	**10 µm**	
Dabbling waterfowl	23.6	
Nearshore aerial birds	8.8	
Surface diving birds	76.3	
Aerial seabirds	4.2	
Wetland wildlife	8.7	
Terrestrial wildlife	< 0.1	
Cetaceans	< 0.1	
Fur-bearing marine mammals	59.3	
Pinnipeds	0.9	
In-Water Impacts	**5 ppb**	**50 ppb**
Demersal - move at bottom	0.1	< 0.1
Demersal – stationary	0.1	< 0.1
Small pelagic fish/invertebrates	0.1	< 0.1
Large pelagic fish	< 0.1	0
Benthic – in sediments	0	0
Planktonic (drift)	< 0.1	0

For the Swinomish Channel Swing Bridge winter (neap tide) 90PD release (Table 7-7), there was surface and shoreline oiling at thicknesses that could cause mortality in 9 km^2 for dabbling waterfowl and 11 km^2 for surface diving birds. For this spill scenario, very limited acute impacts were predicted for cetaceans (whales or dolphins), pinnipeds, aerial seabirds, and terrestrial wildlife. The results from the exposure model for water column organisms indicated there would be concentrations of hydrocarbons

in the water column (or in the sediment) that would cause small areas of mortality in each of the organism types evaluated, all < 0.2 km^2. Species of moderate sensitivity would experience extremely small regions of acute mortality, all < 0.03 km^2. This would have implications for commercial fisheries in that there would be limited acute impacts to fish and shellfish for this one spill event.

Table 7-7: Equivalent area (km^2) of up to 100-percent-predicted mortality for various behavior groups of wildlife, fish, and invertebrates by threshold for the Swinomish Channel Swing Bridge winter (neap tide) 90PD release. Values are the equivalent area of 100-percent mortality for species of high and medium sensitivity to dissolved PAHs from a representative spill.

Behavior Group	Equivalent Area (km^2) of up to 100%-Predicted Mortality At Threshold:	
Surface and Shoreline Impacts	**10 µm**	
Dabbling waterfowl	9.0	
Nearshore aerial birds	3.2	
Surface diving birds	11.0	
Aerial seabirds	0.6	
Wetland wildlife	3.2	
Terrestrial wildlife	< 0.1	
Cetaceans	< 0.1	
Fur-bearing marine mammals	8.4	
Pinnipeds	0.1	
In-Water Impacts	**5 ppb**	**50 ppb**
Demersal - move at bottom	< 0.1	< 0.1
Demersal – stationary	< 0.1	< 0.1
Small pelagic fish/invertebrates	< 0.1	< 0.1
Large pelagic fish	< 0.1	0
Benthic – in sediments	0	0
Planktonic (drift)	0.2	< 0.1

For the Swinomish Channel Swing Bridge winter (neap tide) 30PD release (Table 7-8), there was surface and shoreline oiling at thicknesses that could cause mortality in 7 km^2 for dabbling waterfowl and 9 km^2 for surface diving birds. For this spill scenario, very limited acute impacts were predicted for cetaceans (whales or dolphins), pinnipeds, aerial seabirds, and terrestrial wildlife. The results from the exposure model for water column organisms indicated there would be concentrations of hydrocarbons in the

water column (or in the sediment) that would cause small areas of mortality in each of the organism types evaluated, all < 0.1 km^2. Species of moderate sensitivity would not experience regions of acute mortality. This would have implications for commercial fisheries in that there would be limited acute impacts to fish and shellfish for this one spill event.

Table 7-8: Equivalent area (km^2) of up to 100-percent-predicted mortality for various behavior groups of wildlife, fish, and invertebrates by threshold for the Swinomish Channel Swing Bridge winter (neap tide) 30PD release. Values are the equivalent area of 100-percent mortality for species of high and medium sensitivity to dissolved PAHs from a representative spill.

Behavior Group	Equivalent Area (km^2) of up to 100%-Predicted Mortality At Threshold:	
Surface and Shoreline Impacts	**10 µm**	
Dabbling waterfowl	7.2	
Nearshore aerial birds	2.6	
Surface diving birds	8.9	
Aerial seabirds	0.5	
Wetland wildlife	2.6	
Terrestrial wildlife	< 0.1	
Cetaceans	< 0.1	
Fur-bearing marine mammals	6.8	
Pinnipeds	< 0.1	
In-Water Impacts	**5 ppb**	**50 ppb**
Demersal - move at bottom	< 0.1	0
Demersal – stationary	< 0.1	0
Small pelagic fish/invertebrates	< 0.1	0
Large pelagic fish	< 0.1	0
Benthic – in sediments	0	0
Planktonic (drift)	< 0.1	0

7.3 Skagit River Crossing

7.3.1 Overlay Analysis for Skagit River Crossing

The results of the overlay analysis for public access and socioeconomic resources, aquatic resources and aquatic sensitive areas, and avian/terrestrial resources and terrestrial sensitive areas for the Skagit River Crossing scenarios are presented in Table 7-9,

Table 7-10, and Table 7-11, respectively.

The 90PD scenarios for this release location only occasionally affected a greater number of resources than the 30PD scenarios. However, significantly more resources were affected during the summer (high flow) than the winter (low flow) scenarios. All resources except for salmon stocks and freshwater fish distributions were less affected during winter than during the summer scenarios. This can be attributed to the larger extents of oiling from the summer (high flow) scenarios, which oiled Skagit Bay much more extensively, and the similar levels of oiling within Skagit River across seasons.

Table 7-9: Overlay analysis for Skagit River Crossing summer (high flow) and winter (low flow) 30PD and 90PD scenarios. Numbers indicate the counts of public access and socioeconomic resource areas potentially affected by oil.

Layer ID	Area Type(s)	Location/Description/Species	Summer 30PD	Summer 90PD	Winter 30PD	Winter 90PD
1	Beach, park, access	Jensen Access, Milltown Access, North Fork Access, Snee-Oosh Waterfront Park, Spur Road End, Dewey Beach, Hope Island / Skagit County, Rockaway Beach, Similk Beach, Cornet Bay County Park	10	10	3	4
	Archeological site	Cornet Bay Native American Site, Paine Point Native American Site	2	2	0	0
	Airport, artificial reef, boat ramp, marina	Onamac Point, Camano Island Airfield, Blake's RV Park and Marina, Conway Park, Deception Pass State Park (Cornet Bay), Headquarters (WDFW) - Skagit River, LaConner Marina, Maple Grove Boat Ramp, Mariner's Cove Boat Launch, Milltown (WDFW) - Skagit River, Sherman St. Boat Ramp, Swinomish Channel Boat Launch, UTSALADY #1, Cornet Bay Marina, Hope Island State Park, LaConner City Floats, LaConner Marina	17	17	4	9
10	Public access	Unknown, Dewey Beach, Goat Island, Jensen Access, LaConner Marina, Milltown Access, North Fork Access, Northwest Island Marine Park, Sharpe County Park, Swinomish Channel Boat Launch, Skagit Wildlife Recreation Area	14	15	4	12
5	Park, management area, marine sanctuary, nature conservancy, Indian reservation	Swinomish Indian Reservation, San Juan County / Cypress Island MBP, Ebey's Landing NHR, Deception Pass, Dugualla Bay, Padilla Bay NERR	18	18	1	4
	Unknown use, aquaculture, and commercial fishing	Unknown, cultured mussels, Saratoga Pass, Similk Bay, Swinomish, Demersal groundfish fishing, pelagic groundfish fishing, rocky reef groundfish fishing, salmon fishing	36	35	8	13
	Recreational and subsistence fishing	Demersal groundfish fishing, pelagic groundfish fishing, rocky reef groundfish fishing, salmon fishing, Native American salmon fishing	17	17	3	5
12 / 25	Shellfish commercial harvest and growing areas	Swinomish Indian Tribal Community, Trans Ocean Seafoods, Inc., Upper Skagit Indian Tribe, Penn Cove, Point Partridge, Saratoga Pass, Similk Bay, South Skagit Bay, Swinomish	23	26	2	5
15	Shellfish recreational beaches	Ala Spit CP, Blowers Bluff, Deception Pass SP, DNR-142, DNR-144 (Sleeper), DNR-145, FN Onamac Pt, Hope Island SP (North), Jensen Access, N Onamac Pt, S Rocky Pt, S Strawberry Pt, Skagit Waterfowl- South Fork & North Fork Access, West Pass Access, Winas-Maylor Point East and West	21	26	5	7
23	Community water system	City of Anacortes	1	1	1	1
16	Unknown, ceded land, reservation	Treaty of Point Elliott, Swinomish Tribe Reservation	2	2	2	2

Table 7-10: Overlay analysis for Skagit River Crossing summer (high flow) and winter (low flow) 30PD and 90PD scenarios. Numbers indicate the counts of aquatic resources and sensitive areas potentially affected by oil.

Layer ID	Area Type(s)	Location/Description/Species	Summer 30PD	Summer 90PD	Winter 30PD	Winter 90PD
6	Invertebrate concentration area	Unknown, hardshell clams, scallops, softshell clam, Dungeness crab, sea urchins, pandalid shrimp	47	41	10	19
46	Shellfish locations	Abalone, Dungeness crab, hardshell clam, pandalid shrimp, red sea urchin	15	13	3	5
4	Fish spawning areas/ beaches	Chinook salmon (fall), Chinook salmon (spring), chum salmon (fall), coho salmon, native char, pink salmon, sockeye salmon, steelhead (winter), steelhead (summer), Pacific sand lance, surf smelt	138	132	52	82
7	Spawning and pre-spawner areas	Pacific herring	10	7	3	8
44 / 45	Adult holding and spawning areas	Pacific herring	9	6	3	8
47	Spawning habitat	Pacific sand lance	21	20	8	14
48	Spawning habitat	Surf smelt	132	132	11	46
42	Wild salmon stock status - depressed	Chinook salmon, steelhead	25	25	27	28
	Wild salmon stock status - healthy	Bull trout, Chinook salmon, chum salmon, coho salmon, pink salmon, sockeye salmon	33	33	31	31
	Wild salmon stock status - unknown	Bull trout, chum salmon, coho salmon, cutthroat trout, steelhead trout	33	33	34	34
41	Freshwater distribution of fish	Bull trout, Chinook salmon, chum salmon, coho salmon, cutthroat trout, kokanee salmon, pink salmon, rainbow trout, sockeye salmon, steelhead	114	114	87	119
3	Marine mammal haulout points	Harbor seal	14	11	2	8
34	Seal and sea lion haulout locations	Bowman Bay/Deception Island Area, Langley Bay/South Burrows Bay, Padilla Bay/West Channels, Padilla Bay/west of Swinomish Channel, Padilla Bay/Bent Piling/Indian Slough, Saddlebag Island/Huckleberry/Hat Island Area, Seal Rocks, Similk Bay/Log Booms/Kiket Island, Skagit Bay/North Channels/Goat Island/Iki Island, Skagit Bay/Point Brown, Skagit Bay/South Channels, Williamson Rocks	11	6	3	7
28	Observation of listed species - haulout	California sea lion, harbor seal, Stellar sea lion	10	9	4	7

Table 7-11: Overlay analysis for Skagit River Crossing summer (high flow) and winter (low flow) 30PD and 90PD scenarios. Numbers indicate the counts of avian and terrestrial resources and sensitive areas potentially affected by oil.

Layer ID	Area Type(s)	Location/Description/Species	Summer 30PD	Summer 90PD	Winter 30PD	Winter 90PD
8	Unknown bird sites	Unknown	12	13	2	5
	Alcid bird sites	Murre, pigeon guillemot, rhinoceros auklet	17	17	1	2
	Diving bird sites	Common loon, cormorant, Pacific loon, red-throated loon, western grebe	16	16	3	4
	Gull/tern bird sites	Caspian tern, gulls	34	27	7	20
	Waterfowl bird sites	Bufflehead, Goldeneye, harlequin duck, scoters, waterfowl	49	56	10	24
3	Pelagic nesting sites	Seabirds	2	3	0	1
	Raptor nesting sites	Bald eagle	68	67	12	29
	Wading nesting sites	Great blue heron	3	3	0	2
32	Bald eagle nests and communal roosts	Bald eagle	89	87	26	52
39	Seabird colonies	Unknown, alcids, cormorants, others	9	8	2	4
40	National Wetlands Inventory	Estuarine and marine deepwater, estuarine and marine wetland, freshwater emergent wetland, freshwater forested/shrub wetland, riverine	223	212	106	167
35 / 36	Biodiversity areas and corridors	Deception Pass State Park, Hope Island, Fidalgo Island Open Space, Skagit Flats Open Space, Skagit Island, Skagit Wildlife Area and vicinity	5	5	4	5
	Priority habitats (cliffs/bluffs, islands, sloughs, old growth forest, wetlands)	Cliffs/Bluffs, Burrows and Allen Island and Williamson Rocks, Deception Pass State Park, old growth forest, Fidalgo Island wetlands, Hat Slough Marsh and wetlands, Padilla Bay wetlands, Region 4 Saltwater wetlands, Skagit River Delta wetlands, Skagit River wetlands, slough	9	9	3	6
	Wildlife concentrations and occurrences	March Point graveling areas, Ala Spit (formerly Ben Ure Spit), Padilla Bay, Skagit Bay, Padilla Bay Waterfowl Area, Port Susan waterfowl wintering area, Skagit Bay waterfowl staging and wintering area, Whidbey Island waterfowl wintering area	7	5	3	7
28 / 29	Observation of listed species - biotic detection, nest, colony, communal roost, or concentration	Bald eagle, big brown bat, black oystercatcher, Caspian tern, gray wolf, great blue heron, merlin, osprey, peregrine falcon, pileated woodpecker, purple martin, purplish copper, Shaw Island Townsend's vole, snowy owl, Townsend's big-eared bat, western floater, western toad	105	109	32	62

7.3.2

Biological Impacts for Skagit River Crossing

For the Skagit River Crossing high river flow (June) 90PD release (Table 7-12), there was surface and shoreline oiling at thicknesses that could cause mortality in 35 km^2 for dabbling waterfowl and over 914 km^2 for surface diving birds. For this spill scenario, very limited acute impacts were predicted for cetaceans (whales or dolphins) and terrestrial wildlife. The results from the exposure model for water

column organisms indicated there would be concentrations of hydrocarbons in the water column (or in the sediment) that would cause small areas of mortality in each of the organism types evaluated. Species of moderate sensitivity would experience extremely small regions of acute mortality, generally < 0.1 km^2. This would have implications for commercial fisheries in that there would be limited acute impacts to fish and shellfish for this one spill event.

Table 7-12: Equivalent area (km^2) of up to 100-percent-predicted mortality for various behavior groups of wildlife, fish, and invertebrates by threshold for the Skagit River Crossing high river flow (June) 90PD release. Values are the equivalent area of 100-percent mortality for species of high and medium sensitivity to dissolved PAHs from a representative spill.

Behavior Group	Equivalent Area (km^2) of up to 100%-Predicted Mortality At Threshold:	
Surface and Shoreline Impacts	**10 µm**	
Dabbling waterfowl	35.3	
Nearshore aerial birds	13.7	
Surface diving birds	94.8	
Aerial seabirds	5.6	
Wetland wildlife	13.7	
Terrestrial wildlife	< 0.1	
Cetaceans	< 0.1	
Fur-bearing marine mammals	75.1	
Pinnipeds	1.1	
In-Water Impacts	**5 ppb**	**50 ppb**
Demersal - move at bottom	0.8	< 0.1
Demersal – stationary	0.5	< 0.1
Small pelagic fish/invertebrates	0.7	< 0.1
Large pelagic fish	0.9	< 0.1
Benthic – in sediments	< 0.1	0
Planktonic (drift)	2.5	0.4

For the Skagit River Crossing high river flow (June) 30PD release (Table 7-13), there was surface and shoreline oiling at thicknesses that could cause mortality in 16 km^2 for dabbling waterfowl and over 51 km^2 for surface diving birds. Mortality would only occur if the organisms were present in the areas affected by spilled oil. For this spill scenario, very limited acute impacts were predicted for cetaceans

(whales or dolphins), pinnipeds, and terrestrial wildlife. The results from the exposure model for water column organisms indicated there would be concentrations of hydrocarbons in the water column (or in the sediment) that would cause small areas of mortality in each of the organism types evaluated, all < 1.5km^2. Species of moderate sensitivity would experience extremely small regions of acute mortality, all < 0.15 km^2. This would have implications for commercial fisheries in that there would be limited acute impacts to fish and shellfish for this one spill event.

Table 7-13: Equivalent area (km^2) of up to 100-percent-predicted mortality for various behavior groups of wildlife, fish, and invertebrates by threshold for the Skagit River Crossing high river flow (June) 30PD release. Values are the equivalent area of 100-percent mortality for species of high and medium sensitivity to dissolved PAHs from a representative spill.

Behavior Group	Equivalent Area (km^2) of up to 100%-Predicted Mortality At Threshold:	
Surface and Shoreline Impacts	**10 µm**	
Dabbling waterfowl	16.6	
Nearshore aerial birds	6.1	
Surface diving birds	51.6	
Aerial seabirds	2.8	
Wetland wildlife	6.1	
Terrestrial wildlife	< 0.1	
Cetaceans	< 0.1	
Fur-bearing marine mammals	39.9	
Pinnipeds	0.6	
In-Water Impacts	**5 ppb**	**50 ppb**
Demersal - move at bottom	0.2	< 0.1
Demersal – stationary	0.2	< 0.1
Small pelagic fish/invertebrates	0.4	< 0.1
Large pelagic fish	0.3	< 0.1
Benthic – in sediments	0	0
Planktonic (drift)	1.4	0.1

For the Skagit River Crossing low river flow (December) 90PD release (Table 7-14), there was surface and shoreline oiling at thicknesses that could cause mortality in 11 km^2 for dabbling waterfowl and over 21 km^2 for surface diving birds. For this spill scenario, very limited acute impacts were predicted for

cetaceans (whales or dolphins) and terrestrial wildlife. The results from the exposure model for water column organisms indicated there would be concentrations of hydrocarbons in the water column (or in the sediment) that would cause small areas of mortality in each of the organism types evaluated, generally < 2 km^2. Species of moderate sensitivity would experience extremely small regions of acute mortality, generally < 0.1 km^2. This would have implications for commercial fisheries in that there would be limited acute impacts to fish and shellfish for this one spill event.

Table 7-14: Equivalent area (km^2) of up to 100-percent-predicted mortality for various behavior groups of wildlife, fish, and invertebrates by threshold for the Skagit River Crossing low river flow (December) 90PD release. Values are the equivalent area of 100-percent mortality for species of high and medium sensitivity to dissolved PAHs from a representative spill.

Behavior Group	Equivalent Area (km^2) of up to 100%-Predicted Mortality At Threshold:	
Surface and Shoreline Impacts	**10 µm**	
Dabbling waterfowl	11.0	
Nearshore aerial birds	4.0	
Surface diving birds	21.2	
Aerial seabirds	1.1	
Wetland wildlife	4.0	
Terrestrial wildlife	< 0.1	
Cetaceans	< 0.1	
Fur-bearing marine mammals	16.2	
Pinnipeds	0.2	
In-Water Impacts	**5 ppb**	**50 ppb**
Demersal - move at bottom	1.8	< 0.1
Demersal – stationary	1.5	< 0.1
Small pelagic fish/invertebrates	1.9	< 0.1
Large pelagic fish	1.5	< 0.1
Benthic – in sediments	< 0.1	0
Planktonic (drift)	3.1	0.3

For the Skagit River Crossing low river flow (December) 30PD release (Table 7-15), was surface and shoreline oiling at thicknesses that could cause mortality in 3 km^2 for dabbling waterfowl and 8 km^2 for surface diving birds. Mortality would only occur if the organisms were present in the areas affected by

spilled oil. For this spill scenario, very limited acute impacts were predicted for cetaceans (whales or dolphins), pinnipeds, aerial seabirds, and terrestrial wildlife. The results from the exposure model for water column organisms indicated there would be concentrations of hydrocarbons in the water column (or in the sediment) that would cause small areas of mortality in each of the organism types evaluated, all < 0.6 km^2. Species of moderate sensitivity would experience extremely small regions of acute mortality, all < 0.02 km^2. This would have implications for commercial fisheries in that there would be limited acute impacts to fish and shellfish for this one spill event.

Table 7-15: Equivalent area (km^2) of up to 100-percent-predicted mortality for various behavior groups of wildlife, fish, and invertebrates by threshold for the Skagit River Crossing low river flow (December) 30PD release. Values are the equivalent area of 100-percent mortality for species of high and medium sensitivity to dissolved PAHs from a representative spill.

Behavior Group	Equivalent Area (km^2) of up to 100%-Predicted Mortality At Threshold:	
Surface and Shoreline Impacts	**10 µm**	
Dabbling waterfowl	2.8	
Nearshore aerial birds	1.0	
Surface diving birds	8.0	
Aerial seabirds	0.4	
Wetland wildlife	1.0	
Terrestrial wildlife	< 0.1	
Cetaceans	< 0.1	
Fur-bearing marine mammals	6.1	
Pinnipeds	< 0.1	
In-Water Impacts	**5 ppb**	**50 ppb**
Demersal - move at bottom	0.6	< 0.1
Demersal – stationary	0.3	< 0.1
Small pelagic fish/invertebrates	0.4	< 0.1
Large pelagic fish	0.5	< 0.1
Benthic – in sediments	0	0
Planktonic (drift)	< 0.1	0

7.4 Edmonds Ferry Terminal

7.4.1 Overlay Analysis for Edmonds Ferry Terminal

The results of the overlay analysis for public access and socioeconomic resources, aquatic resources and aquatic sensitive areas, and avian/terrestrial resources and terrestrial sensitive areas for the Edmonds Ferry Terminal scenarios are presented in Table 7-16,

Table 7-17**,** and Table 7-18, respectively.

The 90PD scenarios for this release location occasionally affected a greater number of resources than the 30PD scenarios, as seen for the surf smelt spawning habitat, bald eagle nesting, and wetlands data layers. However, significantly more resources were affected during the winter (high winds) than the summer (low winds) scenarios. Commercial and recreational fishing areas and fish spawning habitats were notably more affected during the winter scenarios, while terrestrial habitats like wetlands were less affected during the winter. This can be attributed to greater oil entrainment and adherence to SPM and settling during the high-wind conditions of the winter scenario.

Table 7-16: Overlay analysis for the Edmonds Ferry Terminal summer (low wind) and winter (high wind) 30PD and 90PD scenarios. Numbers indicate the counts of public access and socioeconomic resource areas potentially affected by oil.

Layer ID	Area Type(s)	Location/Description/Species	Summer 30PD	Summer 90PD	Winter 30PD	Winter 90PD
1	Beach, park, access	Camano Island State Park, Carkeek Park, Cultus Bay Road End, Double Bluff East Beach, Edmonds Underwater Park, Glendale Road End, Glendale-Beaches 100 and 99, Hansville-Beach 69, Kayak Point County Park, Marina Beach South/ Edmonds, Meadowdale County Park, Mukilteo Lighthouse Park, Picnic Point County Park, Point No Point, Beach 68, Richmond Beach County Park, Sunlight County Park	6	6	11	12
	Aquaculture, boat ramp, diving, equipment, ferry, marina	Camano Island State Park, Clinton - Mukilteo Ferry, Clinton Ferry Landing, Dave Mackie Park, Edmonds - Kingston Ferry, Edmonds Ferry Landing, Edmonds Jetty, Edmonds Marina (Port of), Edmonds Oil Dock, Edmonds Underwater Park, Eglon Boat Launch, Gedney Island, Hat Island Community, Kayak Point County Park, Kingston Cove Marina, Kingston Ferry Landing, MSRC Spill Response Equipment, Mukilteo Lighthouse Park, Mukilteo State Park, Mutiny Bay Ramp, NRCES Spill Response Equipment, Port Of Kingston/ Kingston Cove Marina, Possession Beach Waterfront Park, Possession Point, Richmond Beach (Entry), The Trees (Boeing Creek)	15	15	13	15
10 / 11	Public access	Edmonds Underwater Park, Olympic Beach Park, Edmonds Marina Beach Park, Edmonds Marina Dog Park	4	4	2	2
5	Park, management area	Brackett's Landing Shoreline Sanctuary, Camano Island, Everett Jetty	1	1	3	3
	Unknown use, aquaculture, and commercial fishing	Unknown, Kingston, Possession Sound, South West Whidbey, demersal groundfish fishing, pelagic groundfish fishing, rocky reef groundfish fishing, salmon fishing	37	41	77	77
	Recreational and subsistence fishing	Demersal groundfish fishing, pelagic groundfish fishing, rocky reef groundfish fishing, salmon fishing, Native American salmon fishing	20	20	41	41
12 / 25	Shellfish commercial harvest and growing areas	Jamestown S'Klallam Tribe, Kingston, Lower Elwha S'Klallam Tribe, Lummi Indian Business Council, Port Gamble S'Klallam Tribe, Possession Sound, Saratoga Pass, South West Whidbey, Suquamish Seafoods, Suquamish Tribe, Swinomish Indian Tribal Community, The Tulalip Tribes	29	31	34	34
15	Shellfish recreational beaches	Camano Island SP, Dave Mackie CP, DNR-68, DNR-69, DNR-100, DNR-101, DNR-99, Double Bluff SP, E Elger Bay, Fn Camano Hd, Fs Mabana, Kayak Point CP, Mabana, Meadowdale CP, Mukilteo SP, Ne Cultus Bay, Picnic Pt CP, Richmond Beach, S Mukilteo Pk, S Sandy Pt, Scatchet Hd, South Useless Bay, Unnamed, W Elger Bay	3	3	20	22
16	Ceded land, reservation	Treaty of Point Elliott, Tulalip Tribe Reservation	1	1	2	2

Table 7-17: Overlay analysis for the Edmonds Ferry Terminal summer (low wind) and winter (high wind) 30PD and 90PD scenarios. Numbers indicate the counts of aquatic resources and sensitive areas potentially affected by oil.

Layer ID	Area Type(s)	Location/Description/Species	Summer 30PD	Summer 90PD	Winter 30PD	Winter 90PD
6	Invertebrate concentration area	Unknown, geoduck, hardshell clams, giant octopus, Dungeness crab, pandalid shrimp	36	53	96	100
43	Locations of subtidal geoduck clams	Apple Cove Point North, Apple Tree Cove, Elliott Point, Gedney Island North and South, Kingston, Picnic Point, Picnic Point North, Pilot Point, President Point, Randall, Richmond Beach	7	7	6	6
46	Shellfish locations	Dungeness crab, geoduck, hardshell clam, pandalid shrimp, subtidal hardshell clam	14	14	19	19
4	Fish spawning areas / beaches	Coho salmon, Pacific sand lance, surf smelt	7	7	32	34
7	Spawning and pre-spawner areas	Pacific herring	0	0	5	6
44 / 45	Adult holding and spawning areas	Pacific herring	0	0	5	6
47	Spawning habitat	Pacific sand lance	6	6	26	26
48	Spawning habitat	Surf smelt	6	6	37	62
9	Marine mammal haulout points	California sea lion, harbor seal	3	3	7	8
28	Observation of listed species - haulout	California sea lion	1	1	2	2

Table 7-18: Overlay analysis for the Edmonds Ferry Terminal summer (low wind) and winter (high wind) 30PD and 90PD scenarios. Numbers indicate the counts of avian and terrestrial resources and sensitive areas potentially affected by oil.

Layer ID	Area Type(s)	Location/Description/Species	Summer 30PD	Summer 90PD	Winter 30PD	Winter 90PD
8	Unknown bird sites	Unknown	0	0	4	6
	Alcid bird sites	Murre, pigeon guillemot, rhinoceros auklet	2	2	7	7
	Diving bird sites	Pacific loon, red-throated loon, western grebe	4	4	13	15
	Gull/tern bird sites	Caspian tern, gulls	8	8	22	25
	Waterfowl bird sites	Bufflehead, Goldeneye, scaup, scoters, waterfowl	7	8	34	35
3	Pelagic nesting sites	Seabirds	2	2	0	0
	Raptor nesting sites	Bald eagle	15	15	34	46
	Wading nesting sites	Great blue heron	1	1	3	3
32	Bald eagle nests	Bald eagle	28	28	37	43
39	Seabird colonies	Unknown, alcids, cormorants, others	3	3	0	0
40	National Wetlands Inventory	Estuarine and marine deepwater, estuarine and marine wetland	28	41	7	7
35 / 36	Biodiversity areas and corridors	Boeing Creek Unos, Carkeek Park And Environs - Seattle, Gedney Island open space, Lower Chenault Creek open space, Meadowdale Park, SW Snohomish County open space, Puget Sound to I-5	3	3	4	4
	Priority habitats (cliffs/bluffs, eelgrass meadows, wetlands)	Cliffs/bluffs, eelgrass meadows, mouth of Snohomish River, Snohomish River Estuary, Lake Washington wetlands, Mukilteo wetlands, Region 6 Saltwater wetlands	1	1	4	4
	Wildlife concentrations and occurrences	Gray whale, mountain quail, waterfowl concentrations	1	1	2	2
28 / 29	Observation of listed species - biotic detection, nest, colony	Bald eagle, great blue heron, mountain quail, Northern goshawk, osprey, Purple martin	28	28	29	32

7.4.2

Biological Impacts for Edmonds Ferry Terminal

For the Edmonds Ferry Terminal summer low wind (August) 90PD release (Table 7-19), there was surface and shoreline oiling at thicknesses that could cause mortality in 4 km^2 for aerial seabirds and ~74 km^2 for surface diving birds. Mortality would only occur if the organisms were present in the areas affected by spilled oil. For this spill scenario, very limited acute impacts were predicted for cetaceans (whales or dolphins), pinnipeds, wetland wildlife, nearshore aerial birds, and terrestrial wildlife. The results from the exposure model for water column organisms indicated there would be concentrations of hydrocarbons in the water column (or in the sediment) that would cause small areas of mortality in

each of the organism types evaluated, all < 0.5 km^2. Species of moderate sensitivity would experience extremely small regions of acute mortality, all < 0.02 km^2. This would have implications for commercial fisheries in that there would be limited acute impacts to fish and shellfish for this one spill event.

Table 7-19: Equivalent area (km^2) of up to 100-percent-predicted mortality for various behavior groups of wildlife, fish, and invertebrates by threshold for the Edmonds Ferry Terminal summer low-wind (August) 90PD release. Values are the equivalent area of 100-mortality for species of high and medium sensitivity to dissolved PAHs from a representative spill.

Behavior Group	Equivalent Area (km^2) of up to 100%-Predicted Mortality At Threshold:	
Surface and Shoreline Impacts	**10 µm**	
Dabbling waterfowl	1.6	
Nearshore aerial birds	0.6	
Surface diving birds	74.3	
Aerial seabirds	3.9	
Wetland wildlife	0.5	
Terrestrial wildlife	< 0.1	
Cetaceans	< 0.1	
Fur-bearing marine mammals	56.8	
Pinnipeds	0.8	
In-Water Impacts	**5 ppb**	**50 ppb**
Demersal - move at bottom	0.1	< 0.1
Demersal – stationary	0.1	< 0.1
Small pelagic fish/invertebrates	0.3	< 0.1
Large pelagic fish	0.3	< 0.1
Benthic – in sediments	0	0
Planktonic (drift)	0.4	< 0.1

For the Edmonds Ferry Terminal summer low wind (August) 30PD release (Table 7-20), there was surface and shoreline oiling at thicknesses that could cause mortality in ~4 km^2 for aerial seabirds and ~69 km^2 for surface diving birds. Mortality would only occur if the organisms were present in the areas affected by spilled oil. For this spill scenario, very limited acute impacts were predicted for cetaceans (whales or dolphins), pinnipeds, wetland wildlife, nearshore aerial birds, and terrestrial wildlife. The

results from the exposure model for water column organisms indicated there would be concentrations of hydrocarbons in the water column (or in the sediment) that would cause small areas of mortality in each of the organism types evaluated, all < 0.2 km^2. Species of moderate sensitivity would experience extremely small regions of acute mortality, all < 0.03 km^2. This would have implications for commercial fisheries in that there would be limited acute impacts to fish and shellfish for this one spill event.

Table 7-20: Equivalent area (km^2) of up to 100-percent predicted mortality for various behavior groups of wildlife, fish, and invertebrates by threshold for the Edmonds Ferry Terminal summer low-wind (August) 30PD release. Values are the equivalent area of 100-percent mortality for species of high and medium sensitivity to dissolved PAHs from a representative spill.

Behavior Group	Equivalent Area (km^2) of up to 100%-Predicted Mortality At Threshold:	
Surface and Shoreline Impacts	**10 µm**	
Dabbling waterfowl	1.3	
Nearshore aerial birds	0.4	
Surface diving birds	68.9	
Aerial seabirds	3.6	
Wetland wildlife	0.4	
Terrestrial wildlife	< 0.1	
Cetaceans	< 0.1	
Fur-bearing marine mammals	52.6	
Pinnipeds	0.7	
In-Water Impacts	**5 ppb**	**50 ppb**
Demersal - move at bottom	0.1	< 0.1
Demersal – stationary	< 0.1	< 0.1
Small pelagic fish/invertebrates	0.2	< 0.1
Large pelagic fish	0.1	< 0.1
Benthic – in sediments	0	0
Planktonic (drift)	0.1	< 0.1

For the Edmonds Ferry Terminal winter high-wind (January) 90PD release (Table 7-21), there was surface and shoreline oiling at thicknesses that could cause mortality in 3 km^2 for dabbling waterfowl and 28 km^2 for surface diving birds. Mortality would only occur if the organisms were present in the areas

affected by spilled oil. For this spill scenario, very limited acute impacts were predicted for cetaceans (whales or dolphins), pinnipeds, and terrestrial wildlife. The results from the exposure model for water column organisms indicated there would be concentrations of hydrocarbons in the water column (or in the sediment) that would cause small areas of mortality in each of the organism types evaluated, all < 3 km^2. Species of moderate sensitivity would experience extremely small regions of acute mortality, all < 0.1 km^2. This would have implications for commercial fisheries in that there would be limited acute impacts to fish and shellfish for this one spill event.

Table 7-21: Equivalent area (km^2) of up to 100-percent-predicted mortality for various behavior groups of wildlife, fish, and invertebrates by threshold for the Edmonds Ferry Terminal winter high-wind (January) 90PD release. Values are the equivalent area of 100-percent mortality for species of high and medium sensitivity to dissolved PAHs from a representative spill.

Behavior Group	Equivalent Area (km^2) of up to 100%-Predicted Mortality At Threshold:	
Surface and Shoreline Impacts	**10 µm**	
Dabbling waterfowl	2.7	
Nearshore aerial birds	1.0	
Surface diving birds	27.7	
Aerial seabirds	1.4	
Wetland wildlife	1.0	
Terrestrial wildlife	< 0.1	
Cetaceans	< 0.1	
Fur-bearing marine mammals	21.1	
Pinnipeds	0.3	
In-Water Impacts	**5 ppb**	**50 ppb**
Demersal - move at bottom	0.5	< 0.1
Demersal – stationary	0.6	< 0.1
Small pelagic fish/invertebrates	0.6	< 0.1
Large pelagic fish	0.4	< 0.1
Benthic – in sediments	< 0.1	< 0.1
Planktonic (drift)	2.7	< 0.1

For the Edmonds Ferry Terminal winter high-wind (January) 30PD release (Table 7-22), there was surface and shoreline oiling at thicknesses that could cause mortality in ~1 km^2 for dabbling waterfowl and ~17 km^2 for surface diving birds. Mortality would only occur if the organisms were present in the areas affected by spilled oil. For this spill scenario, very limited acute impacts were predicted for cetaceans (whales or dolphins), pinnipeds, wetland wildlife, nearshore aerial birds, aerial seabirds, and terrestrial wildlife. The results from the exposure model for water column organisms indicated there would be concentrations of hydrocarbons in the water column (or in the sediment) that would cause small areas of mortality in each of the organism types evaluated, all < 0.5 km^2. Species of moderate sensitivity would experience extremely small regions of acute mortality, all < 0.03 km^2. This would have implications for commercial fisheries in that there would be limited acute impacts to fish and shellfish for this one spill event.

Table 7-22: Equivalent area (km^2) of up to 100-percent-predicted mortality for various behavior groups of wildlife, fish, and invertebrates by threshold for the Edmonds Ferry Terminal winter high-wind (January) 30PD release. Values are the equivalent area of 100-percent mortality for species of high and medium sensitivity to dissolved PAHs from a representative spill.

Behavior Group	Equivalent Area (km^2) of up to 100%-Predicted Mortality At Threshold:	
Surface and Shoreline Impacts	**10 µm**	
Dabbling waterfowl	1.1	
Nearshore aerial birds	0.4	
Surface diving birds	16.8	
Aerial seabirds	0.9	
Wetland wildlife	0.4	
Terrestrial wildlife	< 0.1	
Cetaceans	< 0.1	
Fur-bearing marine mammals	12.8	
Pinnipeds	0.2	
In-Water Impacts	**5 ppb**	**50 ppb**
Demersal - move at bottom	< 0.1	0
Demersal – stationary	0.1	< 0.1
Small pelagic fish/invertebrates	0.2	< 0.1
Large pelagic fish	< 0.1	0
Benthic – in sediments	< 0.1	< 0.1

Behavior Group	Equivalent Area (km^2) of up to 100%-Predicted Mortality At Threshold:	
Planktonic (drift)	0.4	< 0.1

8 Discussion and Conclusions

In general, conditioned Bakken crude is a light oil with low density and viscosity. It remains predominantly on the surface of the water, forming extensive slicks and evaporating rapidly. On average, approximately 53 percent is predicted to evaporate from the spills originating at the Swinomish Channel Swing Bridge release location, 49 percent from the spills originating at the Skagit River Crossing release location, and 53 percent from the spills originating at the Edmonds Ferry Terminal release location.

Swinomish Channel Swing Bridge

The general extents of the trajectories varied between the summer (spring tide) and the winter (neap tide) scenarios. During the summer, the oil was transported farther north and covered a larger footprint over the region. During the winter, the oil was localized to a smaller region within Padilla Bay. In each scenario, oil traveled south in the Swinomish Channel as the direction of the current changed with the tides.

The spring tide in the summer led to larger overall extents of oiling, but lower total hydrocarbon concentrations on the shoreline and in the sediments, and lower surface oil thickness. However, the neap tide in the winter resulted in smaller extents of oiling, higher concentrations on the shoreline and in the sediments, and higher overall surface oil thicknesses.

In general, the extents from the 90PD and 30PD trajectories were similar; however, 90PD scenarios could travel farther and oil shorelines more extensively. Additionally, the 90PD scenarios resulted in thicker surface oil, higher dissolved aromatics, and more extensive shoreline and sediment oiling.

At the end of each 48-hour simulation, the fates results provided a similar overall prediction of how released oil at this location would behave. Roughly 50 percent of the released oil evaporated, 20 to 30 percent of the oil remained on the water surface, 13 to 28 percent stranded on the nearby shorelines, and very little oil entrained, decayed, or adhered to sediment.

Overlay results followed similar trends to those observed in the trajectories. The 90PD scenarios generally affected numbers of resources more than or similar to the 30PD scenarios. In addition, the greater extent of oiling during the spring tide in the summer scenarios led to more resources being affected than during neap tide conditions in the winter scenarios.

The degree of biological impacts varied between scenarios, but the groups most affected were similar. For the Swinomish Channel Swing Bridge summer (spring tide) 30PD and 90PD scenarios, dabbling waterfowl (24 to 27 km^2), fur-bearing mammals (59 to 78 km^2), and surface-diving birds (76 to 100 km^2)

experienced the greatest acute mortality due to surface/shoreline oiling, while in-water acute toxicity impacts were minimal (≤ 0.8 km^2 in 90PD) across all aquatic behavior groups and sensitivity levels. During the winter (neap tide) scenarios, dabbling waterfowl (7 to 9 km^2), fur-bearing mammals (7 to 8 km^2), and surface-diving birds (9 to 11 km^2) experienced greater areas of predicted mortality than other biotic groups, but the overall impact was lower. In-water acute toxicity was lower during the winter scenarios than the summer scenarios, with all areas of mortality ≤ 0.2 km^2 at 5 ppb sensitivity. The mass balance percentages for winter and summer scenarios were similar at this location, likely explaining the similar biotic impacts across seasons.

Skagit River Crossing

The trajectories varied slightly between the summer (high flow) and the winter (low flow) scenarios. In each scenario, oil traveled down the Skagit River, through both the north and south forks, then entered Skagit Bay. During the summer, the oil traveled farther into Skagit Bay and into the Rosario Strait. During the winter, the oil was localized to a smaller region within Skagit Bay. Additionally, the oil had the potential to travel up Swinomish Channel and into Padilla Bay.

Generally, the low flow conditions resulted in smaller overall regions of affected areas. High flow conditions resulted in enhanced downstream transport and more substantial oiling of Skagit Bay.

The extents from the 90PD and 30PD trajectories were similar; however, 90PD scenarios could travel farther and oil shorelines more extensively. Additionally the 90PD scenarios resulted in thicker surface oil, higher dissolved aromatics, and more extensive shoreline and sediment oiling.

At the end of the 48-hour simulation, the fates in each of the scenarios provided a similar overall picture of how released oil at this location would behave. Roughly 44 to 50 percent of the released oil evaporated, 0 to 7 percent of the oil remained on the water surface, 40 to 55 percent stranded on the nearby shorelines, and very little oil entrained, decayed, or adhered to sediment. Substantially more oil stranded on shorelines primarily due to the release location in the Skagit River.

Overlay results followed similar trends to those observed in the fates trajectories. Larger extents of oiling due to the high river flow in the summer led to more resources potentially being affected than in the winter during low river flow conditions.

The degree of biological impacts varied between scenarios, but the groups most affected were similar. For the Skagit River Crossing summer (high flow) 30PD and 90PD scenarios, dabbling waterfowl (17 to 35 km^2), fur-bearing mammals (40 to 75 km^2), and surface-diving birds (52 to 95 km^2) experienced the greatest acute mortality due to surface/shoreline oiling, while in-water acute toxicity impacts were minimal (< 0.5 km^2 in 90PD) across most aquatic behavior groups and sensitivity levels. Only sensitive drifting plankton experienced acute morality greater than 1 km^2 during the summer scenarios (1.4 km^2

30PD, 2.5 km^2 90PD). During the winter (low flow) scenarios, dabbling waterfowl (3 to 11 km^2), fur-bearing mammals (6to– 16 km^2), and surface-diving birds (8 to 21 km^2) experienced greater areas of predicted mortality than other biotic groups, but the overall impact was lower. In-water acute toxicity was highest in the winter 90PD scenarios, with all groups except benthic infauna experiencing areas of mortality from 1.5 to 3.1 km^2 at 5 ppb sensitivity. This is possibly due to higher surface and water column mass balances of spilled oil during this scenario, compared to others at this release location.

Edmonds Ferry Terminal

The trajectories varied substantially between the summer (low wind) and the winter (high wind) scenarios. In the summer scenarios, when wind speeds were generally low, the oil traveled to the south and west and remained close to the release location. The low winds resulted in more localized impacts, due to limited transport, which led to less shoreline oiling. During the winter, high winds resulted in extensive transport of surface oil with the oil traveling primarily toward the north. The high-wind conditions also entrained oil into the water column by inducing surface breaking waves, which resulted in high concentrations of oil and dissolved aromatics in the water column and on the sediments.

Overall, the extents from the 90PD and 30PD trajectories were similar; however, 90PD could travel farther and oil shorelines more extensively. Additionally the 90PD resulted in thicker surface oil, higher dissolved aromatics, and more extensive shoreline and sediment oiling.

The resulting fates from the scenarios at the Edmonds Ferry Terminal release location were substantially different between the winter and summer scenarios. In the summer, roughly 52 to 53 percent of the released oil evaporated, 42 to 43 percent of the oil remained on the water surface, 3 percent stranded on the nearby shorelines, and very little oil entrained, decayed, or adhered to sediment. In the winter, roughly 52 to 53 percent of the released oil evaporated, 5 to 12 percent of the oil remained on the water surface, 12 to 29 percent stranded on the nearby shorelines, 5 to 11 percent entrained in the water column, 9 to 12 percent adhered to sediment, and very little oil decayed. During the high-wind winter season, there was substantially more oil in water column due to entrainment, and therefore adhered to sediment.

Overlay results followed similar trends to those observed in the fates trajectories. Occasionally, the 90PD scenarios affected numbers of resources more than or similar to the 30PD scenarios. For this release location, the winter scenario with high winds had the potential to affect more resources than the summer scenario during low-wind conditions.

The degree of biological impacts varied between scenarios, but the groups most affected were similar. For the Edmonds Ferry Terminal summer (low wind) 30PD and 90PD scenarios, fur-bearing mammals (53 to 57 km^2) and surface-diving birds (70 to 74 km^2) experienced the greatest acute mortality due to

surface/shoreline oiling, while in-water acute toxicity impacts were minimal (< 0.5 km^2 in 90PD) across all aquatic behavior groups and sensitivity levels. During the winter (high wind) scenarios, the same patterns of relative impact were seen to a lesser degree. As in the summer scenarios, fur-bearing mammals (13 to 21 km^2) and surface-diving birds (17 to 28 km^2) experienced greater areas of predicted mortality than other biotic groups, but the overall impact was lower. In-water acute toxicity was similar across seasons, except that drifting plankton had a greater area of mortality at 5 ppb in the winter 90PD scenario (2.7 km^2) than in any other scenario, likely due to greater surface oil entrainment in high-wind conditions.

Overall Summary

A crude-by-rail derailment is a very rare occurrence (Etkin 2016). Furthermore, a derailment that results in a loss of containment is even less likely. Finally, if an event were to occur, responders would be on scene to help mitigate any potentially negative impacts.

Under the assumption that this extremely unlikely event had occurred and that no response would be provided (i.e., unmitigated), oil spill modeling was conducted using the SIMAP™ trajectory, fate, and biological impacts model. The model results were used to predict the potential impacts that could result in the unlikely event of a release into water. To capture some of the potential geographic and environmental variability, three representative hypothetical release locations were investigated, under two environmental conditions, and two release volumes of conditioned Bakken crude oil. In addition, two biological sensitivities were investigated to determine the potential impacts a release could have on sensitive and average sensitivity species.

Trajectory and fates results were used to demonstrate that although roughly 50 percent of the oil was predicted to evaporate with the 48-hour modeled period, extensive shoreline and surface oiling was possible. Furthermore, under high-wind conditions, entrainment of surface oil into the water column was possible. A portion of this entrained oil and dissolved aromatics could result in sediment oiling.

In general, larger volumes (90PD, compared with 30PD) of oil resulted in larger numbers of potentially affected resources and larger acute biological impacts. Environmental conditions that resulted in further transport of oil also resulted in larger numbers of potential impacts. Generally, the 90PD scenarios led to larger numbers of potentially affected resources and more acute biological impacts.

An overlay analysis was used to determine the potential impacts a release could have on identified resources located near the hypothetical release locations. The overlay assessment included a count of any identified resource features (points, lines, or polygons) that were intersected by the trajectory of the released oil. Identified resources included socioeconomic resources (e.g., parks, management areas, public access points, fishing areas), aquatic resources (e.g., shellfish locations, fish spawning areas, seal

haulout points), and avian and terrestrial resources (e.g., bird colonies, nesting areas, wetlands, biodiversity corridors, and wildlife observations). In addition, biological impacts modeling was used to predict the equivalent areas of 100-percent mortality for each scenario for surface and shoreline impacts, as well as in-water impacts at two different sensitivity thresholds. In general, spilling larger volumes of oil resulted in larger potential impacts and larger numbers of potentially affected resources. Environmental conditions that resulted in further transport of oil also resulted in larger numbers of potential impacts.

While it is understood that the identified scenarios are in no way intended to predict a specific future event, the results presented in this document have demonstrated a range of potential trajectory and fates, as well as the predicted impacts that may result based on geographic criteria, environmental variability, and biological sensitivities. In the unlikely event that a derailment and loss of containment of the magnitude modeled here (5,700 to 20,000 bbl of crude oil) were to occur and enter a waterway, the resulting impacts have the potential to be both significant and adverse.

9 References

Aamo, O.M., M. Reed, and P. Daling, 1993. A laboratory based weathering model: PC version for coupling to transport models. In Proceedings of the 16th Arctic and Marine Oil Spill Program (AMOP) Technical Seminar, Environmental Protection Service, Emergencies Science Division, Environment Canada, Ottawa, ON, Canada, pp. 617-626.

Albers, P.H., 1980. Transfer of Crude Oil from Contaminated Water to Bird Eggs. Environmental Research 22(2): 307-314.

Albers, P.H. and R.C. Szaro, 1978. Effects of No. 2 Fuel Oil on Common Eider Eggs. Marine Pollution Bulletin 9: 138-139.

American Society of Civil Engineers (ASCE), 1969. Design and Construction of Sanitary and Storm Sewers. Manuals and Reports of Engineering Practice, Published by the American Society of Civil Engineers, No. 37, New York.

American Society of Civil Engineers Task Committee on Modeling Oil Spills (ASCE), 1996. State-of-the-art Review of Modeling Transport and Fate of Oil Spills, Water Resources Engineering Division, ASCE, Journal of Hydraulic Engineering 122(11): 594–609.

Anderson, J.W., S.L. Kiesser, R.M. Bean, R.M., R.G. Riley, and B.L. Thomas, 1981. Toxicity of chemically dispersed oil to shrimp exposed to constant and decreasing concentrations in a flowing system, Proceedings 1981 Oil Spill Conference, American Petroleum Institute, Washington, D.C., API Publication No. 4334, p. 69-75.

Anderson, J.W., 1985. Toxicity of dispersed and undispersed Prudhoe Bay crude oil fractions to shrimp, fish, and their larvae. American Petroleum Institute Publication No. 4441, Washington, D.C., USA, August 1985, 52p.

Anderson, J.W., R.G. Riley, S.L. Kiesser, and J. Gurtisen, 1987. Toxicity of dispersed and undispersed Prudhoe Bay crude oil fractions to shrimp and fish. In Proceedings 1987 Oil Spill Conference (Prevention, Behavior, Control, Cleanup), Tenth Biennial, American Petroleum Institute, Washington, D.C., pp.235-240.

Anderson, E., D. Mendelsohn and E. Howlett. 1995. The OILMAPWin/WOSM Oil Spill Model: Application to Hindcast a River Spill. Proceedings of the Eighteenth Arctic and Marine Oilspill Program (AMOP) Technical Seminar. June 14-16, 1995. Edmonton, Alberta Canada pp. 793.

Blum, D.J. and R.E. Speece, 1990. Determining chemical toxicity to aquatic species, Environmental Science and Technology. 24: 284–293.

Bradbury, S., R. Carlson, and T. Henry, 1989. Polar narcosis in aquatic organisms. Aquatic Toxicology and Hazard Assessment 12: 59–73.

City of Edmonds Washington, 2016. Edmonds GIS. Available: http://www.edmondswa.gov/gis-text.html. Accessed February 2016.

Clark, R.B., 1984. Impact of Oil Pollution on Seabirds. Environmental Pollution (Series A) 33: 1–22.

Coastal Engineering Research Center (CERC), 1984. Shore Protection Manual, Vol. I. Coastal Engineering Research Center, Department of the Army, Waterways Experiment Station, U.S. Army Corps of Engineers, Vicksburg, Mississippi, 1,105 p. plus 134 p. in appendices.

CSE/ASA/BAT, 1986. Development of a Coastal Oil Spill Smear Model. Phase 1: Analysis of Available and Proposed Models, Prepared for Minerals Management Service by Coastal Science & Engineering, Inc. (CSE) with Applied Science Associates, Inc. (ASA) and Battelle New England Research Laboratory (BAT), 121 p.

Daling, P.S. and P.J. Brandvik, 1988. A Study of the Formation and Stability of Water-in-Oil Emulsions. In Proceedings of the 11th Arctic and Marine Oil Spill Program Technical Seminar. Emergencies Science Division, Environment Canada, Ottawa, ON, Canada, pp. 153–170.

Daling, P.S. and P.J. Brandvik, 1991. Characterization and prediction of the weathering properties of oils at sea – A manual for the oils investigated in the DIWO project. IKU SINTEF Group report 91.037, DIWO report no. 16 02.0786.00/16/91, 29 May 1991, 140p.

Daling, P.S., D. Mackay, N. Mackay, and P.J. Brandvik, 1990. Droplet size distributions in chemical dispersion of oil spills: Towards a mathematical model. Oil and Chemical Pollution 7: 173–198.

Daling, P.S., O.M. Aamo, A. Lewis, and T. Strom-Kritiansen, 1997. SINTEF/IKU Oil-Weathering Model: Predicting Oil's Properties at Sea. In Proceedings 1997 Oil Spill Conference, Publication No. 4651, American Petroleum Institute, Washington, D.C., pp. 297–307.

Delvigne, G.A.L., 1993. Natural dispersion of oil by different sources of turbulence. Proc. Oil Spill Conf,-1993. Sponsored by U.S. Coast Guard, EPA and API, Tampa, FL, March, pp. 415–419.

Delvigne, G.A.L. and C.E. Sweeney, 1988. Natural Dispersion of Oil. Oil and Chemical Pollution 4: 281–310.

Di Toro, D.M. and J.A. McGrath, 2000. Technical basis for narcotic chemicals and polycyclic aromatic hydrocarbon criteria. II. Mixtures and sediments. Environmental Toxicology and Chemistry 19(8): 1971–1982.

Di Toro, D.M., J.A. McGrath, and D.J. Hansen, 2000. Technical basis for narcotic chemicals and polycyclic aromatic hydrocarbon criteria. I. Water and tissue. Environmental Toxicology and Chemistry 19(8): 1951–1970.

Engelhardt, F.R., 1983. Petroleum Effects on Marine Mammals. Aquatic Toxicology 4: 199–217.

Etkin, D., 2016. Crude-by-Rail Spill Risk Analysis for Proposed Shell Anacortes Rail Unloading Facility (ARUF): Rail Spill Probability and Volume Analysis. Submitted to HDR Inc. for presentation to the co-lead agencies Skagit County and Washington State Department of Ecology, March 2016.

Fay, J.A., 1971. Physical processes in the spread of oil on a water surface. In Proceedings, Conference on Prevention and Control of Oil Spills, sponsored by API, EPA, and US Coast Guard, American Petroleum Institute, Washington, D.C., June 15 17, 1971, pp. 463–467.

Fingas, M., 1996. The Evaporation of Crude Oil and Petroleum Products. PhD Dissertation, McGill University, Montreal, Canada, 181 p.

Fingas, M., 1997. The Evaporation of Oil Spills: Prediction of Equations Using Distillation Data. In Proceedings of the 20th Arctic and Marine Oil Spill Program (AMOP) Technical Seminar, Emergencies Science Division, Environment Canada, Ottawa, ON, Canada, pp. 1–20.

Fingas, M.F., 1998. Studies on the Evaporation of Crude Oil and Petroleum Products: II. Boundary Layer Regulation. Journal of Hazardous Materials, Vol. 57, pp. 41–58.

Fingas, M.F., 1999. The Evaporation of Oil Spills: Development and Implementation of New Prediction Methodology. In Proceedings of the 1999 International Oil Spill Conference, American Petroleum Institute, Washington, D.C., pp. 281–287.

Fingas, M., B. Fieldhouse, and J.V. Mullin, 1997. Studies of Water-in-Oil Emulsions: Stability Studies. In: Proceedings of 20th Arctic and Marine Oil Spill Program (AMOP) Technical Seminar, Emergencies Science Division, Environment Canada, Ottawa, ON, Canada, pp. 21–42.

Fischer, H.B., 1973. Longitudinal Dispersion and Turbulent Mixing in Open Channel Flow. Annual Review of Fluid Mechanics: pp. 59–78.

French, D.P., 1991. Estimation of exposure and resulting mortality of aquatic biota following spills of toxic substances using a numerical model, Aquatic Toxicology and Risk Assessment: Fourteenth Volume, ASTM STP 1124, (M.A. Mayes and M.G. Barron, Eds.) American Society for Testing and Materials, Philadelphia, pp. 35–47.

French, D.P. and F.W. French III, 1989. The biological component of the CERCLA Type A damage Assessment Model system. Oil and Chemical Pollution 5:125 163.

French, D.P. and H. Rines, 1997. Validation and use of spill impact modeling for impact assessment. Proceedings, 1997 International Oil Spill Conference, Fort Lauderdale, Florida, American Petroleum Institute Publication No. 4651, Washington, DC, pp. 829–834.

French, D., M. Reed, K. Jayko, S. Feng, H. Rines, S. Pavignano, T. Isaji, S. Puckett, A. Keller, F.W. French III, D. Gifford, J. McCue, G. Brown, E. MacDonald, J. Quirk, S. Natzke, R. Bishop, M. Welsh, M. Phillips, and B.S. Ingram, 1996. Final Report, The CERCLA Type A Natural Resource Damage

Assessment Model for Coastal and Marine Environments (NRDAM/CME), Technical Documentation, Vol. I - V., Office of Environmental Policy and Compliance, U.S. Department of the Interior, Washington, DC, Contract No. 14-0001-91-C-11.

French, D.P., H. Rines, and P. Masciangioli, 1997. Validation of an Orimulsion spill fates model using observations from field test spills. Proceedings, Twentieth Arctic and Marine Oil Spill Program Technical Seminar, Vancouver, Canada, June 10-13, 1997.

French, D., H. Schuttenberg, and T. Isaji, 1999. Probabilities of Oil Exceeding Thresholds of Concern: Examples from an Evaluation for Florida Power and Light. In Proceedings of the 22nd Arctic and Marine Oil Spill Program (AMOP) Technical Seminar, June 2-4, 1999, Calgary, Alberta, Environment Canada, pp. 243–270.

French McCay, D., 2001. Development and Application of an Oil Toxicity and Exposure Model, OilToxEx. Final Report to NOAA Damage Assessment Center, Silver Spring, MD, January 2001, 50 pp. plus appendices.

French McCay, D.P., 2002. Development and Application of an Oil Toxicity and Exposure Model, OilToxEx. Environmental Toxicology and Chemistry 21(10): 2080–2094.

French McCay, D.P., 2003. Development and Application of Damage Assessment Modeling: Example Assessment for the North Cape Oil Spill. Marine Pollution Bulletin, Volume 47, Issues 9–12, September-December 2003, pp. 341–359.

French McCay, D.P., 2004. Oil spill impact modeling: Development and validation. Environmental Toxicology and Chemistry 23(10): 2441–2456.

French McCay, D.P, 2009. State-of-the-Art and Research Needs for Oil Spill Impact Assessment Modeling. In Proceedings of the 32nd AMOP Technical Seminar on Environmental Contamination and Response, Emergencies Science Division, Environment Canada, Ottawa, ON, Canada, pp. 601–653.

French McCay, D. and J.R. Payne, 2001. Model of Oil Fate and Water concentrations with and without application of dispersants. In Proceedings of the 24th Arctic and Marine Oil Spill Program (AMOP) Technical Seminar, Emergencies Science Division, Environment Canada, Ottawa, ON, Canada, pp. 601–653.

French McCay, D.P. and J.J. Rowe, 2004. Evaluation of Bird Impacts in Historical Oil Spill Cases Using the SIMAP Oil Spill Model. In Proceedings of the 27th Arctic and Marine Oil Spill Program (AMOP) Technical Seminar, Emergencies Science Division, Environment Canada, Ottawa, ON, Canada, pp. 421–452.

Geraci, J.R. and D.J. St. Aubin, 1988. Synthesis of Effects of Oil on Marine Mammals, Report to U.S. Department of the Interior, Minerals Management Service, Atlantic OCS Region, OCS Study, MMS 88 0049, Battelle Memorial Institute, Ventura, CA, 292 p.

Grossman, E.E., A. Stevens, G. Gelfenbaum, and C. Curran, 2007. Nearshore circulation and water column properties in the Skagit River Delta, northern Puget Sound, Washington - Juvenile Chinook salmon habitat availability in the Swinomish Channel: U.S. Geological Survey Scientific Investigations Report 2007-5120, 97 pp.

Gundlach, E.R., 1987. Oil Holding Capacities and Removal Coefficients for Different Shoreline Types to Computer Simulate Spills in Coastal Waters. In Proceedings of the 1987 Oil Spill Conference, pp. 451–457.

Hines, A.L. and R.N. Maddox, 1985. Mass Transfer Fundamentals and Application. Prentice-Hall, Inc., Englewood Cliffs, New Jersey, 542 p.

Hodson, P.V., D.G. Dixon, and K.L.E. Kaiser, 1988. Estimating the Acute Toxicity of Waterborne Chemicals in Trout from Measurements of Median Lethal Dose and the Octanol-Water Partition Coefficient. Journal of Environmental Toxicology and Chemistry 7:443–454.

Hoffman, D.J., 1978. Embryotoxic Effects of Crude Oil in Mallard Ducks and Chicks. Toxicology and Applied Pharmacology 46: 183–190.

Homer, C.G.,J.A. Dewitz, L. Yang, S. Jin, P. Danielson, G. Xian, J. Coulston, N.D. Herold, J.D. Wickham, and K. Megown, 2015. Completion of the 2011 National Land Cover Database for the conterminous United States-Representing a decade of land cover change information. Photogrammetric Engineering and Remote Sensing, v. 81, no. 5, pp. 345–354. Available: http://www.mrlc.gov/nlcd2011.php. Accessed January 2016.

Incardona, J.P., M.G. Carls, L. Holland, T.L. Linbo, D.H. Baldwin, M.S. Myers, K.A. Peck, M. Tagal, S.D. Rice, and N.L. Scholz, 2015. Very low embryonic crude oil exposures cause lasting cardiac defects in salmon and herring. Scientific Reports 5.

Jenssen, B.M., 1994. Review article: effects of oil pollution, chemically treated oil, and cleaning on thermal balance of birds. Environmental Pollution. 86(2):207–215.

Jenssen, B. M. and M. Ekker, 1991a. Dose Dependent Effects of Plumage-Oiling on Thermoregulation of Common Eiders Somateria mollissima Residing in Water. Polar Research 10: 579–84.

Jenssen, B. M. and M. Ekker, 1991b. Effects of Plumage Contamination with Crude Oil Dispersant Mixtures on Thermoregulation in Common Eiders and Mallards. Archives of Environmental Contamination and Toxicology 20: 398–403.

Jones, R.K., 1997. A Simplified Pseudo-Component of Oil Evaporation Model. In Proceedings of the 20th Arctic and Marine Oil Spill Program (AMOP) Technical Seminar, Environment Canada, pp. 43–61.

Khangaonkar T. and W. Long, 2016. Sensitivity of Circulation in the Skagit River Estuary to Sea Level Rise and Future Flows. Northwest Science (in press).

Khangaonkar T., Z. Yang, T.Y. Kim, and M. Roberts, 2011. Tidally averaged circulation in Puget Sound sub-basins: Comparison of historical data, analytical model, and numerical model. Estuarine, Coastal and Shelf Science 93(4):305–319. doi:10.1016/j.ecss.2011.04.016.

King, K.A. and C.A. Lefever, 1979. Effects of Oil Transferred from Incubating Gulls to Their Eggs. Marine Pollution Bulletin 10: 319–321.

Kirstein, B.E., J.R. Clayton, C. Clary, J.R. Payne, D. McNabb, Jr., G. Fauna, and R. Redding, 1987. Integration of Suspended Particulate Matter and Oil Transportation Study. Minerals Management Service, OCS Study MMS87-0083, Anchorage, Alaska, 216 p.

Kolluru, V., M.L. Spaulding, and E. Anderson, 1994. A three dimensional subsurface oil dispersion model using a particle based approach. In Proceedings of 17th Arctic and Marine Oil Spill Program (AMOP) Technical Seminar, Vancouver, British Columbia, June 8–10, 1994, Emergencies Science Division, Environment Canada, Ottawa, ON, Canada, pp. 867–893.

Kooijman, S.A.L.M., 1981. Parametric analysis of mortality rates in bioassays. Water Research 15:107–119.

Kouwen, N., S.F. Mousavi, V.P. Singh, and D.K. Frevert, 2002. WATFLOOD/SPL9 hydrological model and flood forecasting system. Mathematical models of large watershed hydrology, pp. 649–685.

Kullenberg, G. (ed.), 1982. Pollutant transfer and transport in the sea. Volume I. CRC Press, Boca Raton, Florida, 227 p.

Lehr, W.J., D. Wesley, D. Simecek-Beatty, R. Jones, G. Kachook, and J. Lankford, 2000. Algorithm and interface modifications of the NOAA oil spill behavior model. In Proceedings of the 23rd Arctic and Marine Oil Spill Program (AMOP) Technical Seminar, Vancouver, BC, Environmental Protection Service, Environment Canada, pp. 525–539.

Lunel, T., 1993a. Dispersion: Oil droplet size measurements at sea. In Proceedings of the 16th Arctic Marine Oilspill Program (AMOP) Technical Seminar, Environment Canada, Calgary, Alberta, June 7–9, 1993, pp. 1023–1056.

Lunel, T., 1993b. Dispersion: Oil droplet size measurements at sea. In Proceedings of the 1993 Oil Spill Conference, pp. 794–795.

Lyman, C.J., W.F. Reehl, and D.H. Rosenblatt, 1982. Handbook of Chemical Property Estimation Methods. McGraw-Hill Book Co., New York, 960 p.

Mackay, D. and P.J. Leinonen, 1977. Mathematical model of the behavior of oil spills on water with natural and chemical dispersion. Prepared for Fisheries and Environment Canada. Economic and Technical Review Report EPS-3-EC-77-19, 39 p.

Mackay, D. and R.M. Matsugu, 1973. Evaporation rates of liquid hydrocarbon spills on land and water. Canadian Journal of Chemical Engineering 51: 434–439.

Mackay, D. and W. Zagorski, 1982. Water-In-Oil Emulsions. Environment Canada Manuscript Report EE-34, Ottawa, Ontario, Canada, 93p.

Mackay, D., S. Paterson, and K. Trudel, 1980. A mathematical model of oil spill behavior. Department of Chemical and Applied Chemistry, University of Toronto, Canada, 39p.

Mackay, D, W.Y. Shiu, K. Hossain, W. Stiver, D. McCurdy, and S. Peterson, 1982. Development and calibration of an oil spill behavior model. Report No. CG-D-27-83, U.S. Coast Guard, Research and Development Center, Groton, Connecticut, 83p.

Mackay, D., W.Y. Shiu, and K.C. Ma, 1992. Illustrated Handbook of Physical-Chemical Properties and Environmental Fate for Organic Chemicals, Vol. I-IV. Lewis Publishers, Inc., Chelsea, Michigan.

Malins, D.C. and H.O. Hodgins, 1981. Petroleum and marine fishes: a review of uptake, disposition, and effects. Environmental Science & Technology 15(11):1272-1280.

McAuliffe, C.D., 1989. The Weathering of Volatile Hydrocarbons from Crude Oil Slicks on Water. In Proceedings of the 1989 Oil Spill Conference, San Antonio, Texas, American Petroleum Institute, Washington, D.C., pp. 357–364.

McCarty, L.S., 1986. The Relationship Between Aquatic Toxicity QSARs and Bioconcentration for Some Organic Chemicals. Journal of Environmental Toxicology Chemistry 5:1071–1080.

McCarty, L.S., and D. Mackay, 1993. Enhancing Ecotoxicological Modeling and Assessment. Journal of Environmental Science and Technology 27(9):1719–1728.

McCarty, L.S., D. Mackay, A.D. Smith, G.W. Ozburn, and D.G. Dixon, 1992a. Residue-based Interpretation of Toxicity and Bioconcentration QSARs from Aquatic Bioassays: Neutral Narcotic Organics. Journal of Environmental Toxicology and Chemistry 11:917–930.

McCarty, L.S., G.W. Ozburn, A. D. Smith, and D.G. Dixon, 1992b. Toxicokinetic modeling of mixtures of organic chemicals. Environmental Toxicology and Chemistry 11: 1037–1047.

Milton, S., P. Lutz, and G. Shigenaka, 2003. Oil Toxicity and Impacts on Sea Turtles. In Shigenaka, G. (ed.), Oil and Sea Turtles: Biology, Planning, and Response. National Oceanic and Atmospheric Administration, 116 p.

National Oceanic and Atmospheric Administration (NOAA), 2016a. Office of Response and Restoration – Environmental Sensitivity Index (ESI) Maps. Available: http://response.restoration.noaa.gov/maps-and-spatial-data/environmental-sensitivity-index-esi-maps.html. Accessed January 2016.

National Oceanic and Atmospheric Administration (NOAA), 2016b. National Centers for Environmental Information NGDC Coastal DEMs. Available: http://www.ngdc.noaa.gov/dem/squareCellGrid/search. Accessed: January 2016.

National Oceanic and Atmospheric Administration (NOAA), 2016c. Office of Response and Restoration – Download ESI Maps and GIS Data: Washington. Available: http://response.restoration.noaa.gov/maps-and-spatial-data/download-esi-maps-and-gis-data.html#Washington. Accessed: March 2016.

National Park Service (NPS), 2016. North Cascades National Park, Washington - Bald Eagle Surveys. Available: http://www.nps.gov/noca/learn/nature/bald-eagle-surveys.htm. Accessed March 2016.

National Research Council (NRC), 1985. Oil in the Sea: Inputs, Fates and Effects. National Academy Press, Washington, D.C., 601 p.

National Research Council (NRC), 2002. Oil in the Sea III: Inputs, Fates and Effects. National Academy Press, Washington, D.C., 446 p.

Neff, J.M. and J.W. Anderson, 1981. Response of Marine Animals to Petroleum and Specific Petroleum Hydrocarbons. Applied Science Publishers Ltd., London and Halsted Press Division, John Wiley & Sons, NY., 177 p.

Neff, J.M., J.W. Anderson, B.A. Cox, R.B. Laughlin, Jr., S.S. Rossi, and H.E. Tatem, 1976. Effects of petroleum on survival respiration, and growth of marine animals. In Sources, Effects and Sinks of Hydrocarbons in the Aquatic Environment. American Institute of Biological Sciences, Washington, D.C., pp. 515–539.

Nirmalakhandan, N. and R.E. Speece, 1988. Structure-activity relationships, quantitative techniques for predicting the behavior of chemicals in the ecosystem. Environmental Science and Technology 22:606-615.

Okubo, A., 1971. Oceanic diffusion diagrams. Deep-Sea Research 8:789–802.

Okubo, A. and R.V. Ozmidov, 1970. Empirical dependence of the coefficient of horizontal turbulent diffusion in the ocean on the scale of the phenomenon in question. Atmospheric and Ocean Physics 6(5):534–536.

Payne, J.R. and G.D. McNabb Jr., 1984. Weathering of Petroleum in the Marine Environment. Marine Technology Society Journal 18(3):24–42.

Payne, J.R., B.E. Kirstein, G.D. McNabb, Jr., J.L. Lambach, R. Redding R.E. Jordan, W. Hom, C. deOliveria, G.S. Smith, D.M. Baxter, and R. Gaegel, 1984. Multivariate analysis of petroleum weathering in the marine environment – sub Arctic. Environmental Assessment of the Alaskan Continental Shelf, OCEAP, Final Report of Principal Investigators, Vol. 21 and 22, Feb. 1984, 690 p.

Payne, J.R., B.E. Kirstein, J.R. Clayton, Jr., C. Clary, R. Redding, G.D. McNabb, Jr., and G. Farmer, 1987. Integration of suspended particulate matter and oil transportation study. Final Report. Minerals Management Service, Environmental Studies Branch, Anchorage, AK. Contract No. 14-12-0001-30146, 216 p.

Peakall, D.B., P.G. Wells, and D. Mackay, 1985. A Hazard Assessment of Chemically Dispersed Oil Spills and Seabirds - A Novel Approach. In Proceedings of the 8th Technical Semi Annual Arctic Marine Oil Spill Program, Environmental Canada, Edmonton, AB, pp. 78–90.

Puget Sound Lidar Consortium (PSLC), 2016. Public domain high-resolution topography for the Pacific Northwest. Available: http://pugetsoundlidar.ess.washington.edu. Accessed February 2016.

Reed, M. and E. Gundlach, 1989. Hindcast of the Amoco Cadiz event with a coastal zone oil spill model. Oil and Chemical Pollution 5: 451–476.

Rice, S.D., J.W. Short, and J.F. Karinen, 1977. Comparative oil toxicity and comparative animal sensitivity, D.A. Wolfe (ed.). Fate and Effects of Petroleum Hydrocarbons in Marine Ecosystems and Organisms. Pergamon Press, NY, pp. 78–94.

Saha, S., et al., 2010. NCEP Climate Forecast System Reanalysis (CFSR) 6-hourly Products, January 1979 to December 2010. Research Data Archive at the National Center for Atmospheric Research, Computational and Information Systems Laboratory. http://dx.doi.org/10.5065/D69K487J.

Schwartz, M., L. Bromwell, J. Kiefer, W. Reigner, W. Winkler, and B. Manley, 2002. Hydrodynamic Simulations of Restoration Alternative 1 Tenoroc Fish Management Area. Stormwater Management Conference, Orlando, Florida, December 4–6, 2002.

Seo, I.W. and K.O. Baek, 2004. Estimation of the Longitudinal Dispersion Coefficient Using the Velocity Profile in Natural Streams. Journal of Hydraulic Engineering. March 2004.

Shannon & Wilson, Inc. (S&W), 2011. Skagit River Levee General Investigation (GI) Levee Risk and Reliability Analysis – Skagit County, Washington. Report submitted to: USACE Seattle District. 21-1-21 199-003. Available: http://www.skagitcounty.net/PublicWorksSalmonRestoration/Documents/2011JAN31_SkagitGI_LeveeRiskandReliabilityReport.pdf. Accessed January 2016.

Shigenaka, G., 2002. Chapter 2. Oil Toxicity. In Oil Spills in Mangroves: Planning and Response Considerations, R. Hoff (ed.), National Oceanic and Atmospheric Administration, Office of Response and Restoration (OR&R), 70 p.

Snohomish County Marine Resources Committee (MRC), 2016. Maps of Snohomish County Marine Resources. Available: http://www.snocomrc.org/Resources/Marine-Resource-Maps.aspx. Accessed January 2016.

Socolofsky, S.A., and G.H. Jirka, 2004. Environmental Fluid Mechanics Draft Textbook.

Spies, R.B., S.D. Rice, D.A. Wolfe, and B.A. Wright, 1996. The Effects of the Exxon Valdez Oil Spill on the Alaskan Coastal Environment. In Proceedings of the Exxon Valdez Oil Spill Symposium 18, American Fisheries Society, Bethesda, MD, pp. 1–16.

Sprague, J.B., 1969. Measurement of pollutant toxicity to fish. I. Bioassay methods for acute toxicity. Water Research 3: 793–821.

Stiver, W. and D. Mackay, 1984. Evaporation rate of oil spills of hydrocarbons and petroleum mixtures. Environmental Science and Technology 18: 834–840.

Swartz, R.C., D.W. Schults, R.J. Ozretich, J.O. Lamberson, F.A. Cole, T.H. DeWitt, M.S. Redmond, and S.P. Ferraro, 1995. PAH: A Model to Predict the Toxicity of Polynuclear Aromatic Hydrocarbon Mixtures in Field-Collected Sediments. Journal of Environmental Toxicology and Chemistry 14(11): 1977–1987.

Tatem, H.E., B.A. Cox, and J.W. Anderson, 1978. The toxicity of oils and petroleum hydrocarbons to estuarine crustaceans. Estuarine and Coastal Marine Science 6:365–373.

Thorpe, S.A., 1984. On the Determination of K in the Near Surface Ocean from Acoustic Measurements of Bubbles. Journal of Physical Oceanography 14: 855–863.

U.S. Environmental Protection Agency (US EPA), 2003. Procedures for the Derivation of Equilibrium Partitioning Sediment benchmarks (ESBs) for the Protection of Benthic Organisms (PDF). PAH Mixtures. EPA-600-R-02-013. Office of Research and Development. Washington, DC.

U.S. Environmental Protection Agency (US EPA), 2008. Procedures for the Derivation of Equilibrium Partitioning Sediment benchmarks (ESBs) for the Protection of Benthic Organisms (PDF). Compendium of Tier 2 Values for Nonionic Organics. U.S. Environmental Protection Agency, Office of Research and Development: Washington DC. EPA/600/R-02/016. PB2008-107282. March 2008.

U.S. Geological Survey (USGS), 2016a. Hydrography – National Hydrography Dataset, Watershed Boundary Dataset. Available: http://nhd.usgs.gov/. Accessed January 2016.

U.S. Geological Survey (USGS), 2016b. National Water Information System: Web Interface. USGS 12200500 Skagit River Near Mount Vernon, WA. Available: http://waterdata.usgs.gov/nwis/inventory?agency_code=USGS&site_no=12200500. Accessed January 2016.

U.S. Geological Survey (USGS), 2016c. Surface water data for USA: USGS Surface-Water Monthly Statistics for USGS 12200500 Skagit River Near Mount Vernon, WA. Available: http://waterdata.usgs.gov/nwis/monthly?. Accessed February 2016.

Vargo, S., P. Lutz, D. Odell, E. Van Vleep, and G. Bossart, 1986. Final Report: Study of Effects of Oil on Marine Turtles. Technical Report OCS Study MMS 86-0070. Vol. 2, 181 p.

Varhaar, H.J.M, C.J. VanLeeuwen, and J.L.M. Hermens, 1992. Classifying Environmental Pollutants, 1: Structure-activity Relationships for Prediction of Aquatic Toxicity. Chemosphere 25:471–491.

Varoujean, D.H., D.M. Baltz, B. Allen, D. Power, D.A. Schroeder, and K.M. Kempner, 1983. Seabird Oil Spill Behavior Study, Vol 1: Executive Summary, Volume 2: Technical Report, Volume 3: Appendices. Final Report to U.S. Dept. of the Interior, Minerals Management Service, Reston, VA, by Nero and Associates, Inc., Portland, OR, MMS QN TE 83 007, NTIS #PB84 17930, 365 p.

Washington State Department of Natural Resources (WA DNR), 2016. Nearshore Habitat Inventory. Available: http://www.dnr.wa.gov/programs-and-services/aquatics/aquatic-science/nearshore-habitat-inventory. Accessed January 2016.

Washington State Department of Ecology (WA DOE), 2014. Washington State Coastal Atlas. Available: https://fortress.wa.gov/ecy/coastalatlas/Default.aspx. Accessed January 2016.

Washington State Department of Ecology (W DOE), 2015. Padilla Bay: National Estuarine Research Reserve. http://www.padillabay.gov. Accessed December, 2015.

Washington State Department of Ecology (WA DOE), 2016. GIS Data: Ecology's Statewide Data Sets. Available: http://www.ecy.wa.gov/services/gis/data/data.htm. Accessed March 2016.

Washington State Department of Fish and Wildlife (WDFW), 2016. Conservation: Priority Habitats and Species. Available: http://wdfw.wa.gov/mapping/phs. Accessed March 2016.

Washington State Department of Health (WA DOH), 2016. Downloadable Data Sets. Available: http://www.doh.wa.gov/DataandStatisticalReports/DataSystems/GeographicInformationSystem/DownloadableDataSets. Accessed March 2016.

Wolfe, J.L. and R.J. Esher, 1981. Effects of Crude Oil on Swimming Behavior and Survival in the Rice Rat. Environmental Research 26: 486–489.

Youssef, M. and M.L. Spaulding, 1993. Drift current under the action of wind waves, Proceedings of the 16th Arctic and Marine Oil Spill Program Technical Seminar, Calgary, Alberta, Canada, pp. 587–615.

10 Appendix A: Overlay Analysis Resource Figures

The following figures represent the spatial extent of the resources investigated for the overlay analysis that was conducted in Section 7. Each figure corresponds to a different GIS data layer that was used in the analysis. Refer to Table 7-1 for each data layer and source. The name of each resource is embedded as a title within the legend for each figure. The hypothetical release locations are depicted on each map.

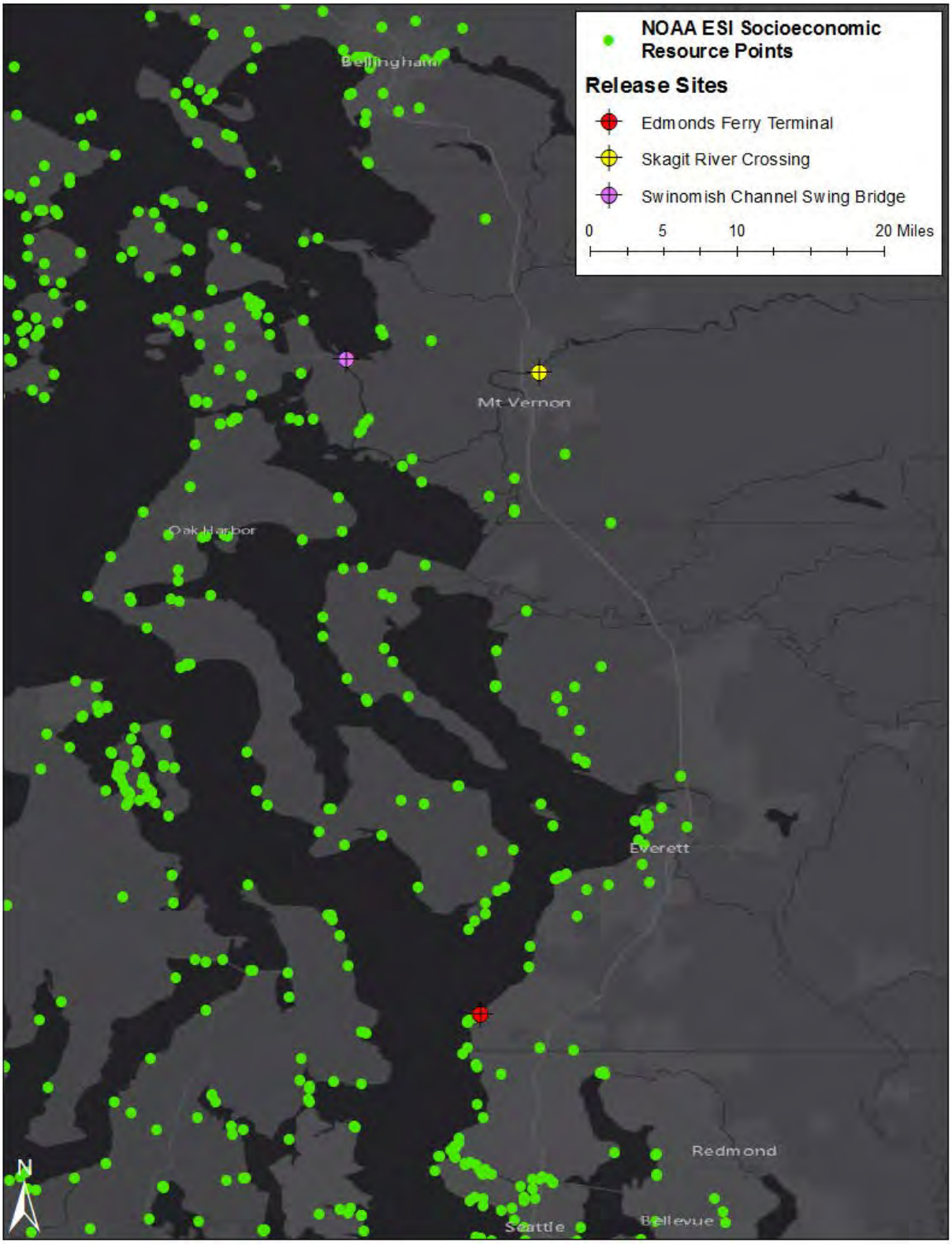
NOAA ESI Socioeconomic Resource Points
Release Sites
Edmonds Ferry Terminal
Skagit River Crossing
Swinomish Channel Swing Bridge
0
5
10
20 Miles
Bellingham
Mt Vernon
Oak Harbor
Everett
Redmond
Seattle
Bellevue
N

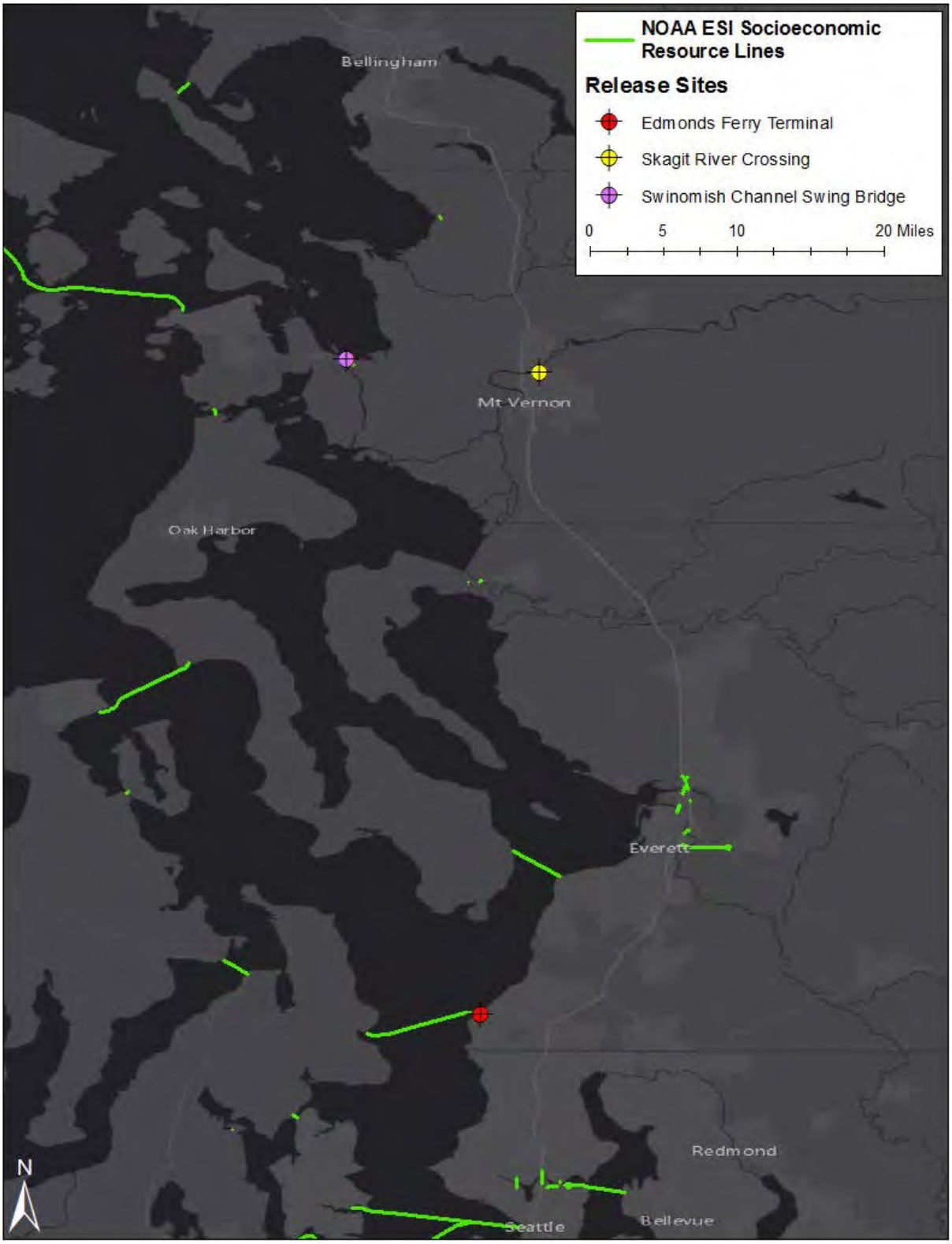
NOAA ESI Socioeconomic Resource Lines
Release Sites
Edmonds Ferry Terminal
Skagit River Crossing
Swinomish Channel Swing Bridge
0
5
10
20 Miles
Bellingham
Mt Vernon
Oak Harbor
Everett
Redmond
Seattle
Bellevue
N

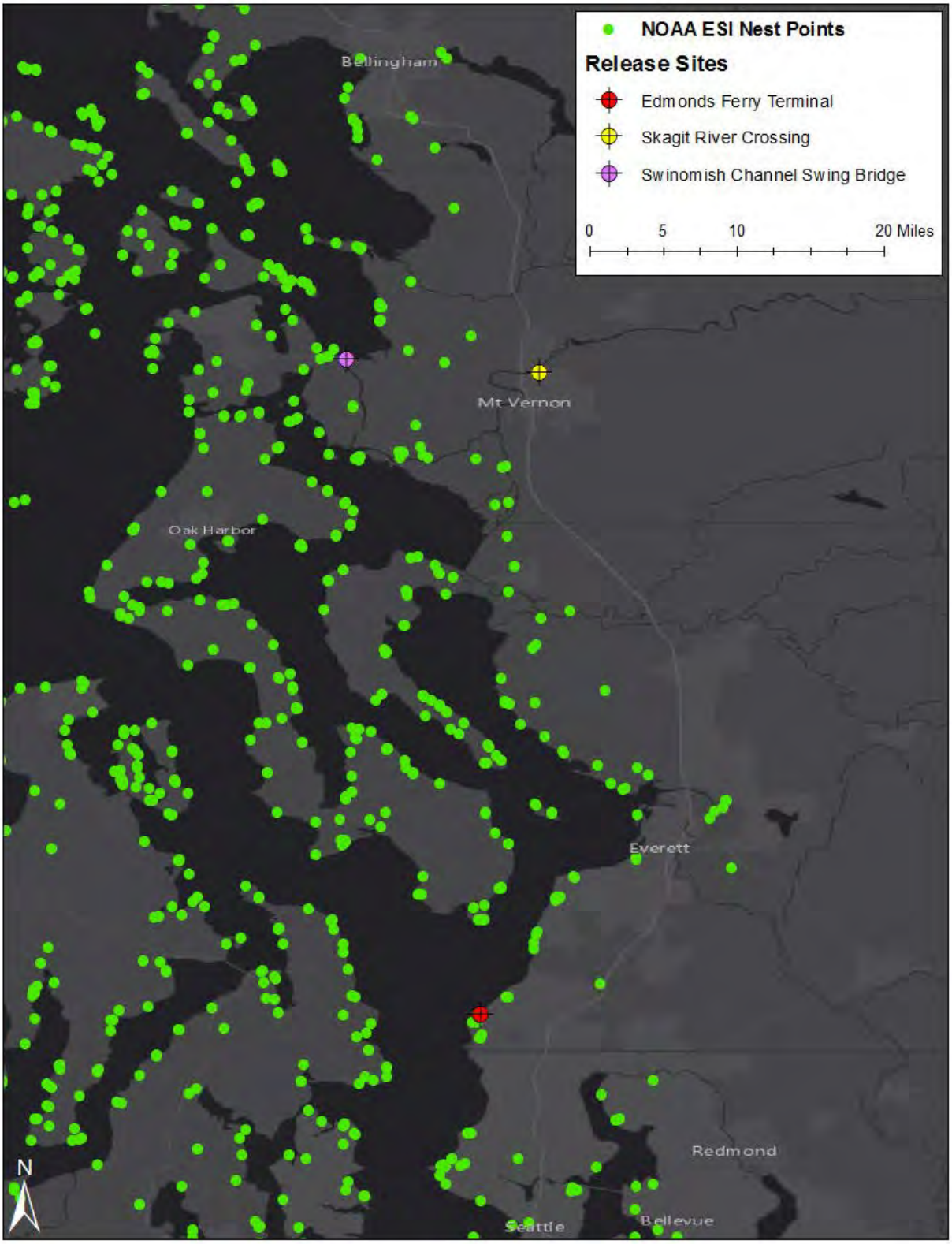
NOAA ESI Nest Points
Release Sites
Edmonds Ferry Terminal
Skagit River Crossing
Swinomish Channel Swing Bridge
0
5
10
20 Miles
Bellingham
Mt Vernon
Oak Harbor
Everett
Redmond
Seattle
Bellevue
N

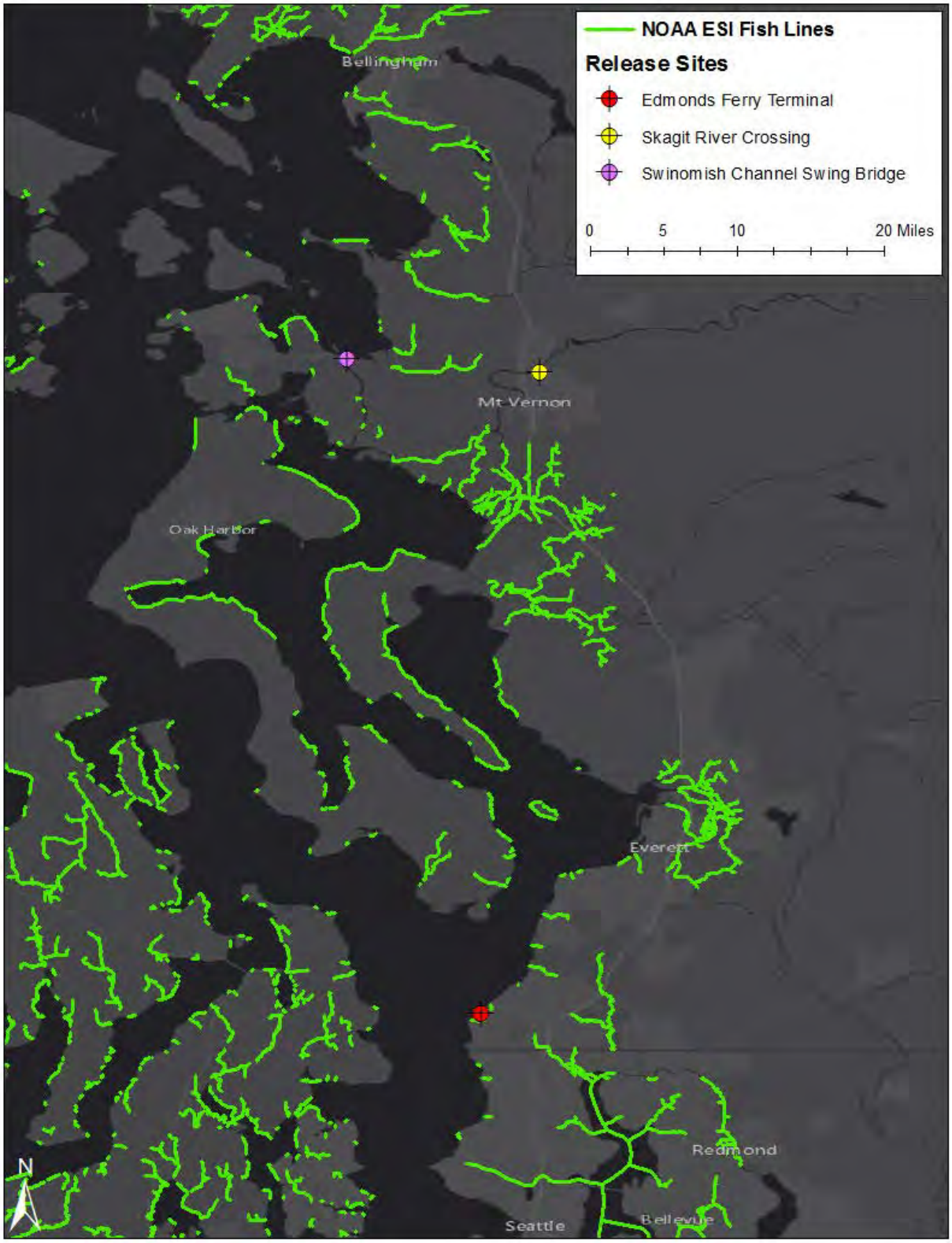
NOAA ESI Fish Lines
Release Sites
Edmonds Ferry Terminal
Skagit River Crossing
Swinomish Channel Swing Bridge
0
5
10
20 Miles
Bellingham
Mt Vernon
Oak Harbor
Everett
Redmond
Seattle
Bellevue
N

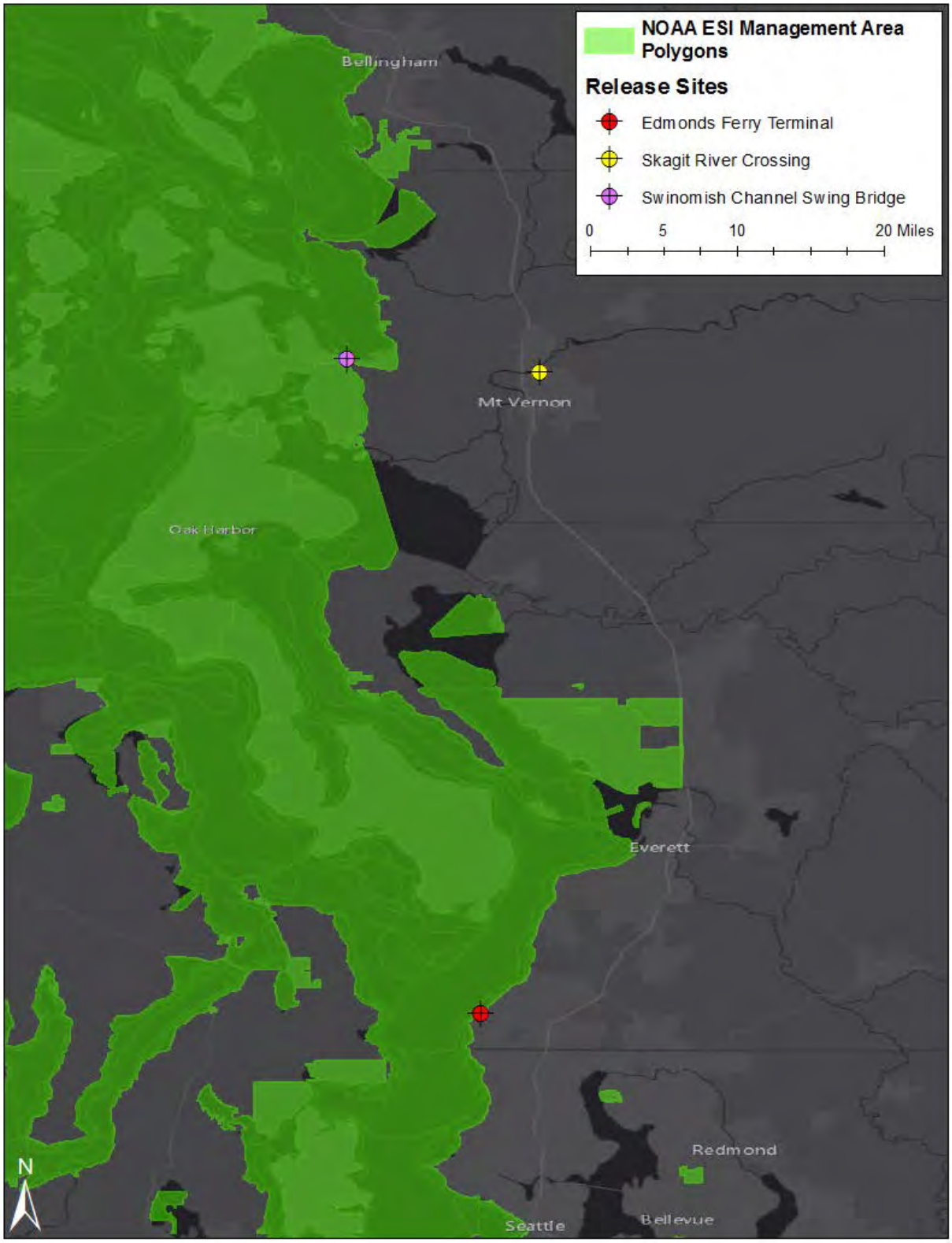
NOAA ESI Management Area Polygons
Release Sites
Edmonds Ferry Terminal
Skagit River Crossing
Swinomish Channel Swing Bridge
0
5
10
20 Miles
Bellingham
Mt Vernon
Oak Harbor
Everett
Redmond
Seattle
Bellevue
N

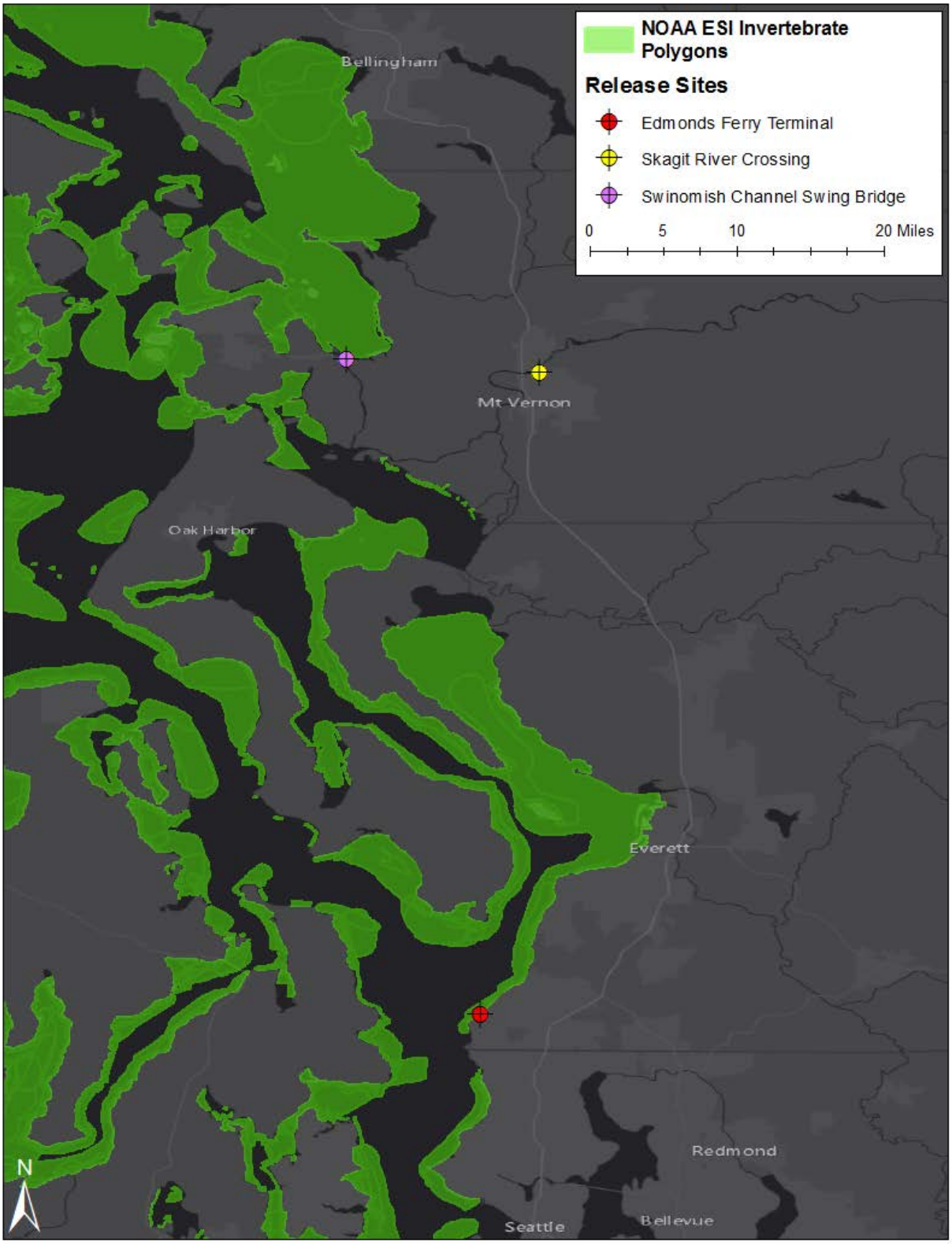
NOAA ESI Invertebrate Polygons
Release Sites
Edmonds Ferry Terminal
Skagit River Crossing
Swinomish Channel Swing Bridge
0
5
10
20 Miles
Bellingham
Mt Vernon
Oak Harbor
Everett
Redmond
Seattle
Bellevue
N

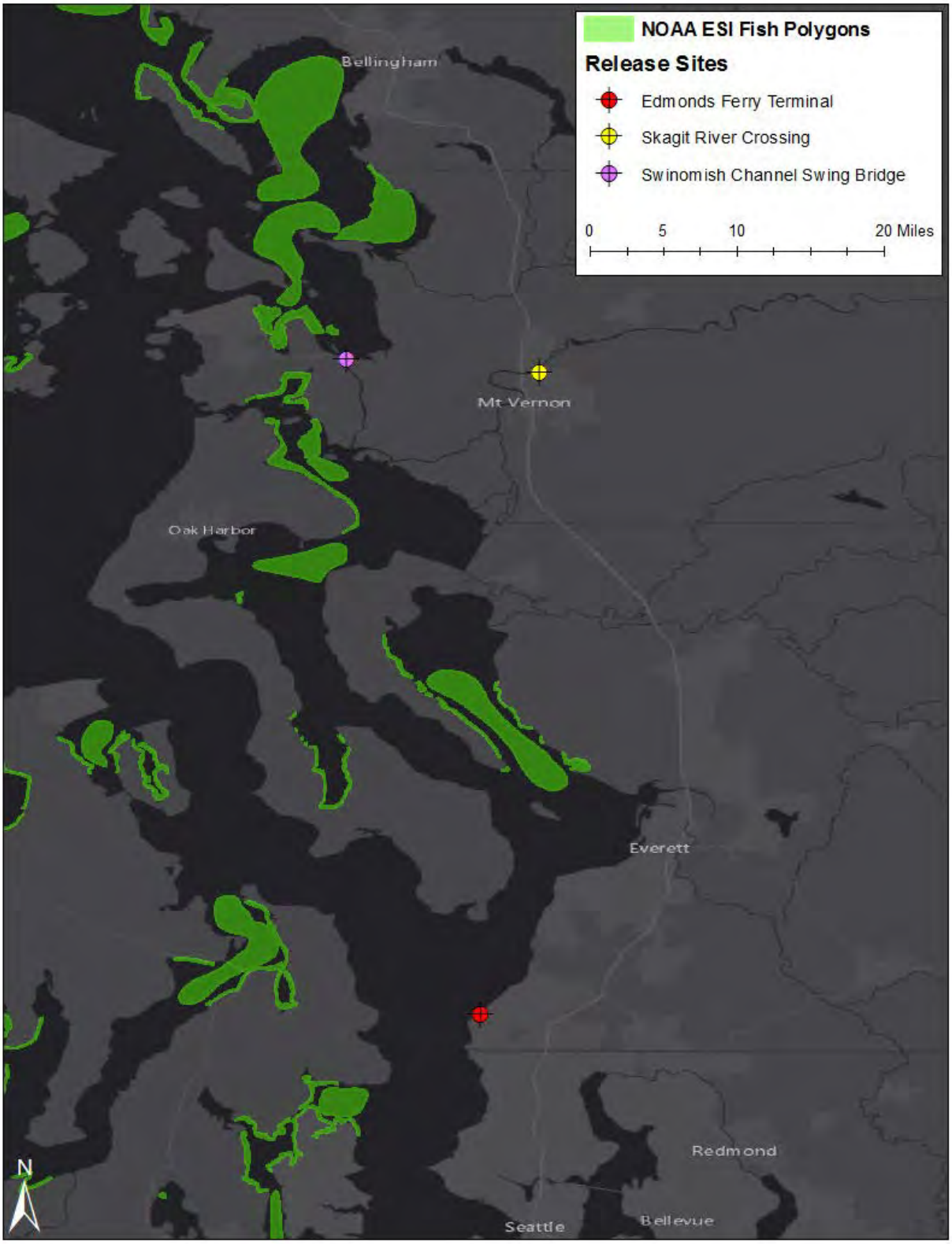
NOAA ESI Fish Polygons
Release Sites
Edmonds Ferry Terminal
Skagit River Crossing
Swinomish Channel Swing Bridge
0
5
10
20 Miles
Bellingham
Mt Vernon
Oak Harbor
Everett
Redmond
Seattle
Bellevue
N

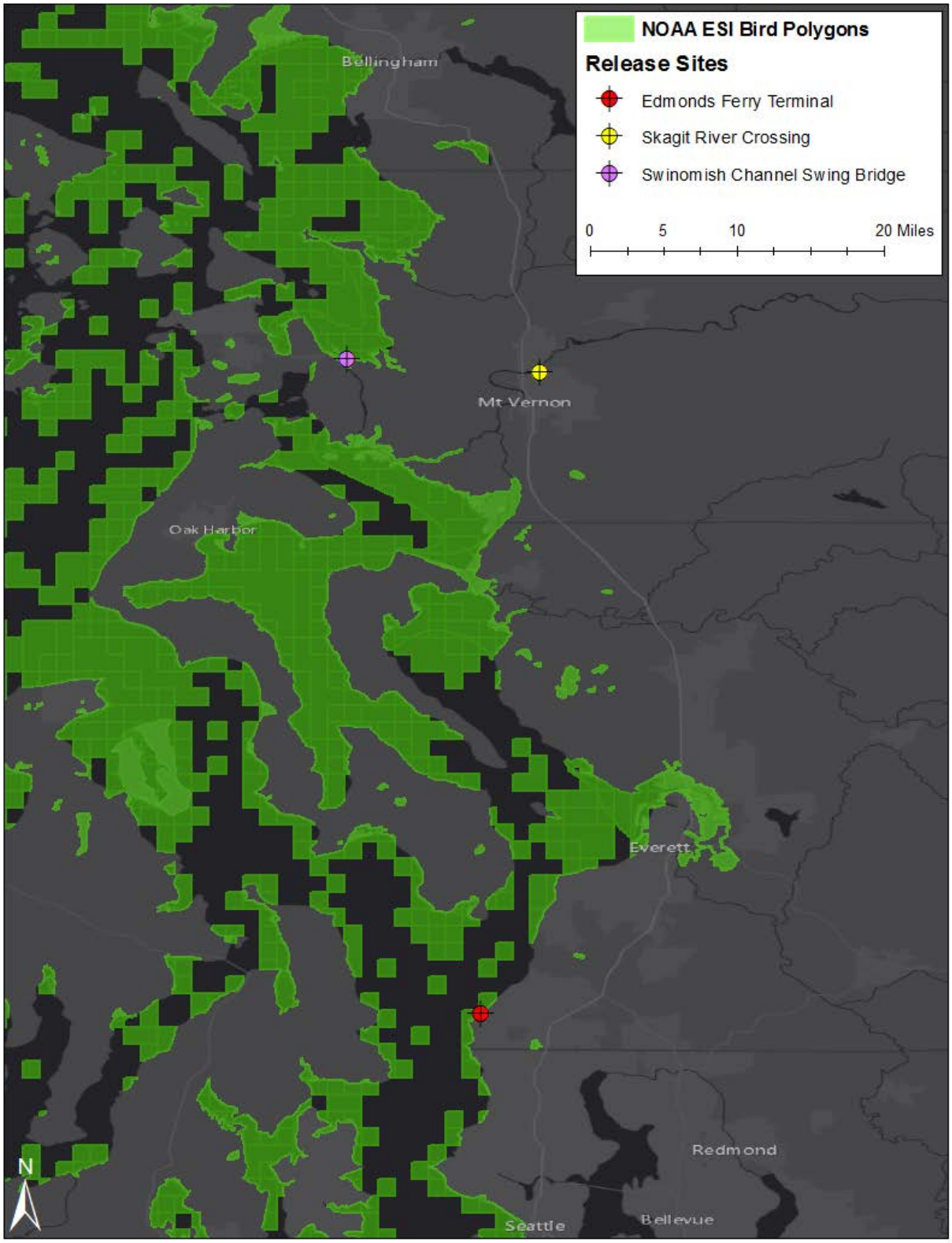
NOAA ESI Bird Polygons
Release Sites
Edmonds Ferry Terminal
Skagit River Crossing
Swinomish Channel Swing Bridge
0
5
10
20 Miles
Bellingham
Mt Vernon
Oak Harbor
Everett
Redmond
Seattle
Bellevue
N

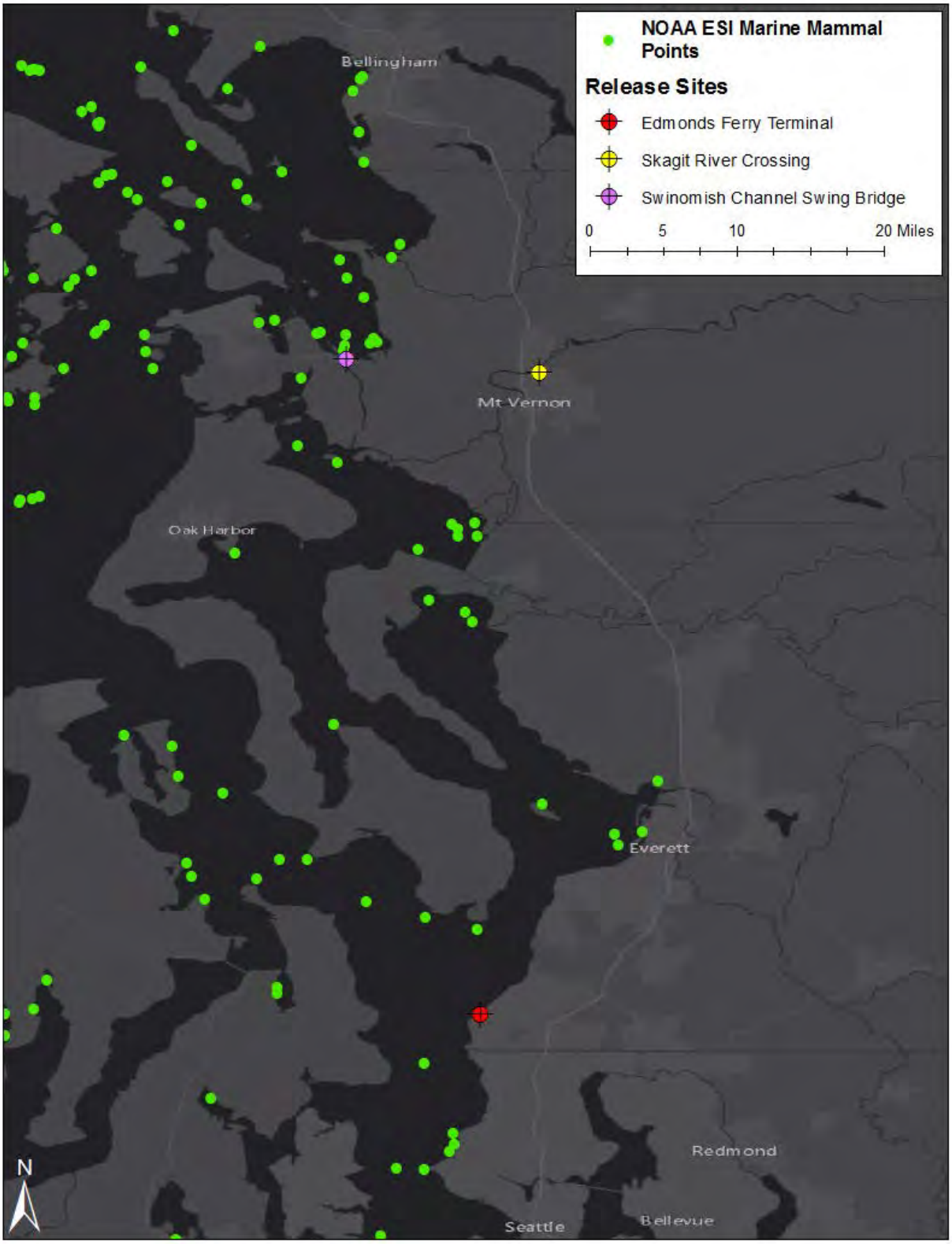
NOAA ESI Marine Mammal Points
Release Sites
Edmonds Ferry Terminal
Skagit River Crossing
Swinomish Channel Swing Bridge
0
5
10
20 Miles
Bellingham
Mt Vernon
Oak Harbor
Everett
Redmond
Seattle
Bellevue
N

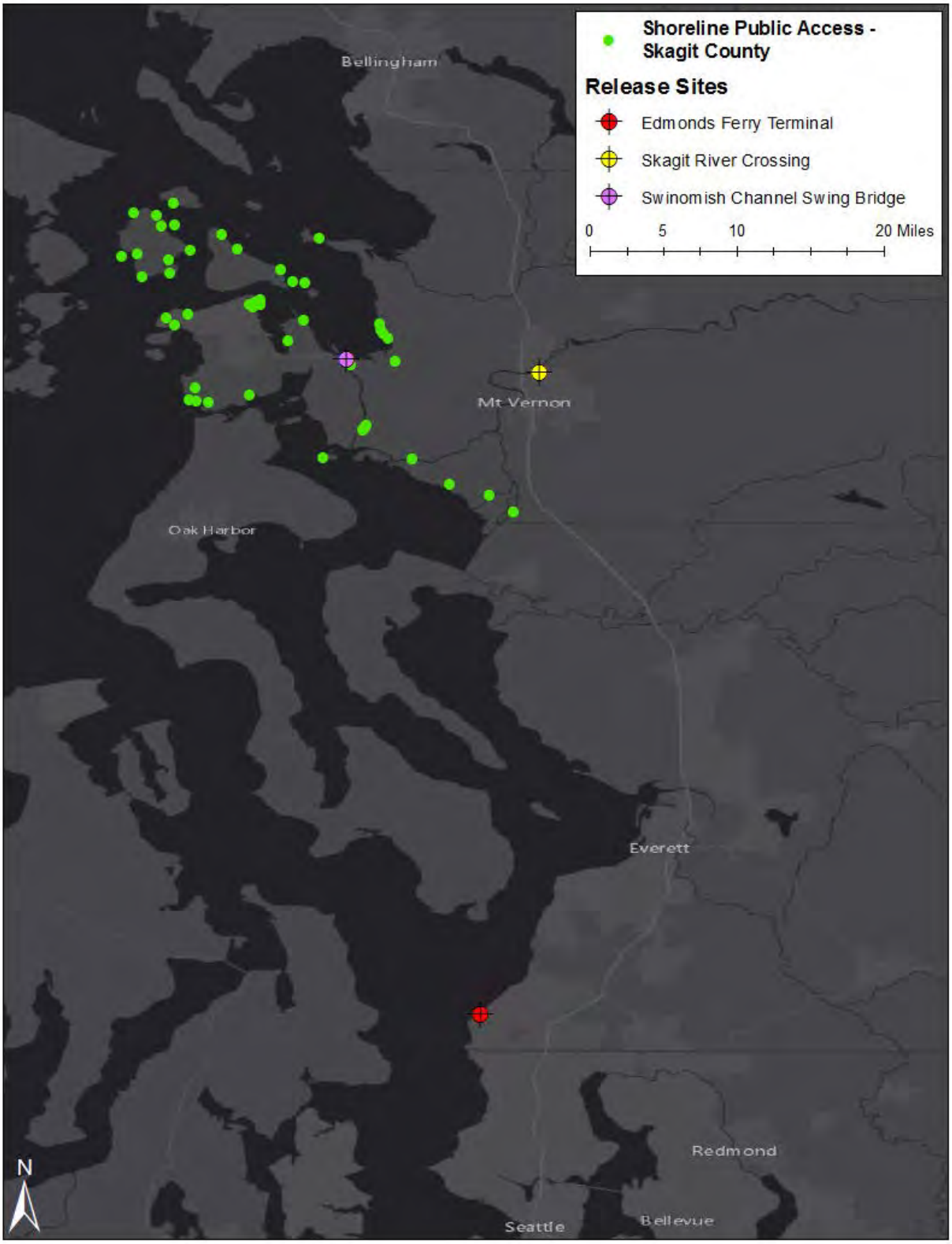
Shoreline Public Access - Skagit County
Release Sites
Edmonds Ferry Terminal
Skagit River Crossing
Swinomish Channel Swing Bridge
0
5
10
20 Miles
Bellingham
Mt Vernon
Oak Harbor
Everett
Redmond
Seattle
Bellevue
N

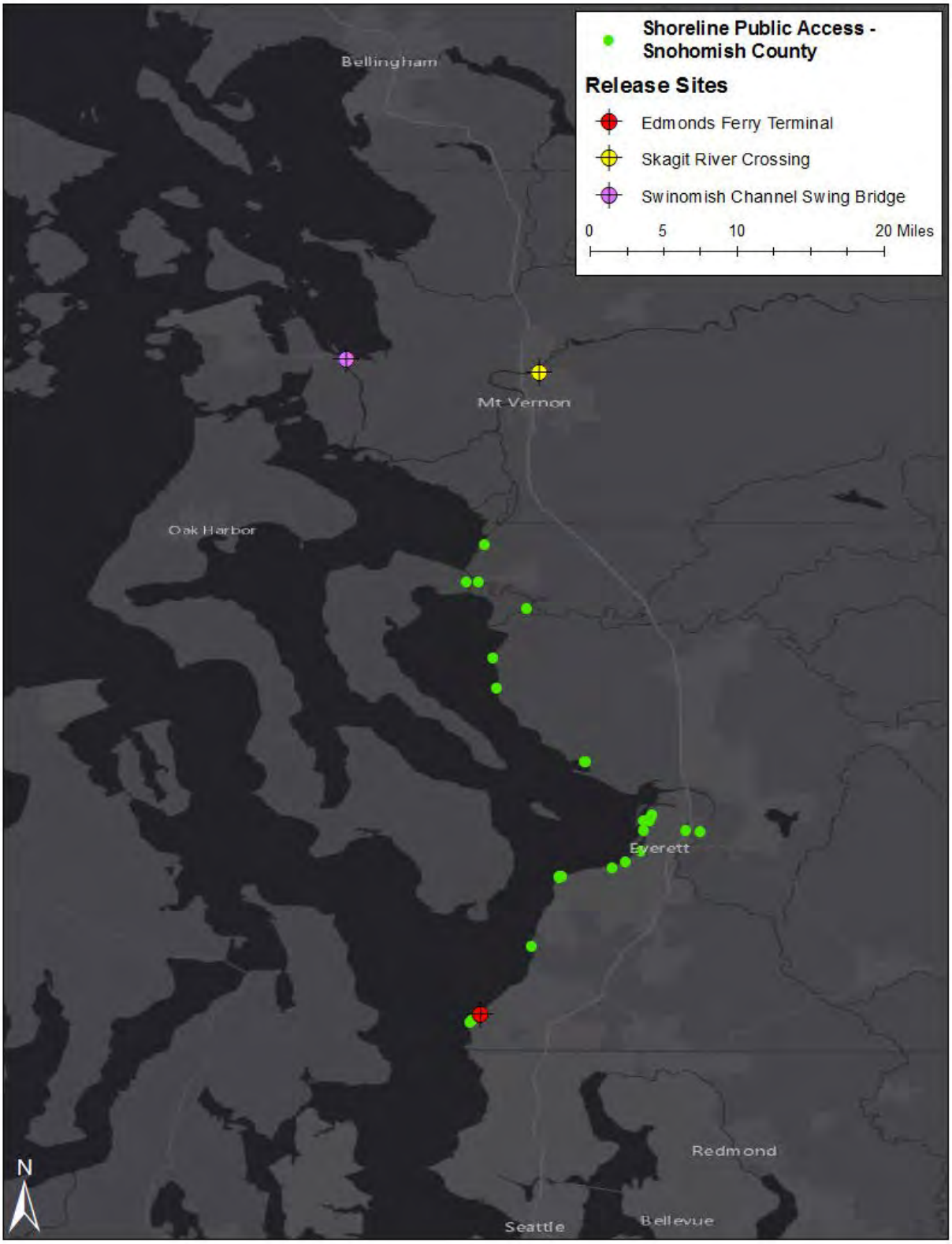
Shoreline Public Access - Snohomish County
Release Sites
Edmonds Ferry Terminal
Skagit River Crossing
Swinomish Channel Swing Bridge
0
5
10
20 Miles
Bellingham
Mt Vernon
Oak Harbor
Everett
Redmond
Seattle
Bellevue
N

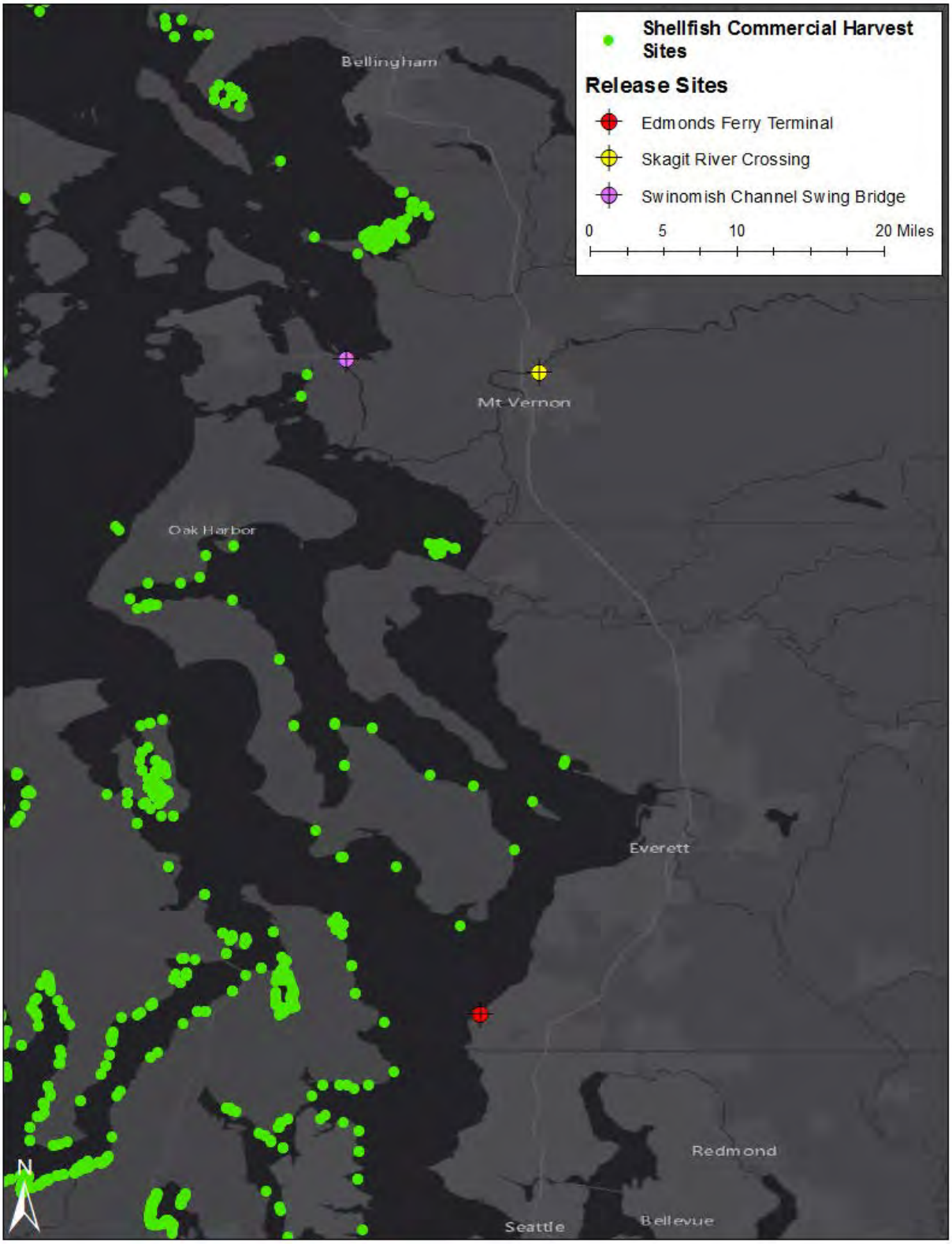
Shellfish Commercial Harvest Sites
Release Sites
Edmonds Ferry Terminal
Skagit River Crossing
Swinomish Channel Swing Bridge
0
5
10
20 Miles
Bellingham
Mt Vernon
Oak Harbor
Everett
Redmond
Seattle
Bellevue
N

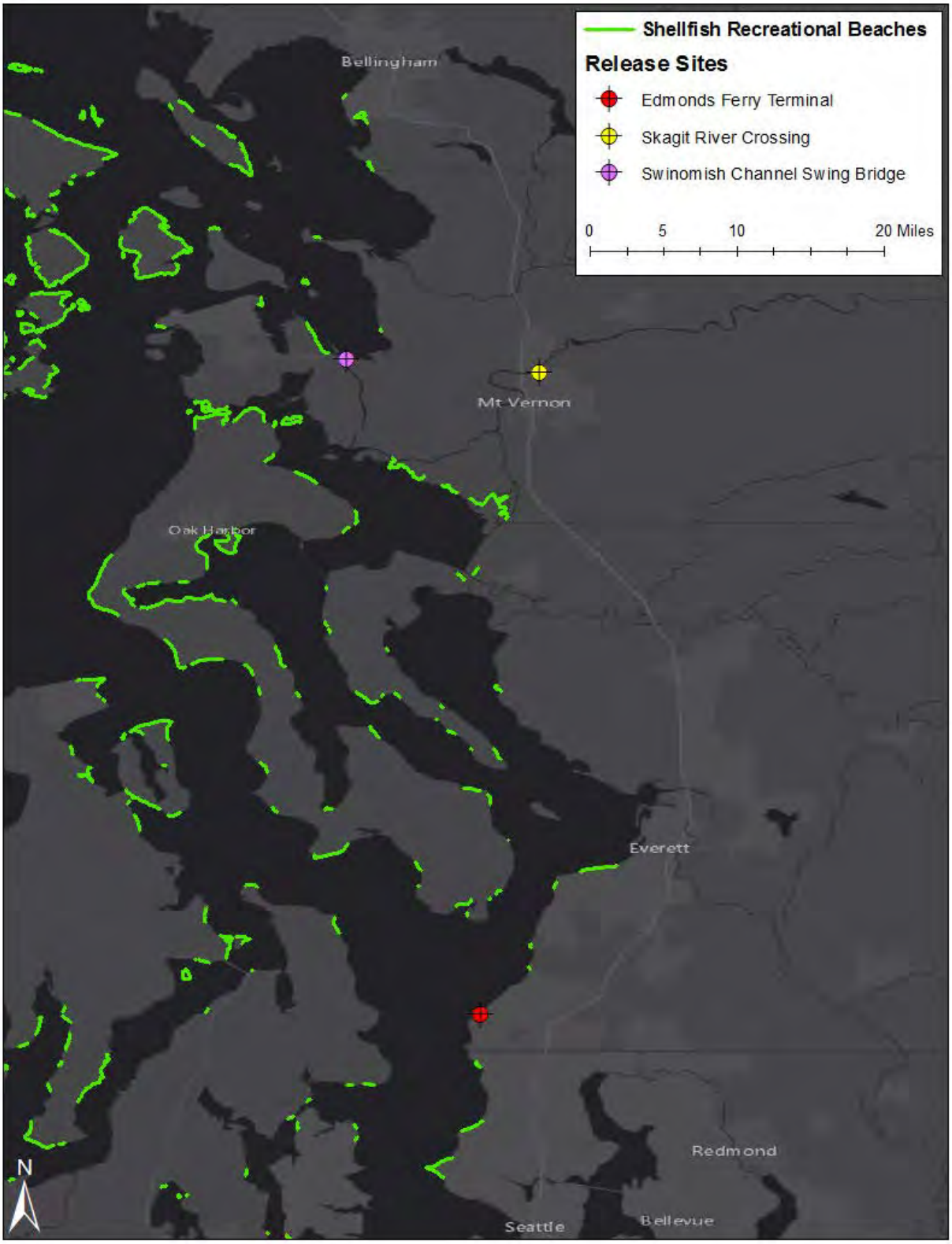
Shellfish Recreational Beaches
Release Sites
Edmonds Ferry Terminal
Skagit River Crossing
Swinomish Channel Swing Bridge
0
5
10
20 Miles
Bellingham
Mt Vernon
Oak Harbor
Everett
Redmond
Seattle
Bellevue
N

Tribal Lands
Release Sites
Edmonds Ferry Terminal
Skagit River Crossing
Swinomish Channel Swing Bridge
0
5
10
20 Miles
Bellingham
Mt Vernon
Oak Harbor
Everett
Redmond
Seattle
Bellevue
N

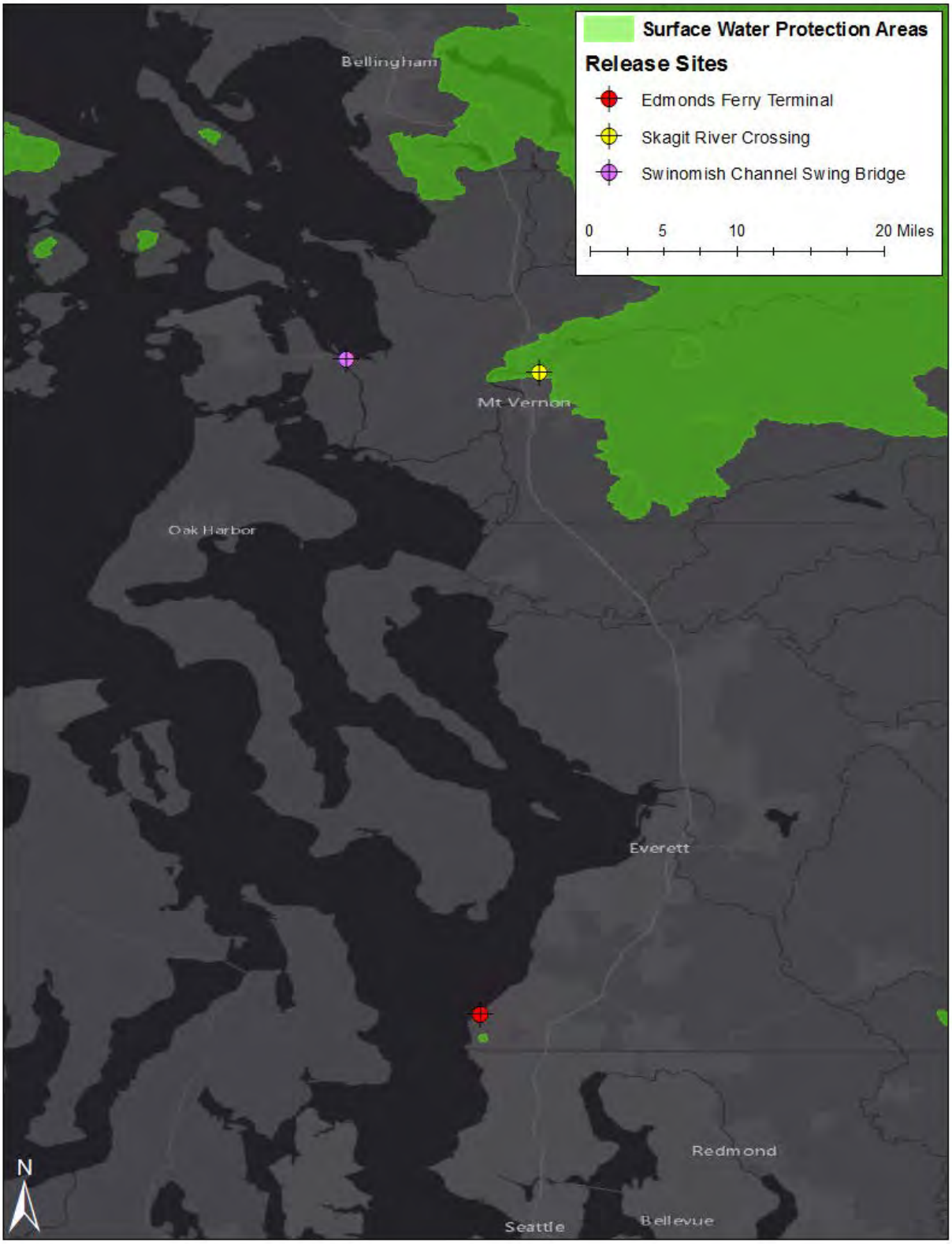
Surface Water Protection Areas
Release Sites
Edmonds Ferry Terminal
Skagit River Crossing
Swinomish Channel Swing Bridge
0
5
10
20 Miles
Bellingham
Mt Vernon
Oak Harbor
Everett
Redmond
Seattle
Bellevue
N

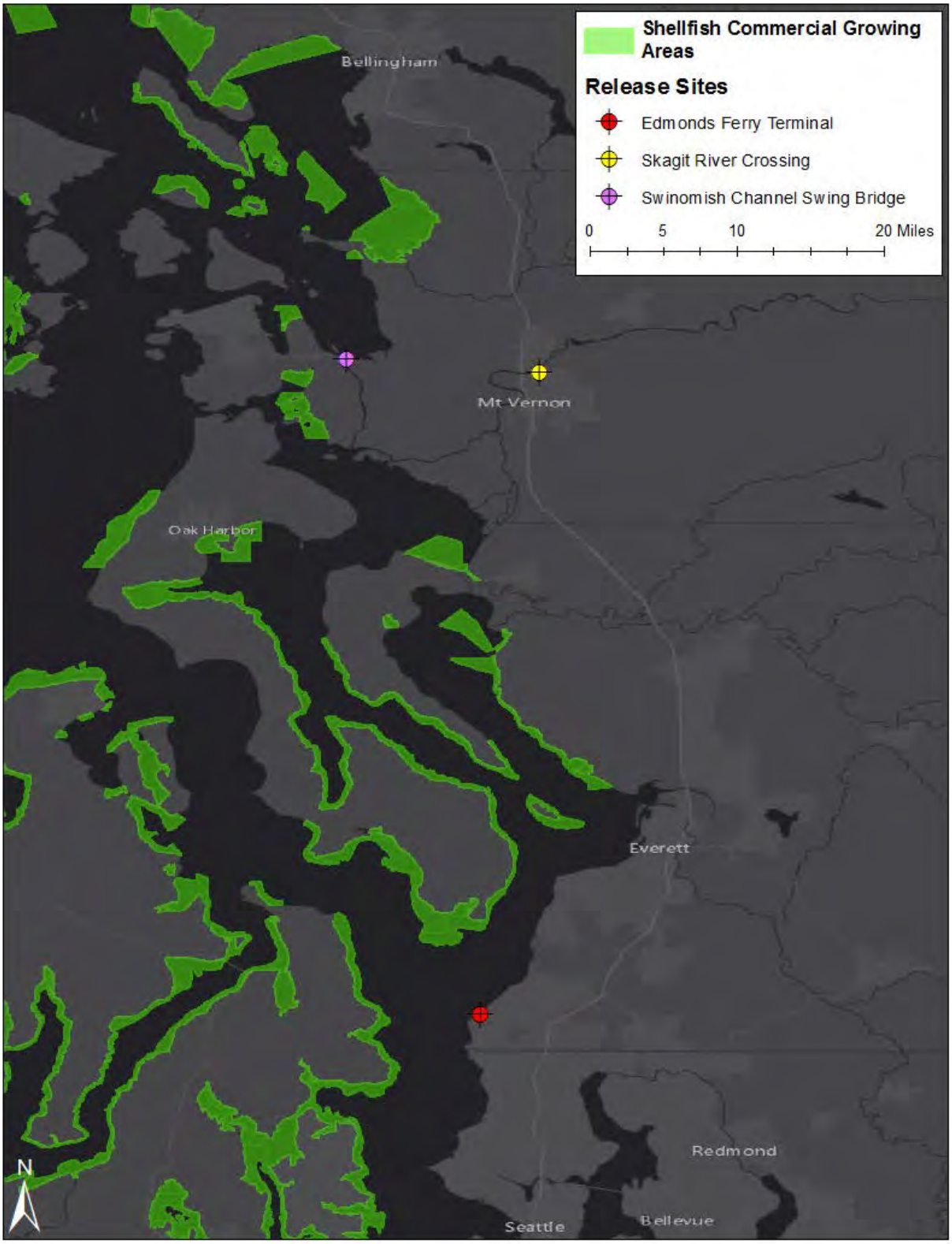
Shellfish Commercial Growing Areas
Release Sites
Edmonds Ferry Terminal
Skagit River Crossing
Swinomish Channel Swing Bridge
0
5
10
20 Miles
Bellingham
Mt Vernon
Oak Harbor
Everett
Redmond
Seattle
Bellevue
N

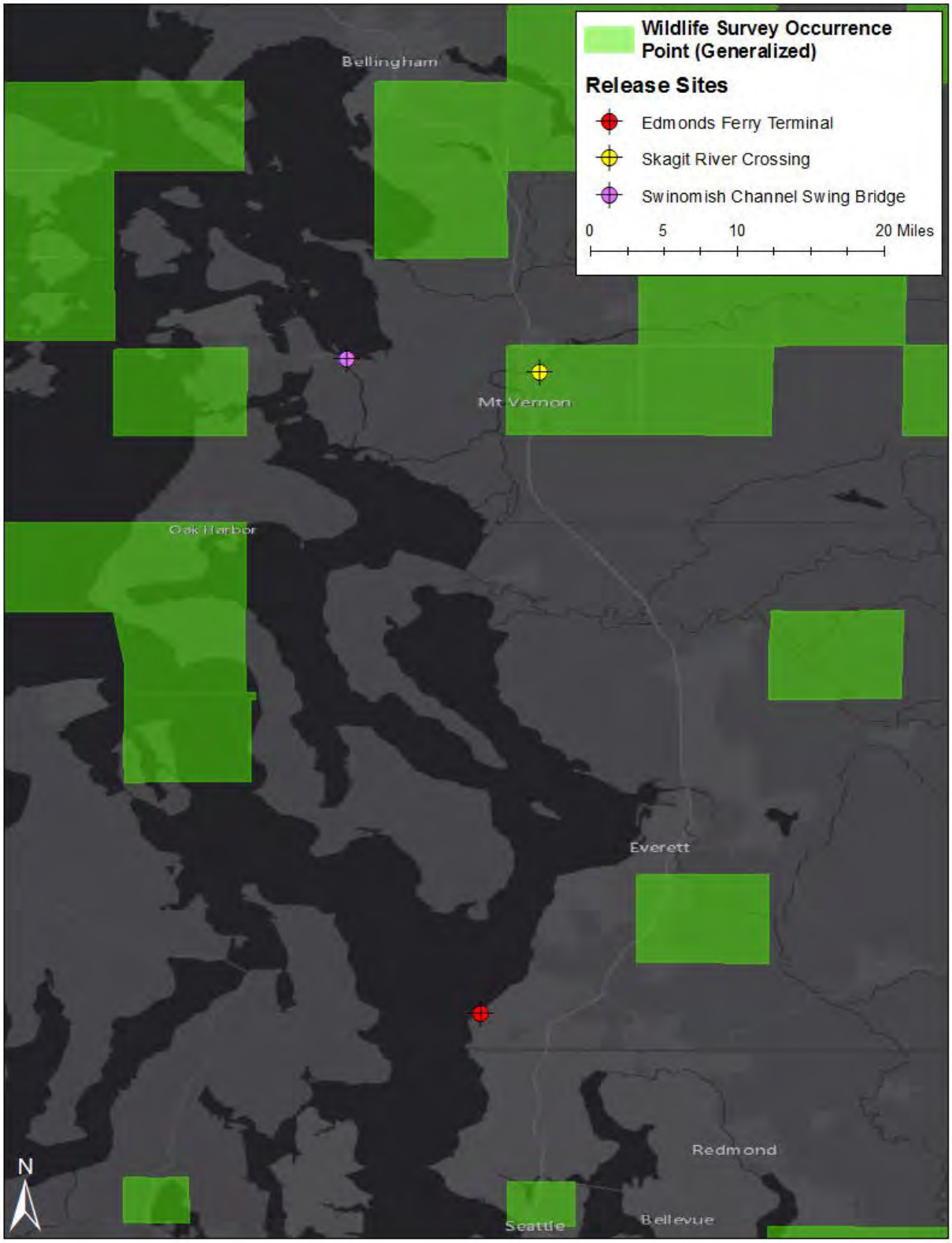
Wildlife Survey Occurrence Point (Generalized)
Release Sites
Edmonds Ferry Terminal
Skagit River Crossing
Swinomish Channel Swing Bridge
0
5
10
20 Miles
Bellingham
Mt Vernon
Oak Harbor
Everett
Redmond
Seattle
Bellevue
N

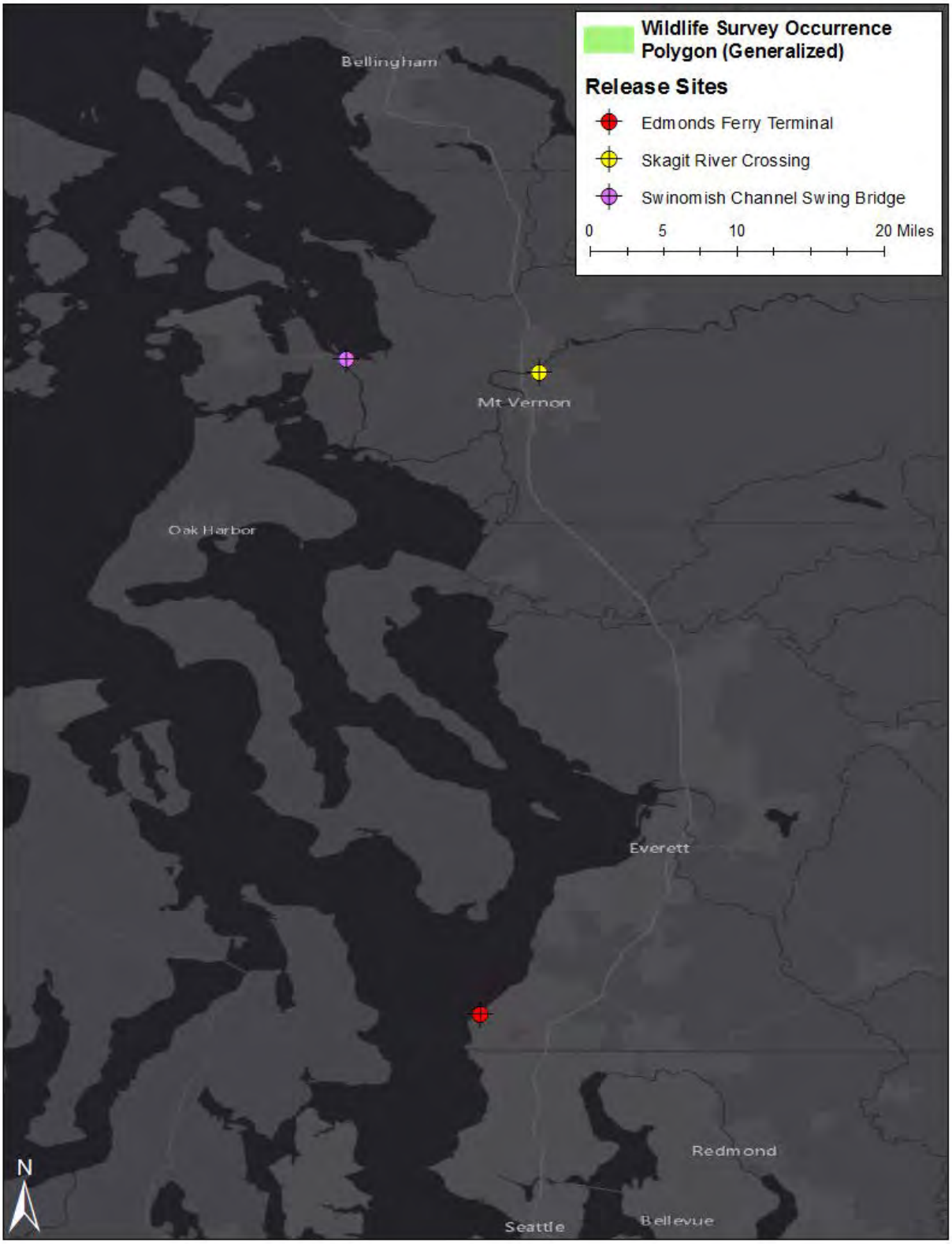
Wildlife Survey Occurrence Polygon (Generalized)
Release Sites
Edmonds Ferry Terminal
Skagit River Crossing
Swinomish Channel Swing Bridge
0
5
10
20 Miles
Bellingham
Mt Vernon
Oak Harbor
Everett
Redmond
Seattle
Bellevue
N

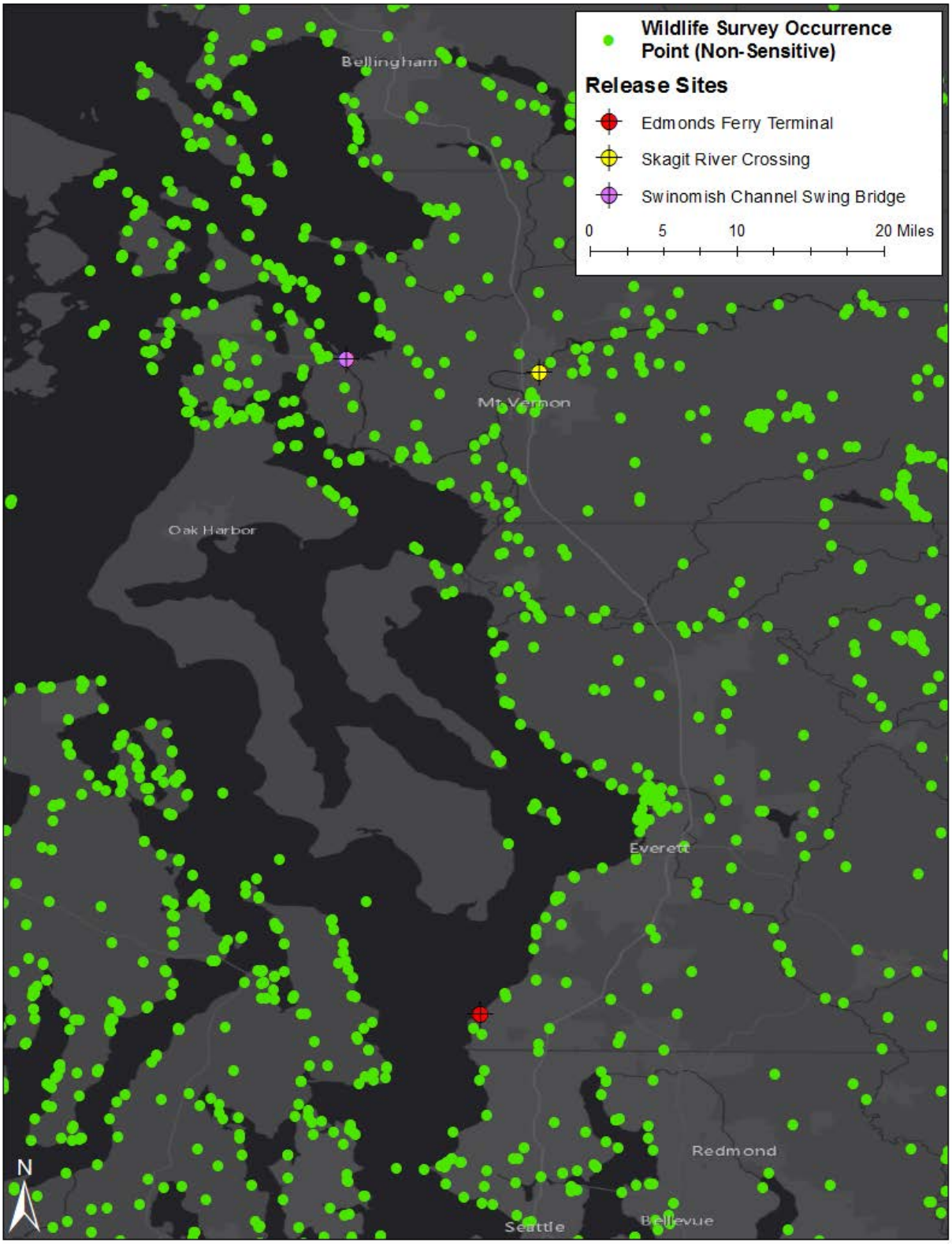
Wildlife Survey Occurrence Point (Non-Sensitive)
Release Sites
Edmonds Ferry Terminal
Skagit River Crossing
Swinomish Channel Swing Bridge
0
5
10
20 Miles
Bellingham
Mt Vernon
Oak Harbor
Everett
Redmond
Seattle
Bellevue
N

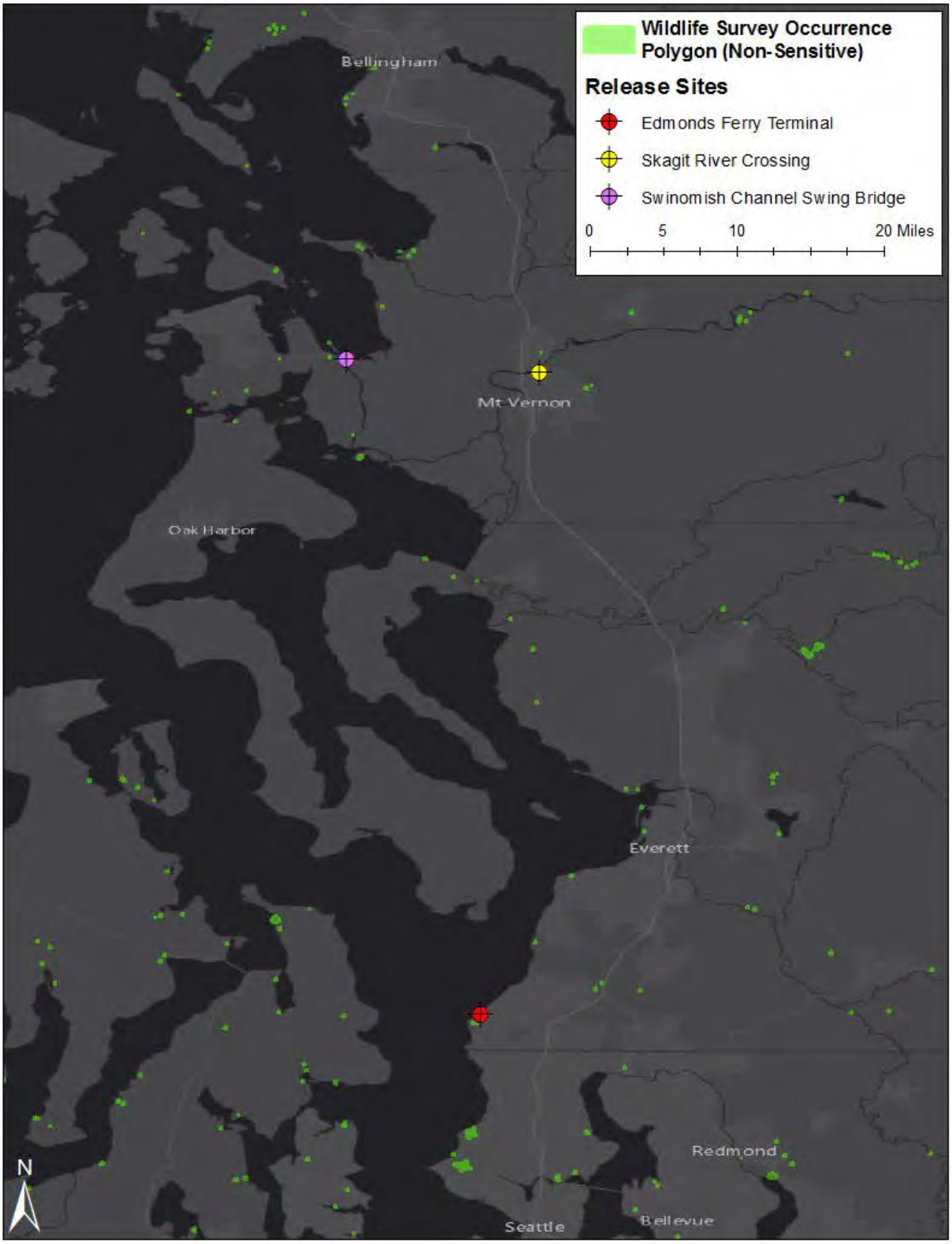
Wildlife Survey Occurrence Polygon (Non-Sensitive)
Release Sites
Edmonds Ferry Terminal
Skagit River Crossing
Swinomish Channel Swing Bridge
0
5
10
20 Miles
Bellingham
Mt Vernon
Oak Harbor
Everett
Redmond
Seattle
Bellevue
N

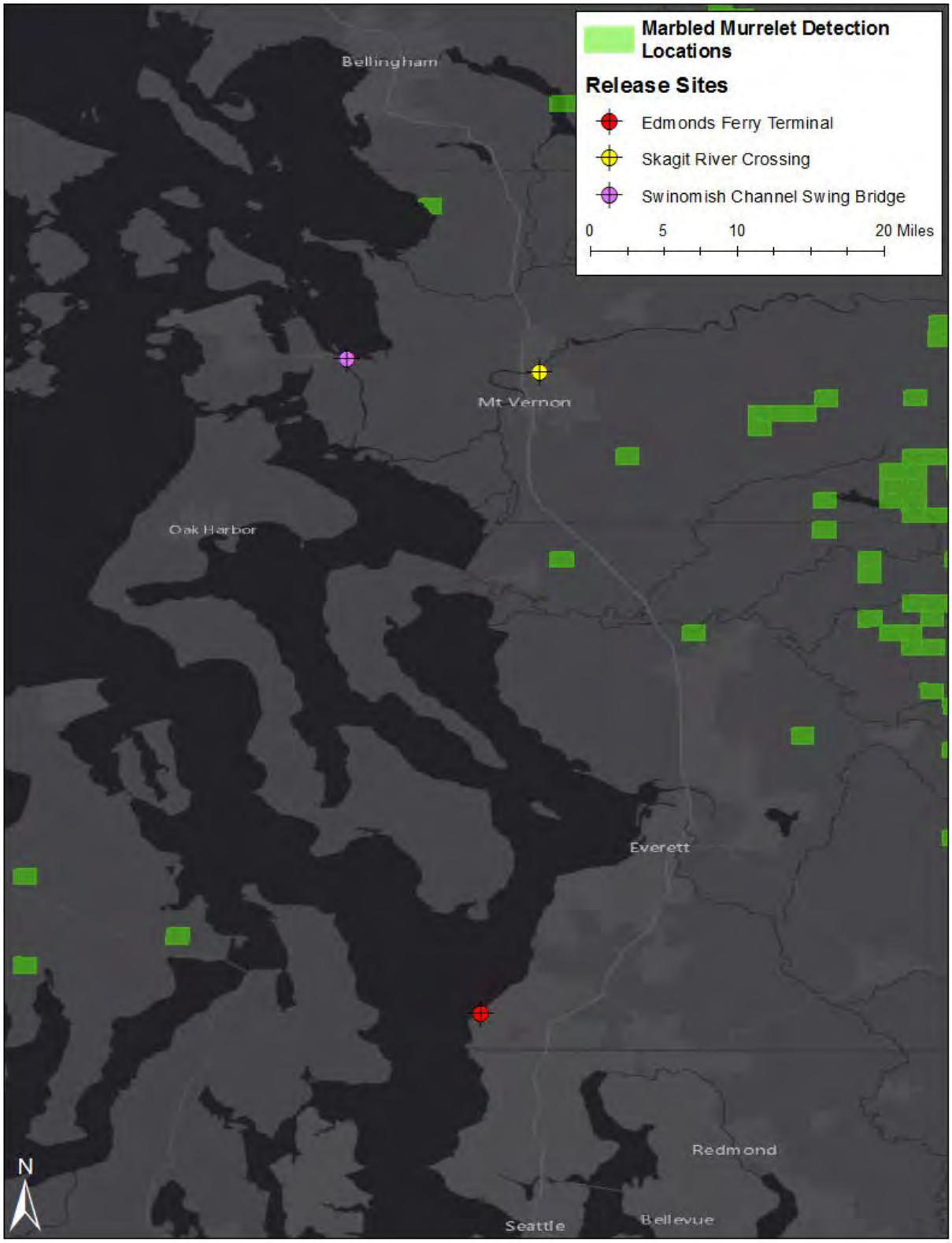
Marbled Murrelet Detection Locations
Release Sites
Edmonds Ferry Terminal
Skagit River Crossing
Swinomish Channel Swing Bridge
0
5
10
20 Miles
Bellingham
Mt Vernon
Oak Harbor
Everett
Redmond
Seattle
Bellevue
N

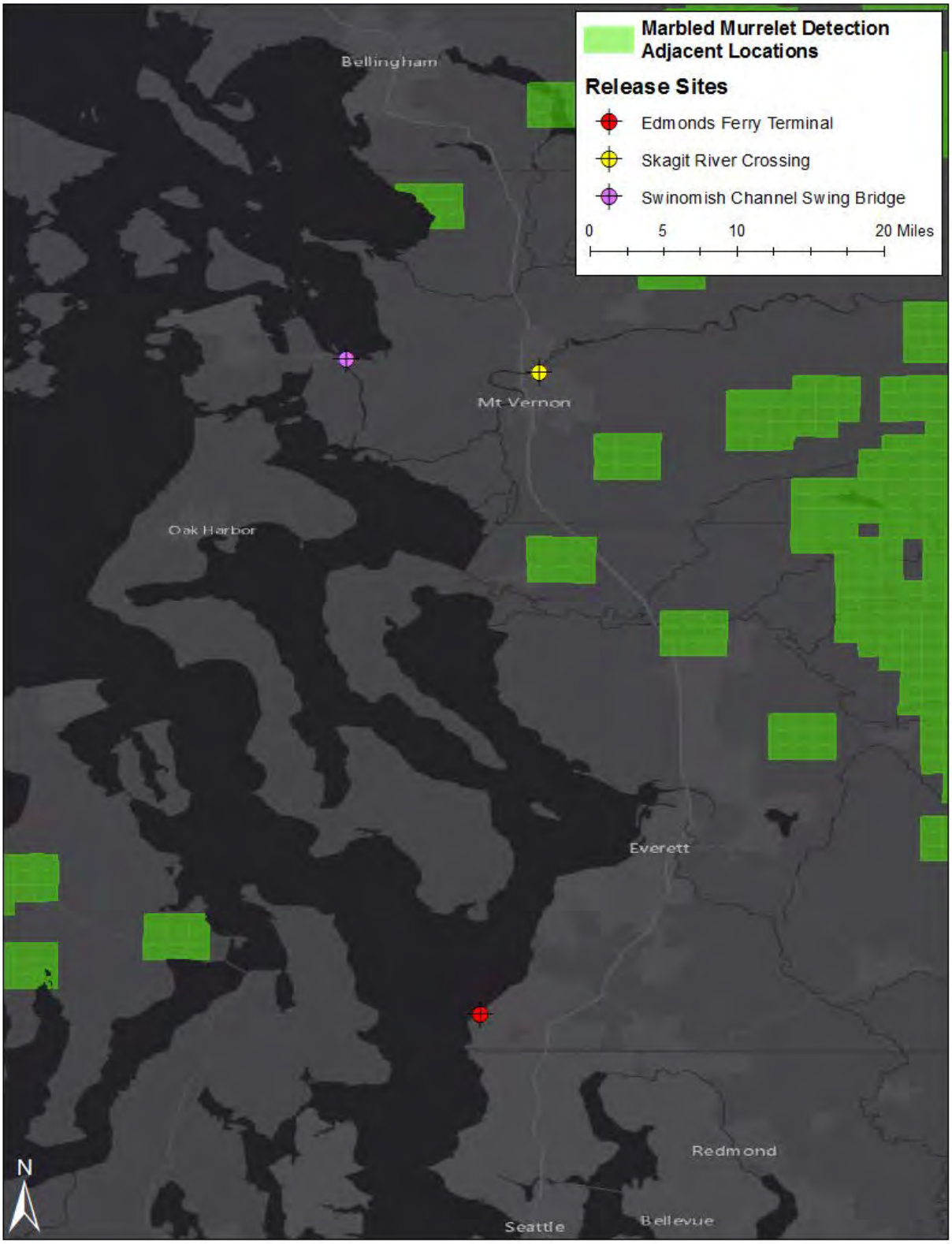
Marbled Murrelet Detection Adjacent Locations
Release Sites
Edmonds Ferry Terminal
Skagit River Crossing
Swinomish Channel Swing Bridge
0
5
10
20 Miles
Bellingham
Mt Vernon
Oak Harbor
Everett
Redmond
Seattle
Bellevue
N

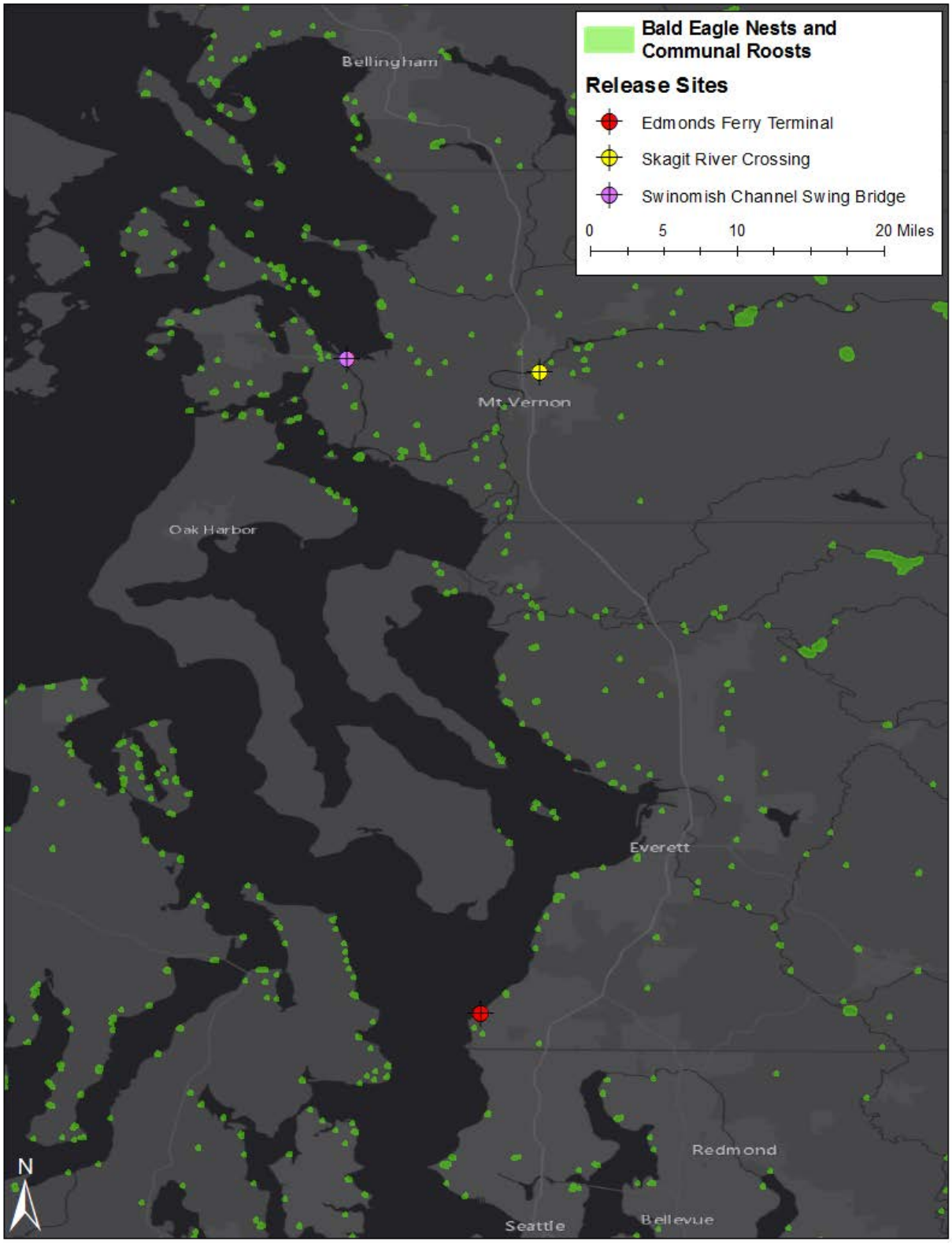
Bald Eagle Nests and Communal Roosts
Release Sites
Edmonds Ferry Terminal
Skagit River Crossing
Swinomish Channel Swing Bridge
0
5
10
20 Miles
Bellingham
Mt Vernon
Oak Harbor
Everett
Redmond
Seattle
Bellevue
N

Spotted Owl Sites
Release Sites
Edmonds Ferry Terminal
Skagit River Crossing
Swinomish Channel Swing Bridge
0
5
10
20 Miles
Bellingham
Mt Vernon
Oak Harbor
Everett
Redmond
Seattle
Bellevue
N

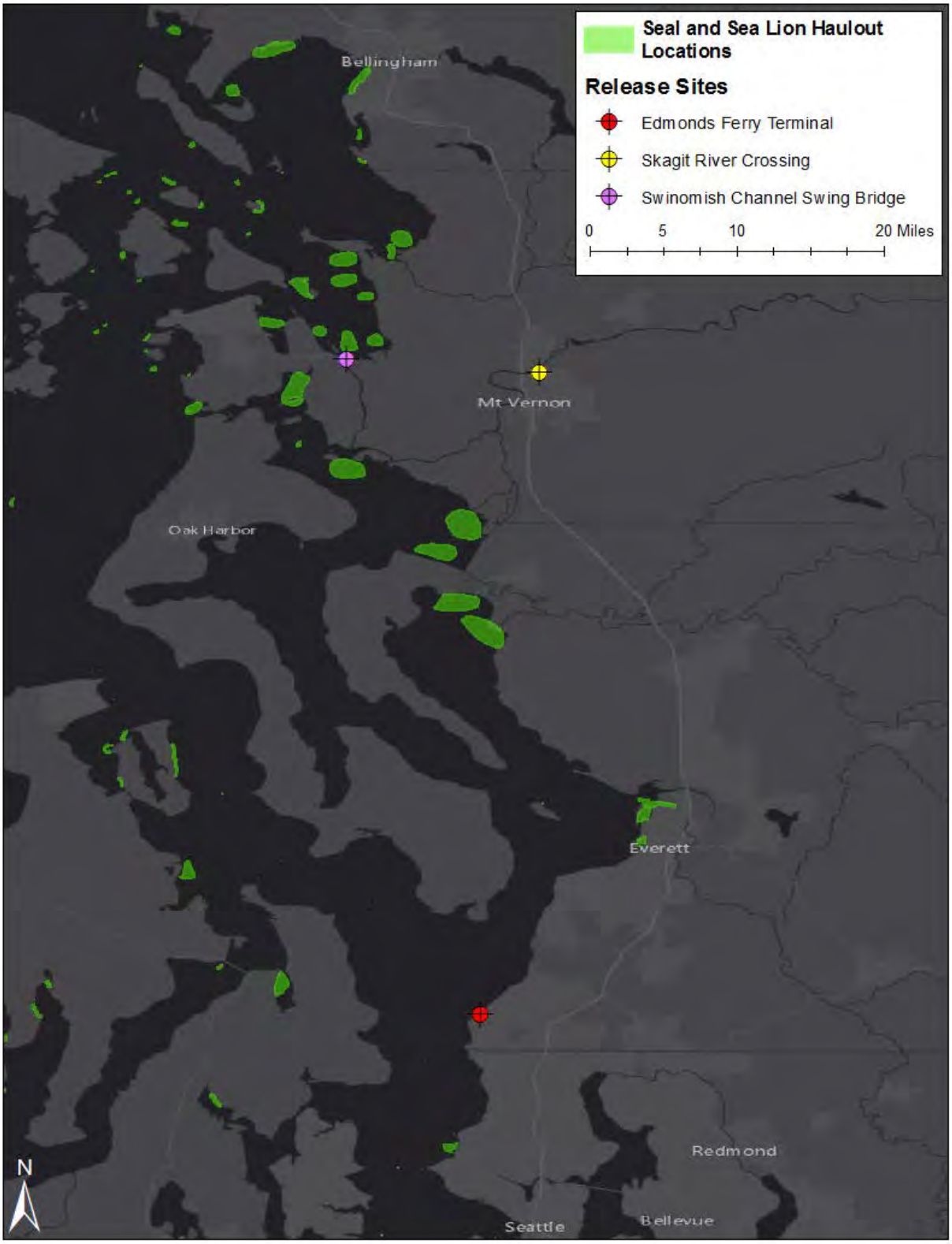
Seal and Sea Lion Haulout Locations
Release Sites
Edmonds Ferry Terminal
Skagit River Crossing
Swinomish Channel Swing Bridge
0
5
10
20 Miles
Bellingham
Mt Vernon
Oak Harbor
Everett
Redmond
Seattle
Bellevue
N

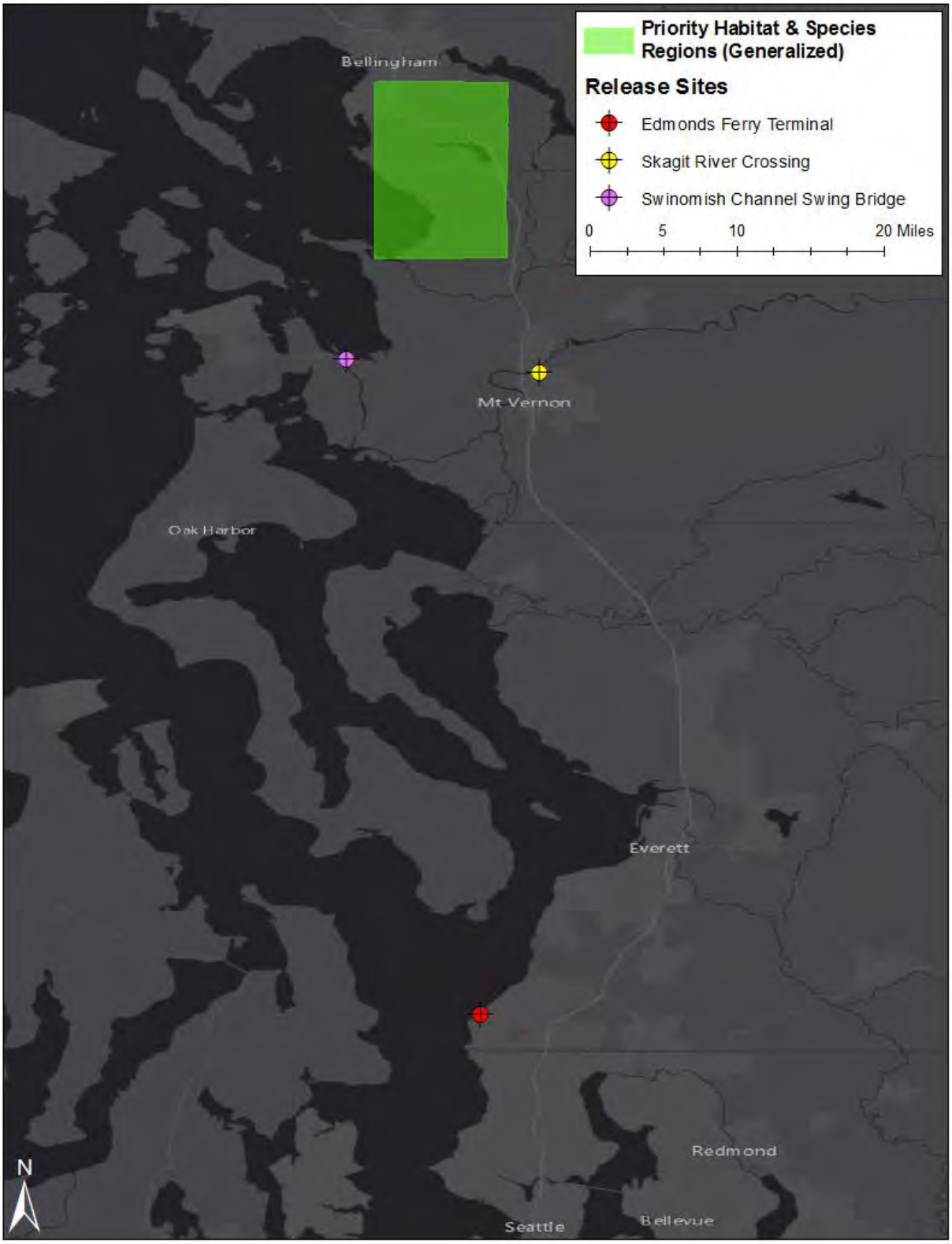
Priority Habitat & Species Regions (Generalized)
Release Sites
Edmonds Ferry Terminal
Skagit River Crossing
Swinomish Channel Swing Bridge
0
5
10
20 Miles
Bellingham
Mt Vernon
Oak Harbor
Everett
Redmond
Seattle
Bellevue
N

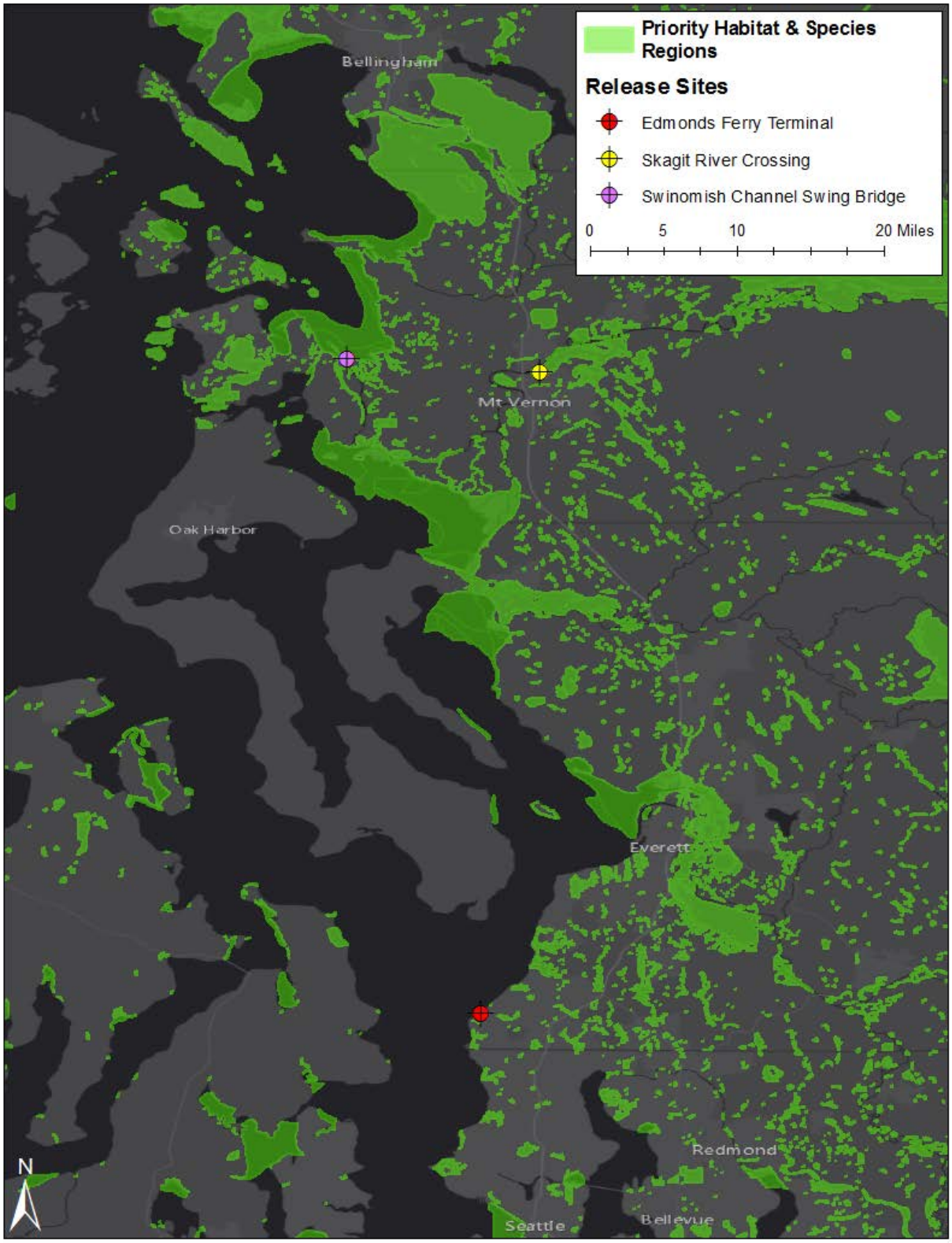
Priority Habitat & Species Regions
Release Sites
Edmonds Ferry Terminal
Skagit River Crossing
Swinomish Channel Swing Bridge
0
5
10
20 Miles
Bellingham
Mt Vernon
Oak Harbor
Everett
Redmond
Seattle
Bellevue
N

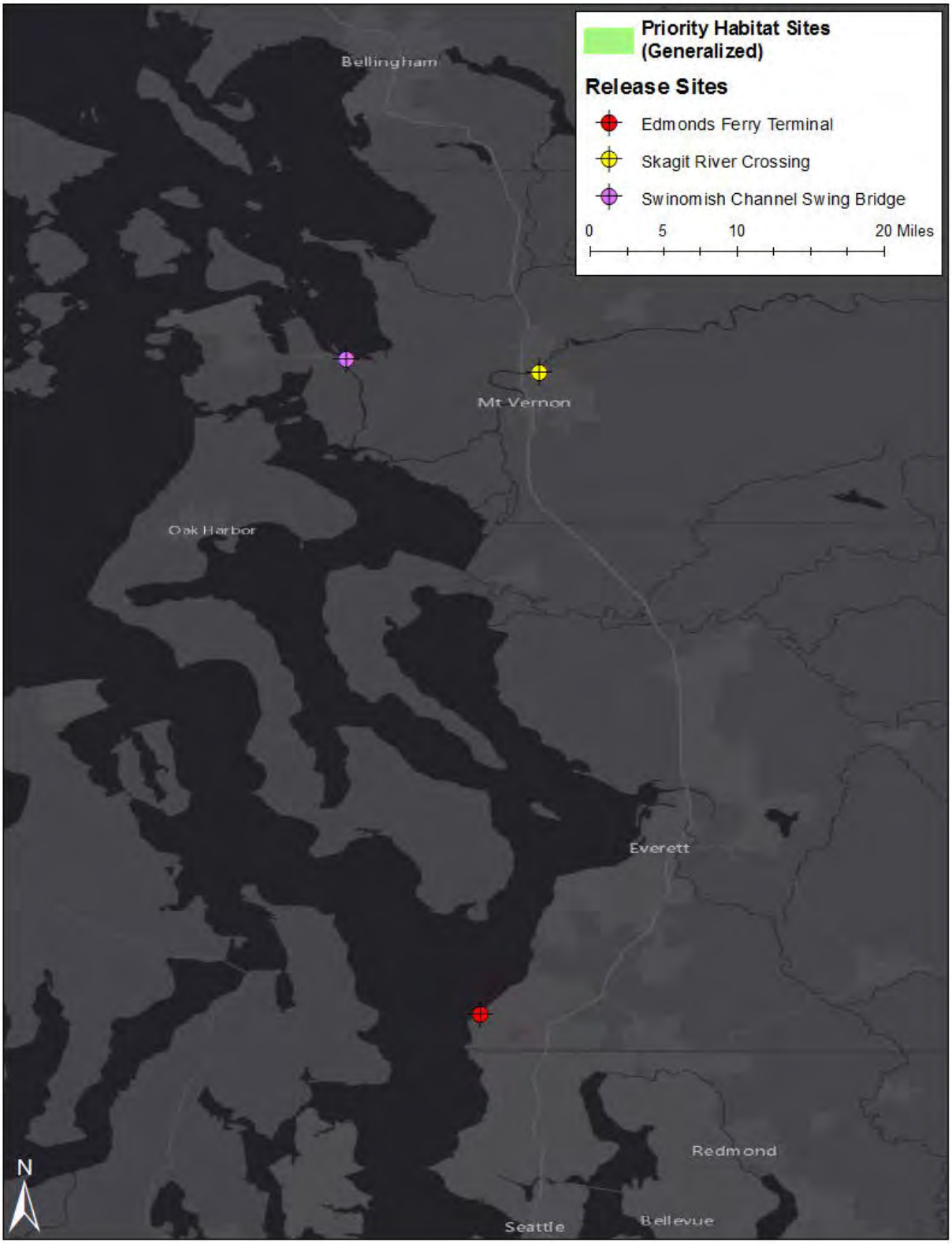
Priority Habitat Sites (Generalized)
Release Sites
Edmonds Ferry Terminal
Skagit River Crossing
Swinomish Channel Swing Bridge
0
5
10
20 Miles
Bellingham
Mt Vernon
Oak Harbor
Everett
Redmond
Seattle
Bellevue
N

Priority Habitat Sites
Release Sites
Edmonds Ferry Terminal
Skagit River Crossing
Swinomish Channel Swing Bridge
0
5
10
20 Miles
Bellingham
Mt Vernon
Oak Harbor
Everett
Redmond
Seattle
Bellevue
N

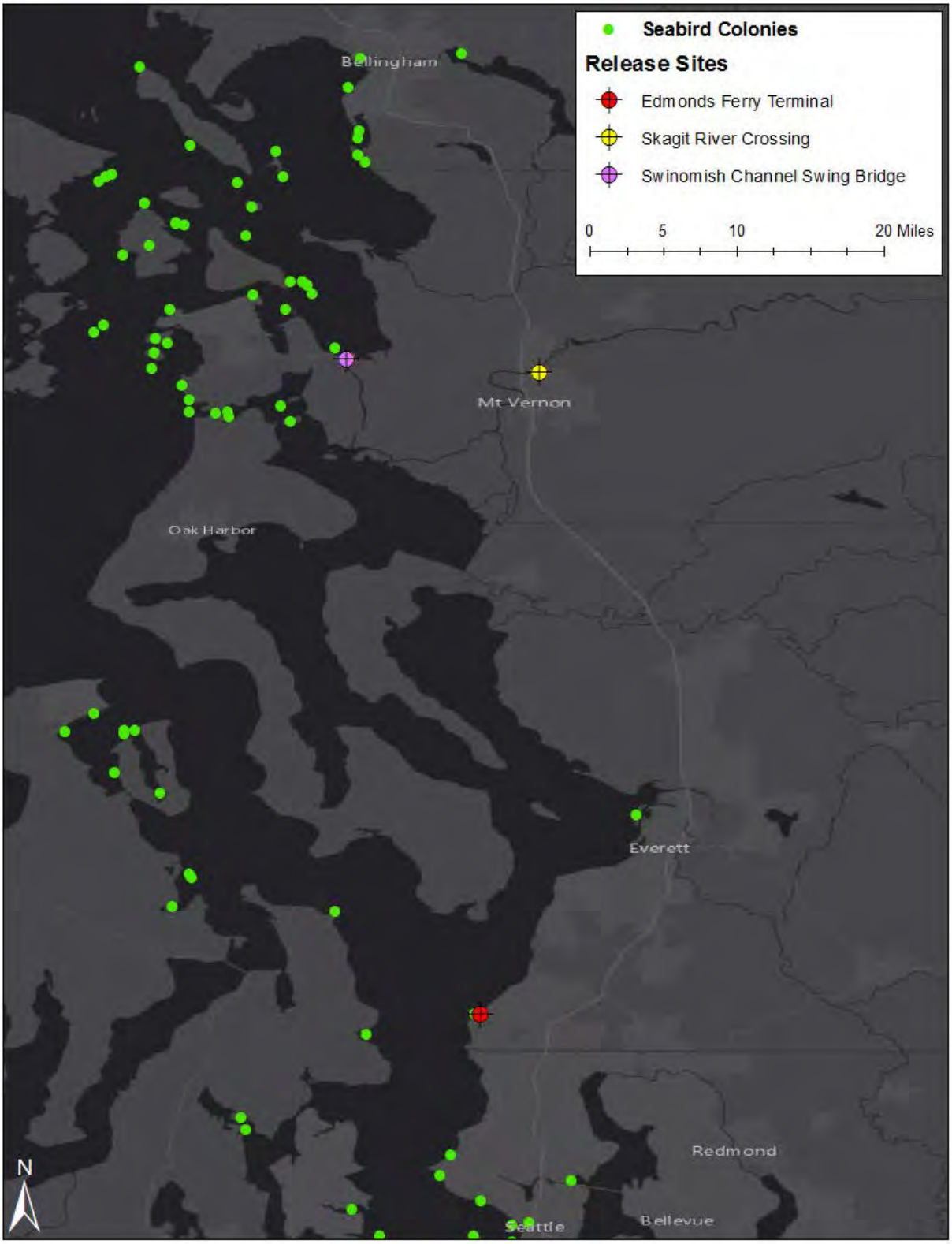
Seabird Colonies
Release Sites
Edmonds Ferry Terminal
Skagit River Crossing
Swinomish Channel Swing Bridge
0
5
10
20 Miles
Bellingham
Mt Vernon
Oak Harbor
Everett
Redmond
Bellevue
Seattle
N

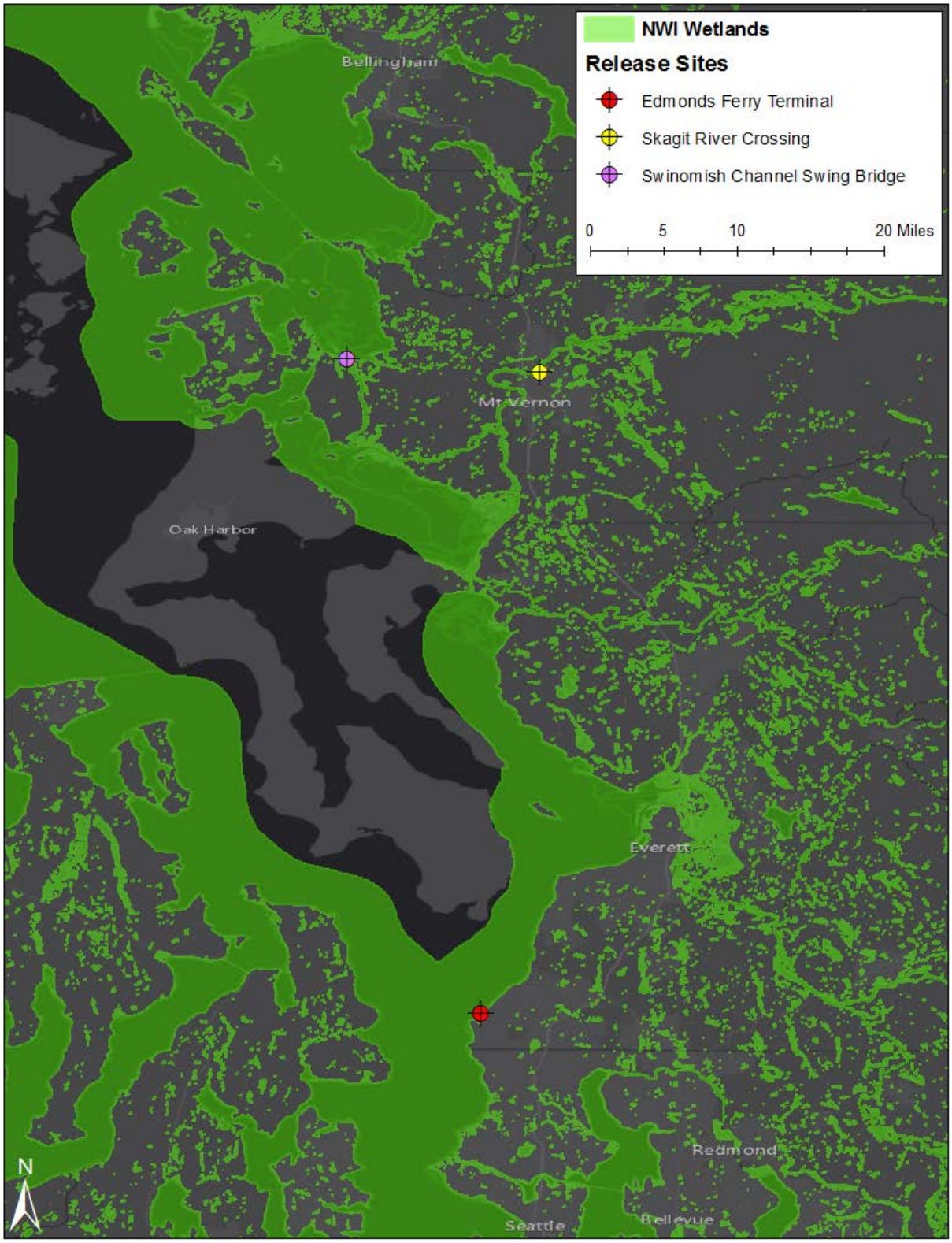
NWI Wetlands
Release Sites
Edmonds Ferry Terminal
Skagit River Crossing
Swinomish Channel Swing Bridge
0
5
10
20 Miles
Bellingham
Mt Vernon
Oak Harbor
Everett
Redmond
Seattle
Bellevue
N

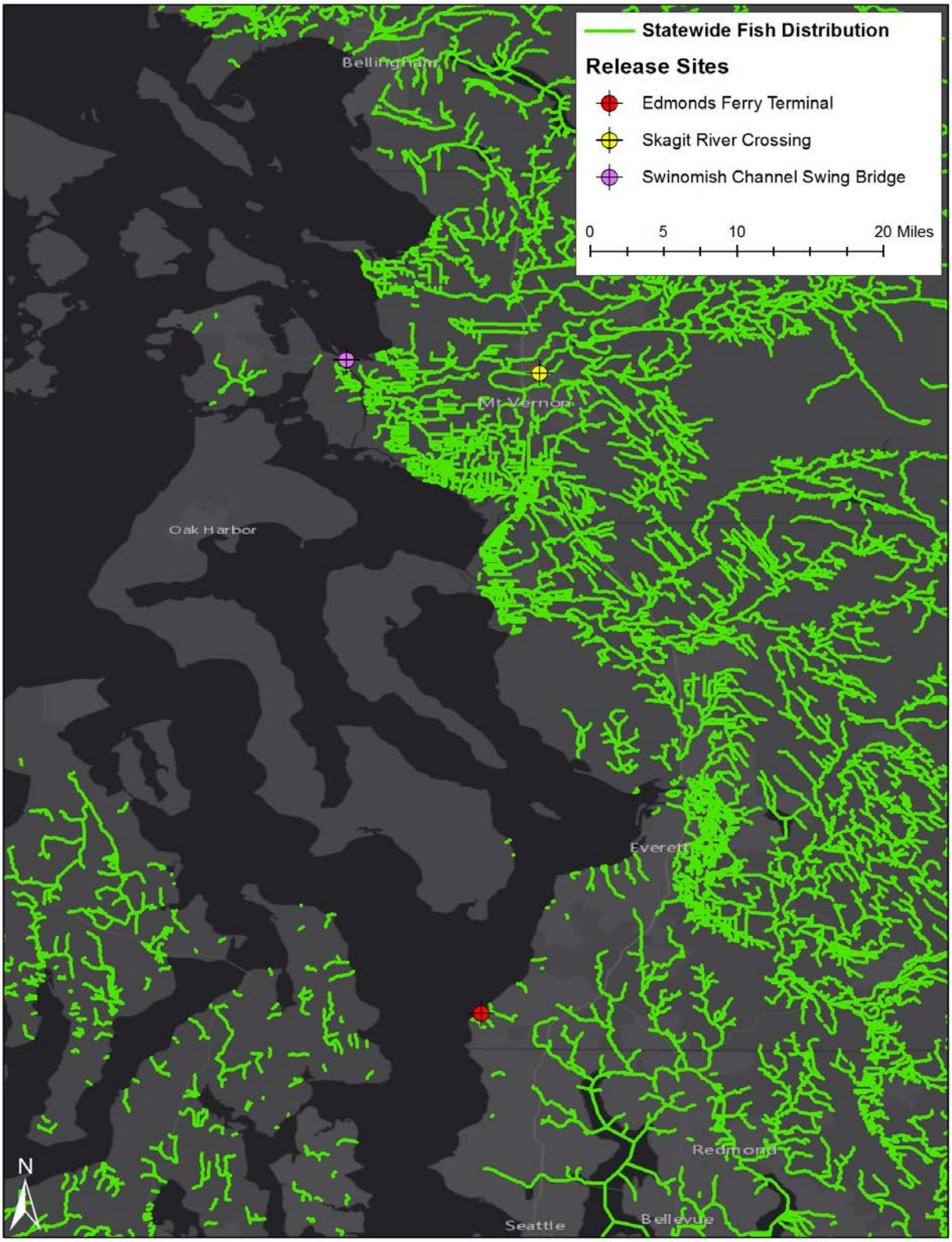
Statewide Fish Distribution
Release Sites
Edmonds Ferry Terminal
Skagit River Crossing
Swinomish Channel Swing Bridge
0
5
10
20 Miles
Bellingham
Mt Vernon
Oak Harbor
Everett
Redmond
Seattle
Bellevue
N

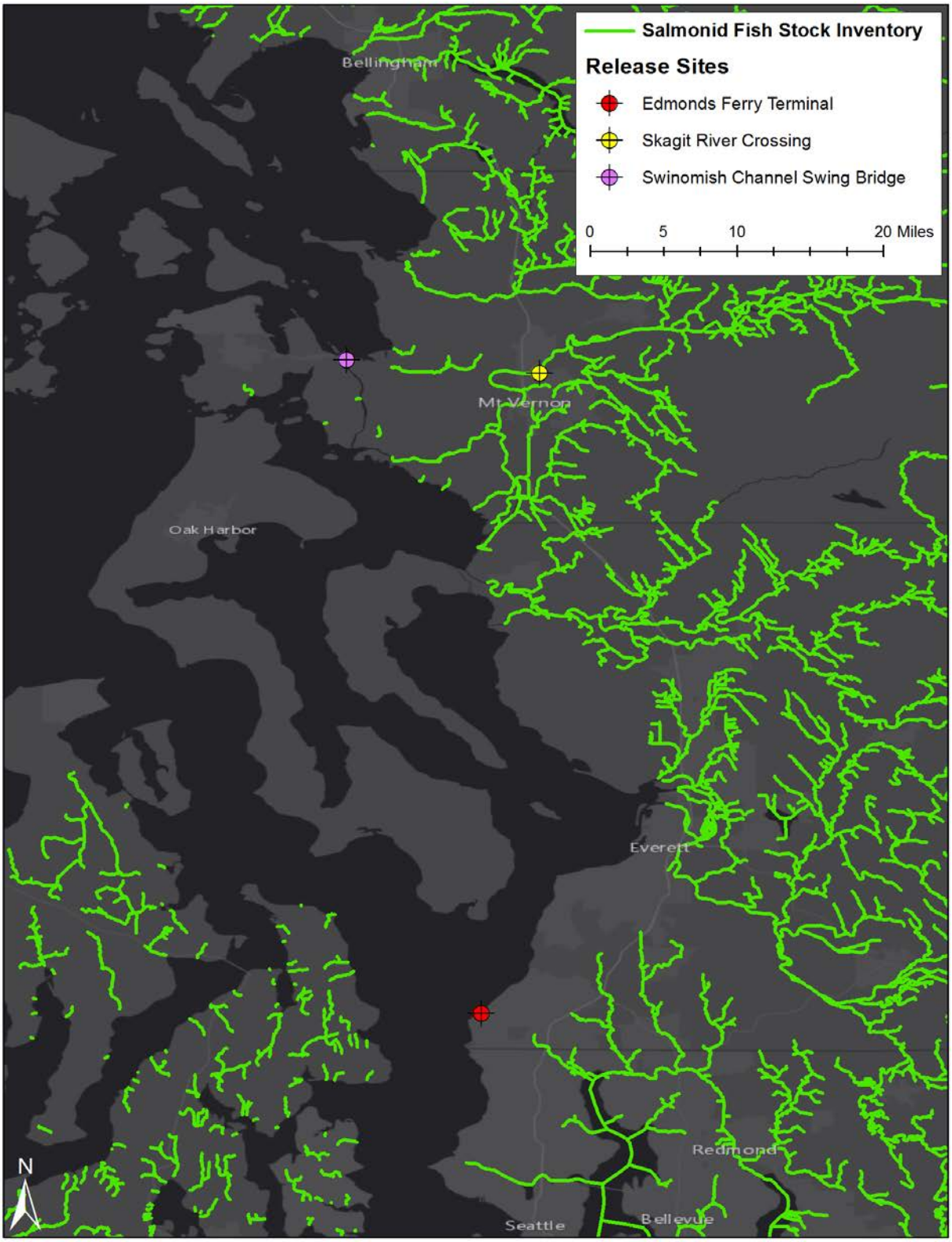
Salmonid Fish Stock Inventory
Release Sites
Edmonds Ferry Terminal
Skagit River Crossing
Swinomish Channel Swing Bridge
0
5
10
20 Miles
Bellingham
Mt Vernon
Oak Harbor
Everett
Redmond
Seattle
Bellevue
N

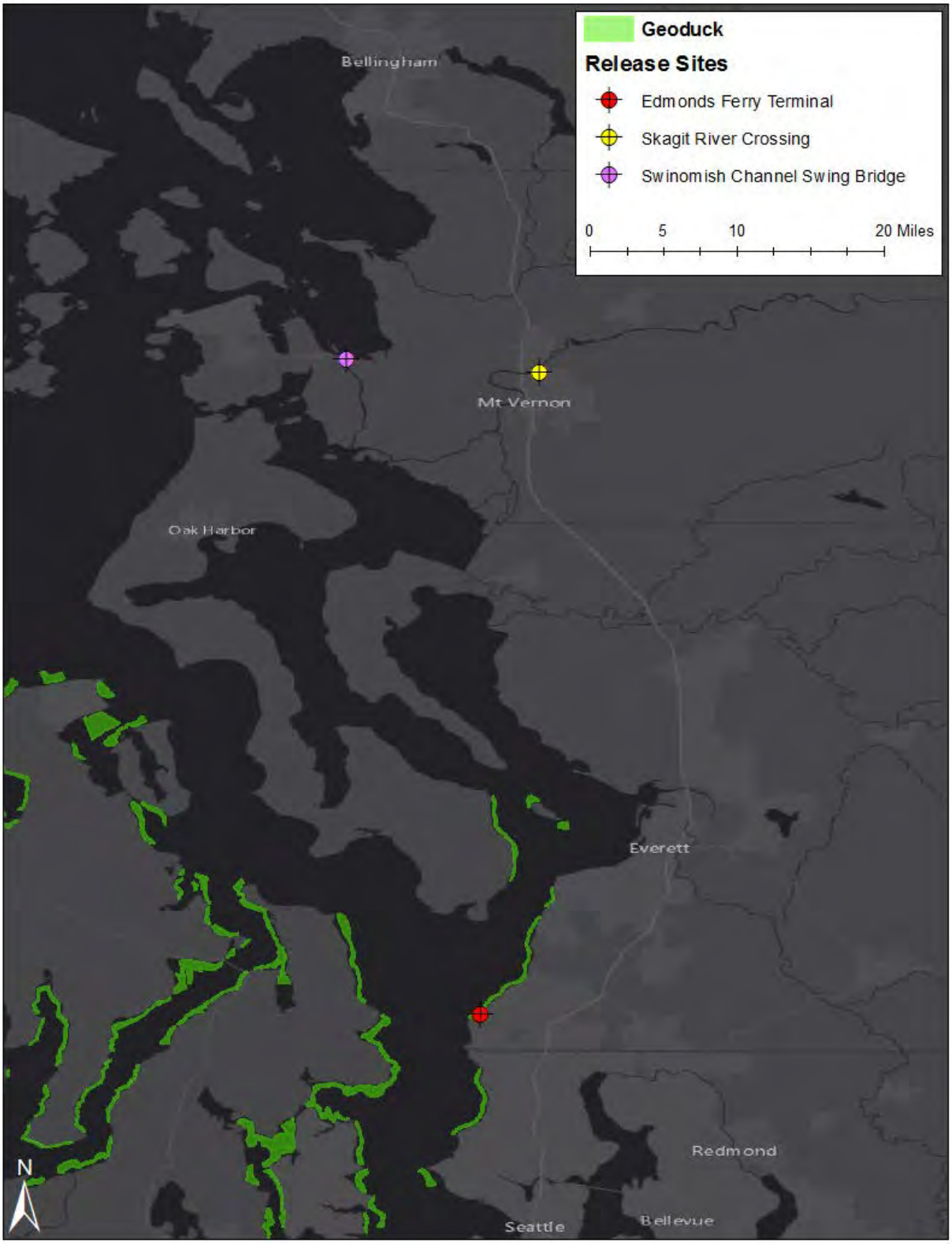
Geoduck
Release Sites
Edmonds Ferry Terminal
Skagit River Crossing
Swinomish Channel Swing Bridge
0
5
10
20 Miles
Bellingham
Mt Vernon
Oak Harbor
Everett
Redmond
Seattle
Bellevue
N

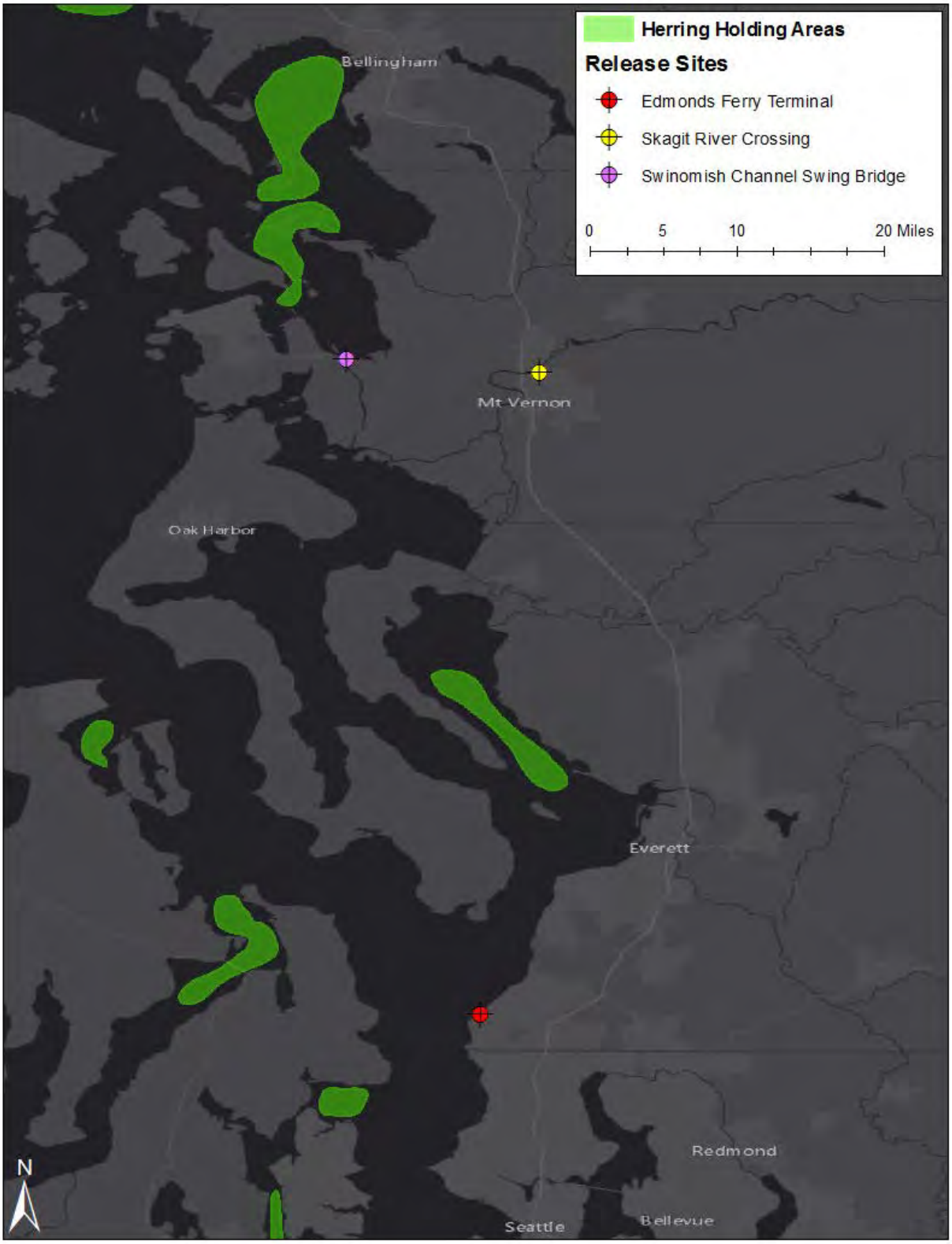
Herring Holding Areas
Release Sites
Edmonds Ferry Terminal
Skagit River Crossing
Swinomish Channel Swing Bridge
0
5
10
20 Miles
Bellingham
Mt Vernon
Oak Harbor
Everett
Redmond
Seattle
Bellevue
N

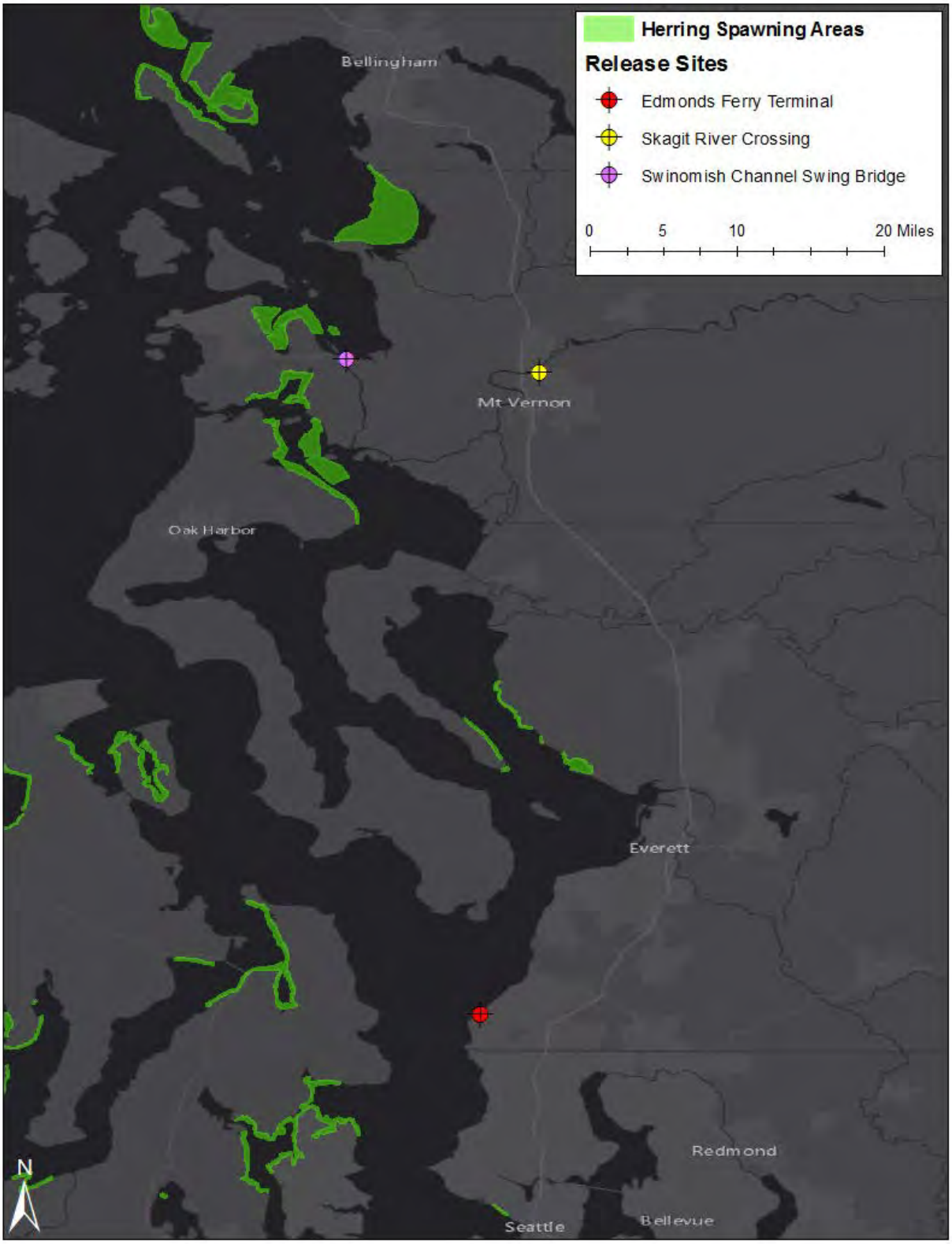
Herring Spawning Areas
Release Sites
Edmonds Ferry Terminal
Skagit River Crossing
Swinomish Channel Swing Bridge
0
5
10
20 Miles
Bellingham
Mt Vernon
Oak Harbor
Everett
Redmond
Seattle
Bellevue
N

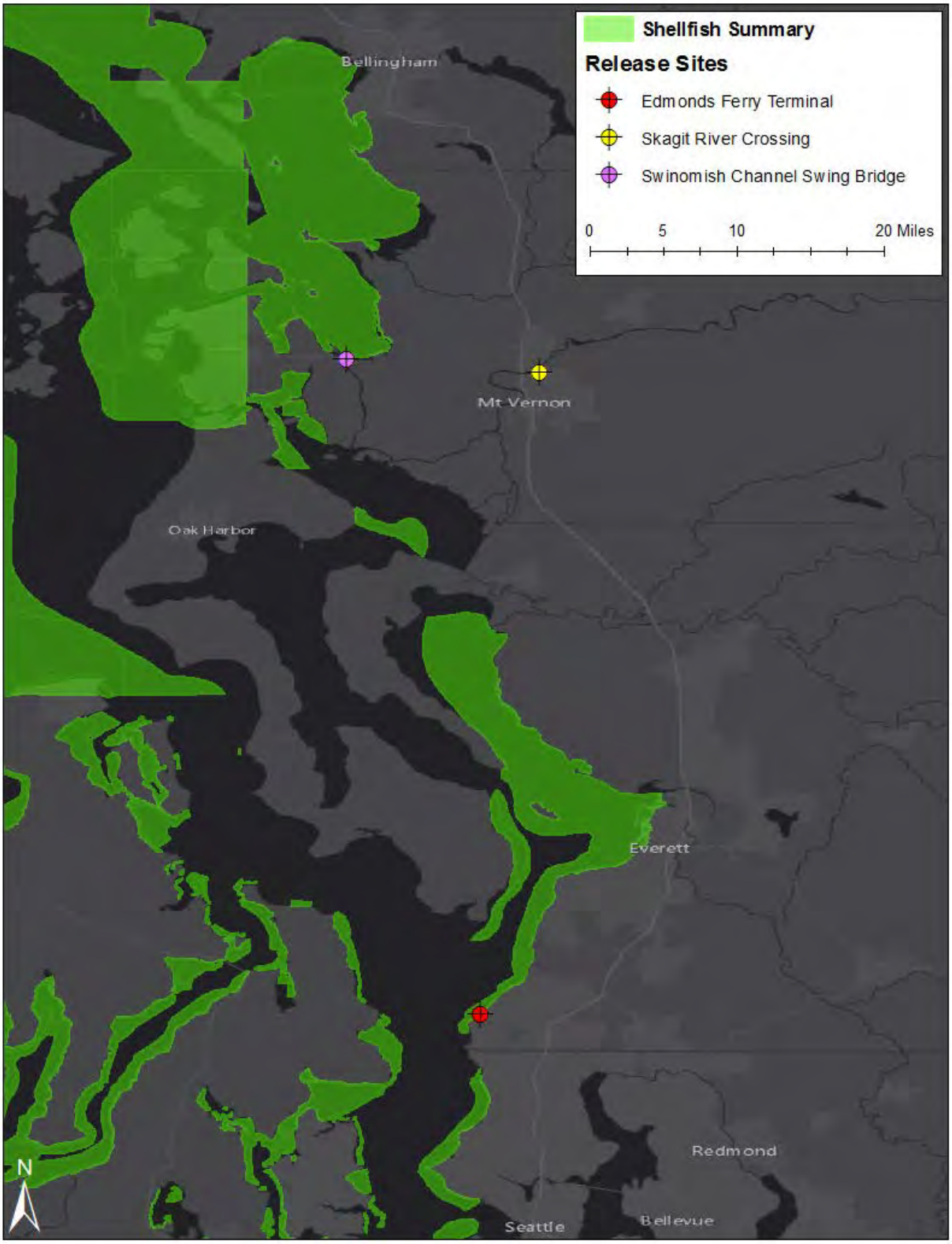
Shellfish Summary
Release Sites
Edmonds Ferry Terminal
Skagit River Crossing
Swinomish Channel Swing Bridge
0
5
10
20 Miles
Bellingham
Mt Vernon
Oak Harbor
Everett
Redmond
Seattle
Bellevue
N

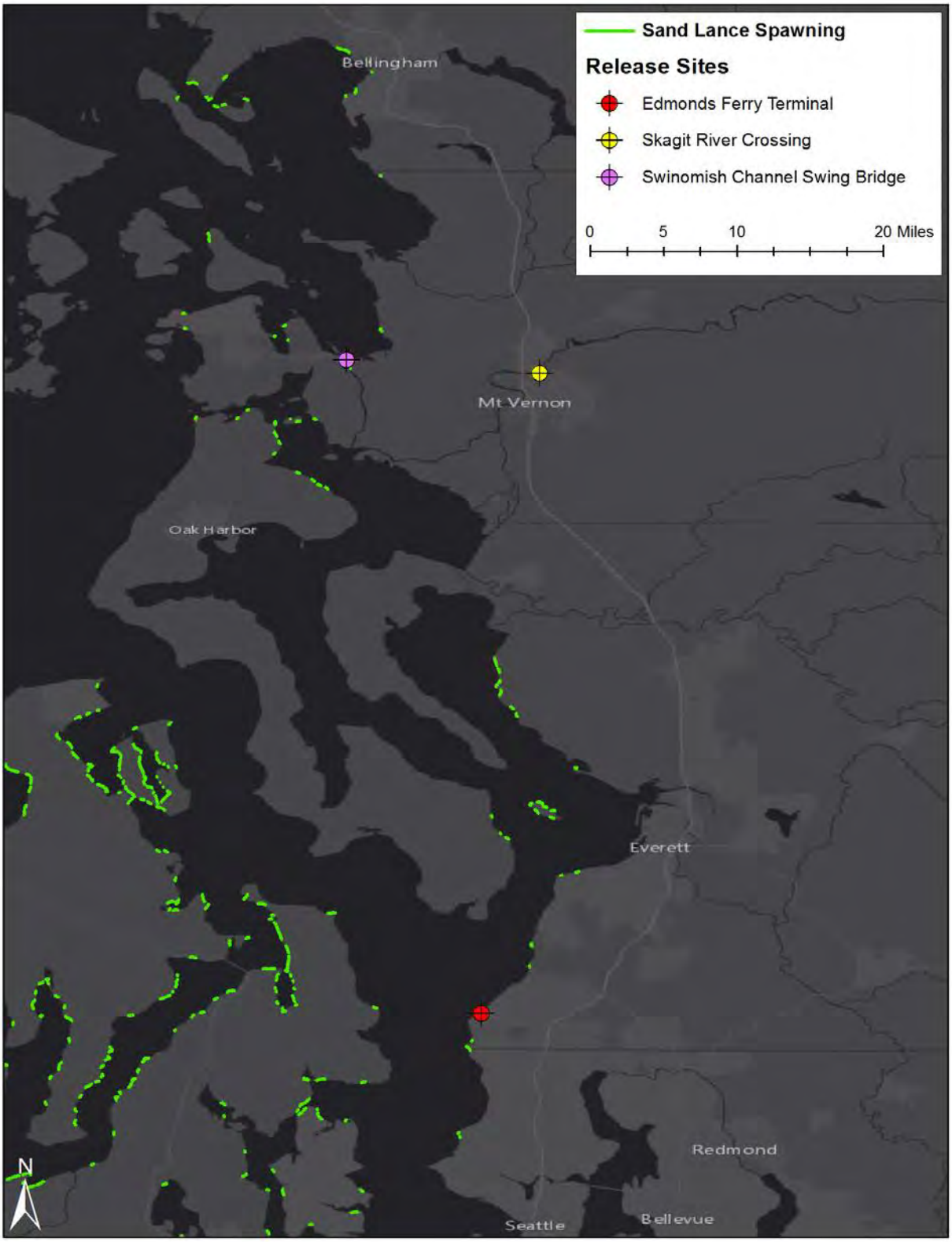
Sand Lance Spawning
Release Sites
Edmonds Ferry Terminal
Skagit River Crossing
Swinomish Channel Swing Bridge
0
5
10
20 Miles
Bellingham
Mt Vernon
Oak Harbor
Everett
Redmond
Seattle
Bellevue
N

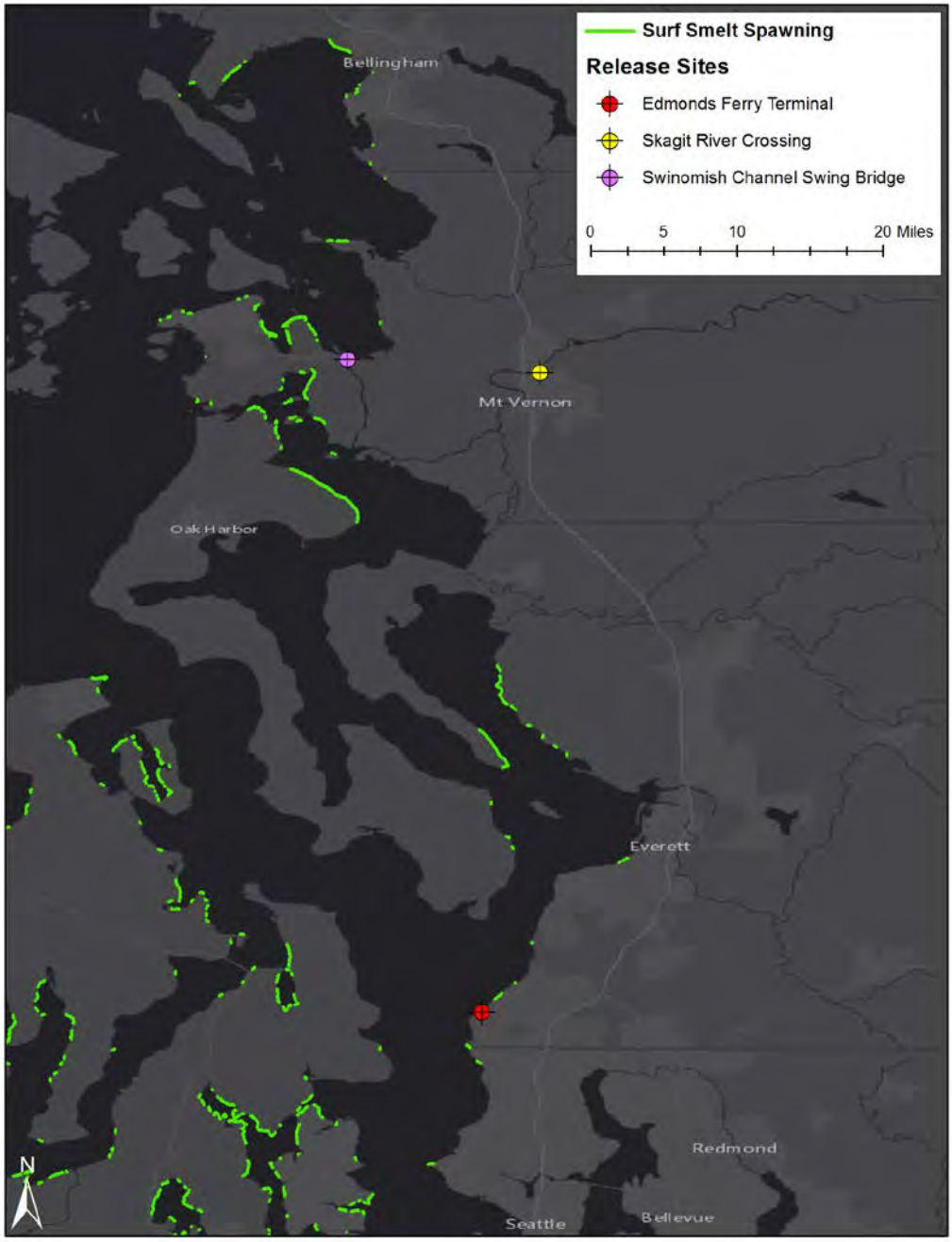
Surf Smelt Spawning
Release Sites
Edmonds Ferry Terminal
Skagit River Crossing
Swinomish Channel Swing Bridge
0
5
10
20 Miles
Bellingham
Mt Vernon
Oak Harbor
Everett
Redmond
Seattle
Bellevue
N